

EXPERIMENTAL RESEARCH ON A 400KW HIGH POWER  
DENSITY MHD GENERATOR

O.K. Sanju, J. Teno, J.W. Lothrop, and S.W. Po

AVCO EVERETT RESEARCH LABORATORY

TECHNICAL REPORT AFAPL-TR-71-5

May 1971

Reproduced From  
Best Available Copy

NATIONAL TECHNICAL  
INFORMATION SERVICE

AIR FORCE AERO PROPULSION LABORATORY  
AIR FORCE SYSTEMS COMMAND  
Wright-Patterson Air Force Base, Ohio

When Government drawings, specifications, or other data are used for any purpose other than in connection with a definitely related Government procurement operation, the United States Government thereby incurs no responsibility nor any obligation whatsoever; and the fact that the government may have formulated, furnished, or in any way supplied the said drawings, specifications, or other data, is not to be regarded by implication or otherwise as in any manner licensing the holder or any other person or corporation, or conveying any rights or permission to manufacture, use, or sell any patented invention that may in any way be related thereto.

Copies of this report should not be returned unless return is required by security considerations, contractual obligations, or notice on a specific document.

Unclassified

Security Classification

DOCUMENT CONTROL DATA - R&D		
(Security classification of title, body of abstract and indexing annotation must be entered when the overall report is classified)		
1. ORIGINATING ACTIVITY (Corporate author) Avco Everett Research Laboratory 2385 Revere Beach Parkway Everett, Massachusetts		2a. REPORT SECURITY CLASSIFICATION Unclassified
		2b. GROUP
3. REPORT TITLE Experimental Research on a 400 KW High Power Density MHD Generator		
4. DESCRIPTIVE NOTES (Type of report and inclusive dates) Final Technical Report		
5. AUTHOR(S) (Last name, first name, initial) Sonju, O. K., Teno, J., Lothrop, J. W., Petty, S. W.		
6. REPORT DATE December 1970	7a. TOTAL NO. OF PAGES 180	7b. NO. OF REFS
8a. CONTRACT OR GRANT NO. F33615-67-C-1019	8b. ORIGINATOR'S REPORT NUMBER(S) Final Technical Report	
a. PROJECT NO.		
c.	9b. OTHER REPORT NO(S) (Any other numbers that may be assigned this report)	
d.	AFAPL-TR-71-5	
10. AVAILABILITY/LIMITATION NOTICES Distribution of this document is unlimited.		
11. SUPPLEMENTARY NOTES	12. SPONSORING MILITARY ACTIVITY Air Force Aero Propulsion Laboratory, Air Force Systems Command, USAF, Wright-Patterson Air Force Base, Ohio	
13. ABSTRACT An MHD Generator Laboratory was designed, constructed and placed in operation at the USAF Aero Propulsion Laboratory. The Laboratory is described and operating, maintenance, safety and calibration instructions and procedures are given. In support of other APL programs, the Laboratory was utilized to demonstrate experimentally that seeding of hydrocarbon-oxygen combustion gases with cesium salts would result in a factor of two improvement in electrical conductivity as compared with potassium seeding. A high specific power output ( $0.5 \text{ MW/kg sec}^{-1}$ ) MHD generator at the 300-400 kilowatt output level was designed and built for cyanogen-oxygen operation. The design of the generator is described, as are the modifications to the AERL Mark II facility which were required in order to test the generator. Excessive overlap of the magnetic field at the channel ends could not be avoided. Also, because of a lack of knowledge relative to heat transfer to the walls at the time the generator was designed, the wall in practice operated colder and caused the downstream electrode drop to be excessive. Power takeoff and diffuser pressure recovery were adversely affected because of the combination of all these effects. Cyanogen operation was terminated due to unavailability of sufficient quantities of chlorine free cyanogen for experimental operation, and high power studies with toluene commenced. In spite of the system imperfections encountered, the ability of an MHD generator to produce high specific output in the sub-megawatt power range with conventional hydrocarbon fuels was conclusively demonstrated although even more impressive performance should be readily attainable. These results should speed the utilization of MHD in those situations where its single unit power capability, compactness, low weight, and power output flexibility are believed to be unique.		

DD FORM 1 JAN 64 1473

Unclassified

Security Classification

Unclassified

Security Classification

14. KEY WORDS	LINK A		LINK B		LINK C	
	ROLE	WT	ROLE	WT	ROLE	WT
1. MHD Generators						
2. Electric Generators						
3. Light Megawatt Power Supplies						
4. Compact DC Megawatt Generator						
5. Gas Conductivities						
6. MHD Facility						
7. Operating Procedure for MHD Laboratory						
8. Flightweight MHD						
9. Cyanogen Fueled MHD						
10. Cesium Seeding of MHD Gases						
11. Effect of Chlorine on Conductivity						
12. Toluene Fueled MHD						

#### INSTRUCTIONS

1. **ORIGINATING ACTIVITY:** Enter the name and address of the contractor, subcontractor, grantee, Department of Defense activity or other organization (*corporate author*) issuing the report.

2a. **REPORT SECURITY CLASSIFICATION:** Enter the overall security classification of the report. Indicate whether "Restricted Data" is included. Marking is to be in accordance with appropriate security regulations.

2b. **GROUP:** Automatic downgrading is specified in DoD Directive 5200.10 and Armed Forces Industrial Manual. Enter the group number. Also, when applicable, show that optional markings have been used for Group 3 and Group 4 as authorized.

3. **REPORT TITLE:** Enter the complete report title in all capital letters. Titles in all cases should be unclassified. If a meaningful title cannot be selected without classification, show title classification in all capitals in parenthesis immediately following the title.

4. **DESCRIPTIVE NOTES:** If appropriate, enter the type of report, e.g., interim, progress, summary, annual, or final. Give the inclusive dates when a specific reporting period is covered.

5. **AUTHOR(S):** Enter the name(s) of author(s) as shown on or in the report. Enter last name, first name, middle initial. If military, show rank and branch of service. The name of the principal author is an absolute minimum requirement.

6. **REPORT DATE:** Enter the date of the report as day, month, year, or month, year. If more than one date appears on the report, use date of publication.

7a. **TOTAL NUMBER OF PAGES:** The total page count should follow normal pagination procedures, i.e., enter the number of pages containing information.

7b. **NUMBER OF REFERENCES:** Enter the total number of references cited in the report.

8a. **CONTRACT OR GRANT NUMBER:** If appropriate, enter the applicable number of the contract or grant under which the report was written.

8b, 8c, & 8d. **PROJECT NUMBER:** Enter the appropriate military department identification, such as project number, subproject number, system numbers, task number, etc.

9a. **ORIGINATOR'S REPORT NUMBER(S):** Enter the official report number by which the document will be identified and controlled by the originating activity. This number must be unique to this report.

9b. **OTHER REPORT NUMBER(S):** If the report has been assigned any other report numbers (either by the originator or by the sponsor), also enter this number(s).

10. **AVAILABILITY/LIMITATION NOTICES:** Enter any limitations on further dissemination of the report, other than those

imposed by security classification, using standard statements such as:

- (1) "Qualified requesters may obtain copies of this report from DDC."
- (2) "Foreign announcement and dissemination of this report by DDC is not authorized."
- (3) "U. S. Government agencies may obtain copies of this report directly from DDC. Other qualified DDC users shall request through \_\_\_\_\_."
- (4) "U. S. military agencies may obtain copies of this report directly from DDC. Other qualified users shall request through \_\_\_\_\_."
- (5) "All distribution of this report is controlled. Qualified DDC users shall request through \_\_\_\_\_."

If the report has been furnished to the Office of Technical Services, Department of Commerce, for sale to the public, indicate this fact and enter the price, if known.

11. **SUPPLEMENTARY NOTES:** Use for additional explanatory notes.

12. **SPONSORING MILITARY ACTIVITY:** Enter the name of the departmental project office or laboratory sponsoring (paying for) the research and development. Include address.

13. **ABSTRACT:** Enter an abstract giving a brief and factual summary of the document indicative of the report, even though it may also appear elsewhere in the body of the technical report. If additional space is required, a continuation sheet shall be attached.

It is highly desirable that the abstract of classified reports be unclassified. Each paragraph of the abstract shall end with an indication of the military security classification of the information in the paragraph, represented as (TS), (S), (C), or (U).

There is no limitation on the length of the abstract. However, the suggested length is from 150 to 225 words.

14. **KEY WORDS:** Key words are technically meaningful terms or short phrases that characterize a report and may be used as index entries for cataloging the report. Key words must be selected so that no security classification is required. Identifiers, such as equipment model designation, trade name, military project code name, geographic location, may be used as key words but will be followed by an indication of technical context. The assignment of links, rules, and weights is optional.

Unclassified

Security Classification



AFAPL-TR-71-5

EXPERIMENTAL RESEARCH ON A 400 KW HIGH POWER  
DENSITY MHD GENERATOR

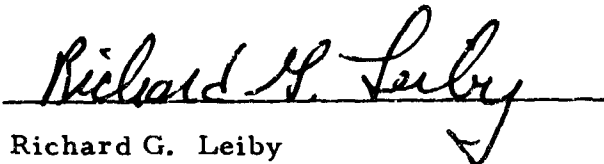
O. K. Sonju, J. Teno, J. W. Lothrop and S. W. Petty

## FOREWORD

This is the final report on the USAF Aero Propulsion Laboratory MHD Laboratory and on a compact, low weight, high power, MHD Generator Preliminary Test Program. This work was sponsored under Project 3145 Task 314526 and Contract F33615-67-C-1019 "Experimental Research on a 400 kW High Power Density MHD Generator" with the USAF Aero Propulsion Laboratory, Wright-Patterson Air Force Base, Dayton, Ohio. This report was submitted by the authors December 1970.

The authors of this report appreciate the assistance of the members of the staff of the Aero Propulsion Laboratory, most notably Mr. R. Cooper and Dr. J. Holt who guided and participated in the program.

This Technical Report has been reviewed and is approved.

A handwritten signature in dark ink, reading "Richard G. Leiby", is written over a horizontal line. The signature is fluid and cursive, with a large initial 'R' and a stylized 'L'.

Richard G. Leiby  
Chief  
Propulsion and Power Branch  
Aerospace Power Division

## ABSTRACT

An MHD Generator Facility was designed, constructed and placed in operation at the USAF Aero Propulsion Laboratory. The Facility is described and operating, maintenance, safety and calibration instructions and procedures are given. In support of other APL programs, the Facility was utilized to measure conductivity of hydrocarbon-oxygen combustion gases seeded with cesium salts. A factor of two improvement in electrical conductivity as compared with potassium seeding was observed.

A high specific power output ( $0.5 \text{ MW/kg sec}^{-1}$ ) MHD generator at the 300-400 kilowatt output level was designed and built for cyanogen-oxygen operation. The design of the generator is described, as are the modifications to the AERL Mark II facility which were required in order to test the generator. Excessive overlap of the magnetic field at the channel ends could not be avoided. Also, because of a lack of knowledge relative to heat transfer to the walls at the time the generator was designed, the wall in practice operated colder and caused the downstream electrode drop to be excessive. Power takeoff and diffuser pressure recovery were adversely affected because of the combination of all these effects. Cyanogen operation was terminated due to unavailability of sufficient quantities of chlorine free cyanogen for experimental operation, and high power studies with toluene were commenced. In spite of the system imperfections encountered the ability of an MHD generator to produce high specific output in the submegawatt power range with conventional hydrocarbon fuels was conclusively demonstrated, although even more impressive performance should be readily attainable. These results should speed the utilization of MHD in those situations where its single unit power capability, compactness, low weight, and power output flexibility are believed to be unique.

## TABLE OF CONTENTS

	<u>Page</u>
I. INTRODUCTION, SUMMARY AND CONCLUSIONS	1
1. Introduction	1
2. Summary	6
3. Conclusion	7
II. THE APL MHD GENERATOR FACILITY	9
1. Introduction	9
2. MHD Generator System	11
a. General	11
b. Combustion Chamber	18
c. Supersonic Expansion Nozzle	21
d. MHD Channel	21
e. Supersonic Diffuser	28
3. Description of Facility	28
a. Introduction	28
b. Oxidizer System (Figures 18 and 19)	28
c. Fuel System (Figures 20-23)	35
d. Nitrogen System (Figures 24 and 25)	40
e. Pilot Combustion System (Figures 24 and 25)	40
f. Water System (Figures 26-28)	40
g. Exhaust System	46
h. Load Resistor	46
i. Seeder	46
j. Instrumentation	49
k. Control System (Figures 31-35)	49
4. Operation of Facility	55
a. Pre-run Procedure	55
b. Normal Run	57
c. Test	60
d. Procedures for Toxic Fuels	60

	<u>Page</u>
5. Maintenance	63
a. Safety	63
b. Burner, Nozzle, and Diffuser	63
c. Channel Maintenance	64
d. Fuel System Maintenance	66
e. Maintenance of Gas Systems	67
f. Seeder	68
g. Control System	69
6. Safety in Handling Cyanogen	69
7. Calibration Data	69
a. Oxidizer Venturi	69
b. Fuel System	69
c. Water System	80
d. Seeder	80
e. Magnet	80
III. APL FACILITY CHECKOUT	85
1. System Checks	85
2. Burner Tests	85
3. Magnet Tests	85
4. Seeder	86
5. Conclusions	86
IV. CONDUCTIVITY MEASUREMENTS AT APL	87
V. INSTALLATION OF GENERATOR COMPONENTS IN THE AERL MARK II FACILITY	91
1. Introduction	91
2. Magnet Modifications	91
3. Assembly of Generator	92
4. Modification of Facility	92
5. Burner Modification	95
VI. EXPERIMENTS WITH CYANOGEN FUEL AT AERL	97
1. Introduction	97
2. Experimental Results	97
3. Conclusions and Recommendations	110
VII. ANALYSIS OF HALL MHD GENERATOR	113
1. Thermodynamic Equilibrium Calculations	113
2. Calculation of Channel Inlet Conditions	118

	<u>Page</u>
3. MHD Channel Performance Analysis	119
4. Inputs and Outputs for the Hall Generator Off-Design Program	123
5. Diagonal Generator Analysis Program	127
VIII. GENERATOR TESTING WITH CONVENTIONAL HYDROCARBON FUELS AT AERL	129
1. Introduction and Summary	129
2. Examination of Alternate Fuel-Oxidizer Combinations	130
3. Experimental Program	142
4. Experimental Results and Comparison with Theory	146
5. Conclusions and Recommendations	166
APPENDIX 1 - LIQUID SEED SYSTEM	167
APPENDIX 2 - HALL MHD GENERATOR ANALYTIC COMPUTER PROGRAM	171

## LIST OF ILLUSTRATIONS

<u>Figure</u>		<u>Page</u>
1	A View of the 400 kW High Specific Power Output MHD Generator.	4
2	Typical Performance Data Obtained During Experimental Program with High Specific Power Output MHD Generator in the AERL MK II Facility.	5
3	Schematic Illustration of Major Equipment and Systems of the APL MHD Generator Facility.	10
4	Schematic Illustration of the MHD Generator System	12
5	Variation of the Calculated Flow Parameters as a Function of Distance Along the Channel at the Design Condition; Combustion of Cyanogen and Oxygen with Cesium Seed; Mass Flow 0.7 kg/sec.	16
6	Variable Area Profile Characteristics of the Channel.	17
7	Assembly Drawing of the Combustion Chamber.	19
8	Photograph of the Assembled Combustion Chamber.	20
9	Drawing of the Mach 2.15 Rectangular Expansion Nozzle.	22
10	Photograph of the Rectangular Expansion Nozzle.	23
11	Assembly Drawing of the Heat Sink, Segmented Electrode, Peg Insulator Wall MHD Channel.	24
12	View of Completed Channel with Two Walls Removed.	26
13	View of Completed Channel with One Peg Wall Raised	27
14	Assembly Drawing of the Supersonic Diffuser.	29
15	View of the Assembled Diffuser.	30
16	View Inside Facility Looking Toward Combustion Chamber and Field Coil.	31

<u>Figure</u>		<u>Page</u>
17	Close Up View of the Combustion Chamber End of the APL MHD Generator Laboratory.	32
18	Main Oxygen System - APL MHD Generator Facility	33
19	Oxygen System Assembly - APL MHD Generator Facility	34
20	Cyanogen Rated Fuel System Layout	36
21	Cyanogen Fuel System Piping Layout.	37
22	Cyanogen Ventilating System Layout.	38
23	Photograph of the Cyanogen Fuel Storage and Ventilating System.	39
24	Nitrogen and Pilot System Schematic - APL MHD Generator Facility	41
25	Nitrogen and Pilot System Piping Layout - APL MHD Generator Facility	42
26	Cooling Water System Schematic - APL MHD Generator Facility	43
27	Cooling Water Piping Layout, I.	44
28	Cooling Water Piping Layout, II.	45
29	The Load Resistor Bank - APL MHD Generator Facility	47
30	Photograph of the Powder Seed Feeder.	48
31	Control System 1: AC Line, Water Cooling, Fuel Vent, and Auxiliary Power - APL MHD Generator Facility	50
32	Control System 2: Pilot Test, Run and Purge.	51
33	Control System 3: Burner, Seeder, Magnet, Fuel Alarm, Entrance Alarm.	52
34	Drawing of the Control and Instrumentation Assembly - APL MHD Generator Facility	53
35	View of Control and Instrumentation Assembly and Observation Window.	54



<u>Figure</u>		<u>Page</u>
36	Oxidizer Venturi Calibration - $O_2$ .	70
37	Oxidizer Venturi Calibration - $N_2/O_2 = 1/2$ .	71
38	Oxygen Mollier Diagram.	72
39	Calibration of 3 Sets of Fuel Oxidizers.	73
40	Seeder Calibration - 20 and 40 Tooth Rotors.	81
41	Magnetic Field Strength vs Winding Current at the Center of the APL Magnet.	82
42	Magnetic Field Distribution at 2.3 Tesla Center Field for the APL Magnet	83
43	Results of Conductivity Tests with JP-4 and Oxygen.	89
44	Axial Distribution of Flux Density of the Modified AERL Mark II Magnet.	93
45	Photograph of the Generator Setup at AERL	94
46	Mollier Curve for $C_2 N_2 + 2 O_2$ with 0.5% (Molar) Cs.	98
47	Electrical Diagram for Conductivity Tests with Voltage Applied Along the Channel.	100
48	Electrical Diagram for Conductivity Tests with Voltage Applied Across the Channel at Electrode Pair 28.	101
49	Observed Axial Voltage Distribution with Voltage Applied Along the Channel.	102
50	Observed Transverse Voltage Distribution with Voltage Applied Across the Channel at Electrode Pair 28.	103
51	Observed and Predicted Values of Electrical Conductivity for Combustion Products of Cyanogen and Oxygen as a Function of Seed Rate; $T = 2790^\circ K$ and $P = 0.54$ atm.	106
52	Predicted Distributions of Pressure, Temperature, Conductivity, and Area; Mass Flows of 0.68 kg/sec of Cyanogen and Oxygen.	107
53	Electrical Diagram for Hall Parameter Test.	108

<u>Figure</u>		<u>Page</u>
54	Mollier Chart, $C_2N_2 + O_2$ , C/O = 1 Seeding Rate of 0.5 Mole %.	115
55	Typical Computer Output Data for Hall Generator Calculations.	125
56	Mollier Chart for a Stoichiometric Mixture of Toluene and Oxygen with Two Weight Percent Cesium Added.	143
57	Magnetic Field Distribution of the Mark II Magnet with Short Pole Pieces at a Maximum Field of 3.5 Tesla.	144
58	Insulator Heat Transfer as a Function of Axial Distance Along Channel When Burning Toluene and Oxygen; Mass Flow = 0.6 kg/sec; B = 0.	148
59	Measured Static Pressure Distribution in the Channel and the Diffuser when Burning Toluene and Oxygen; Mass Flow = 0.6 kg/sec; B = 0.	149
60	Static Pressure Distribution in the Channel and Diffuser when Burning Toluene and Oxygen. Mass Flow = 0.8 kg/sec; B = 0.	150
61	Observed and Predicted Axial Voltage Distributions for the APL Generator; Mass Flow = 0.6 kg/sec.	153
62	Predicted V-I Characteristics for the APL Generator with 0.8 kg/sec Mass Flow and a Peak Field of 2.6 Tesla.	154
63	A Schematic of the Electrical Wiring Diagram Used in Run No. 13.	156
64	Observed and Predicted Axial Voltage Distributions.	157
65	Transverse Current in Amperes per Electrode as a Function of Axial Distance Along the Channel.	158
66	Transverse Voltage Distribution at Electrode Pair Number 28.	159
67	Transverse Voltage Distribution at Electrode Pair Number 81.	160
68	Axial Voltage Distribution for 400 kW Test.	161
69	Transverse Current Distribution in Amperes per Electrodes for 400 kW Test	162

<u>Figure</u>		<u>Page</u>
70	Axial Pressure Distributions for Unloaded and Loaded MHD Generator During 400 kW Test.	163
71	Predicted V-I Characteristics with 0.8 kg/sec Mass Flow and a Peak Field of 3.5 Tesla.	165
72	Experimental Setup of Liquid Seed System at AERL.	168

## SECTION I

### INTRODUCTION, SUMMARY AND CONCLUSIONS

#### 1. INTRODUCTION

This is the Final Report of Contract F33615-67-C-1019, "Experimental MHD Generator Research," between the USAF Aero Propulsion Laboratory (APL) and the Avco Everett Research Laboratory (AERL). The period of performance for the work is June 1967 through December 1970.

Two main objectives of the program may be identified:

- 1) Design, construction and startup of the APL MHD Generator Facility.
- 2) Demonstration of high specific power output ( $0.5 \text{ MW sec/kg}$ ) from a combustion-driven MHD generator using liquid fuels and stored oxidizers at output power levels of several hundred kilowatts.

Both of the main objectives were achieved.

Implementation of the APL MHD Generator Facility was a straightforward application of techniques utilized for many years at AERL, and proven in several thousand MHD generator connected operations. Complications due to the necessity of using toxic cyanogen fuel were also dealt with using techniques developed previously at AERL. The APL MHD Generator Facility (including the MHD generator itself) is described in Section II along with operating, maintenance, safety and calibration procedures for the as built installation. It is our understanding that the Facility is presently being modified by APL but, as AERL has not been responsible for, nor connected with these modifications, they are not described here.

Although the APL Facility was not operated on cyanogen during the program, checkout was carried out using JP-4 as is described in Section III. In support of other APL sponsored programs, the relative merit of potassium and cesium salts as seed materials in hydrocarbon-oxygen flames was examined in the Laboratory using the Hall MHD generator previously supplied under Contract AF 33(615)-3027 as a conductivity test rig. This work is described in Section IV. The motivation for the work was to confirm that hydroxide formation would not

reduce or eliminate the expected advantages of higher conductivity from cesium. The experiments confirmed that a factor of two improvement in conductivity would be obtained in the temperature range of interest.

The original intention was to carry out the high specific power output program using the APL Facility. However, the program was modified so that this portion of the work was done at AERL using the existing Mark II facility. In order to do this, it was necessary to modify the Mark II combustion system. Other modifications were also required in load resistors and instrumentation. Finally, the Mark II magnet pole force contour was altered in an attempt to confine the intense field to the APL channel which was much smaller than channels usually employed with the Mark II. These modifications were not too effective, in that the performance of the generator was adversely affected in terms of power takeoff and diffuser pressure recovery due to excessive field overlap of the channel ends. The Mark II modifications are described in Section V.

Examination of the electrical properties of seeded cyanogen-oxygen combustion gases is discussed in Section VI. These gases are of interest because of the very high conductivity to be expected after expansion to high velocity due to the extreme flame temperature and lack of water vapor in these combustion gases. This high conductivity combined with storability offers the potential of high specific power output, compactness and lightweight for specialized applications such as exo-atmospheric generation of large amounts of power for limited duration. For these applications, these advantages can outweigh the adverse effects due to the toxicity of cyanogen. Production of cyanogen in the United States is extremely limited, with only one supplier capable of delivering the quantities required by this program and others at AERL. The Government was to have supplied the cyanogen fuel to AERL specification, for use in these experiments, but was unable to obtain a tolerable delivery date. Accordingly, it was arranged that initial quantities would be "borrowed" from other AERL programs, and this cyanogen was used in the conductivity experiments. To our surprise, the conductivity was one seventh or less of the expected value, a discrepancy which was traced to an impurity content of approximately two percent (2%) of chlorine, a level entirely inconsistent with the specifications to which the material was procured. As no cyanogen of the required purity was available on an acceptable delivery schedule, the decision was made to suspend these experiments in favor of the more important goal of demonstration of high specific power output with conventional hydrocarbon fuels and oxygen as described in Section VIII.

The AERL Hall MHD generator design program was supplied to APL as a part of the program. As high power Hall generators will normally operate in the supersonic impulse mode, a boundary layer stability calculation is an important feature of this program, and applies equally well to the high power channel used in the present experiments. The Hall generator design program is described in Section VII.

As is described in Section VIII, the specific power output objective of  $0.5 \text{ MW/Kg sec}^{-1}$  was achieved using an MHD generator designed for a completely different and much higher energy propellant combination than the conventional hydrocarbon-oxygen system that was actually used, and under other particularly unfavorable circumstances. The power level varied from 300-400 kilowatts for this specific output. We believe that achievement of the  $0.5 \text{ MW/Kg sec}^{-1}$  specific output objective under these much less than ideal conditions should provide a convincing demonstration of the unique ability of liquid fueled MHD to satisfy requirements for large amounts of power for limited periods. Additionally, the specific power output objective was achieved at very modest magnetic field strengths (as low as 2.6 Teslas) demonstrating conclusively that the very high field strengths previously considered (6 Teslas) are not essential. The present results show that extremely light weight superconducting field coils are feasible for air- or spaceborne systems. Additionally, the performance was achieved at modest combustion pressures of 10 atm or less showing that the higher pressures previously considered are not necessary. Thus, it is believed that this work represents a significant advance in the state of the art in MHD generators, providing opportunity for immediate utilization while still leaving plenty of room for improvement with modest additional effort.

Figure 1 shows the assembled APL generator in position to be inserted into the Mark II magnet at AERL. The magnetic field provided by this large (1.7 meter long) magnet excessively overlapped the ends of the active channel, and interfered with power takeoff and diffuser recovery. Nonetheless, high performance was achieved as is illustrated by Figure 2 which presents the important data from one 400 kilowatt run at a mass flow of  $0.8 \text{ kg/sec}$ . Close correlation and comparison of these typical pressure, transverse current and voltage distributions for twenty six (26) such runs, and numerous special purpose non-power generation runs with expected values has yielded a good understanding of the operation of this generator and the ability to predict accurately the performance of new designs. We believe there is little doubt that the performance could be markedly improved by operation of a similar generator designed for use with hydrocarbon-oxygen combustion gases in a more favorable magnetic field distribution.

The real reason for this successful demonstration of high specific power output at the submegawatt level is not so much the details of the channel design itself, but rather the choice of sensible combustion conditions with which to drive the generator. The relatively low combustion pressure is selected specifically to match the mass flow-power characteristics desired in the generator. It is easily demonstrated that previous projects in which high specific output at the same power levels as are of interest here were required, were fatally compromised by the selection of extremely high and unrealistic combustion pressures, which led to:

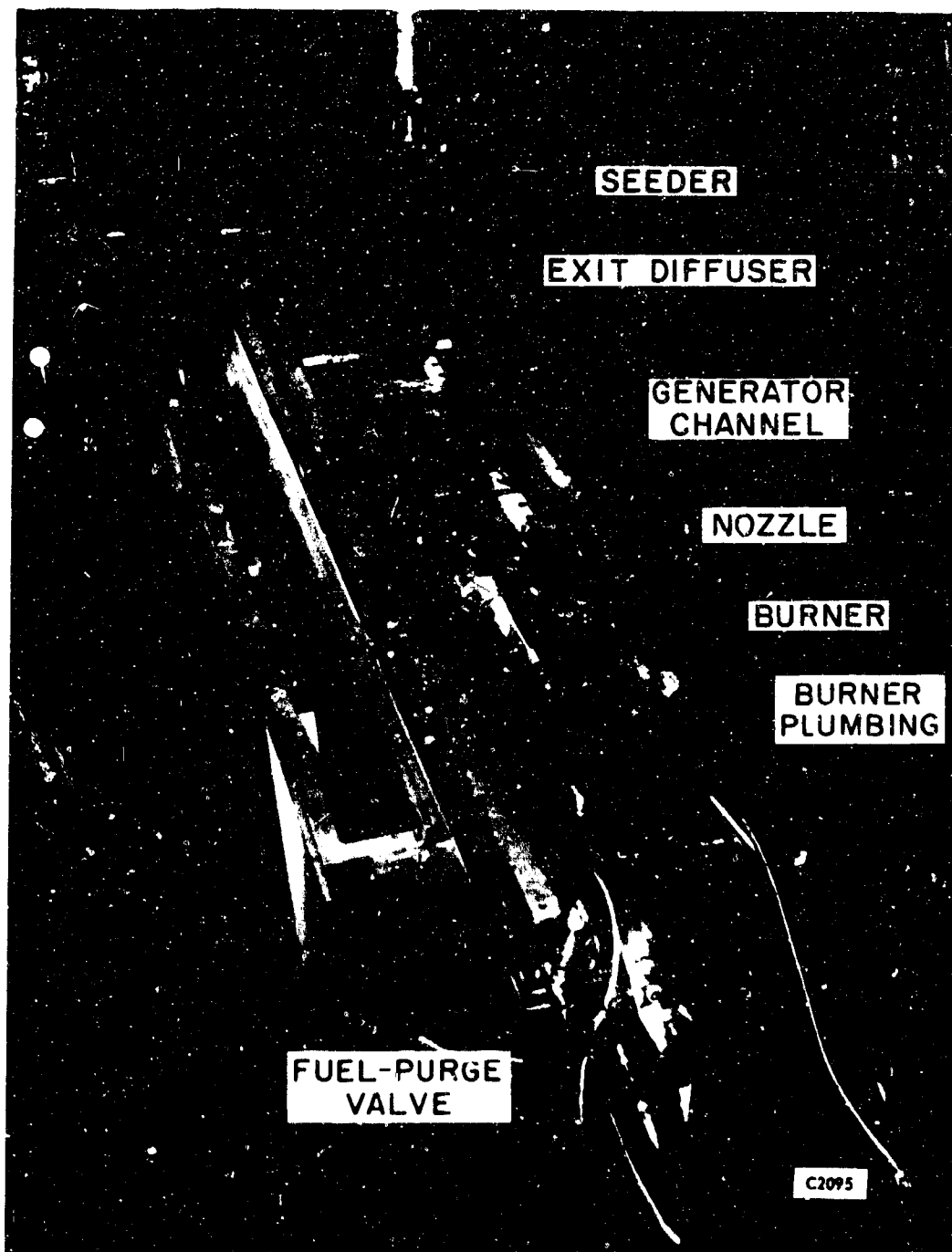
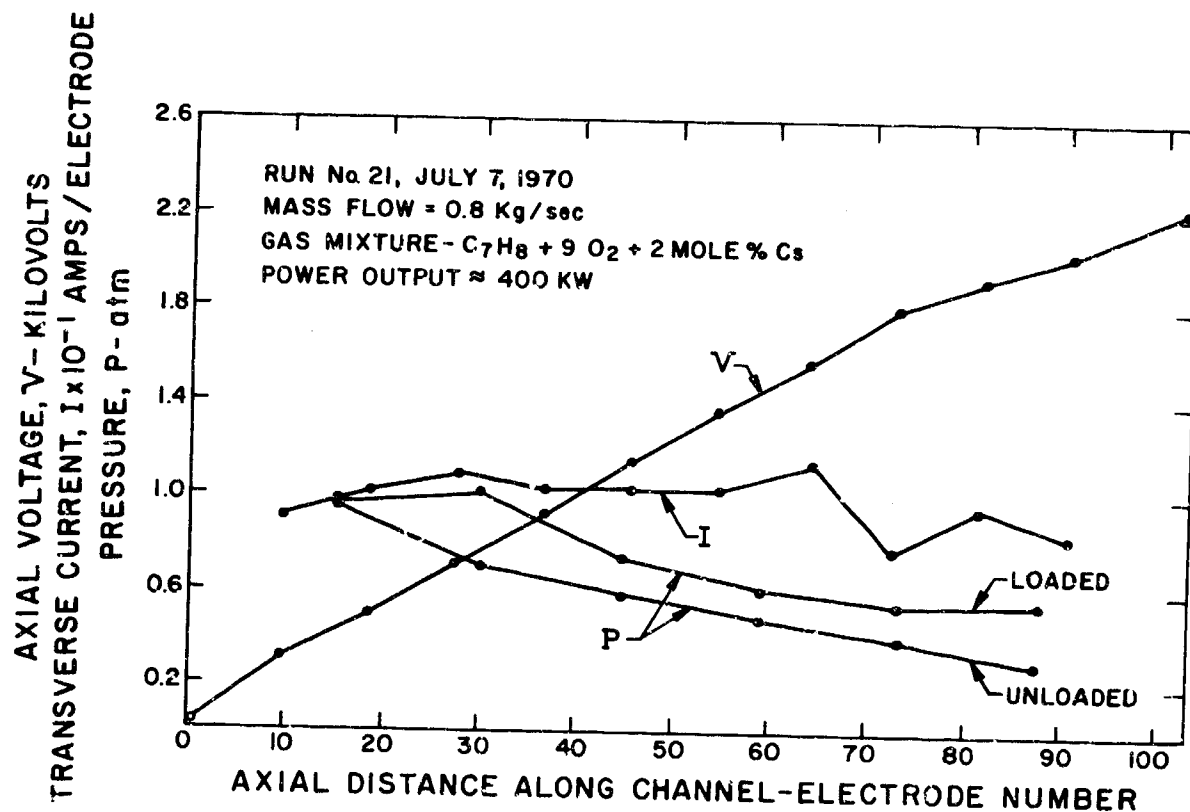


Figure 1 A View of the 400 kW High Specific Power Output MHD Generator.



C5978

Figure 2 Typical Performance Data Obtained During Experimental Program with High Specific Power Output MHD Generator in the AERL MK II Facility.



- 1) Excessive heat transfer rates in the MHD channel and nozzle and burner.
- 2) Excessively high magnetic field strength requirements taxing or exceeding the state of the art.
- 3) Conductivity reduction due to high pressure KOH formation.
- 4) Low utilization of the available pressure ratio.

It is hoped that the results of Section VIII will be useful in demonstrating that high specific output can be achieved without dangerous overstressing of the MHD generator and superconducting field coil.

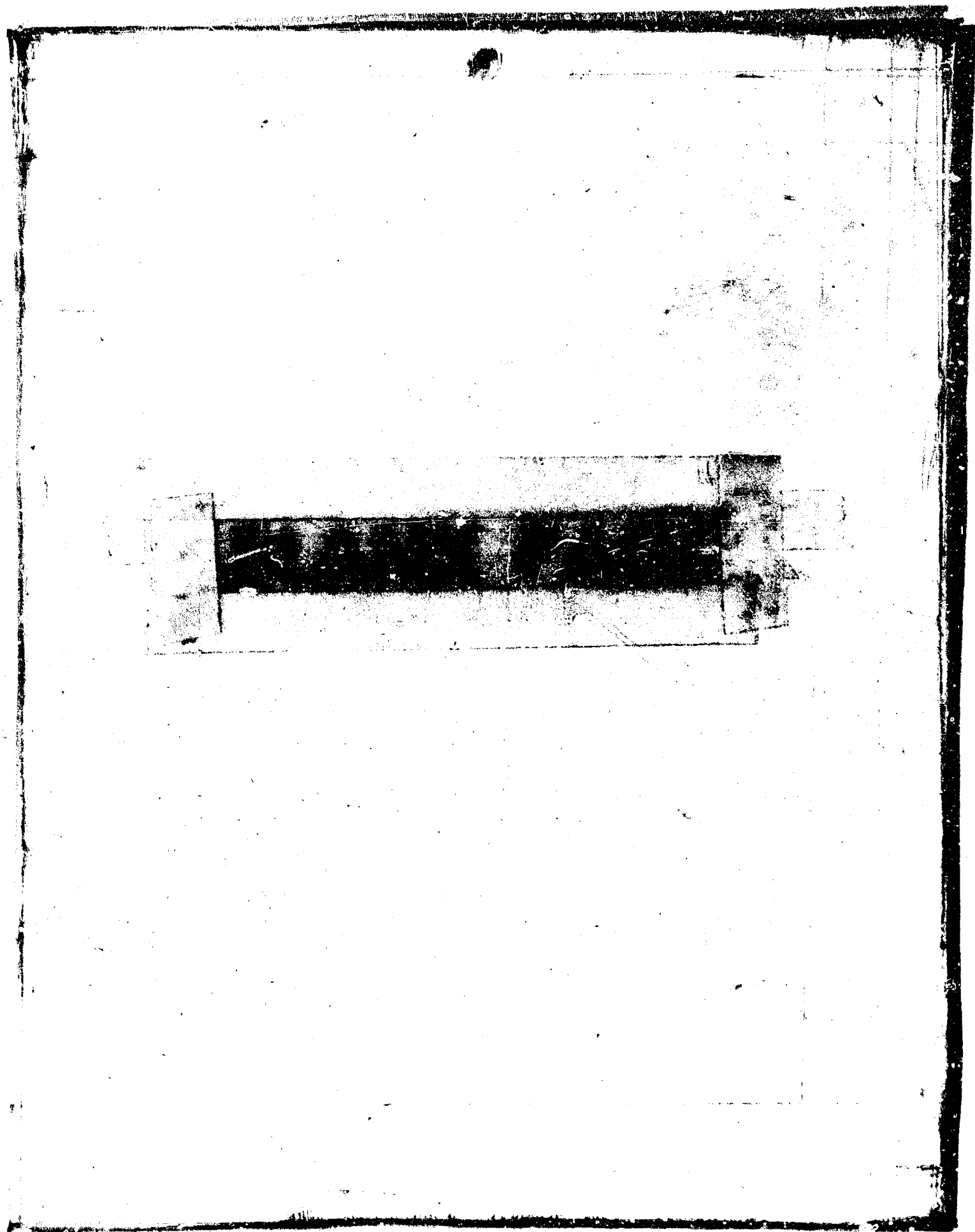
Metric units are utilized throughout this report with the exception of the engineering drawings and instrument calibration curves which are dimensioned in English units. A non-dimensional unit of pressure, the atmosphere (atm), is employed, and is the ratio of the pressure in  $\text{N/m}^2$  to  $1.015 \times 10^5 \text{ N/m}^2$ .

## 2. SUMMARY

- 1) The APL MHD Generator Facility was implemented, calibrated and activated.
- 2) The Laboratory was utilized to confirm that seeding with a cesium salt would yield a factor of two improvement in combustion gas conductivity as compared with the same amount of potassium salt seed by volume of gas temperatures of interest to other APL programs.
- 3) The AERL Mark II facility was modified to accept the APL MHD generator operating on cyanogen-oxygen.
- 4) Electrical property measurements on seeded cyanogen-oxygen combustion projects were terminated due to the impossibility of obtaining adequate supplies of cyanogen free of electron robbing chlorine impurity.
- 5) The AERL Hall MHD generator design program was supplied to APL.
- 6) Specific MHD power output of  $0.5 \text{ MW/kg sec}^{-1}$  was demonstrated using conventional hydrocarbon-oxygen combustion gases at power levels of 300-400 kilowatts, and magnetic fields of 2.6-3.5 Tesla. It is believed that the conditions under which these studies were carried out leave room for considerable improvement in specific power output above this figure.

### 3. CONCLUSION

The ability of an MHD generator to produce high specific power output in the sub-megawatt power range has been conclusively demonstrated, although even more impressive performance should be readily attainable. The results should speed utilization of MHD in those situations where its single unit power capability, compactness, low weight, and power output flexibility are believed to be unique.



## SECTION II

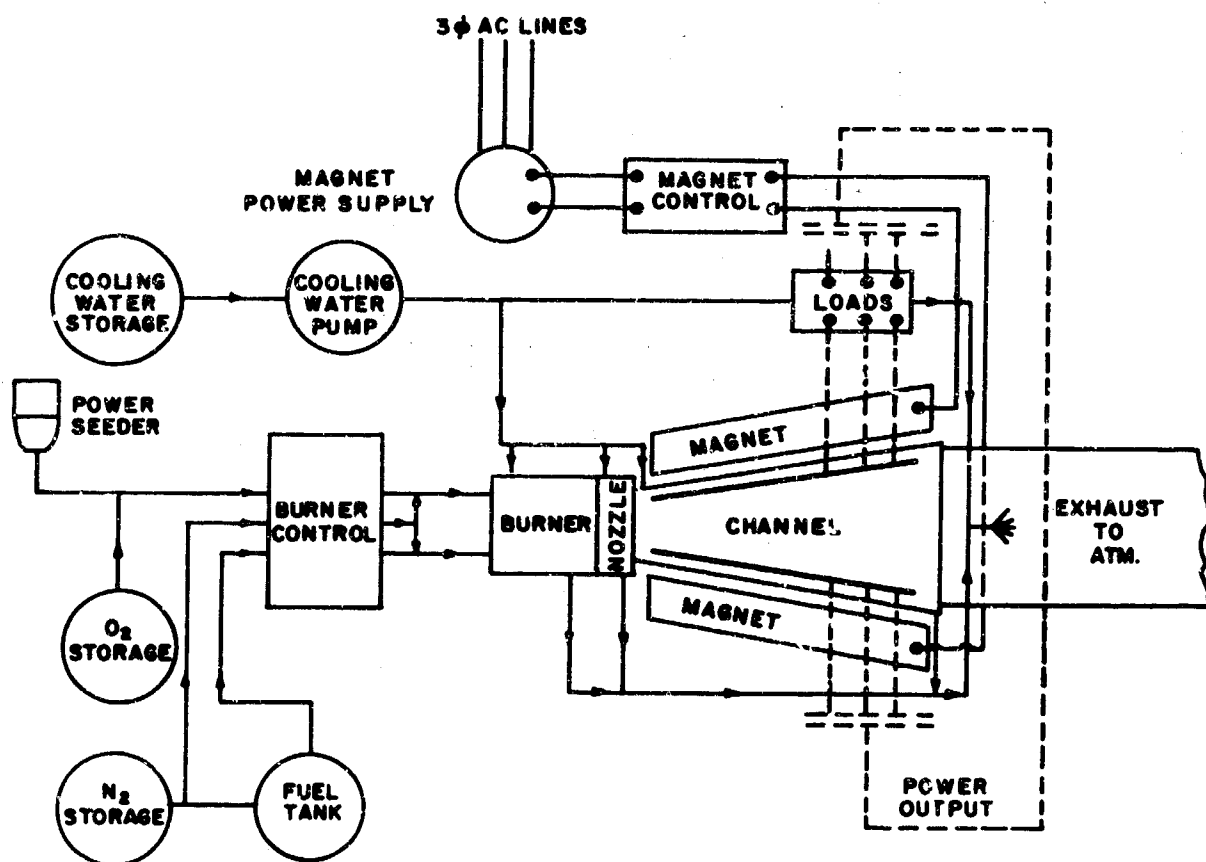
### THE APL MHD GENERATOR FACILITY

#### I. INTRODUCTION

The following is a description of and will also serve as an operating and maintenance manual for the MHD Generator Facility installed in Cell #1, Building 71, at Wright-Patterson Air Force Base, Ohio. Each of the essential components or subsystems of the Facility is described, and its normal performance or operating range is defined. Operating procedures for both normal and emergency situations are described. A section is devoted to procedure for operating the cyanogen rated fuel system. Maintenance of the Facility is described and finally a section on calibration data is included.

The Facility, including rectangular channel, nozzle, and diffuser, was constructed by Avco Everett Research Laboratory under Contract F33615-67-C-1019. The burner, and circular Hall channel, nozzle, and diffuser, and the magnet were previously supplied by Avco under Contract AF 33(615)-3027. Since operating instructions were not supplied for these latter items, suitable instructions have been included where necessary in this Section. The magnet power supply and the essential electrical and water services for the Facility have been supplied by the Air Force to AERL specifications.

Figure 3 is a schematic showing the major components and subsystems of the APL MHD Generator Facility. The oxidizer supply (GOX or simulated  $N_2O_4$ ) is stored in a high pressure trailer supplied by a gas vendor, and is delivered to the combustion chamber through appropriate controls and regulators. Powdered seed is injected directly into the oxygen line and is blown into the burner with the oxygen. Fuel is supplied to the burner from a nitrogen "push fed" tank. The fuel system is fully rated for cyanogen. A spark-ignited ethane (or methane) - oxygen pilot burner provides reliable ignition for the main combustion chamber. Cooling water is supplied to the combustion chamber and nozzle, and, in addition, is sprayed into the diffuser exit to quench the high temperature exhaust gases prior to discharge. A load resistor bank provides for versatile output coupling to the generator which is of heat sink, segmented electrode, peg wall construction with the negative terminal grounded. Suitable control and performance instrumentation complete the Facility.



C 5980

Figure 3 Schematic Illustration of Major Equipment and Systems of the APL MHD Generator Facility.

Laboratory specifications include:

Oxidizer:	Gaseous oxygen or nitrogen-oxygen mixture
Oxidizer Flow Rate:	1.0 kg/sec max.
Fuel:	Nitrogen push fed liquid, cyanogen rated
Fuel Flow Rate:	0.40 kg/sec max. Liquid hydrocarbon or cyanogen
Total Flow Rate:	1.4 kg/sec max. (3.1 lb/sec max.)
Seed:	Fowdered potassium carbonate in oxidizer line; .03 kg/sec max. flow (2% by weight at 1.4 kg/sec)
Ignition:	Spark ignited oxygen-ethane (or methane) pilot burner
Combustion Pressure:	$10^6$ N/m <sup>2</sup> max. (150 psia, 10 atm)
Magnet Field Strength:	2.3 teslas water cooled
Magnet Dimension:	0.19 x 0.25 m cross-section x 0.6 m long
Run Duration:	4 sec at max. flow, 8 sec. at 0.7 kg/sec.
Maximum Output Voltage:	4 kv positive (diffuser)

The data presented in Section VIII of this Report indicate that a maximum MHD power output of approximately 1000 kilowatts (one megawatt) could be achieved with conventional hydrocarbon fuels and oxygen in the APL MHD Generator Facility at various flow rates.

## 2. MHD GENERATOR SYSTEM

### a. General

Figure 4 is an overall portrayal of the MHD generator which is defined to consist of the following components:

- 1) Watercooled combustion chamber and directly attached manifolding
- 2) Watercooled supersonic expansion nozzle
- 3) Heat sink MHD channel (segmented electrode and peg wall)
- 4) Heat sink supersonic diffuser

The combustion chamber was provided to APL under previous Contract AF 33(615)-3027; additional sets of fuel injectors were supplied to permit operation at the high fuel flow rates when cyanogen is used. The other components were supplied as a part of the present contract.

At contract inception in June 1967, the intent was to utilize the Hall MHD generator equipment supplied under AF 33(615)-3027 for low power

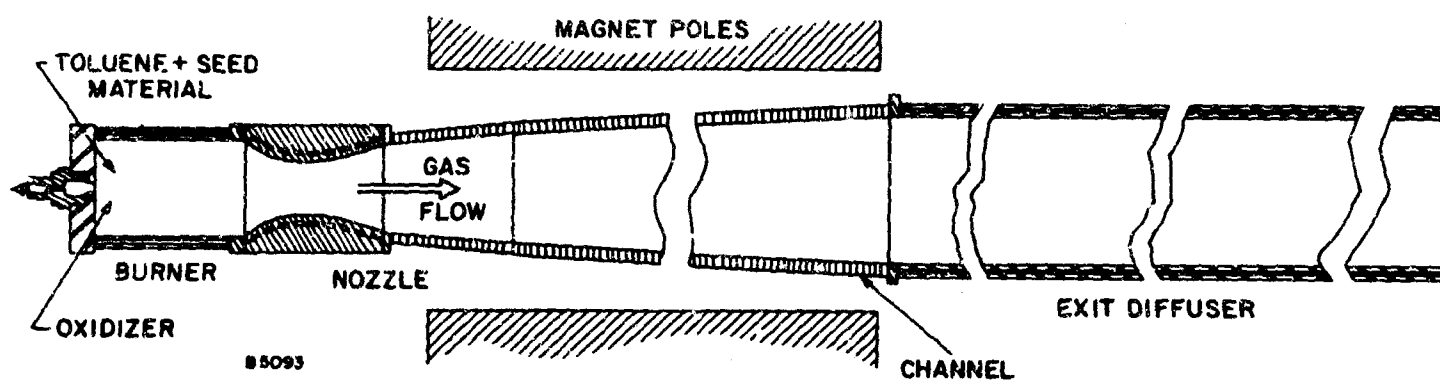


Figure 4 Schematic Illustration of the MHD Generator System

fundamental studies of gas properties, electrode phenomena, etc. in the facility to be constructed. Almost immediately, however, the objective was changed to demonstration of high specific power output (in excess of 0.5 megawatts/kg sec<sup>-1</sup>) at a power level of 300 kilowatts using cyanogen fuel. It should be noted here that the 0.5 megawatt/kg sec<sup>-1</sup> specific power output was ultimately achieved, with ordinary hydrocarbon fuels and without the necessity to use cyanogen. However, as the facility design was specifically intended to support the cyanogen fueled MHD generator, some details of the generator design are presented here before a description of the facility. The chronological development and use of the APL high power generator is given below:

<u>Date</u>	<u>Event</u>
June 1967	Contract inception
July 1967	Decision to concentrate on high specific power output experiments
May 1968	Design freeze
December 1968	Generator shipped to APL
April 1969	Decision to conduct high specific power experiments at AERL Mark II facility
September 1969	Generator returned to AERL
January 1970	Inception of C <sub>2</sub> -N <sub>2</sub> experiments in Mark II
April 1970	Inception of Hydrocarbon-oxygen generation experiments in Mark II
September 1970	Experiments concluded, 300 - 400 kilowatts at 0.5 megawatts/kg sec <sup>-1</sup> achieved

The generator channel loft for cesium seeded cyanogen-oxygen was determined using both segmented electrode and diagonal design and off-design programs as they existed at AERL in early 1968. The design analysis is similar to those presented in Section VII for the Hall configuration MHD generator with the proper form of the tensor Ohm's Law for the segmented electrode and diagonal generator being utilized. In these analyses, fixed parameters included:

Mass Flow:	0.68 kg/sec
Magnetic Field Strength:	2.3 Tesla max.



Generator Length: 0.70 meters pole pieces, 0.85 meters overall

Combustion pressure: 10 atm (1 atm =  $10^5$  N/m<sup>2</sup>)

Parameters which were varied included:

Fuel-oxygen ratio (F/O)

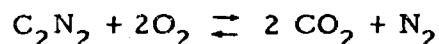
Channel inlet Mach number

Wall angle for diagonal configurations

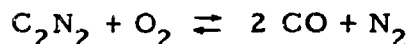
Seed concentration

Loading

In connection with F/O ratio, it was found that combustion to CO<sub>2</sub> rather than to CO offered the best route to high performance. The reaction (with oxygen)



while producing an adiabatic flame temperature considerably below that of

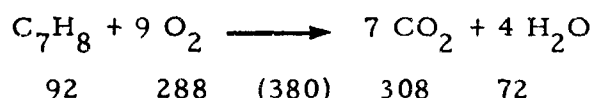
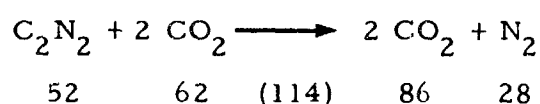


nonetheless leads to considerably higher temperatures and conductivity in the channel after expansion to similar Mach number due to the large energy of dissociation at the flame temperature burning to CO<sub>2</sub>. Additionally, combustion to CO<sub>2</sub> releases a higher energy/unit mass, produces an exhaust free of combustible and poisonous CO, and economizes on cyanogen utilization for a given mass flow. Finally, combustion to CO<sub>2</sub> leads to designs which are less sensitive to variable factors which may not be too well known in advance such as burner heat loss and combustion efficiency. A Mollier diagram for C<sub>2</sub>N<sub>2</sub> + 2 O<sub>2</sub> seeded with 0.5 Cs by volume is given in Figure 46 during discussion of the cyanogen experiments, and is discussed there.

For fixed combustion conditions, the inlet Mach number influences the velocity, density and temperature gradients in the channel. With a high inlet M, thermodynamic conditions in the channel remain relatively constant, and most of the output is extracted from the kinetic energy of the flow, i. e., the generator operates in the impulse mode. The generator will be relatively easy to diagonalize, the area ratio modest to simplify construction, the power density high, and modest magnetic field gradient requirements. On the other hand, the impulse generator is susceptible to boundary layer separation, and the desired power output per unit mass flow could not be achieved entirely in the impulse mode (as in LORHO) so that a combination of impulse and reaction resulted. An inlet Mach number of 2.1 was selected as the best compromise between the practical advantages of impulse operation, and the need to protect the design against boundary layer separation. In general, the exit velocity must be greater than 75%-80% of the inlet velocity in order to prevent separation.

Important parameters of the final design are indicated in Figure 5. The compromise between impulse (decreasing velocity) and reaction (falling pressure) is seen. The calculated power output with some allowance for electrode drop was approximately 500 kilowatts at a mass flow of 0.70 kg/sec for a specific power output of 0.72 MW/kg sec<sup>-1</sup>. Although subsequent more refined calculations with more accurate electrode drop and boundary layer effects, reduced the indicated output to 400 kilowatts, this figure does exhibit the great potential of cyanogen when the ultimate in performance is desired. In a given case, the difficulties in using cyanogen would need to be carefully weighed against the performance advantages.

The equations for the reactions of cyanogen with oxygen and toluene with oxygen are:



These equations show that a higher weight percentage of cyanogen is required to produce a given weight of working gas than for the case of toluene. On the other hand, the mole weights of the combustion products are more or less the same. A third fact to note is that all of the constituents in liquid form have a specific gravity not unlike that of water. In the case of cyanogen less oxygen would need to be carried but then the handling problems of the cyanogen must be taken into account. In the case of toluene (which would be representative of the typical hydrocarbon fuel) a higher percentage of liquid oxygen would need to be handled. Assuming the same conductivities for both mixtures, both the specific weights and specific volumes required to produce a given output would be comparable. However, the conductivity of the cyanogen-oxygen combustion products are relatively higher which would ultimately show up as a reduced requirement for fixed weight which of course is very significant for airborne applications.

To allow flexibility with regard to the aerodynamics of the channel, specifically the boundary layer behavior, the channel was designed with moveable electrode walls so that the area ratio of the channel could be varied by 20%. In Figure 6 the area distribution for the extreme positions of the selected channel design are plotted.

Although the potential of cyanogen as a high performance fuel was not demonstrated due to events described in Section VII as well as earlier inability to run with cyanogen at APL, the goal of 0.5 MW/kg sec<sup>-1</sup> was achieved using an ordinary hydrocarbon fuel with oxygen at output levels of 300-400 kilowatts. The fact that this performance was achieved with relative ease and with a channel intended for use with other higher energy

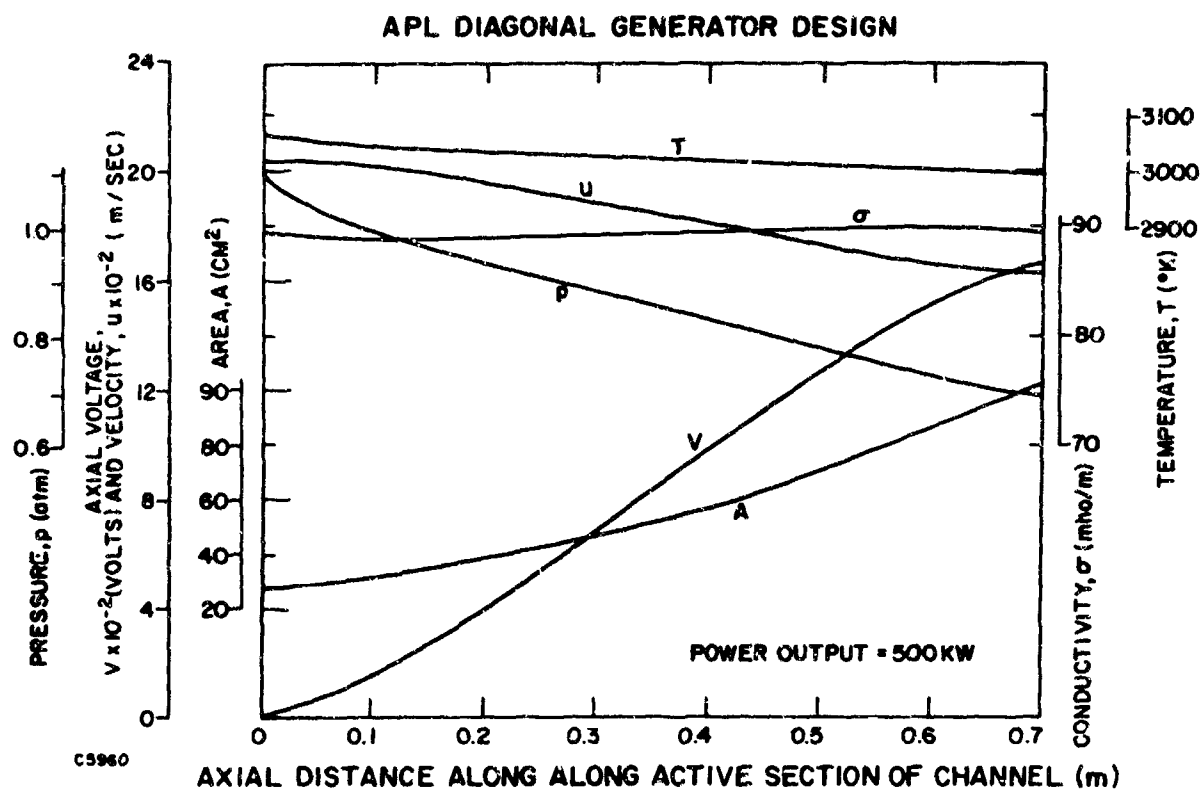


Figure 5 Variation of the Calculated Flow Parameters as a Function of Distance Along the Channel at the Design Condition; Combustion of Cyanogen and Oxygen with Cesium Seed; Mass Flow 0.7 kg/sec.

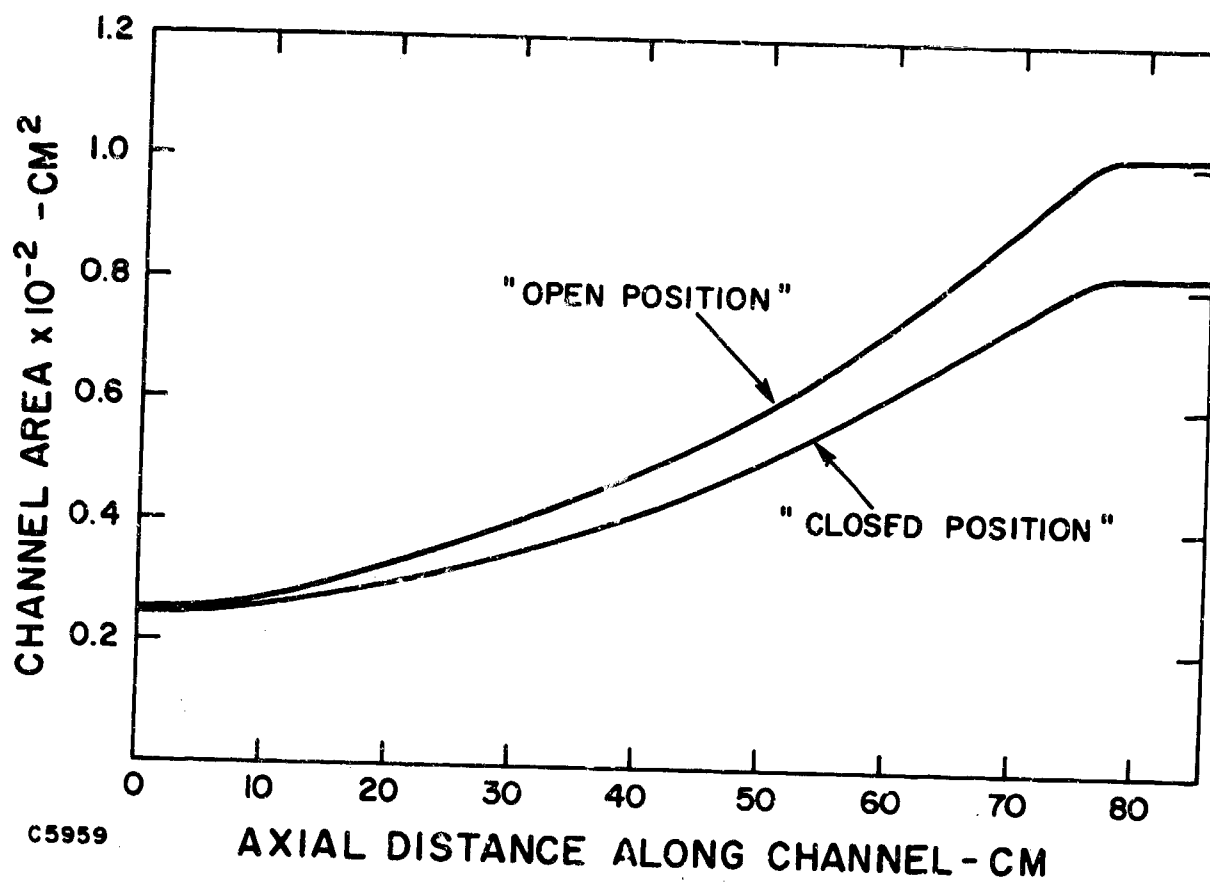


Figure 6 Variable Area Profile Characteristics of the Channel.

propellants and under other unfavorable conditions (as described in Section VIII) is, we believe, impressive testimony to the real potential of MHD in high power, limited duty cycle applications.

#### b. Combustion Chamber

The burner is a water cooled rocket-type combustion chamber designed to burn liquid fuels with gaseous oxidizers at pressure up to 10 atm. A spark ignited pilot burner is used to provide a continuous high intensity ignition source for the main burner. Figure 7 shows details of the burner assembly, while Figure 8 is a photograph of the completed burner.

The injection and combustion system has been designed to produce flexibility in the choice of fuel and oxidizer and to permit a large variation in flow rate. The chamber volume is large so as to permit complete combustion even with relatively slow burning propellant combinations. The oxidizer injectors are designed for use with gaseous oxidizers. The flow in the injectors is normally sonic so that small variations in chamber pressure will not influence oxidizer flow. The use of unusually large fuel/oxidizer ratios or a nozzle of small throat area will cause the flow through the oxidizer injectors to become subsonic which should be avoided. The oxidizer flow rate may be varied over a wide range simply by adjusting the injection pressure, the flow being directly proportional to pressure provided the injectors are sonic. The maximum flow rate for oxygen or oxygen-nitrogen mixtures is approximately 0.8 kg/sec with the present injectors. However, this flow may be increased to 1.0 kg/sec by enlarging the injectors.

The fuel injectors are not capable of such wide flow range as the oxidizer injectors due to the fact that the liquid fuel is incompressible. Therefore, the fuel injectors have been made replaceable. The fuel injectors are changed by removing the fuel manifold and removing the fittings on the burner to which the manifold attaches. These fittings incorporate a piece of small diameter tubing which is the injector. Three sets of fuel injectors have been provided. The smallest set is intended for use with hydrocarbon fuels (Toluene, JP4, etc.) with a nominal flow rate of 0.12 kg/sec. The other two sets are for use with cyanogen with a flow rate of 0.30 or 0.40 kg/sec and may also be used with hydrocarbon fuels at maximum oxidizer flow rates and/or low O/F ratio. The fuel flow may be adjusted by varying the fuel pressure but the following limits must be observed. The fuel tank pressure should not exceed 450 psi for cyanogen and 1000 psi for hydrocarbons. The injection pressure drop should not be less than approximately 10 atm.

Maximum total flow capability is approximately 1.4 kg/sec (3.0 lb/sec). The results presented in Section VIII indicate that, with the magnetic field provided, power levels up to one megawatt can be produced in this facility using hydrocarbon fuels with oxygen or nitrogen tetroxide.

The burner water cooling system has been designed to provide a large margin of safety so that during normal operation the possibility of a burnout

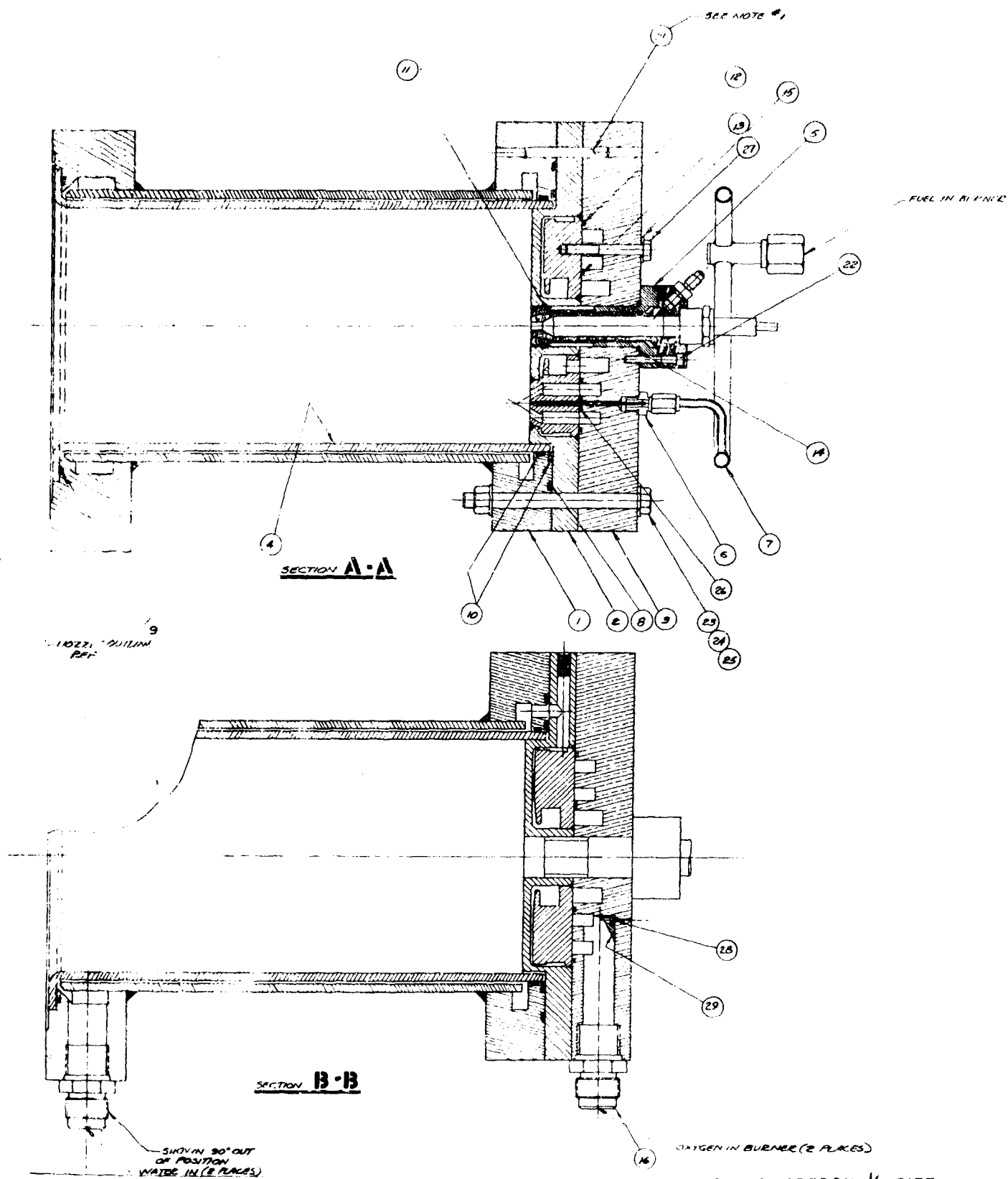


Figure 7 Assembly Drawing of the Combustion Chamber.

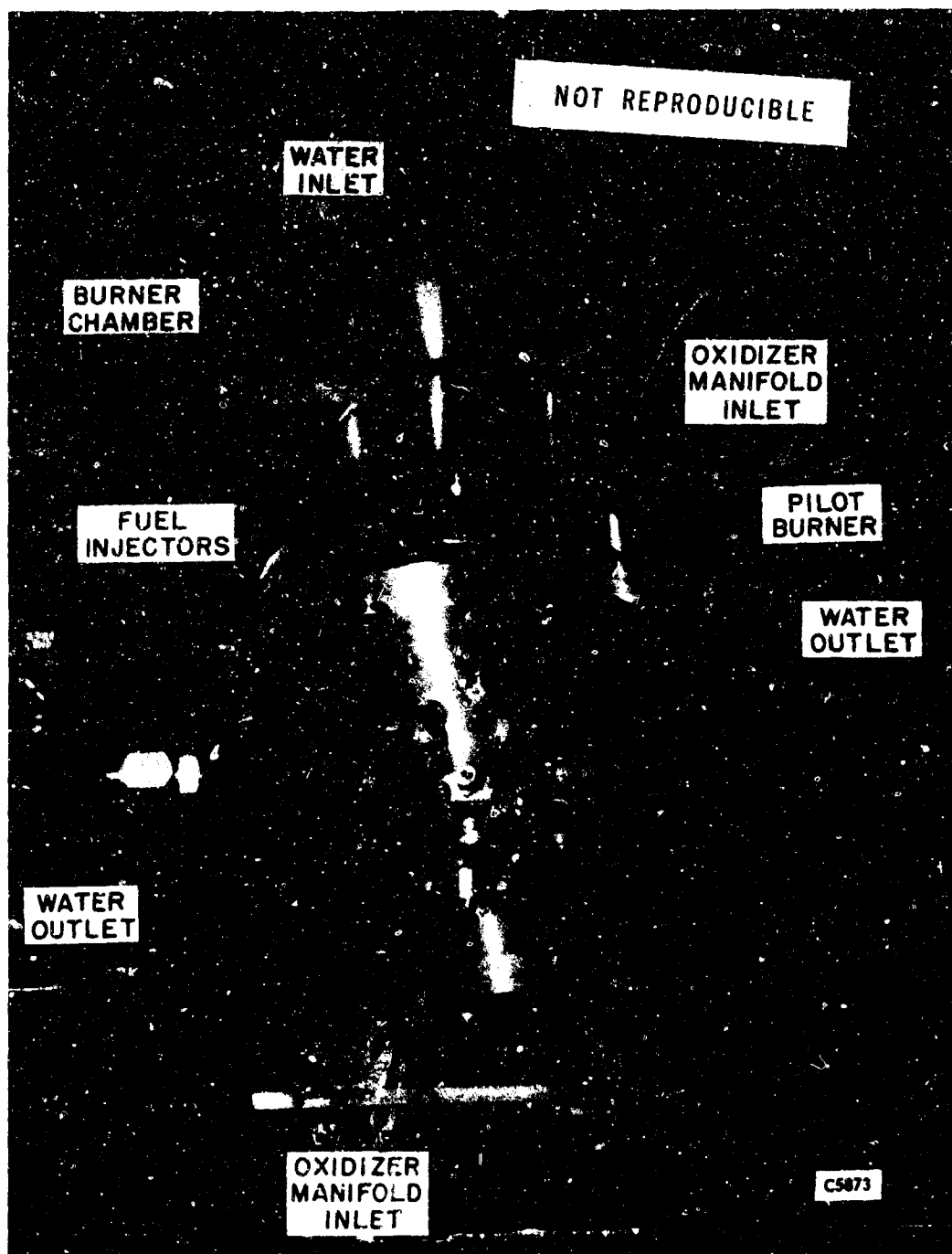


Figure 8 Photograph of the Assembled Combustion Chamber.

is remote. However, operation with high flow rates and high chamber pressure may cause gradual thermal distortion of the burner chamber. High energy propellant combinations result in high heat transfer rates and tend to produce more rapid distortion. Only those parts exposed to hot gas, namely the burner liner, injector plate, and the pilot burner, are liable to distort. The burner should be capable of a large number of firings without hot part replacement provided a water flow of 140/gpm is maintained and provided the water temperature rise is under 100°F.

The pilot is a small spark ignited burner which uses ethane or methane and oxygen as propellants. Normal operating condition for the pilot is approximately 0.01 kg/sec total flow at a chamber pressure of 10 atm but the pilot has been operated to 16 atm. An injection pressure of 22 atm (both propellants) will normally be used. The pilot burner nozzle throat will be sonic at main chamber pressures below 5 atm (60 psig) but will go subsonic at higher main chamber pressures.

#### c. Supersonic Expansion Nozzle

Two nozzles are provided for use with this facility. The first is a circular nozzle designed and constructed under a previous contract (AF 33(615)-3027) and intended for use with the circular Hall channel constructed under the above contract. The design conditions for this nozzle were: chamber pressure 5.5 atm, exit pressure .25 atm, Mach number 2.5. The fuel and oxidizer combination was toluene with nitrogen-oxygen mixture ( $N_2/O_2 = 1$ ). As in the case of the burner, ample water cooling is provided so that the operating limits of flow and pressure are equivalent to those for the burner.

The second nozzle is designed for use with the channel supplied under the present contract. This unit is a water-cooled copper nozzle having a rectangular outlet to match the channel. The design Mach number is 2.15 with a chamber pressure of 10 atm and an exit pressure of 1.1 atm. The cooling of this nozzle is compatible with the capability of the burner. When burning cyanogen and oxygen with a flow rate of 0.68 kg/sec, a water temperature rise of 20°C is expected at a flow rate of 120/gpm. This nozzle can also be used with hydrocarbon fuels. The nozzle is shown in Figures 9 and 10.

#### d. MHD Channel

The channel, a drawing of which is shown in Figure 11, consists of a plastic box-shaped pressure vessel with copper heat sink elements attached to the inside walls. The insulating walls are composed of 0.925 cm hexagonal copper pegs on 1.1 cm centers and attached to the walls with screws. The electrode walls are made of 0.6 cm thick copper slabs placed on 0.80 cm centers. The electrodes are attached to the walls by means of a dowel pin and a shouldered stud which also acts as an electrical connection. The spaces between pegs or electrodes are filled with an



GROOVE FOR PARKER O RING\*2-262

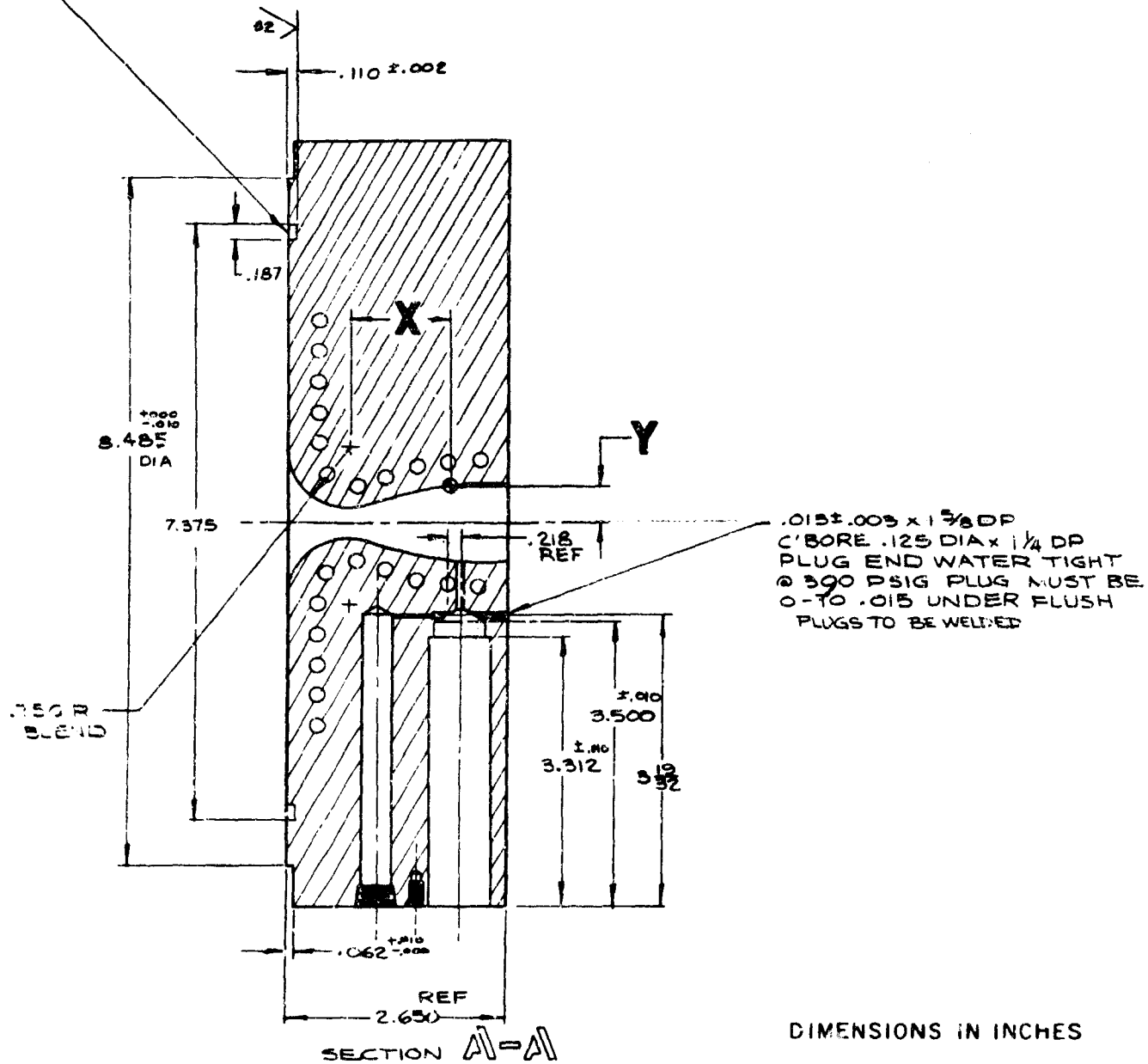
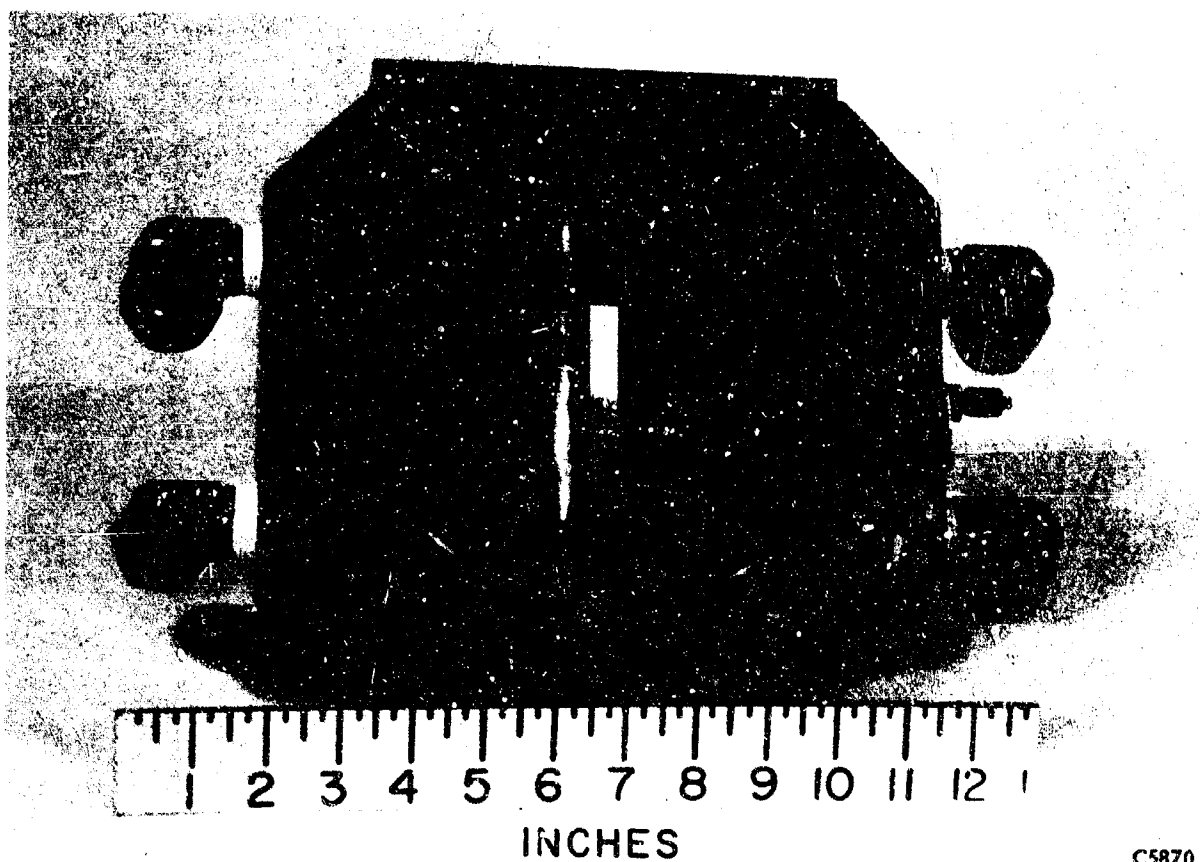


Figure 9 Drawing of the Mach 2.15 Rectangular Expansion Nozzle.



C5870

Figure 10 Photograph of the Rectangular Expansion Nozzle.

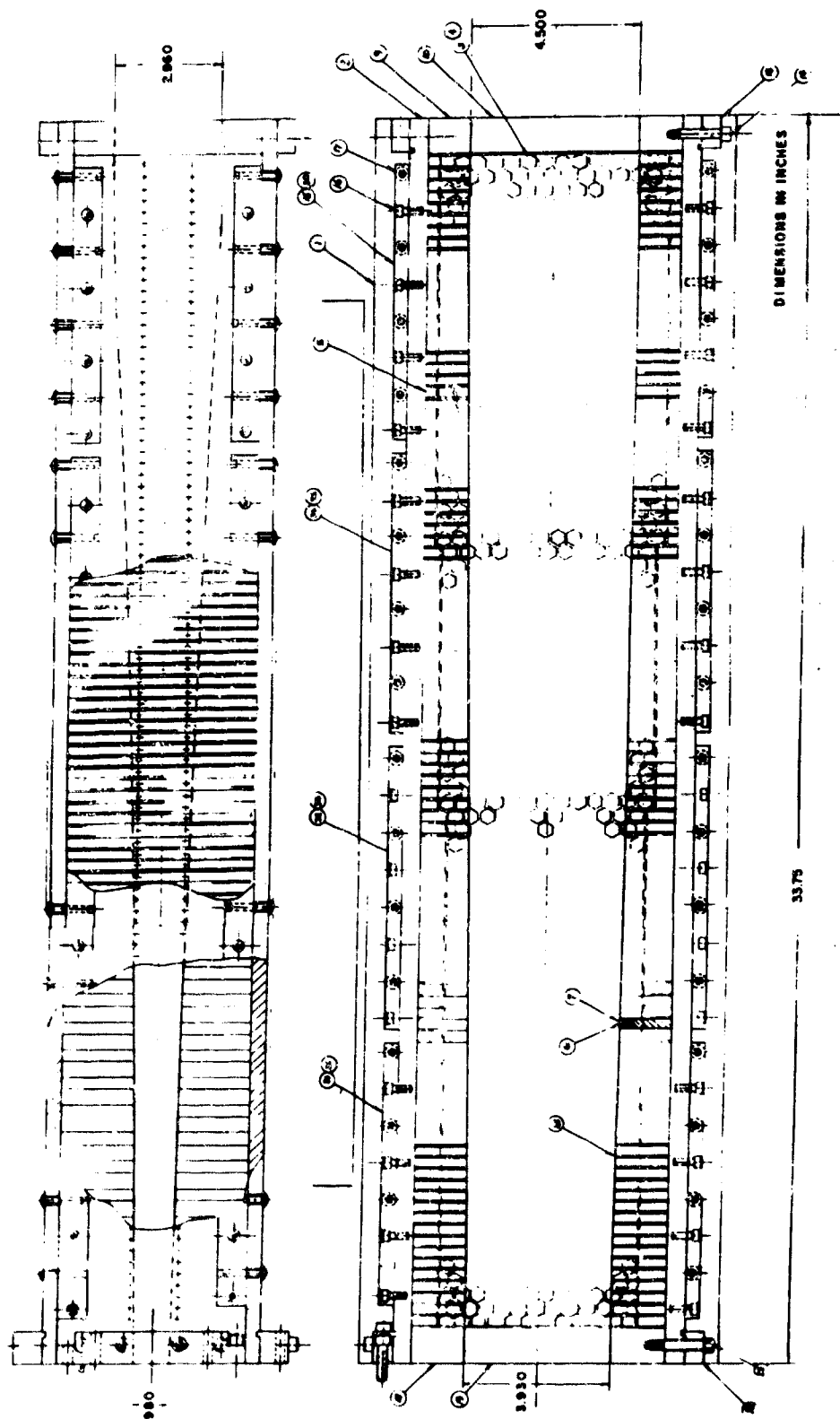


Figure 11 Assembly Drawing of the Heat Sink, Segmented Electrode, Peg Insulator Wall MHD Channel.

insulating refractory. The plastic walls are an epoxy-glass cloth laminate which retains good mechanical properties at a temperature of 205°C. The plastic walls are held together by metal strips which receive the necessary fasteners. The metal strips have been segmented to reduce the possibility of short-circuiting the generator output. Similar fastening strips are provided at the ends to connect the channel to the nozzle and diffuser. The fastening of the electrode walls to the insulating walls has been arranged so that the electrode distance at the channel exit may be increased by 2.5 cm which will increase the channel exit area by approximately 20%. The active surface of the electrodes is provided by a zirconia-based mixture which is troweled into grooves cut in the electrode. The construction closely resembles that used previously for high power heat sink channels,\* but uses finer segmentation for both electrode and insulating walls.

Since the channel is heat sink cooled the run duration is controlled by a limiting temperature which in this case, is the equilibrium temperature that the pegs reach after a run is completed. This equilibrium temperature should not exceed 205°C so as to prevent deterioration of the plastic backing. However, accidental short term exposure of up to 260°C will not cause serious damage. Calculated run duration, observing the 205°C limitation is approximately 8 seconds when using cyanogen and oxygen propellants at 0.70 kg/sec flow and somewhat less with toluene-oxygen at maximum flow rate. Thermocouples are installed on a few pegs in order to monitor their temperature.

Because of the peg type insulating walls and the fine electrode segmentation this channel is capable of operating in all modes possible for a linear channel. Thus it may be connected as a two-terminal single electrode Faraday, segmented electrode multiple output Faraday, two-terminal diagonal Faraday, or a two-terminal Hall generator. The output of each electrode is brought to a terminal board where connections may be made to change the operating mode.

The channel electrical and aerodynamic design program was conducted for two-terminal diagonal Faraday operation using cesium seeded cyanogen-oxygen. The channel Mach number and area distribution were optimized for this condition and are not optimum for other operating modes.

Channel segmentation has been made more than adequate for the electric fields which are expected. Both the electrode and insulating walls are capable of withstanding 5000 V/meter based on 40 V/electrode and 50 V/peg.

Two views of the completed channel are shown in Figures 12 and 13.

---

\*Louis, J. F. et al., "Studies of Fluid Mechanics Using a Large Combustion Driven MHD Generator," Avco Everett Research Laboratory Research Report 145, March 1963.

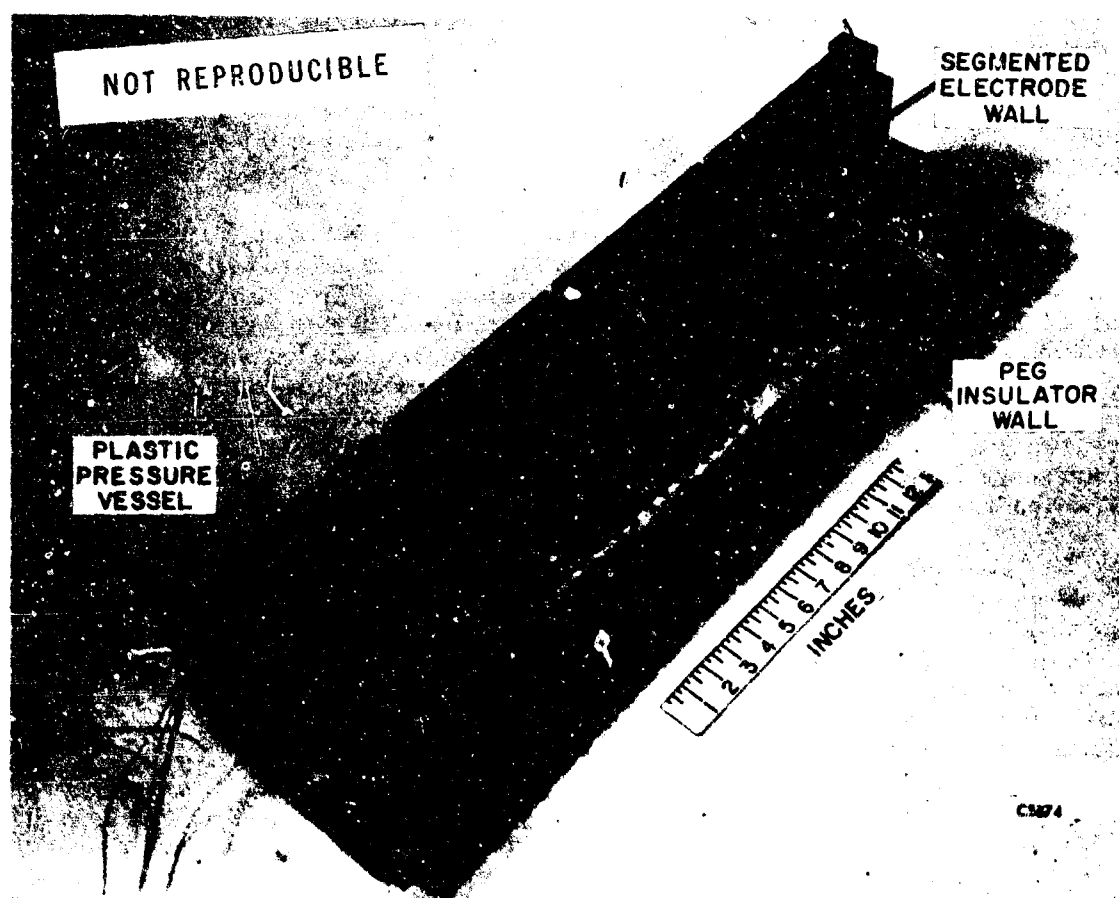


Figure 12 View of Completed Channel with Two Walls Removed.



Figure 13 View of Completed Channel with One Peg Wall Raised.

#### e. Supersonic Diffuser

The diffuser is a heat sink design composed of four copper slabs. The internal passage consists of a straight supersonic section followed by a subsonic section followed by a subsonic diverging section. The heat sink capability is compatible with the channel.

The diffuser walls corresponding to the channel electrode walls are adjustable so as to match the channel outlet.

A drawing of the diffuser is given in Figure 14 and a photograph of the assembled unit in Figure 15.

### 3. DESCRIPTION OF FACILITY

#### a. Introduction

An overall schematic of the Facility was provided in Figure 3. Descriptions of the oxidizer, the fuel, the nitrogen, the pilot burner, the water, and the exhaust systems are presented in this section. The load resistors, the seeder, the magnet, the control system, and the instrumentation are also described. In Figures 16 and 17 photographs of the facility are shown, and labels identifying most of the above items are given. Additional photographs and drawings of various equipments are also presented in this section.

#### b. Oxidizer System (Figures 18 and 19)

Oxidizer for the facility is compressed gas obtained from a standard tube trailer. The oxidizer is normally oxygen and occasionally an oxygen-nitrogen mixture which may simulate  $N_2O_4$  or other  $N_2/O_2$  ratios. Oxidizer from the trailer flows through a control station adjacent to the trailers. In the control station the pressure is reduced to 34 atm or less, depending upon flow requirement. An ON-OFF valve is provided for starting or stopping flow and suitable relief valves are installed to prevent over pressuring the downstream pipeline. With this type of venturi, the flow is always proportional to the upstream pressure and temperature provided the flow remains sonic. A throat pressure tap is provided which will indicate if the flow goes subsonic.

In order to cover the entire possible operating range of burner flow, two venturis have been provided. The smaller venturi produces exactly half of the flow of the larger one at the same pressure and temperature.

The oxidizer flow is routed through the seeder body just upstream of the burner. In the seeder, the oxidizer picks up powder seed, the seed being injected into the burner with the oxidizer.

The oxidizer system is capable of a maximum flow of 1.0 kg/sec. The flow is limited by the pressure rating of the piping downstream of the regulator (500 psi), and may also be limited by the manifolding arrangements in the gas trailer.

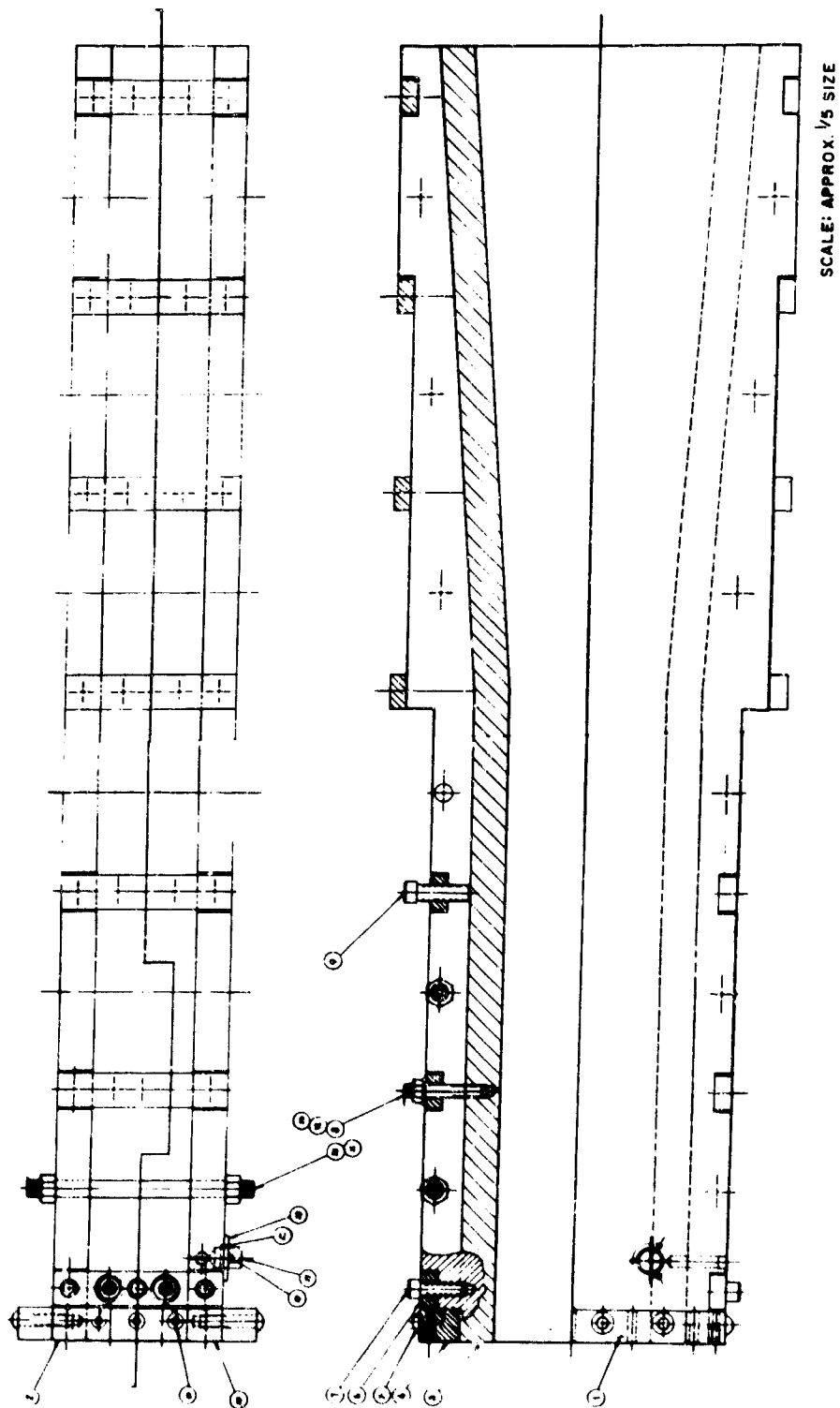


Figure 14 Assembly Drawing of the Supersonic Diffuser.



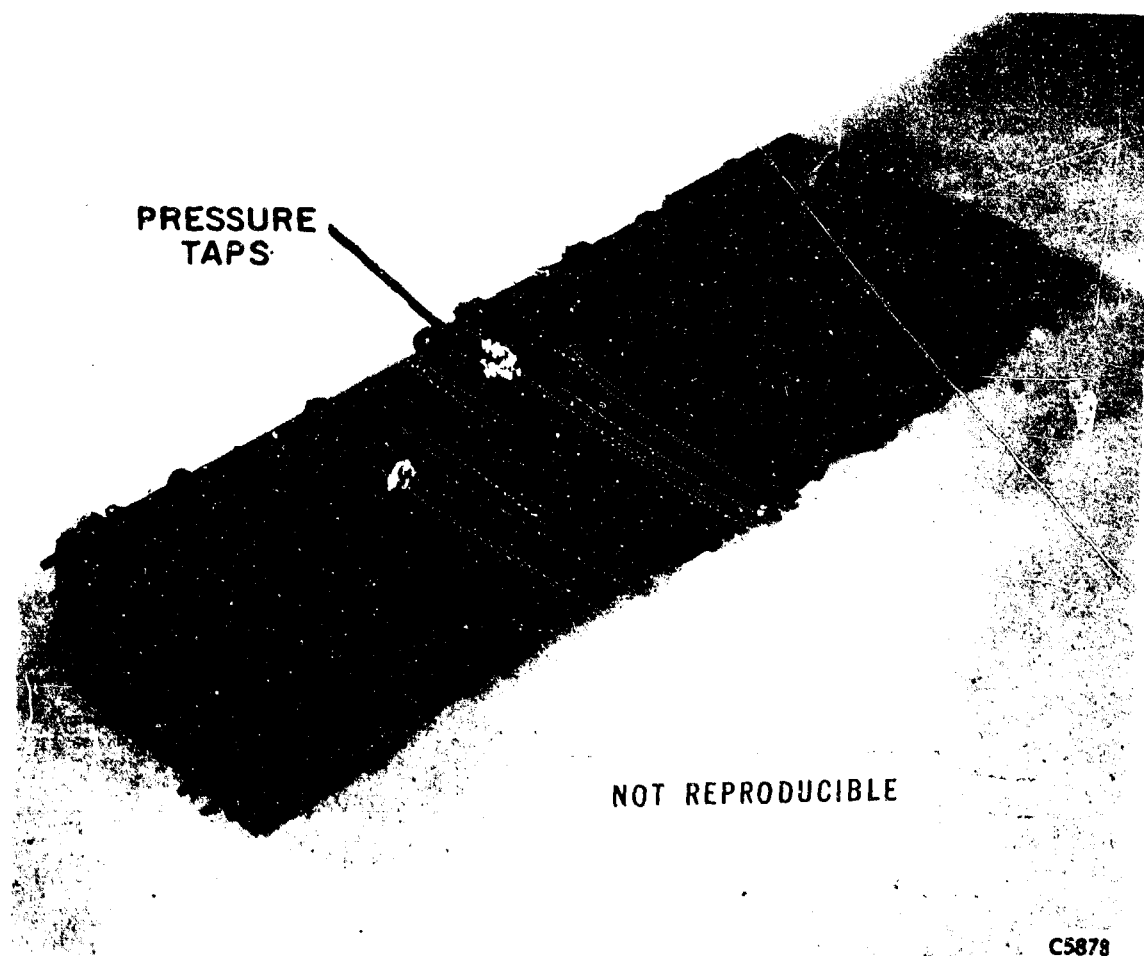


Figure 15 View of the Assembled Diffuser.

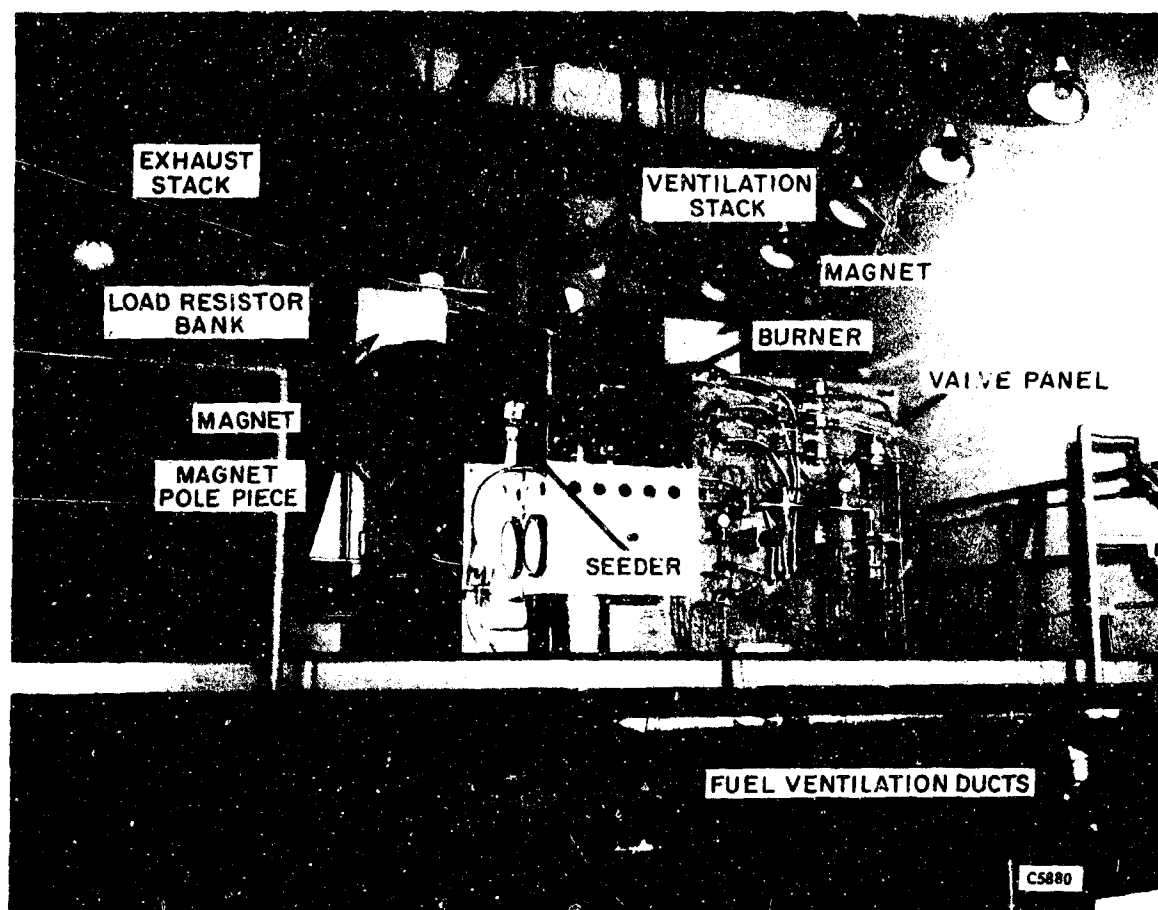


Figure 16 View Inside Laboratory Looking Toward Combustion Chamber and Field Coil.

NOT REPRODUCIBLE

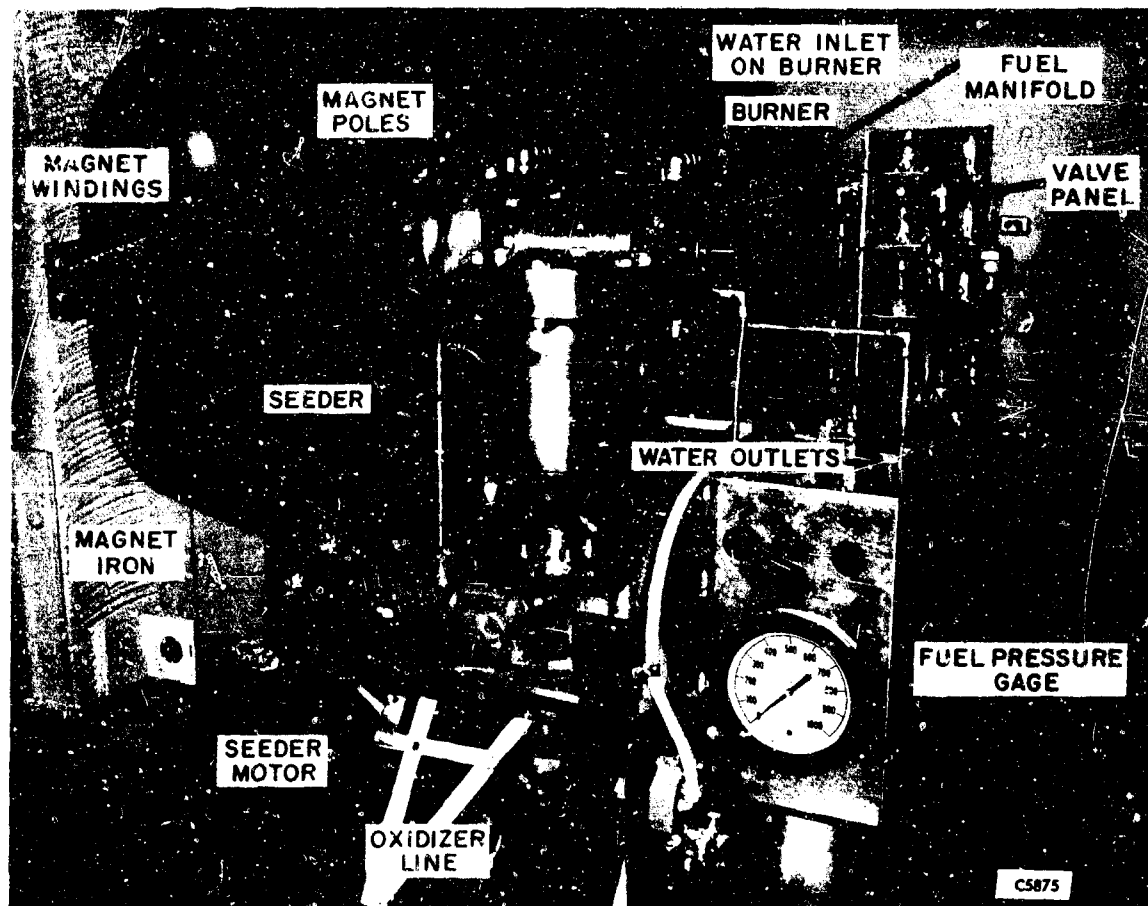


Figure 17 Close Up View of the Combustion Chamber End of the APL MHD Generator Laboratory.

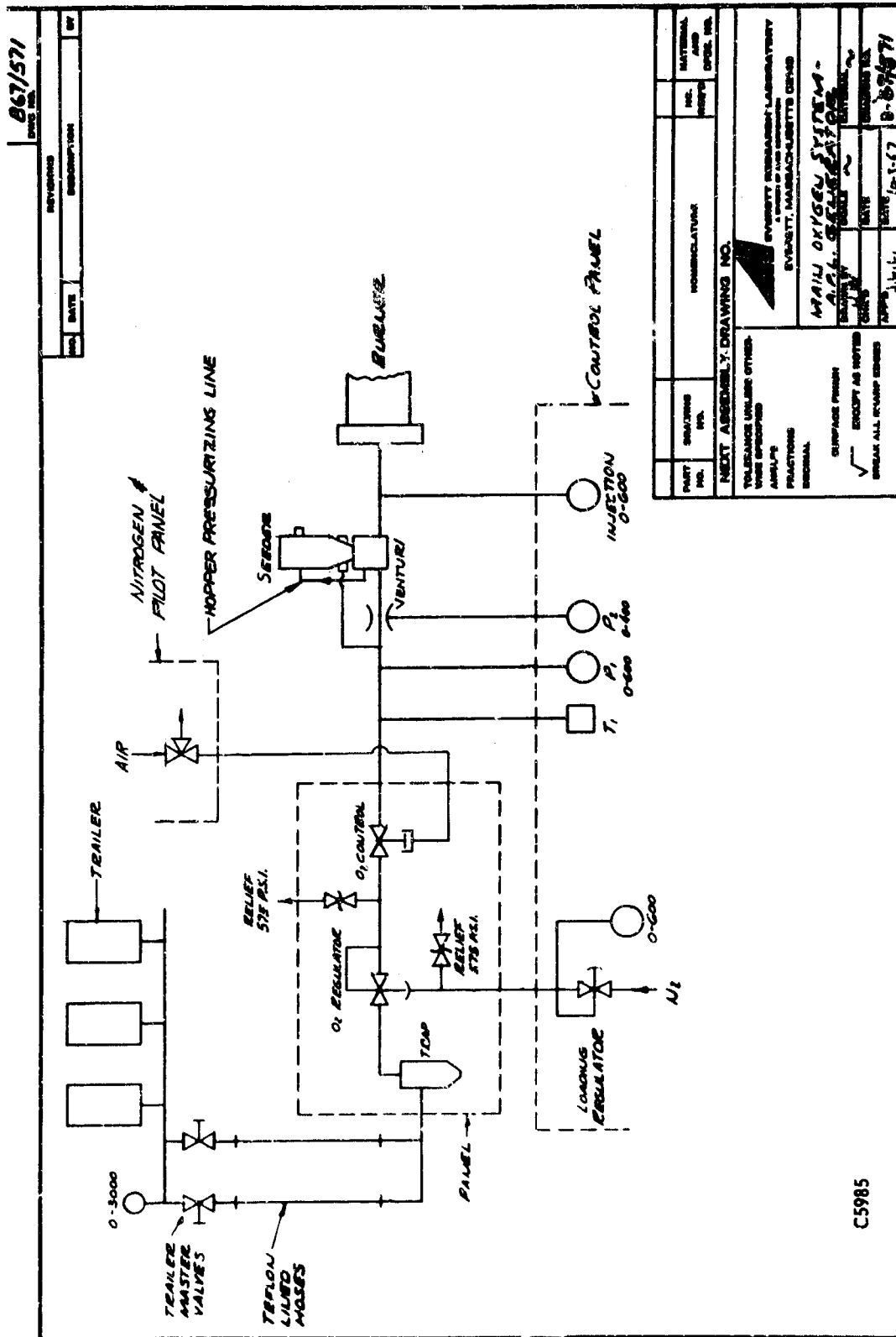


Figure 18 Main Oxygen System - APL MHD Generator Facility

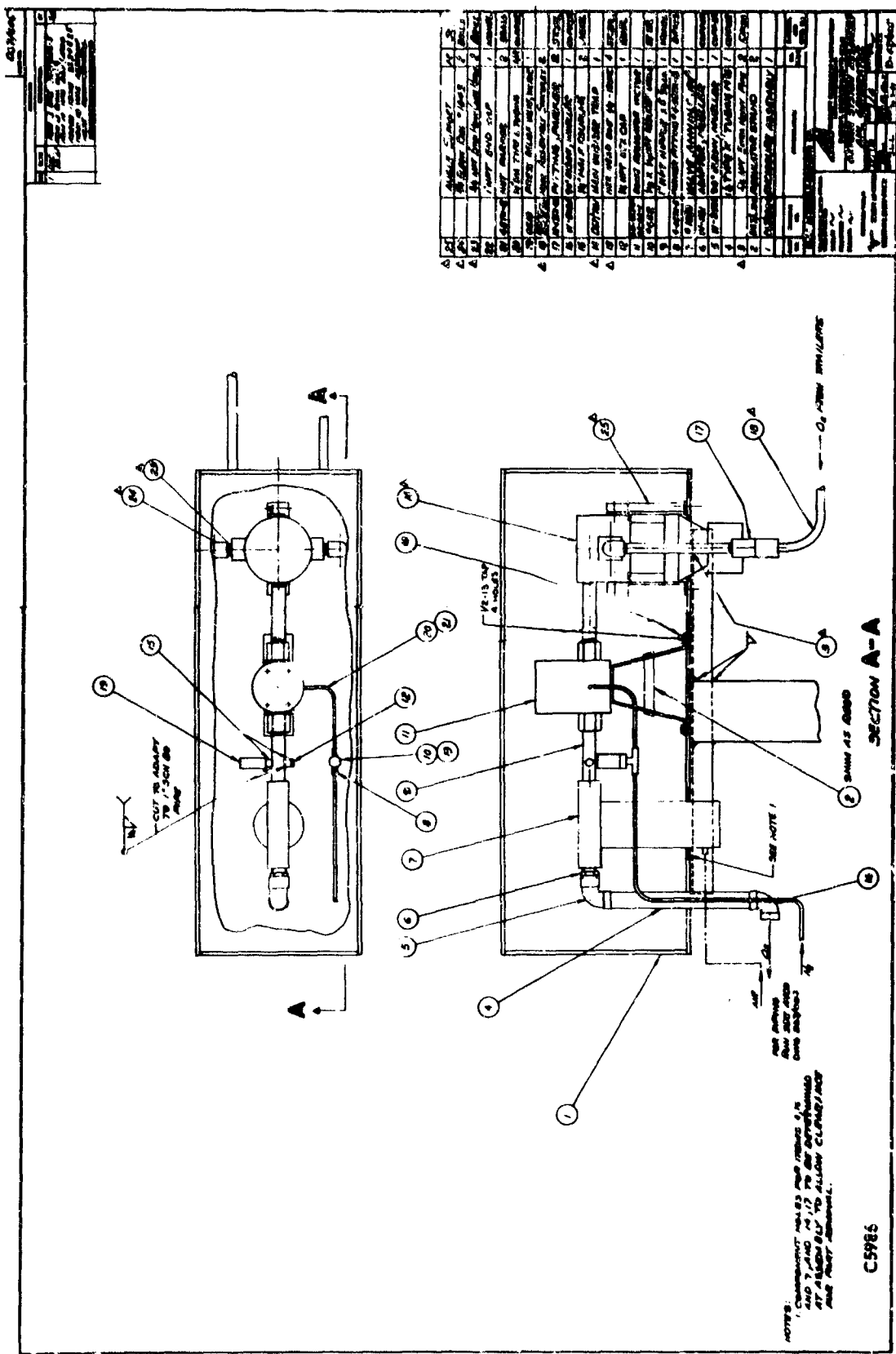


Figure 19 Oxygen System Assembly - APL MHD Generator Facility

### c. Fuel System (Figures 20-23)

The fuel system is designed for the use of cyanogen but is equally suitable for conventional hydrocarbon fuels. Cyanogen is a toxic fuel which has a relatively high vapor pressure of 5 atm at 20°C. Because of the toxicity of cyanogen, the fuel system has been designed to minimize the possibility of leaks and to reduce the hazards associated with leaks.

#### (1) Fuel Piping

As a result of the moderate chamber pressure required in the burner (10 atm max.) it is practical to employ the cyanogen shipping bottle as a fuel tank. Cyanogen is normally shipped in ICC approved containers for which a maximum pressure of 450 psi has been established. A pair of the 100 lb content cylinders manifolded together give adequate flow capacity.

Fuel is forced to the burner by pressurizing the cyanogen cylinders with nitrogen. Nitrogen is supplied from the main nitrogen system through a pressure regulator and check valve to the fuel bottles. On the liquid side, fuel leaves the cylinders through individual air operated ball valves, through a turbine flowmeter, and to an air operated three-way valve at the burner. In a normal burner operating sequence the ball valves open early in this sequence and the actual starting and stopping of the burner is controlled by the three-way valve.

Because of the toxicity of cyanogen the fuel system components have been selected to have pressure ratings much higher than the maximum operating pressure. The majority of the system components have safe working pressures of 2000 psi. The lowest rated component is the three-way valve with a rating of 1440 psi or over three times the maximum working pressure.

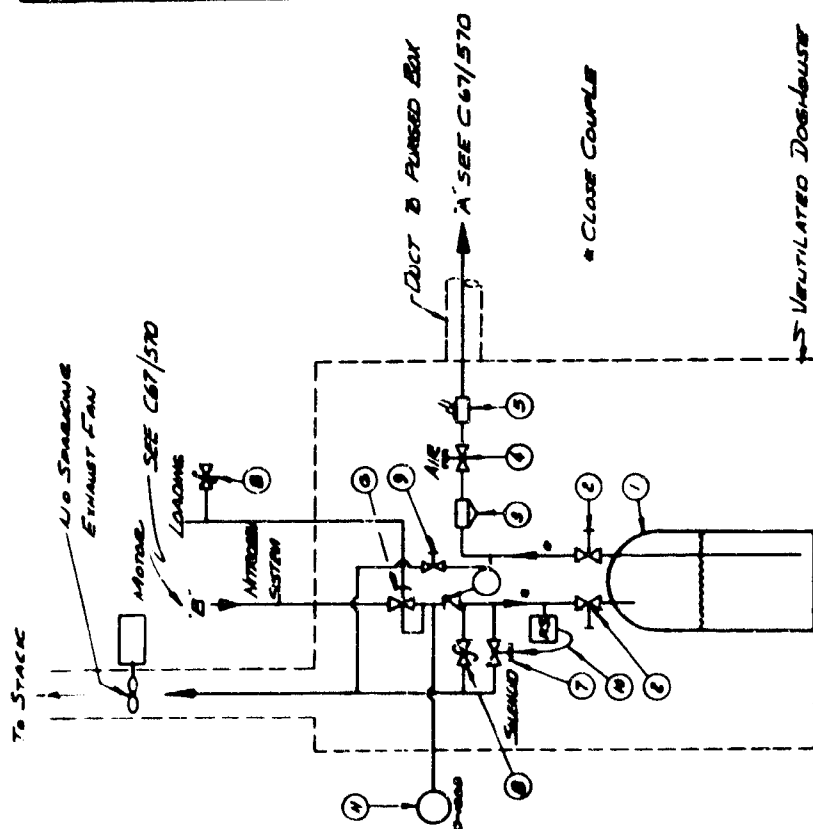
Fuel flow rate is adjusted by varying the nitrogen pressure in the bottles and by changing burner injectors. The maximum flow rate for the fuel system is approximately 0.2 kg/sec.

When the fuel system is to be used for conventional hydrocarbon fuels the cyanogen cylinders are removed, one set of cylinder connections are capped, and a single fuel cylinder is used. This cylinder does not have an integral shut off valve system and therefore, has a flow capability equal to the rest of the fuel system. This cylinder has a capacity of approximately 25 kg of JP4.

#### (2) Line Purging

The fuel system has provision for purging the fuel lines with nitrogen prior to changing bottles or opening the system for maintenance. The purging operation is described fully in Section II-4. Briefly, the majority of liquid fuel may be returned to the bottles, the manual valves on the bottles closed, and the purging continued, venting to atmosphere until the line is clear of cyanogen.

AD	10/1/1980	10/1/1980
COLUMBIA		



NO.	FUNCTION
1	IMMEDIATE INFLATING BOTTLE (ICE CARGO FOR 400 P.S.I.)
2	MANUAL SHUT OFF, INTEREST WITH BOTTLE
3	FUEL FILTER
4	FUEL VALVE, REMOTE CONTROL BALL VALVE
5	FLOWMETER (TURBINE TYPE)
6	FUEL BOTTLE PRESSURIZATION P.S.I. (REMOTE CONT.)
7	FUEL BOTTLE PRESSURES BLIND VALVE (REMOTE CONT.)
8	RELIEF VALVE (SET AT 450 P.S.I.)
9	FUEL LINE VENT VALVE
10	PRESSURE SWITCH
11	PRESSURE GAUGE
12	CHECK VALVE

PLAST REL.	CELLULOSE REL.	NONPOLYMER	WIL. PROB.	INTERNAL AND SPEC. TEL.
NEXT ASSEMBLY-DRAWING NO.				
<p>TELEPHONE (INCLUDE OTHER-          TOWN COUNCIL          ANGLES          FRANCHISES)          REGIONAL</p>				
<p>RECEIPT RESEARCH LABORATORY          1. Receipt for each instrument          EVERTT, MARCH-JULY 1968</p>				
<p>A.P.L. GENERATOR          CHALLOUSE FUEL STATION</p>				
<p>RECEIPT NO. _____          DATE _____          BY _____          FOR _____          TO _____          FROM _____          BY _____          DATE _____          FOR _____          TO _____          FROM _____</p>				
<p>✓ RECEIPT AS NOTED          BREAK A-1, SHARP BEND</p>				
<p>0-67/509</p>				

Figure 20 Cyanogen Rated Fuel System Layout



Figure 21 Cyanogen Fuel System Piping Layout.



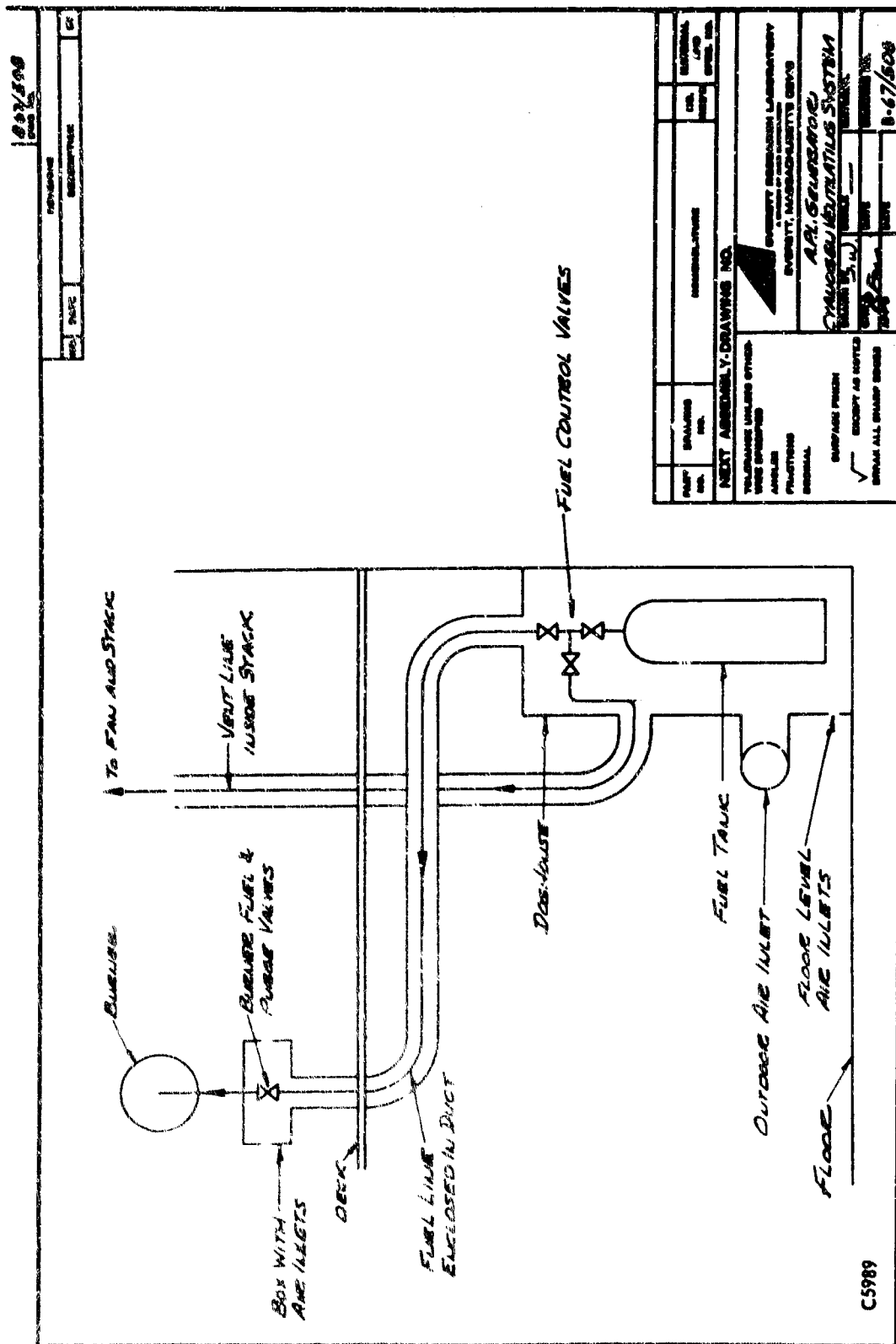
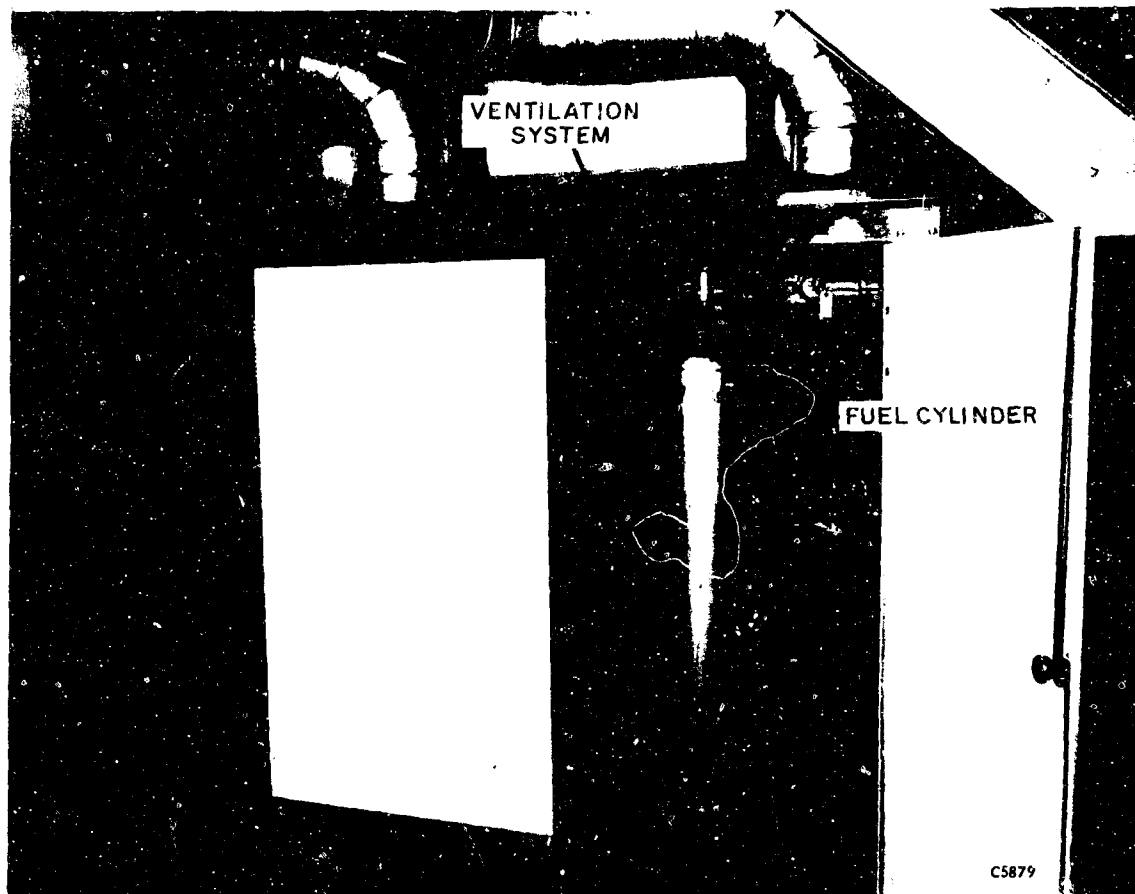


Figure 22 Cyanogen Ventilating System Layout.



NOT REPRODUCIBLE

Figure 23      Photograph of the Cyanogen Fuel Storage and Ventilating System.

### (3) Ventilating System

To reduce the hazard associated with a leak in the fuel line and to provide a method of disposing of cyanogen vapor released during venting and purging operations, the entire fuel system up to the burner has been enclosed in a sheet metal structure. This structure is continuously exhausted by a fan which discharges into an 25 meter stack. Suitable openings in the sheet metal structure allow an air flow of approximately 20,000 lpm. The ventilation apparatus is illustrated in Figures 22 and 23.

#### d. Nitrogen System (Figures 24 and 25)

Nitrogen is used for pressurizing the fuel tank, purging the pilot and main burners and for controlling the gas loaded regulators used in various subsystems. The nitrogen is brought from the supply trailer to the valve panel in the test cell through a 3/4 in. sch. 80 steel pipe. At the valve panel there is a shut off valve and a filter, downstream of which the flow is divided for the various purposes described above. Nitrogen which is used for controlling gas loaded regulators is reduced in pressure at the valve panel before being led into the control room.

The majority of the nitrogen system and the pilot system to be described in the next section are mounted on a valve panel which is placed adjacent to the burner. This was illustrated in Figures 16 and 17.

#### e. Pilot Combustion System (Figures 24 and 25)

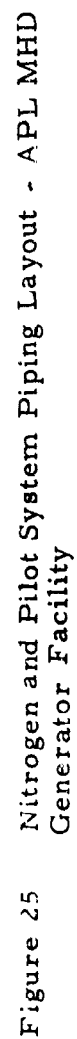
The pilot is supplied with fuel (ethane or methane), oxygen and nitrogen purge by a system of pressure regulators and solenoid valves mounted on the valve panel. Flow rate is controlled by the injection pressure selected and by the size of the injectors in the pilot burner. All three pressure regulators are controlled by a single loading regulator so that the flows of fuel, oxygen, and nitrogen purge will always be in proper proportion. A separate oxygen supply is used for the pilot so that operation will not be affected by changes in the composition of the main oxidizer.

A transistorized ignition system is supplied for the spark ignited pilot. A meter on the control panel indicates the intensity of the spark.

#### f. Water System (Figures 26-28)

A water system supplies cooling water to the burner, nozzle, magnet, load resistor, and exhaust stack. Treated (soft) water is used at a supply pressure of 5 atm for cooling of the load resistor. In addition connections are provided for cooling of a water cooled channel. Treated water pumped to a pressure of 20 atm is supplied for cooling the burner, nozzle, and magnet. Raw water is supplied to spray nozzles in the exhaust stack for cooling the generator exhaust gas.







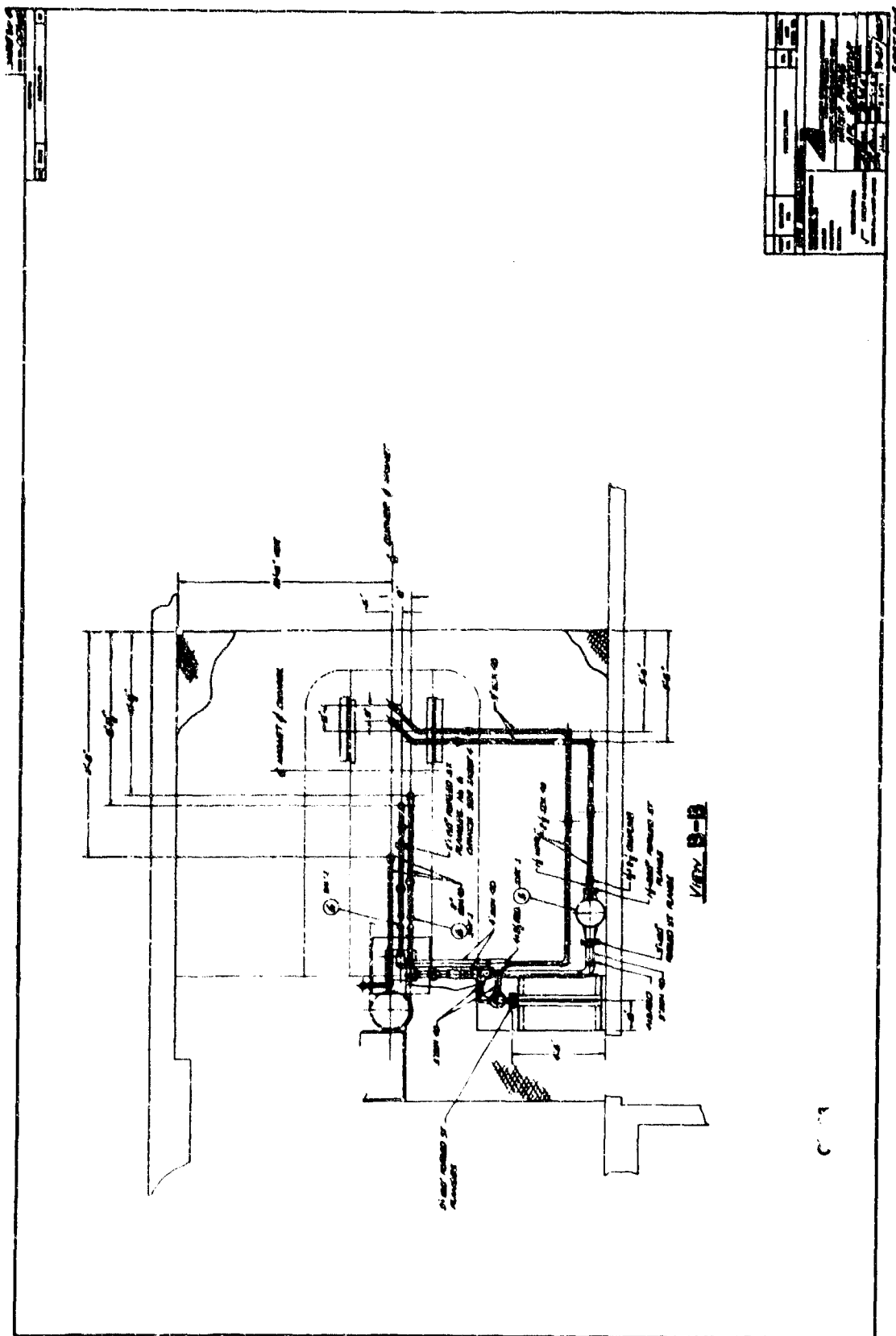


Figure 27 Cooling Water Piping Layout, I.





Each cooling circuit incorporates a flow control orifice which accomplishes one or more of the following objectives:

- a) Flow is measured and controlled to the design values.
- b) A back pressure is produced which is an indication of flowrate and which is sensed by a pressure switch for purposes of safety interlocking.
- c) In the burner and nozzle, a pressure level is maintained in the cooling passages which is higher than the chamber pressure. This is an important safety factor since a small leak will admit water into the combustion chamber, whereas if the water pressure were lower than the chamber pressure a small leak would admit gas into the cooling passage and would result in a disastrous burn out.

Water system calibration data are presented later.

#### g. Exhaust System

The generator exhaust discharges into a 0.6 meter diameter pipe which is provided with a system of spray nozzles to cool the gas and to prevent burn out of the pipe through hot gas impingement. A fan is provided in the stack to provide positive air flow at all times. The fan will induce additional air for the afterburning of fuel-rich mixtures to prevent exhausting of any unburned fuel.

#### h. Load Resistor

A water cooled load resistor is provided for dissipating generator output. The load resistor is made up of thin wall stainless steel tubes which have been grouped to form loads of 0-4, 4, 8, and 16 ohms with a maximum dissipation of 600 kw. The loads are controlled by knife switches which must be opened to secure the desired resistance. Any combination of loads may be selected to get a total resistance between 0 and 32 ohms. The 0-4 ohm load is adjustable by means of sliding clamps to any resistance within its range. For purposes of equalizing current it is desirable to keep all the clamps at approximately the same position. The load resistor bank is shown in Figure 29.

Cooling is accomplished by connecting the ends of the tubes to inlet and outlet water headers. The hoses used for these connections must be nonconducting.

#### i. Seeder

A powder seed feeder (Fig. 30) is utilized which consists of a toothed rotor turning in a housing, which picks up powder from a hopper, and transfers it to the main oxidizer line which runs through the bottom of the housing. The rotor is driven by a variable speed gearmotor at speeds between 20 and 180 rpm. To avoid having a large pressure difference

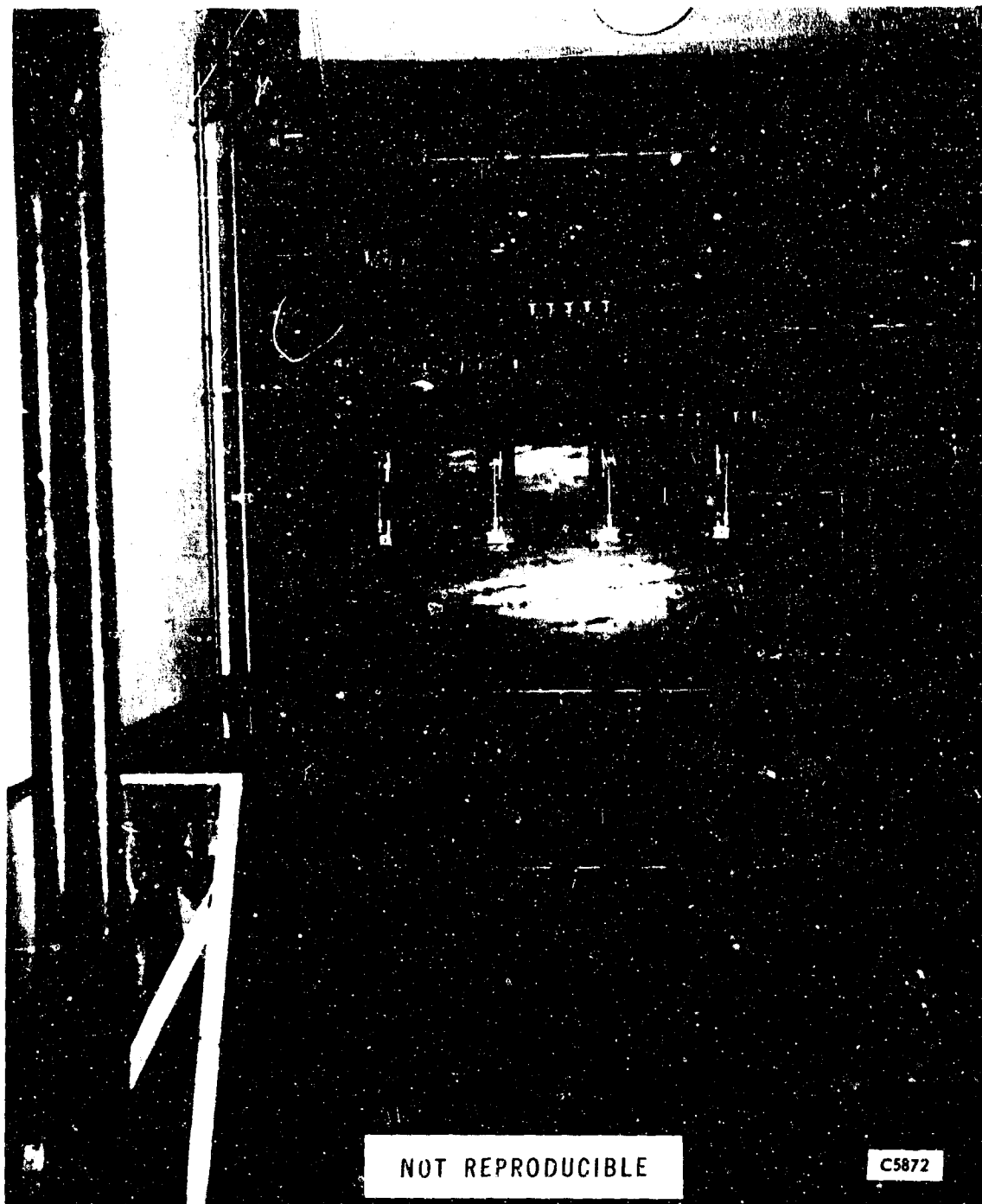


Figure 29 The Load Resistor Tank - APL MHD Generator Facility

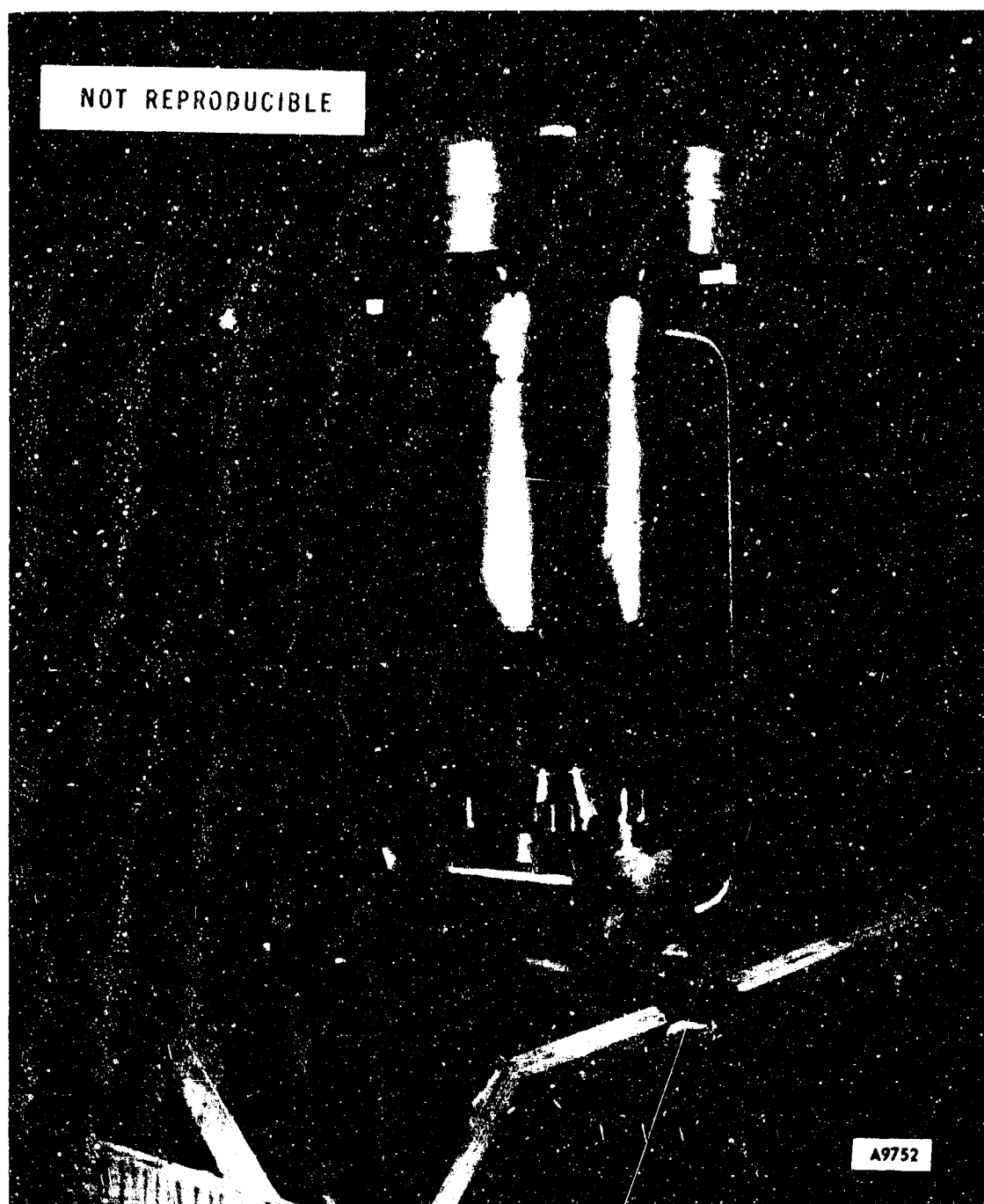


Figure 30 Photograph of the Powder Seed Feeder.

across the rotor the hopper is sealed and is connected by an equalizing line to the oxidizer pipe. The hopper has a capacity of 7 to 10 kg of powder.

A calibration curve of seed flow rate vs speed setting is included later, see Figure 51.

j. Instrumentation

(1) Facility Instrumentation

This group covers flowmeters and temperature and pressure indicators essential to proper operation of the facility. Oxygen flow to the main burner is measured by means of a sonic venturi with the necessary temperature and pressure displayed on the operator's panel. Calibration curves for the oxygen venturis are included later. Fuel flow to the main burner is measured by a turbine meter with analog output displayed on the operator's panel. Additional pressure gages are supplied to show the oxygen injection pressure, the oxygen venturi throat pressure, the fuel tank pressure, and the fuel injection pressure. Pilot system operation is indicated by gages showing the fuel, oxygen, and nitrogen purge pressures. Water system operation is monitored by pressure gages and thermocouple meters for each water circuit. Pilot and main burner chamber pressures are shown by gages on the operator's panel.

A built-in pressure gage calibration feature is provided. Each gage has a small valve and tube connection. Also a test gage and pressure regulator are provided. By connecting a hose between the pressure regulator and the tube connection on the gage to be tested and shutting the small valve, nitrogen may be supplied to both the test gage and the gage under test and their readings compared.

(2) Generator Output Instrumentation

A group of meters and gages are provided for measurement of generator channel performance. Meters are supplied as follows: voltmeter and ammeters for total output, 23 voltmeters and 5 ammeters for voltage and current distributions in the channel, and 32 voltmeters and 30 ammeters for surveying current and voltage distributions at the channel ends. Six compound pressure gages and 9 vacuum gages are provided for measuring static pressure in the channel and diffuser. In addition to the above, essential burner operating information is also displayed on the generator output panel. This information consists of fuel flow, oxygen flow, and chamber pressure. A run clock permits event correlation. The meters and gages have been compactly laid out on panels so that data may be taken photographically.

k. Control System (Figures 31-35)

The control system directs startup, operation and shutdown of the generator, and incorporates interlocks and other safety features to

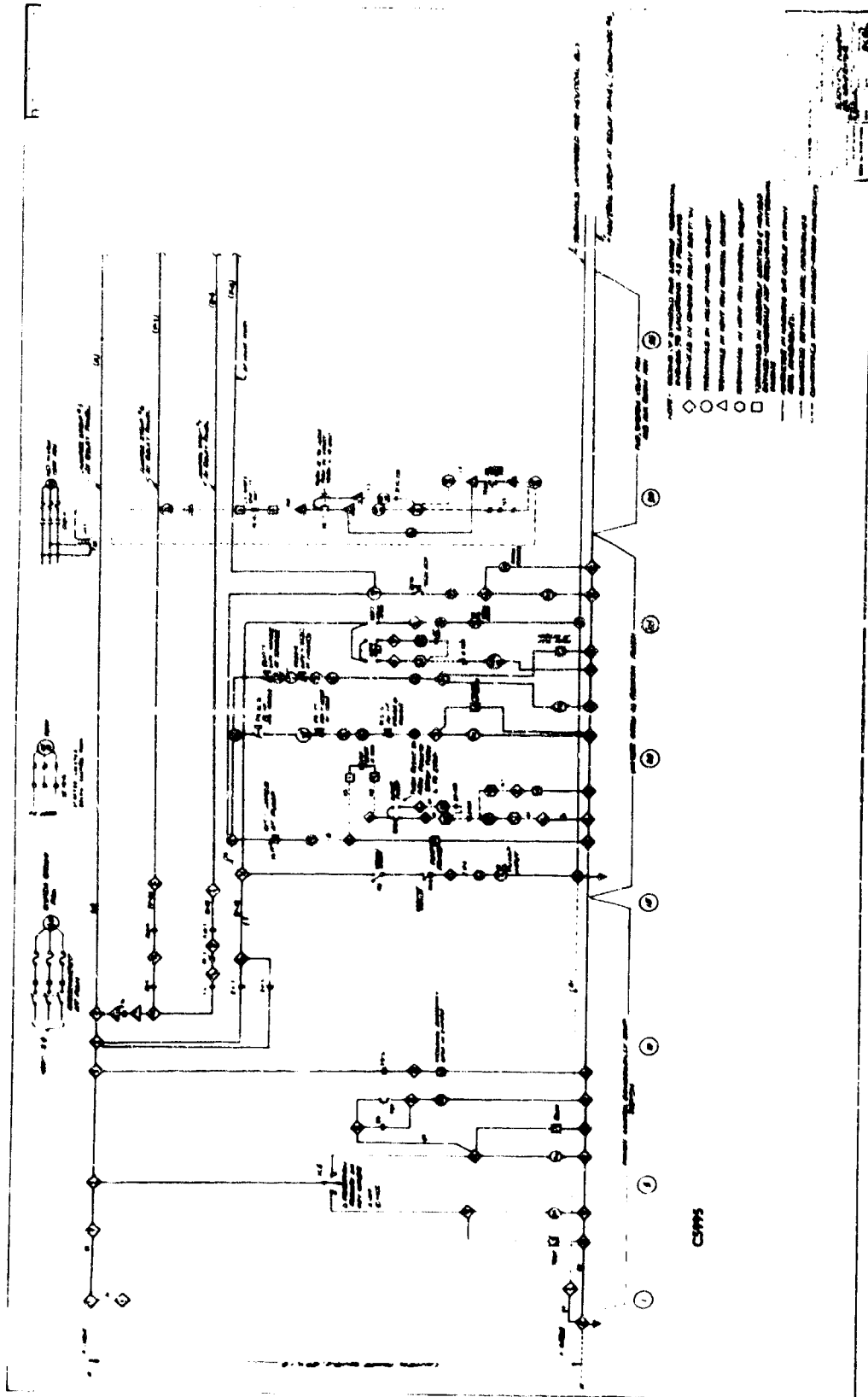


Figure 31 Control System 1: AC Line, Water Cooling, Fuel Vent, and Auxiliary Power - APL MHD Generator Facility



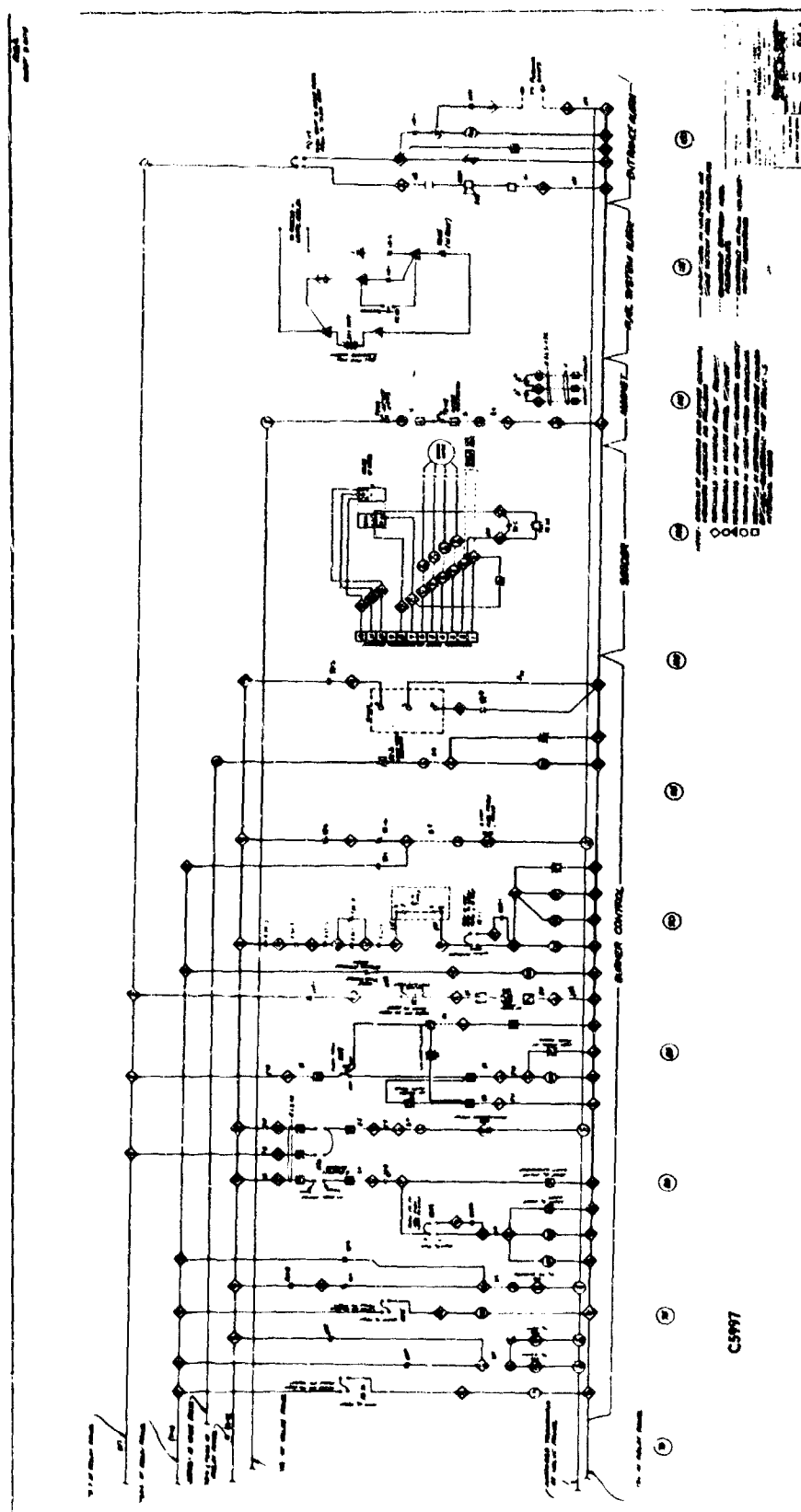


Figure 33 Control System 3: Burner, Seeder, Magnet, Fuel Alarm, Entrance Alarm.

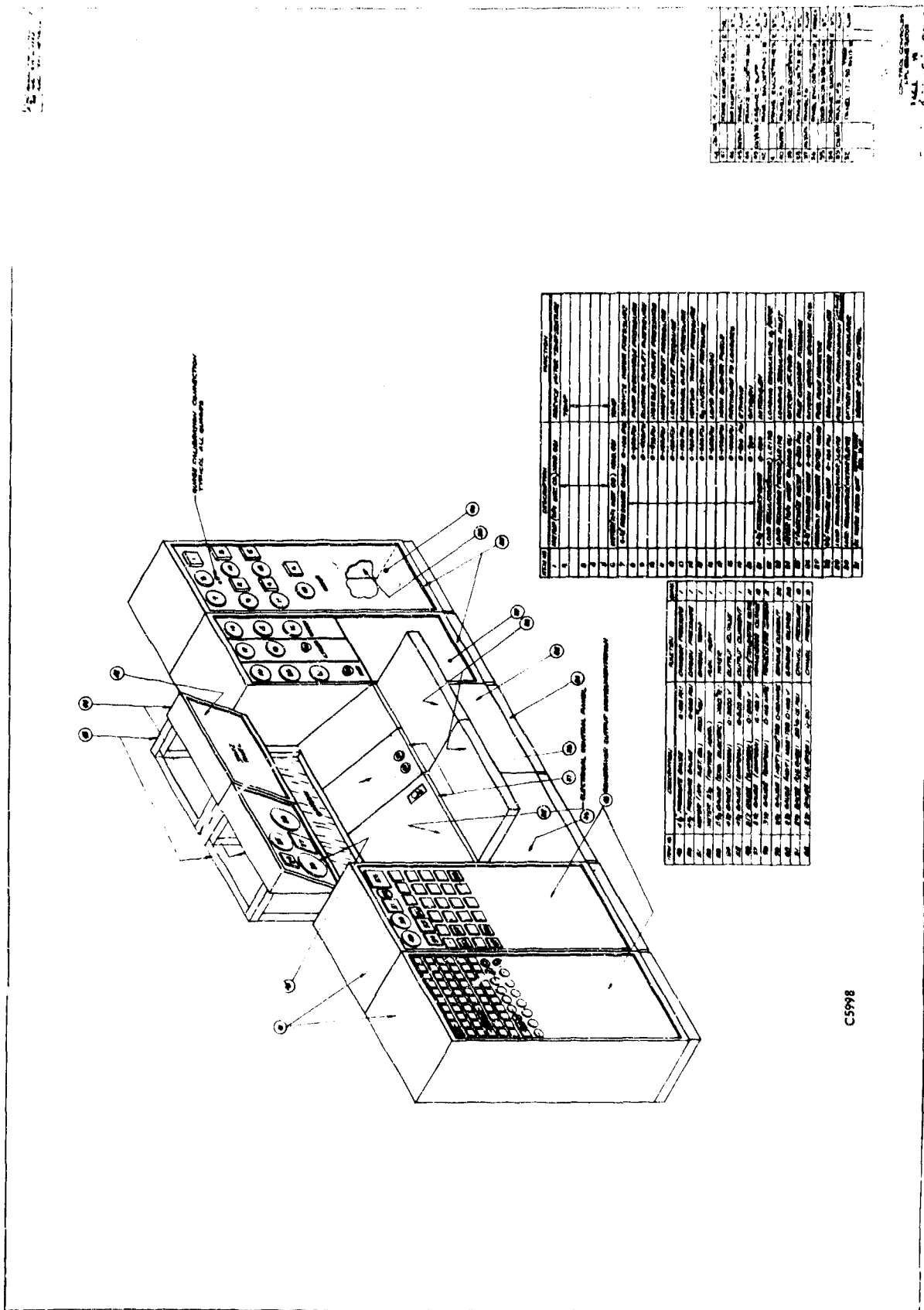


Figure 34 Drawing of the Control and Instrumentation Assembly -  
APL MHD Generator Facility.



NOT REPRODUCIBLE

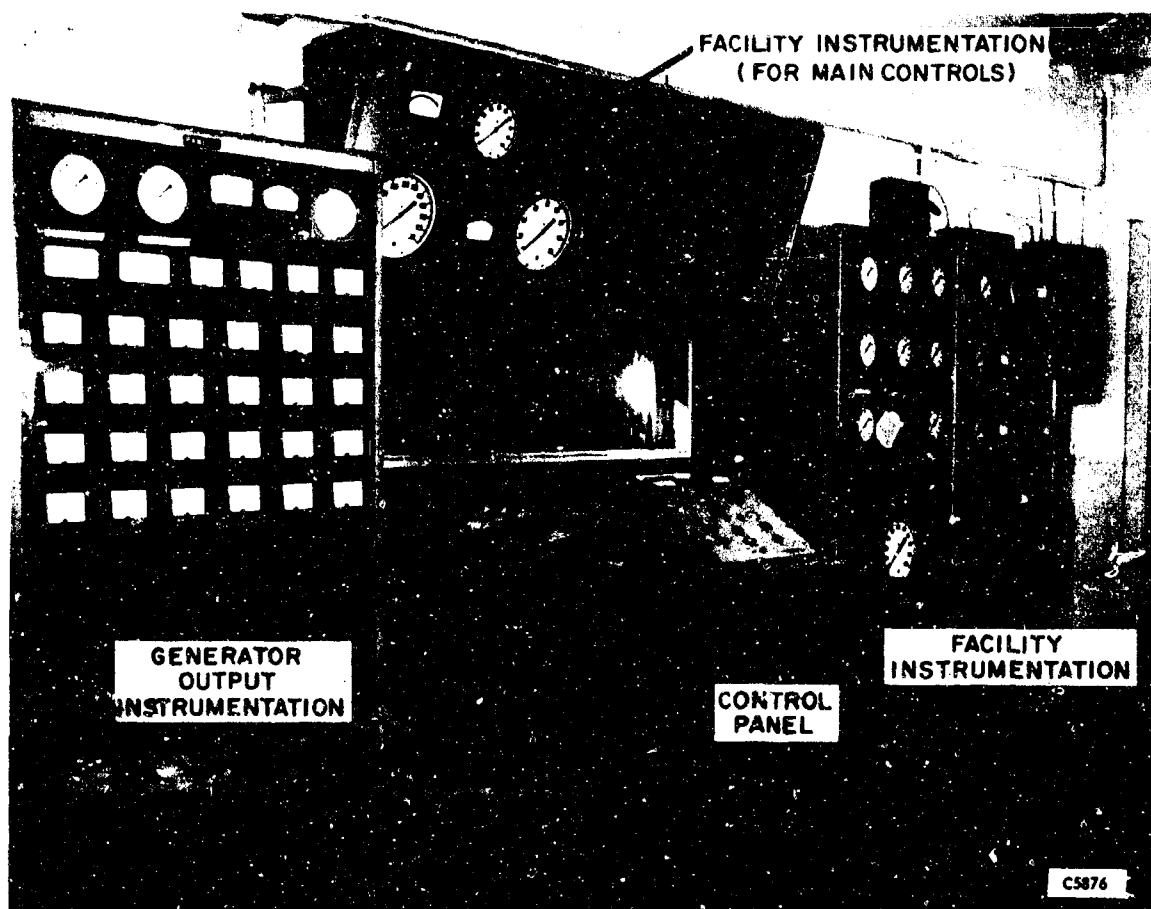


Figure 35 View of Control and Instrumentation Assembly and Observation Window.

prevent operational errors which could lead to difficulty. The operator's controls are contained in a console in the control room. Provision is made for adjusting the pressure and flow in the pilot system and the main burner nitrogen purge, oxygen and fuel systems. Push button stations are provided for operating the water system, nitrogen purge, main burner oxygen pilot start, main burner start, and seeder.

The interlocking system which has been incorporated in the control system is essentially sequential. That is, a proper operating sequence has been established and the control system has been designed to ensure that this sequence is followed. In addition, the interlocking is functional insofar as possible. For instance, cooling water flow is sensed by the orifice-pressure switch system described previously and the pressure switch signal is connected to the control system such that it is impossible to start the burner or the magnet without proper water flow. Operating sequence and interlocking will be further described.

The control system incorporates a test circuit which permits checking system operation independent of interlocks. The test circuit is very useful for troubleshooting.

The control system has been designed to "fail-safe." Thus upon the loss of electrical power or air pressure the system will shut down in an orderly fashion and without damage.

#### (1) Magnet

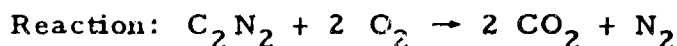
The magnet is a water cooled iron core design producing a field of 2.3 Tesla in a 0.06 x 0.25 x 0.60 meter gas with a power input of 350 kW supplied by a rectifier type power supply. Cooling water to the magnet is supplied from the pumped water circuit. An orifice and pressure switch provide indication of total flow and in addition each cooling circuit in the magnet is provided with a thermal switch. These devices are connected to the magnet power supply to cut off power in the event of improper magnet cooling. The magnet is visible in Figures 16 and 17. Calibration curves for the magnet are given later. The design of this magnet was made under Contract AF33(615)-3027.

### 4. OPERATION OF FACILITY

#### a. Pre-run Procedure

##### (1) Establish Operating Point (example)

The remarks here apply specifically to exchanger operation, but are typical. Generator test conditions for any given run would normally be established by a test plan with appropriate modifications suggested by previous operating experience. Fuel and oxidizer flows in this example are calculated to produce stoichiometric combustion as shown in the following example:



Molecular weights:  $52 + 64 \rightarrow 88 + 28 = 116$

$$\begin{aligned} \text{Fuel flow} &= \frac{52}{116} \times 100 = 44.8\% \text{ of total} \\ \text{Oxygen flow} &= \frac{64}{116} \times 100 = 55.5\% \text{ of total} \end{aligned} \quad \left. \vphantom{\begin{aligned} \text{Fuel flow} \\ \text{Oxygen flow} \end{aligned}} \right\} \text{stoichiometric}$$

For a total mass flow of .670 kg/sec (design point) the fuel flow is 0.32 kg/sec and the oxygen flow is 0.35 kg/sec. The oxidizer venturi flow charts should be consulted to find the venturi pressure required for this flow. For short duration runs the venturi temperature may be estimated from known initial conditions in the storage by using the oxygen Mollier chart. Note that flow =  $f(P)$  and therefore, extremely accurate measurement of temperature is essential.

Fuel flow is controlled by fuel pressure setting. The required pressure may be estimated from the injector flow charts. These charts give an injection pressure drop, to which must be added the expected chamber pressure and any pressure loss in the fuel system. For the example cited above the expected chamber pressure is 10 atm, 15 Ga injectors would be used with a  $\Delta p$  of 12 atm, and the fuel system pressure loss is estimated to be 7 atm producing a total tank pressure of 28 atm.

Seed flow is set by means of calibration curves. These curves have been made for the bulk density stated on them. Whenever a new lot of seed material is received its bulk density must be measured and a suitable correction applied to the calibration curves.

The pilot burner is normally run at a single flow setting which produces approximately 0.01 kg/sec flow. The injection pressure is normally set at approximately 300 psi. A second pilot burner is available which has larger injectors designed for operation at an injection pressure of 225 psi. This pilot is suitable for use when the main burner chamber pressure does not exceed 6 atm. It is important that the pilot injectors remain sonic so that the flow is not influenced by the chamber pressure.

Another part of a normal pre-run procedure is to provide generator electrical hookup and instrumentation connections appropriate to the test to be made.

## (2) Startup of Facility

The following is a check list for starting up the facility and preparing to run the generator:

- a) Turn on the main oxygen and nitrogen supplies by opening the hand valves on the storage trailers.

- b) Turn on pilot oxygen and fuel supplies by opening hand valves on the cylinders in the test cell.
- c) Open nitrogen shut off valve on valve panel.
- d) Check that fuel system ventilating fan is running.
- e) Check that cyanogen detector is operating properly.
- f) Check compressed air and water systems to ensure that air and water are available.
- g) Fill seeder hopper, if necessary.
- h) Set nitrogen pressure to loading regulators at 40 to 50 atm by adjusting the hand regulator on the valve panel.
- i) Turn on cooling water to magnet power supply.
- j) Control system and seeder circuits.
- k) Check flow and check calibration.
- l) Set run timer. Reset run clock on instrumentation panel.
- m) Adjust seeder speed control for desired seed rate.
- n) Open valves on both cyanogen bottles.
- o) All personnel should leave the test cell at this time and the access doors should be shut.
- p) Adjust oxygen loading pressure to approximately 3 atm higher than desired venturi pressure.
- q) Pressurize fuel tanks.
- r) Set pilot system pressure to 22 atm. Note that purge is flowing.
- s) Set main burner purge pressure to equal expected fuel injection pressure. Note that purge is flowing.
- t) Presuming that the instrumentation is ready, the system is now ready for operation.

#### b. Normal Run

##### (1) Startup Sequence

Generator startup is controlled from the operator's control panel. The panel has been arranged so that startup is accomplished by actuating

push buttons in sequence from left to right. A normal shut down is simply the reverse of the start sequence. The procedure is as follows:

- a) Turn key switch to run position.
- b) Turn on warning lights, blow horn.
- c) Start exhaust stack spray. This control also starts the exhaust stack fan.
- d) Turn on service water.
- e) Start water pump.
- f) Turn on magnet power supply and adjust magnet current to required value.
- g) Start nitrogen purge.
- h) Turn on oxygen and adjust flow.
- i) Start pilot burner. Check pilot chamber pressure gage for normal indication (8 to 10 atm).
- j) Start main burner. Check main chamber pressure gage for expected pressure.
- k) Start seeder.
- l) During the run the operator should check the fuel and oxygen flow to make sure they are approximately correct.

## (2) Control Indication

On the operator's panel, the row of lights immediately above the push buttons are pilot lights which indicate that a control has been actuated. The row of lights above the pilot lights indicate when interlocks have functioned. During a normal start, actuation of one push button will start a subsystem, and if this subsystem is functioning normally its interlocks will close and will light the indicator lights over the next push button. Therefore, if the generator should fail to start or should shut down prematurely, the interlock indicators should be examined to determine the cause.

## (3) Interlocking

The interlock system functions as follows:

- a) The stack spray and stack fan must be operating before fuel or oxidizer can be admitted to either the pilot or the main burner.

- b) Service water and the water pump must be operating before either the burner or the magnet can be operated.
- c) When the pilot burner is started its chamber pressure must build up within a certain time period (adjustable up to 2 sec) or else it will shut down.
- d) The pilot chamber pressure must be above a certain (adjustable) value before the main burner can be started.
- e) When the main burner is started, its chamber pressure must build up within a certain time period (adjustable up to 2 sec) or else it will shut down.
- f) The main chamber pressure must be above a certain value before the seeder can be started.
- g) During operation, failure in one subsystem will shut off all other subsystems which follow it in a normal start sequence.

#### (4) Normal Stop

In a normal stop the run timer will shut off the main burner fuel and when burner pressure has decayed, the seeder will stop. Next, the pilot and main oxidizer are stopped. The magnet is turned off. The purge should be allowed to flow for approximately 10 seconds before it is turned off. Finally, the three water system controls are turned off.

#### (5) Emergency Stop

An emergency stop button has been provided which shuts off the seeder, main burner, pilot burner, and main oxygen. The purge, water system, and magnet are not affected. It is recommended that use of this feature be reserved for future emergencies and that it not be used in normal operation.

#### (6) Loss of Services

- a) Loss of 110 V control power will shut down the entire system except for the purge which will remain on.
- b) Loss of 440 V power will immediately shut off the water pump and the magnet. The main and pilot burners will shut off due to lack of water flow. The purge, main oxygen, service water and stack spray will stay on. The fuel ventilating fan will shut off.
- c) Loss of compressed air will shut all air operated valves which will stop the main burner, main oxygen, stack spray, and service water. The pilot, magnet, and water pump will stop due to lack of water flow. The purge will stay on.

### c. Test

The control system key switch has been provided with a test position to allow functional checking of each subsystem. A row of push buttons across the top of the operator's panel are used for this testing. An interlock with the exhaust stack spray and fan control has been provided to prevent the release of fuel or oxidizer into the control room. In addition the test buttons are interlocked to prevent burner operation by pressing the right combination of test buttons.

In view of the use of toxic fuels in this facility the main fuel test control is in the form of a key switch which should discourage inadvertent operation of the fuel valve. It is recommended that the key be removed from this switch, kept in a safe place, and be used only when testing of the main fuel valve is warranted.

It is anticipated that the testing circuits will be used primarily for trouble shooting in the event of a malfunction, and therefore, routine testing will not be necessary. However, the spark plugs used for igniting the pilot burner tend to have a rather short lifetime and it is recommended that the ignition system test be made frequently. The meter in the ignition circuit gives a rough indication of plug condition. If the meter reads low the plug should be removed and inspected, and replaced if necessary.

### d. Procedures for Toxic Fuels

As mentioned previously, the fuel system has design features which reduce the hazards associated with handling toxic fuels. Recommended procedures for the operation of the fuel system will be described in this section.

#### (1) Normal Running Procedure

When connecting cyanogen cylinders the lines and fittings should be checked for leaks before the manual valves on the cylinders are opened. On the liquid side the line may be pressurized with nitrogen from the hand regulator by opening the hand valve (Items 8 and 15 on Figure 25). The air operated ball valves located at each cylinder must be opened by turning on the key switch outside the fuel house. The liquid line will now be pressurized to the manual valves on the fuel cylinders. On the gas side the lines are pressurized by the fuel pressurization regulator which is loaded from the control panel. The lines should be pressurized to 300-400 psi and checked for leaks with a soap solution. All leaks detectable by this method should be repaired.

Before operating, the pressure on the lines should be released. Normal operating procedure was described previously. It is strongly recommended that the fuel system ventilating fan be turned on before any cyanogen is released into the fuel line. This fan should be kept in operation at all times when there is cyanogen in the fuel lines. The cyanogen detector should also be used as a check on the tightness of all fittings.

## (2) Shut Down Procedure

The following is the minimum recommended procedure for shutting down over night or over a weekend. A maximum safety procedure would be to purge the fuel line as described in the next paragraph. The minimum procedure would be:

- a) Unload fuel pressurization regulator.
- b) Shut nitrogen valve on valve panel and bleed off nitrogen downstream of valve.
- c) Vent fuel bottles to minimum pressure.
- d) Release pressure in fuel line by momentarily opening ball valves at fuel bottle by actuating the fuel house key switch.
- e) Leave fuel system ventilating fan on.

NOTE: Extreme caution should be exercised in venting (depressurizing) the fuel bottles. During the venting process, some cyanogen vapor will be released which is diluted with air and is discharged from the ventilating system stack. The cyanogen flow during venting does not exceed 0.01 lbs/sec, and the concentration in the stack will not exceed 1%. During normal atmospheric conditions the mixture discharge from the stack will be rapidly dissipated. However, it is possible that on days with no wind and a low level temperature inversion a relatively high concentration of cyanogen could exist at ground level. Under these circumstances the tanks should not be vented.

## (3) Purging Fuel Lines

Removal of cyanogen from the fuel lines is required for changing fuel bottles, maintenance of the fuel system or the ventilating fan, and is the recommended safety practice whenever the facility is to be shut down for longer than overnight. The procedure is as follows:

- a) Vent fuel bottles to minimum pressure.
- b) Open ball valves on bottles by actuating fuel house key switch.
- c) Set hand regulator on valve panel to approximately 15 atm (Item 8, Figure 25).



- d) Crack open hand valve at valve panel (Item 15, Figure 25). This valve admits nitrogen to the fuel line at the burner. The nitrogen will push liquid cyanogen back into the fuel bottles.
- e) Continued flow will displace the liquid fuel from the lines and will admit nitrogen to the fuel bottles. Allow nitrogen to flow until bottle pressure is nearly equal to the regulator pressure set at Step c. Flow slowly so as not to overspeed the turbine flow meter.
- f) Close hand valve at valve panel.
- g) Vent fuel bottles.
- h) Close manual valves on fuel bottles.
- i) Make sure that fuel system ventilating fan is on.
- j) Open hand valve, Item 11, Figure 21, in fuel house.
- k) Open hand valve on valve panel as in Step d. The fuel line is now being purged with nitrogen. The nitrogen and any cyanogen vapor remaining in the line will be discharged up the ventilating system stack.
- l) Purging should be continued for approximately one-half hour to ensure removal of all cyanogen vapor.
- m) The nitrogen side should also be purged by blowing nitrogen from the pressurization regulator through the vent valve.

There remains a small quantity (about 10 cc) of cyanogen trapped between the check valve (Item 14, Figure 25) and the three-way valve. (Item 10, Figure 25). This may be purged by the following procedure:

- a) Turn off key switch at fuel house.
- b) On control panel turn main key switch to "test."
- c) Turn on stack spray and fan.
- d) Turn on main fuel test key switch.
- e) Introduce nitrogen purge through hand valve on valve panel (Item 15, Figure 25).
- f) Continue purge for at least five (5) minutes.

#### (4) Toxic Gas Detector

The toxic gas detector is used to warn of unsafe concentrations of cyanogen. The detector should be kept in operating condition at all times, following the manufacturer's instruction manual. The detector should be used to monitor the cyanogen level in the test cell and fuel house whenever runs are in progress. In the event of a leak the detector may also be used to determine if a safe atmosphere is present in the control room.

A gas sample mixture has been supplied consisting of 10 ppm of cyanogen in air. The detector sensitivity should be checked periodically using this mixture. The mixture may be transferred to the detector with relatively little dilution by filling a plastic bag from the bottle and transferring the bag to the control room sample tube. The cyanogen concentration in the sample is sufficiently low so as to be not hazardous even if a large amount is accidentally released into the room.

### 5. MAINTENANCE

#### a. Safety

During operation of the generator, deposits will form on the walls due to condensation of seed, slight corrosion of the walls, etc. When using cyanogen fuel it is possible that this deposit may contain some cyanides. Therefore, when disassembling the generator components, precautions should be taken to avoid contact with these deposits. Rubber gloves should be worn and a face mask with filters should be used when scraping out old refractory from the channel. The burner, nozzle, and diffuser, which do not contain refractory may be washed to remove deposits. All of the cyanides which are likely to form are soluble either in water or ammonium hydroxide, and therefore, parts should be washed with a mild ammonium hydroxide solution.

Procedures for operating the cyanogen fuel system were discussed in the previous section. Section II-6 contains more information regarding the safety aspects of handling cyanogen. The importance of careful purging of the fuel lines and the use of self-contained breathing apparatus when opening the fuel system cannot be overemphasized.

#### b. Burner, Nozzle, and Diffuser

It is important to understand that these components do not have unlimited life. The thermal cycling which they experience can produce distortion and cracking (fatigue failures) after prolonged operation. It may be necessary to repair or replace parts which are subject to high heat transfer rates.

The burner liner incorporates a sliding seal at the back plate end to allow for liner expansion. The "O" ring which forms this seal will deteriorate with use and will allow cooling water leakages into the chamber. This leakage will be indicated by water flow from the chamber drain valve when the water pump is run. The interior of the burner may be inspected

by removing the channel and looking in through the nozzle. Do not run cooling water through the burner with the nozzle removed. The nozzle retains the liner in place. To replace the liner "O" ring the nozzle, backplate, and liner must be removed. The liner should be checked for distortion which might relieve the squeeze on the "O" ring. When installing the new "O" ring be sure to lubricate with silicone grease.

Distortion of the liner causes a reduction of its diameter at the backplate end. If this occurs and the liner is otherwise undamaged, the condition can often be corrected by a shop which is experienced at metal spinning.

The burner backplate contains some welds which may be less durable than the base metal. These welds surround the burner injectors. If leakage develops at the welds they may be repairable by chipping out the crack and rewelding.

The pilot burner is also subjected to high heat fluxes. The pilot is of very simple design, and if trouble should develop, it is probably better to replace it than attempt repairs.

Fuel injectors have been made readily replaceable so as to permit wide variations of fuel flow. The injectors consist of a piece of tube which is brazed into the fittings to which the fuel manifold attaches. To replace the injectors, remove the fuel manifold and unscrew the injector assembly from the backplate. When replacing injectors, be sure that the new set have "O" rings in good condition and that the tube is free from dents or burrs. New injectors are readily made by brazing appropriate sizes of hypodermic tubing into the fittings. It is recommended that a set of injectors be made from a single length of tubing to ensure uniformity of inside diameter.

The nozzle is of one piece construction which tends to minimize the possibility of trouble. However, it makes repairs difficult in the event that cracks should occur. If any repair work is attempted in the gas passage, the contour should be preserved so as to maintain the aerodynamic performance.

The diffuser is a completely static component which has no water cooling. Accordingly, no problems are contemplated with the diffuser.

#### c. Channel Maintenance

The channel requires regular maintenance of the refractory materials used as insulator and electrode. These refractories are subject to thermal shock each time the generator is run, and as a result, some spalling and erosion occur. After some period of operation, the channel walls become sufficiently rough to noticeably affect the aerodynamics of the channel and at this time the channel must be disassembled and repaired.

To remove the channel it should be supported by the lifting strap while being disconnected from the diffuser and nozzle. The channel may

then be placed on a bench and disassembled. All loose refractory should be scraped out to provide a firm basis for the new refractory to be applied. It is customary, but not essential, to fill the electrodes first. After the electrode material has set, any surplus which has fallen into the insulator spaces should be removed and then the insulator refractory should be applied. A low temperature bake, at approximately 200°F for several hours, either in an oven or by means of infrared lamps is desirable to secure a hard, dry refractory.

The insulator refractory is Norton Company #1139 Alumina. This is mixed with a water glass (sodium silicate) solution made by diluting commercially available solutions with approximately three parts of water to one part water glass.

The electrode is made up as follows:

74% (by weight) zircoa cast #280 with 5% CaO content

13% zircoa bonding liquid #6

13% zirconium diboride

The first two items are available from Zirconium Corporation of America, Cleveland, Ohio. The last item is available from Kawecki Chemical Company, 220 East 42nd Street, New York, New York.

These mixtures should be of a trowelling consistency and may be applied to the channel walls with a spatula or putty knife.

Reassembly of the channel is done as follows: The plastic walls must be sealed to each other with a silicone rubber sealant. The electrode wall divergence must be adjusted as required for the experimental program. Note that at the inlet end a set of screws position the walls to match the nozzle but at the outlet end the walls are adjustable. Finally, the gaps between the electrode and peg walls must be filled with insulating refractory so as to effectively block gas flow through these gaps. The refractory may be packed into the gaps from the inside of the channel and from the ends using a long metal strip as a tool.

The life of the refractory is prolonged if it can be completely dried before the channel is run. The best way to do this is by a low temperature (150-200°F) bake for several hours.

The sealing of the channel to the nozzle and diffuser is also by silicone rubber sealant. The pressure difference across these joints is small, but a leak could be very damaging due to the high temperature of the combustion products.

The pressure taps in the channel wall tend to collect deposits of seed, etc., and may become plugged. These taps are straight passages, and may be cleaned by removing the connector on the outside of the channel and opening up the hole with a drill.

The channel is necessarily a snug fit in the magnet gap, and therefore, in reinstalling the channel it is important to arrange the power leads and instrumentation connections so that they will not be damaged when the magnet halves are rolled together. A layer of insulation applied to the magnet pole faces will help to prevent short circuits; 0.010" Mylar is recommended.

#### d. Fuel System Maintenance

The fuel system must be kept in good operating condition at all times, and this requirement becomes even more important when cyanogen fuel is in use. A regular inspection procedure is recommended which should be applied at monthly intervals or more frequently if experience indicates the necessity. Before any work is done on the fuel system, it must be drained and purged using the procedure described previously.

During operation of the generator the fuel system should be checked for malfunction. The following checks may be performed without any disassembly:

- a) The cyanogen detector will indicate leaks in the fuel piping. The selector valve should be set to sample air in the fuel house when the fuel bottle valves are opened.
- b) The fuel system gage in front of the control room window shows the nitrogen pressure being supplied to the fuel bottles. Any abnormal operation should be investigated.
- c) When repressurizing the fuel system, the fuel line pressure gage located on the valve panel (Item 21, Figure 25) will not indicate an increase in pressure unless there is a leak through the seat of one or both of the air operated ball valves (Item 9, Figure 21) located at the fuel bottles.
- d) When the burner has been stopped following a run, the pressure gage on the valve panel will not indicate a decrease in pressure unless there is a leak in the piping or through the seat of the three-way valve (Item 10, Figure 25) located at the burner.

When the fuel system is down for maintenance the following checks should be performed:

- a) If any leakage has been indicated by the cyanogen detector, the fuel line should be pressurized with nitrogen from the hand regulator on the valve panel. The pressure should be brought to 20 to 27 atm and leaks should be searched for using a soap solution on all fittings.
- b) The fuel lines between the fuel bottles and the ball valves should be disconnected and by pressurizing the fuel line as above, the ball valves may be checked for leakage.

- c) The fuel filters should be disassembled and cleaned.
- d) The three-way valve at the burner should be checked for leakage through the seat by disconnecting the line to the burner and pressurizing the fuel line as in a.
- e) Following Step d, pressure should be applied at the burner connection of the three-way valve and with this valve opened by means of the key switch on the control panel the check valve (Item 14, Figure 25) may be checked for leakage.
- f) The check valve on the nitrogen side of the fuel system (Item 12, Figure 21) should be checked for leakage through the seat.
- g) The relief valve (Item 10, Figure 21) should be checked for operation by pressurizing with the fuel nitrogen pressurization regulator. If necessary the blow off pressure should be set to 500 psi maximum.
- h) Leaks between the three-way valve and the burner may be detected by turning on the main nitrogen purge and checking with soap solution. This is the only part of the fuel system which is not enclosed by the fuel ventilating system.
- i) All valves should be checked for proper actuation. The three-way fuel valve in particular should operate very rapidly to ensure smooth starting and stopping of the main burner. Sluggish operation of an air operated valve is usually due to dirt and sludge in the lines or the air cylinder.
- j) All fuel line joints which have been broken in the above procedure should be checked for leaks after reassembly.

#### e. Maintenance of Gas Systems

The systems employed to provide fuel, oxygen, and nitrogen purge for the main and pilot burners are functionally similar. Each system has a supply with manual shut-off, a trap or filter, a gas loaded regulator, a relief valve, a solenoid or air operated on-off valve, and generally a check valve. Maintenance consists of periodic cleaning of the filter elements (the nitrogen filter is of the replaceable element type) checking the operation of the relief valves, and overhaul of the regulators and valves when they do not operate properly. Improper valve operation should be obvious during a run. Regulator trouble is indicated either by an uncontrollable rise in outlet pressure which is due to a leaking seat or by a decay in flow which is due to a cracked diaphragm.

Protection against overpressurization has been provided by installing relief valves on the various gas systems. To ensure that this protection is functional the relief valves should be checked for opening pressure.

This checking should be done at least once a year. The blow-off pressure should be adjusted to be 10 to 15% higher than the maximum working pressure. The following pressure settings are recommended.

Main oxygen line	575 psi
Main oxygen regulator loading line	650 psi
Main fuel pressurization line	500 psi for cyanogen 800 psi for other fuels
Main fuel loading line	575 psi for cyanogen 875 psi for other fuels
Pilot oxygen and nitrogen	500 psi
Main burner purge	800 psi
Nitrogen to loaders	800 psi

When overhauling any part of the part of the pilot or main oxygen is very important to maintain a high degree of cleanliness and in particular, to avoid the introduction of any conventional grease or oil into the system. Oxygen in contact with grease or oil may produce a violent explosion. When a lubricant is required in any part of the oxygen system, for instance, on sliding seals in a regulator, a fluorocarbon or silicone based grease should be used.

#### f. Seeder

The seeder needs frequent maintenance in order to secure satisfactory operation. The need for maintenance is due to the hygroscopic nature of the seed material and to the relatively short life of the "O" ring shaft seals.

Proper operation of the seeder requires that the seed be maintained in a very free flowing condition. However, the seed is hygroscopic and will pick up moisture and cake due to careless storage. In addition, the inside of the seeder may accumulate moisture if the hopper is left open or by diffusion back through the pipe lines from the burner. Naturally, this problem will be worse during humid weather. If there is any evidence of caking or moisture in the seeder it must be completely disassembled and flushed with water. After cleaning, all the seeder parts must be completely dried. The shaft seals should be inspected and replaced if necessary. In reassembling the seeder the shaft and seals should be lightly lubricated with fluorocarbon or silicone grease. The interior of the seeder must be kept free of conventional greases or oils due to the fact that the main oxygen supply flows through the seeder.

When a prolonged shut down of the facility is anticipated it is recommended that the seeder be cleaned as above. When cesium carbonate seed is being used it may be removed from the seeder before cleaning and carefully stored. This procedure is very desirable due to the high cost of cesium carbonate. Potassium carbonate, however, is inexpensive and conservation efforts are hardly worthwhile.

#### g. Control System

The electrical control system is designed for simple maintenance. The majority of relays are inexpensive plug-in types which may be replaced if they malfunction.

The pressure switches which are used for protection of the generator components must be adjusted to actuate at approximately 80% of the expected pressures. When generator operating conditions are changed suitable re-adjustments of the pressure switches should be made.

The lines connecting the pilot and main burner chambers to their respective gages and pressure switches must be filled with water to minimize the response time of the system. The connections at the burner tend to accumulate deposits which partially plug the lines. These lines should be blown out periodically and refilled with water.

#### 6. SAFETY IN HANDLING CYANOGEN

Cyanogen is classified as a highly toxic material, and therefore, should be handled with due caution. However, there are many materials which are more toxic which are handled in large quantities in industrial and military installations.

The toxicity of cyanogen is characterized by rapidity of action and by the possibility of complete recovery following exposure provided medical treatment is administered promptly. Cyanogen combustion is utilized in a large number of experiments at AERL. The attached bulletins have been prepared by the safety engineer at AERL for instruction of their own personnel. These bulletins describe the properties of cyanogen and the treatment to be employed in the event of exposure. It is recommended that all people who will be employed in operating the facility become familiar with the contents of these bulletins, and that emergency procedures and facilities be established to at least the extent described.

#### 7. CALIBRATION DATA

##### a. Oxidizer Venturi

Flow characteristics for the two oxidizer venturies are given in Figures 36 and 37. Flow has been calculated for oxygen and for an oxygen-nitrogen mixture simulating  $N_2O_4$ . A temperature-entropy chart is given in Figure 38 for estimating the temperature at the venturi. A constant curve should be followed from the storage temperature and pressure to a predicted venturi pressure where a corresponding venturi temperature may be read.

##### b. Fuel System

Required fuel bottle pressure may be estimated from the injector flow charts (Fig. 39). To the injection pressure drop must be added the



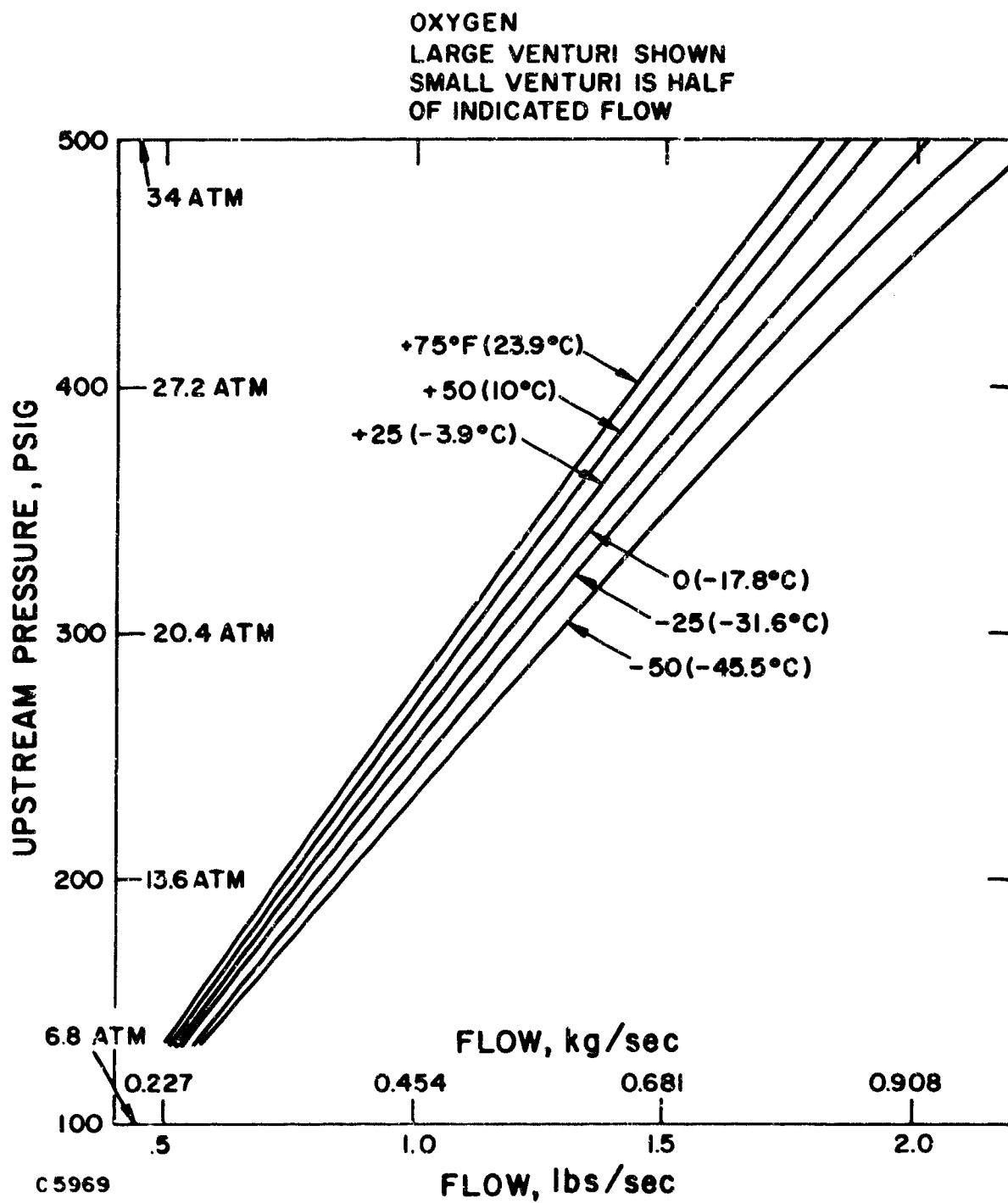


Figure 36 Oxidizer Venturi Calibration - O<sub>2</sub>.

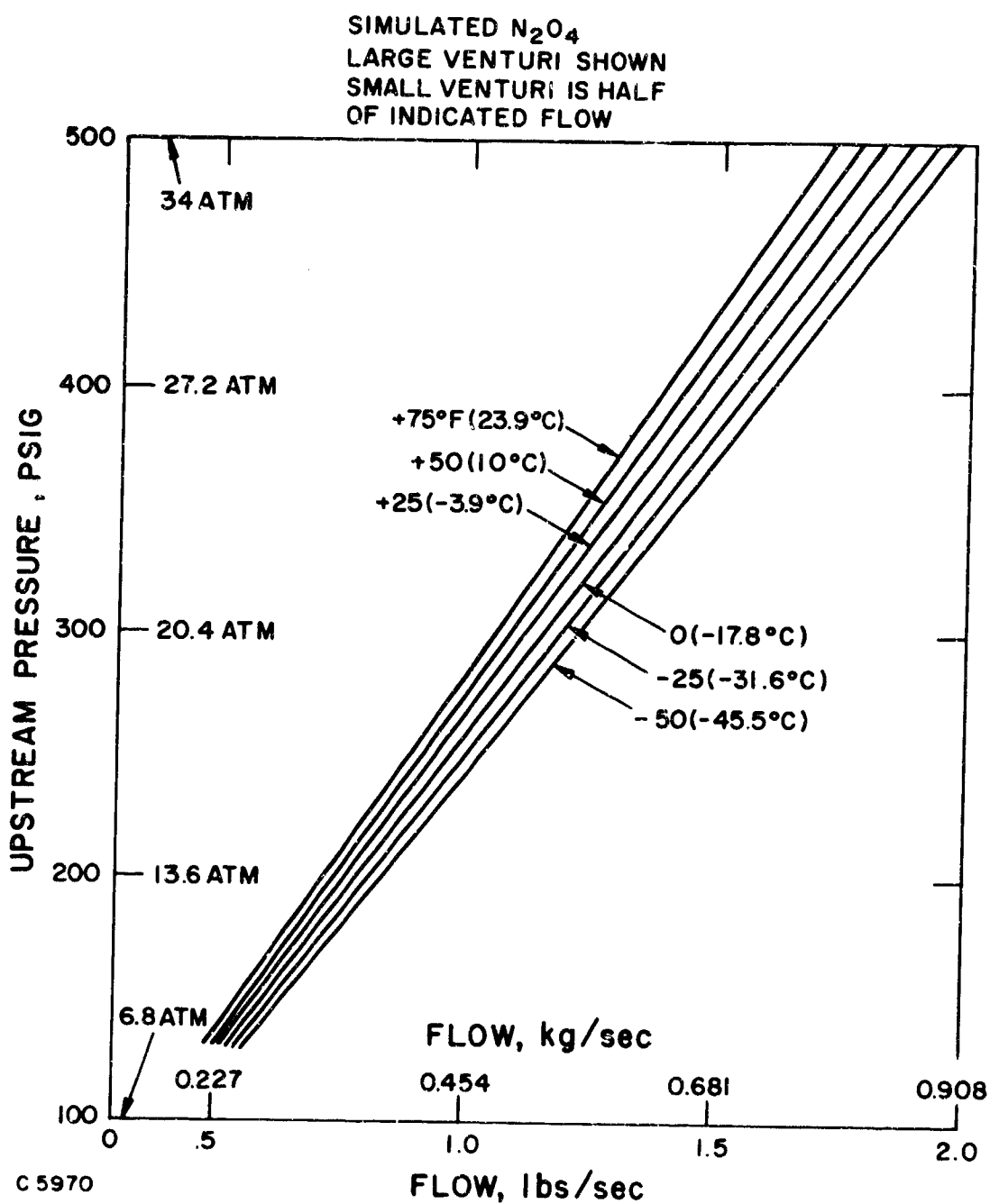


Figure 37 Oxidizer Venturi Calibration ·  $N_2/O_2 = 1/2$ .

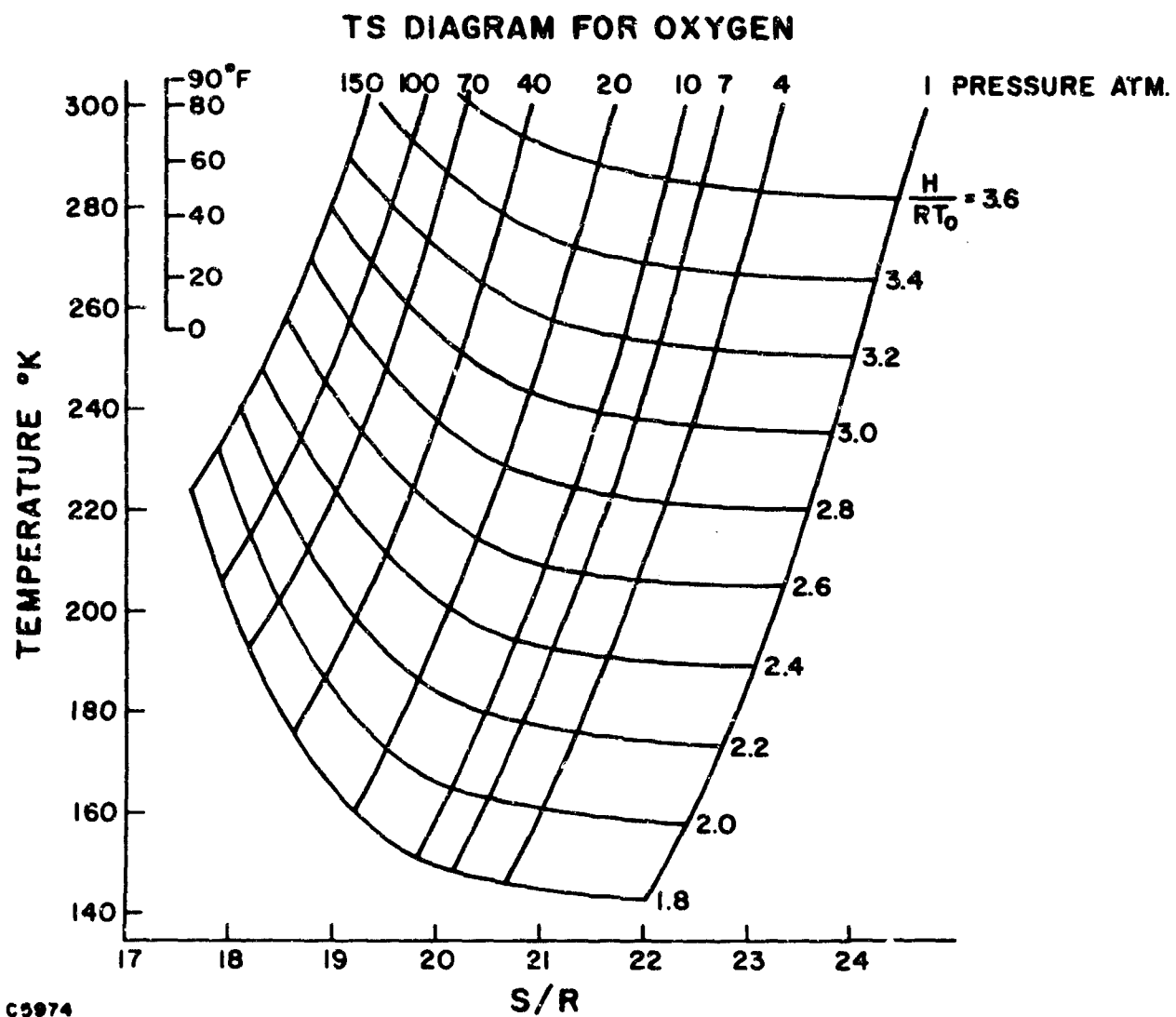


Figure 38 Oxygen Mollier Diagram.

# FUEL INJECTORS FLOW CHARACTERISTICS

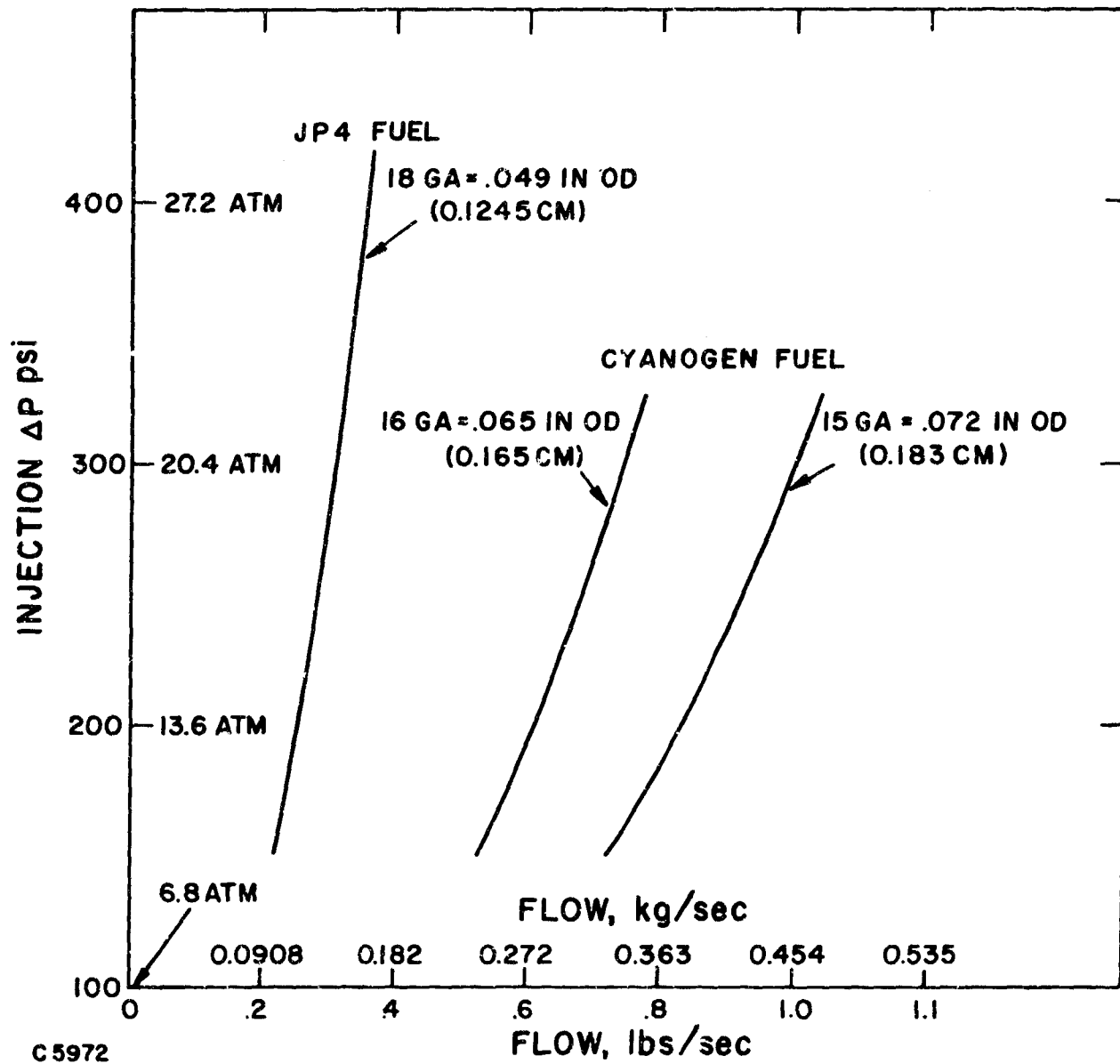
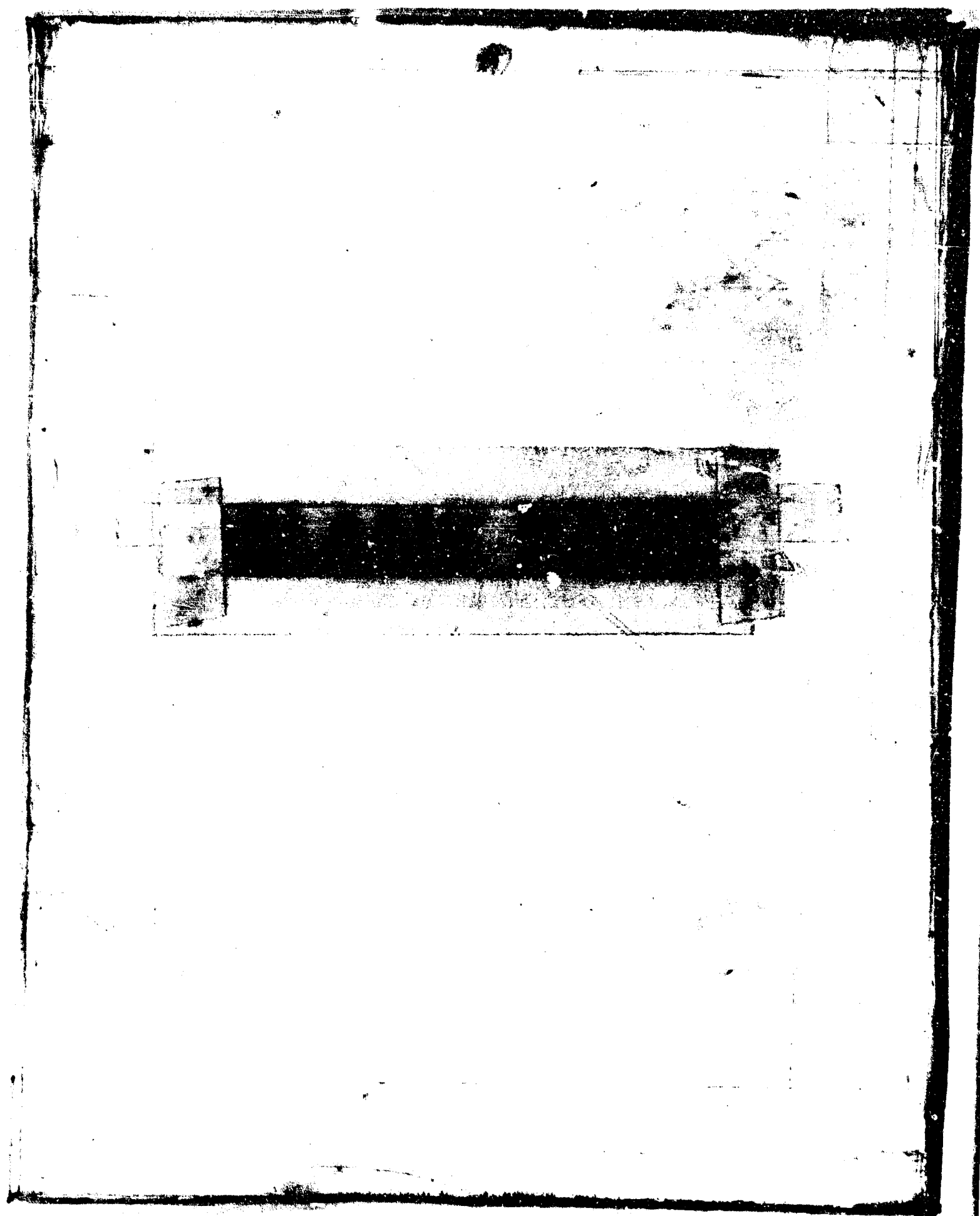


Figure 39 Calibration of 3 Sets of Fuel Oxidizers.



# Safety BULLETIN



**Avco  
EVERETT**  
RESEARCH  
LABORATORY

## SUBJECT:

Cyanogen ( $C_2N_2$ ) and Hydrogen Cyanide (HCN)

	<u>Cyanogen</u>	<u>Hydrogen Cyanide</u>
Molecular Weight	52.04	27.03
Vapor Pressure	60 psig a 20°C 1 atm a -21°C	25.3 psig a 18.1°C 400 mm a 9.8°C
Spec. Volume a 70°F, 1 atm	7.4 cu. ft/lb	
Boiling Point a 1 atm	-6° F (-21° C)	79° F (26° C)
Freezing Point a 1 atm	-18° F (-28° C)	10° F (-13° C)
Vapor Density (Air = 1)	1.67	0.94
Density, Liquid	0.9537 g/cc a bp	.688 a 20°C/4° C water
Critical Temp.	259.8° F (126.55°C)	
Critical Pressure	855.5 psia (58.2 atm)	
Flammability Limits (Air)	6.6-42.6%	5.6-40%
MAC (8 hrs/day)	10 ppm	10 ppm
Flash Point		0° F
Autoignition Temperature		1000° F
Fire Fighting	Water (Soluble 450 cc per 100 cc water)	Water

CYANOGEN (Oxalic Nitrile, Ethane Dinitrile, Prussite) is a colorless, practically odorless, flammable, toxic gas at room temperatures. It is sometimes described as having an almond-like odor. Its uses include a fuel gas for welding and cutting heat-resistant metals, a rocket and missile propellant (with ozone or fluorine), a fumigant, and as an organic chemical synthesizer. It will hydrolyze to cyanide and cyanate, thus its lethal concentration is the same as Hydrogen Cyanide.

Cyanogen polymerizes to paracyanogen when heated to 300°C or exposed to ultraviolet light; is reconverted to Cyanogen at 800°C. In a test, pure Cyanogen remained stable for 18-23 days a 65°C and contained only small quantities of decomposition products after 100 days.

Odor and irritation threshold level detection tests on humans indicate no odor up to 250 ppm but immediate eye irritation shortly followed by nasal irritation at about 16 ppm. Irritations lasted several minutes after the mild exposure. Tests on rats have suggested that Cyanogen is less toxic than Hydrogen Cyanide by an order of magnitude. (3, 4)

HYDROGEN CYANIDE (Hydrocyanic Acid, Prussic Acid) is also colorless but a liquid at room temperatures. It is used principally as a fumigant to kill mice, rats, moths, beetles, cockroaches, insects and the lower forms of life (but not bacteria). In contact with alkaline materials, hydrogen cyanide can polymerize or decompose explosively.

### Hydrogen Cyanide (cont.)

Since concentrations over 300 ppm are absorbed through the skin, neoprene gloves and vapor-tight coveralls are necessary in addition to face mask and air-supplied respirator.

**TOXICITY** Cyanogen and hydrogen cyanide are toxic when inhaled, ingested, or absorbed through the skin. The odor of bitter almonds on the breath, rapid or gasping breathing, and accelerated pulse suggest cyanide poisoning.

Inhalation effects are asphyxiation, lachrymation, irritation of mucous membranes of upper respiratory tract, and pink skin coloration due to the unabsorbed oxygen remaining in the veins.

Cyanides are protoplasmic poisons, which act on tissue cells to inhibit their ability to utilize blood oxygen (i. e., chemical asphyxiation). Cyanides are rapid killers when sufficient amounts are absorbed; but sublethal doses are rapidly detoxified with only slight chronic effects.

Skin absorption effects are minimal from exposures to Cyanogen gas at 10,000 ppm (1%) (3), but dangerous from spills of hydrogen cyanide liquid (4).

The observed effects of hydrogen cyanide on man are as follows (3):

no detectable effects-----	8-10 ppm
slight symptoms after many hours-----	20-40 ppm
tolerated for 1/2 to one hour-----	50-60 ppm
dangerous illness in 1/2 to one hour-----	120-150 ppm
rapidly fatal-----	300 ppm

Exposure to 200 ppm for an hour produces serious symptoms.

Symptoms of poisoning are giddiness, dizziness, feeling of suffocation, headache, fatigue, loss of appetite, nausea.

**HANDLING PRECAUTIONS** Both  $C_2N_2$  and HCN are lethal poisons. **EVERY HANDLER SHOULD KNOW** the PRECAUTIONS and FIRST AID EMERGENCY ACTION (see section on FIRST AID):

- a) Whenever working on a pressurized system, or opening up a system in which these cyanides have been used, wear a SUPPLIED AIR respirator.
- b) Experiment areas should be well-ventilated and under negative pressure with respect to adjacent areas to prevent contamination of the occupied area.
- c) No person should work alone. A second person with a supplied-air respirator and protective clothing and gloves should stand by in a safe area to give help.
- d) Protective clothing should be of rubber or neoprene, including the soles of shoes.

- e) Keep spills hosed down. Wash hands and face (or take a shower) after each exposure.
- f) Use the minimum quantity of cyanide necessary for the experiment.
- g) Don't overlook the FLAMMABLE properties of cyanogen.
- h) Handle full and empty cylinders carefully. Store in a well ventilated area away from strong oxidizers, traffic, and heat. Keep protective cylinder caps in place except during connection to the experiment. Leave some pressure in the "empty" cylinder.
- i) Use stainless steel check valves, and install a vacuum break to prevent suck-back into the cylinder.
- j) LEAK TEST all parts of the system. The presence of cyanogen in air may be detected with MOIST methyl orange-mercuric chloride test papers (color changes from orange to pink or red); or with the MSA hydrogen cyanide detector tube. HCN may be detected with a copper salt and organic indicator on paper, such as the MSA detector.

FIRST AID (SEE INSTRUCTIONS ON ANTIDOTE KIT)

- 1) Quickly move the patient to fresh air and remove contaminated clothing. (The rescuer should wear protective clothing, neoprene gloves and a supplied-air respirator for heavy gas concentrations.)
- 2) Give artificial respiration if not breathing.
- 3) The victim should lie at rest and completely AVOID EXERTION.
- 4) Break an Amyl Nitrite ampoule in a cloth and hold it lightly under the nose of the victim. Work fast, for the ampoule lasts only 15-30 seconds. Repeat 4-5 times at 15-30 second intervals.
- 5) Wash off the residue from a liquid HCN spill or  $C_2N_2$  gas exposure with copious amounts of water. Use a shower if available.
- 6) If seriously exposed, lay the cloth of Amyl Nitrite over the patient's nose and send both the PATIENT and the KIT containing the 10 cc. sodium nitrite, 50 cc. sodium thiosulfate, and the sterilized syringes to the doctor or hospital for intravenous injections by the DOCTOR according to the instructions enclosed with the syringes: first the nitrite, then the thiosulfate. DO NOT STOP the application even if not breathing, but apply artificial respiration.

SPEED IS ESSENTIAL in treating cyanide poisoning. As long as the heart is still beating, the chance of recovery by this treatment is good.

MATERIALS In general with cyanogen, use glass-lined or stainless steel containers. Liquid cyanogen is shipped in ICC-approved steel cylinders under 60 psig pressure. Cylinders have stainless steel valves threaded for 1/8" IPS. There are NO SAFETY DEVICES on the cylinders.



The recommended regulator is brass with a german silver diaphragm and packless control valve for 5 to 50 psig delivery pressures. The stainless steel needle valves, check valves and other fittings are suitable to 65° C temperatures.

#### REFERENCES

- 1) Matheson Co., Inc. GAS DATA BOOK, 4th Ed., 1966
- 2) Matheson Co., Inc. CATALOG 25, April 1965
- 3) McNerney & Schrenk: The Acute Toxicity of Cyanogen, J. of the Am. Ind. Hyg. Assn., April 1960.
- 4) H. B. Elkins: Chemistry of Industrial Toxicology, 1950: discussions with Dr. Elkins (August 1966).
- 5) Eli Lilly & Company Instruction Leaflet with Cyanogen Antidote Package.
- 6) Sax: Dangerous Properties of Industrial Materials (1957); Handbook of Dangerous Materials (1951)

856/1167

COPY FROM  
POTTER AERONAUTICAL CORPORATION  
U. S. Route 22, Union, New Jersey  
POTTERMETER CALIBRATION DATA SHEET

Calibration No. G - R - 867 Model No. 55.0 Serial No. Avco - 1 - 3  
Customer Avco Everett Research Labs. Order No. RL-77009  
No. of Calibrations Required ☐

**METER CONSTRUCTION**

1. Housing Mat. 304 SS
2. Rotor
  - a. Material 304 SS
  - b. Pulsus/Rev. 3
  - c. No. of Blades 6
  - d. Blade Angle 24
3. Bearing Mat. T. C. 883
4. Thrust Stops T. C.
5. Pickup
  - a. Part Number PC 13-70G
  - b. Quantity One
6. Boundary Coefficient 0
7. Weight of Meter \_\_\_\_\_ lb.

**FLUID PROPERTIES**

1. Type Water
2. Viscosity \_\_\_\_\_ cs.
3. SG (measured) .9985
4. Temperature 65° °F
5. Weight of Fluid 2.405 ----- 20. lb.
6. Volume (actual) 2.4051 gal.

**METER FACTORS**

1. Calibration Factor K = 3061.251 cy/gal.
2. Mean Total Cycles (Col. 3) 7362.615
3. (Rate indicator settings) \_\_\_\_\_ cps @ \_\_\_\_\_ gpm  
\_\_\_\_\_ cps @ \_\_\_\_\_ gpm

Pt. No.	Time (Min)	Total Cycles	Approx. Freq. CPS	Actual Freq. CPS	Vol. Flow GPM	Cycles Per Gallon	Dev. %	Press Drop psi	MV (RMS)
1	2450	7362	500		9.81				520
2	2448	7360	500						---
3	2713	7354	450						480
4	3080	7351	400						440
5	3546	7355	350						395
6	4080	7356	300						340
7	4941	7355	250						285
8	6122	7356	200						230
9	8180	7366	150						125
10	1.2280	7379	100						120
11	1.2252	7377	100						---
12	1.6485	7377	75						88
13	1.9000	7361	65		1.26				80
14	2.4290	7257	50x		.9922				59
15	2.7886	6730	40x						46
16	3.2900	6010	30x						34
17	3.3015	6012	30x						---
18	3.6440	5376	25x		.6600				30
19									
20									
21									
22									
23									
24									
25									

\*Cavitation due to Max. Capacity of flow stand  
x Non-linear flow range  
Pressure Test \_\_\_\_\_

Calibrated by: \_\_\_\_\_ Date 10-20-67  
Inspected by: \_\_\_\_\_ Date 10-20-67

chamber pressure and system pressure loss in order to arrive at the required tank pressure.

A turbine flowmeter is used to measure the actual fuel flow. The output instrument is adjustable over a large range so that a convenient full scale reading may be selected. For cyanogen fuel a full scale reading of 1 lb/sec will be particularly convenient. The manufacturer's instruction book should be referred to for calibration instructions. The specific gravity of cyanogen liquid at room temperature is 0.86. The manufacturer's calibration of the meter is attached.

c. Water System

Water system flows and pressures were shown on Figure 26. Note that the orifices provided in the various water circuits both control and measure flow. Any large departures from the pressures shown on this drawing are an indication of trouble in the water system and should be investigated.

d. Seeder

The seeder is provided with a twenty-tooth and a forty-tooth rotor in order to cover the required flow range. The calibration curves given in Figure 40 were obtained using a granular potassium carbonate having an apparent bulk density of 0.30 lbs/in.<sup>3</sup>. When other seed materials are used the bulk density must be measured and the calibration curves corrected.

e. Magnet

Magnetization and field distribution characteristics are given in Figures 41 and 42.

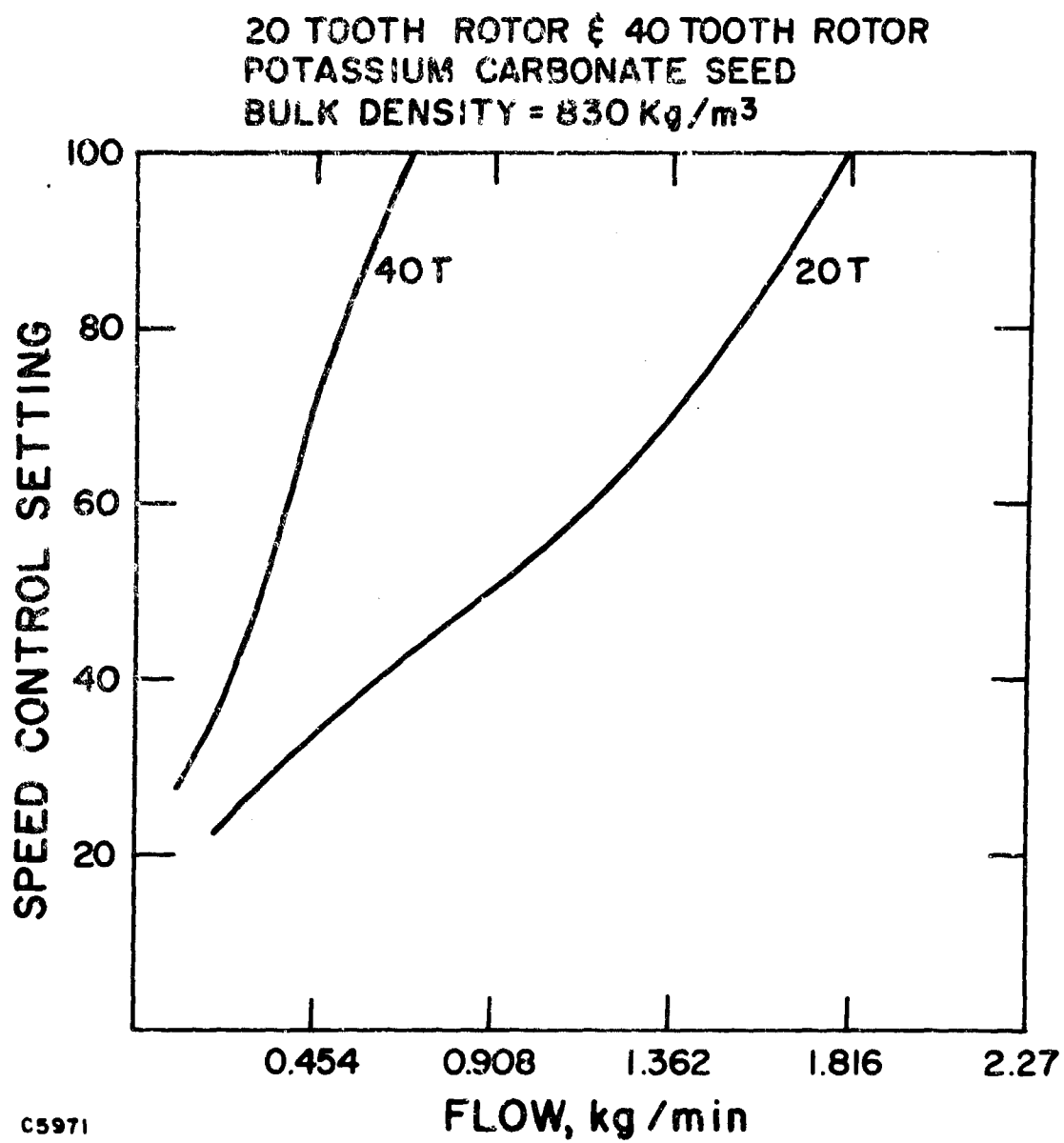


Figure 40 Seeder Calibration - 20 and 40 Tooth Rotors.

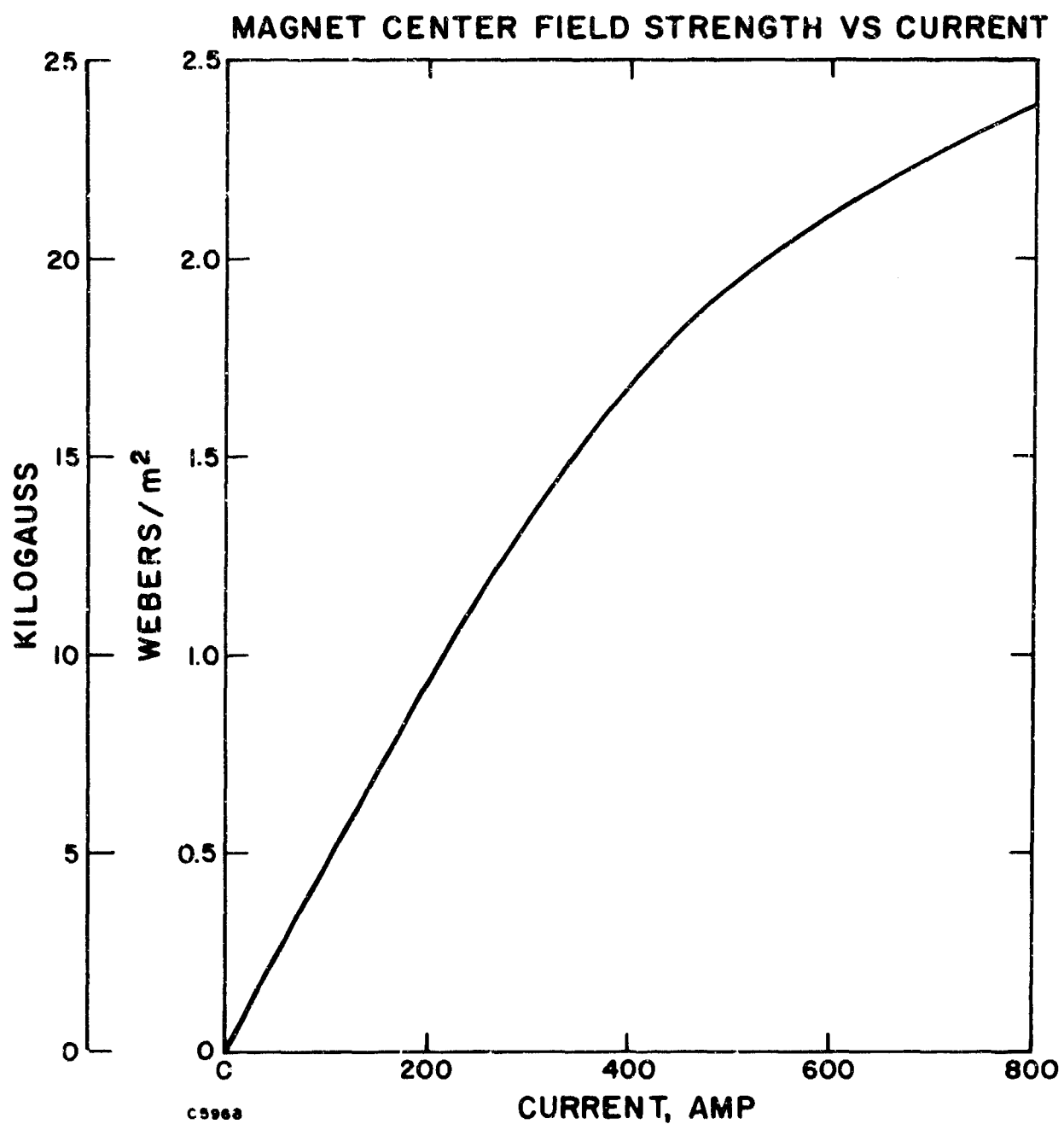
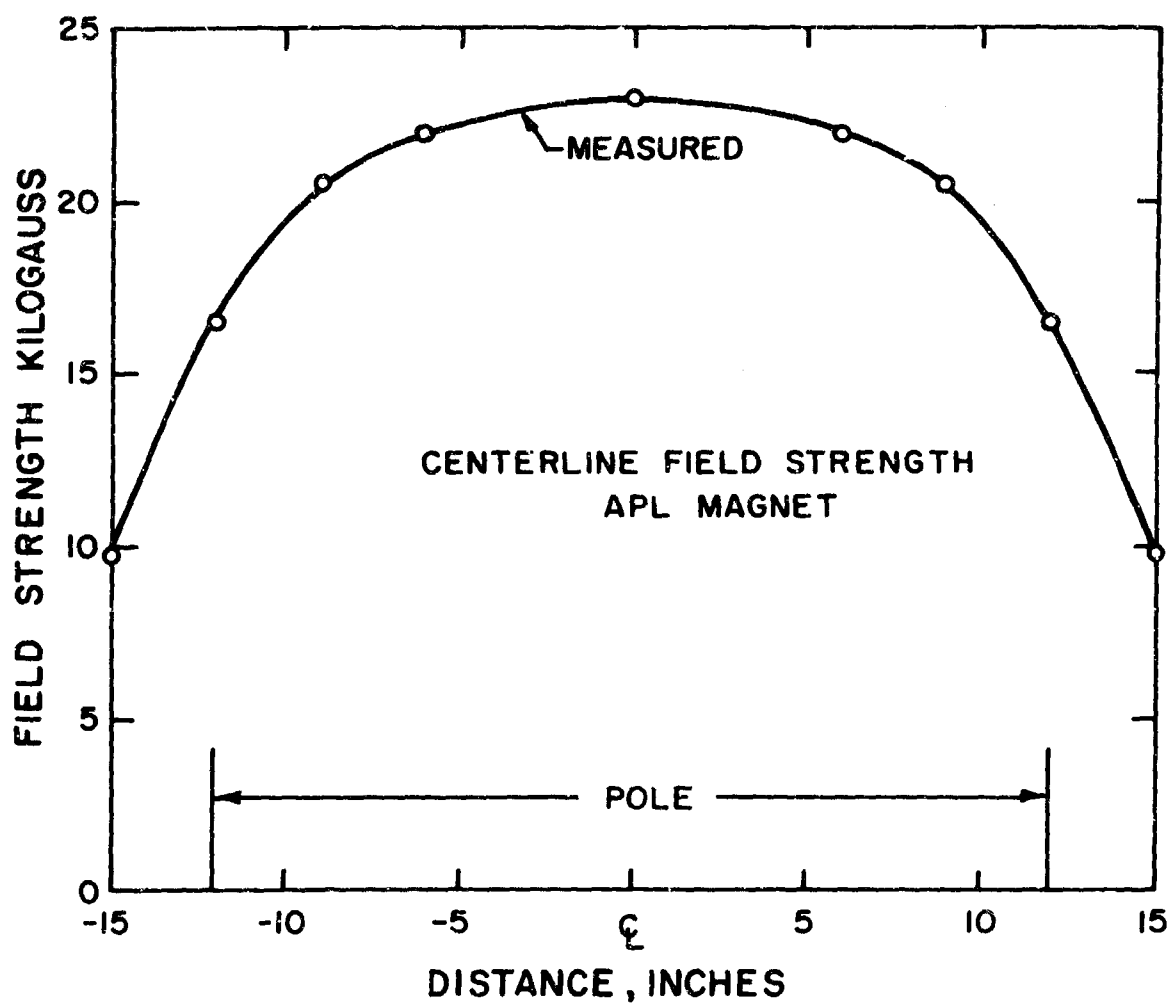
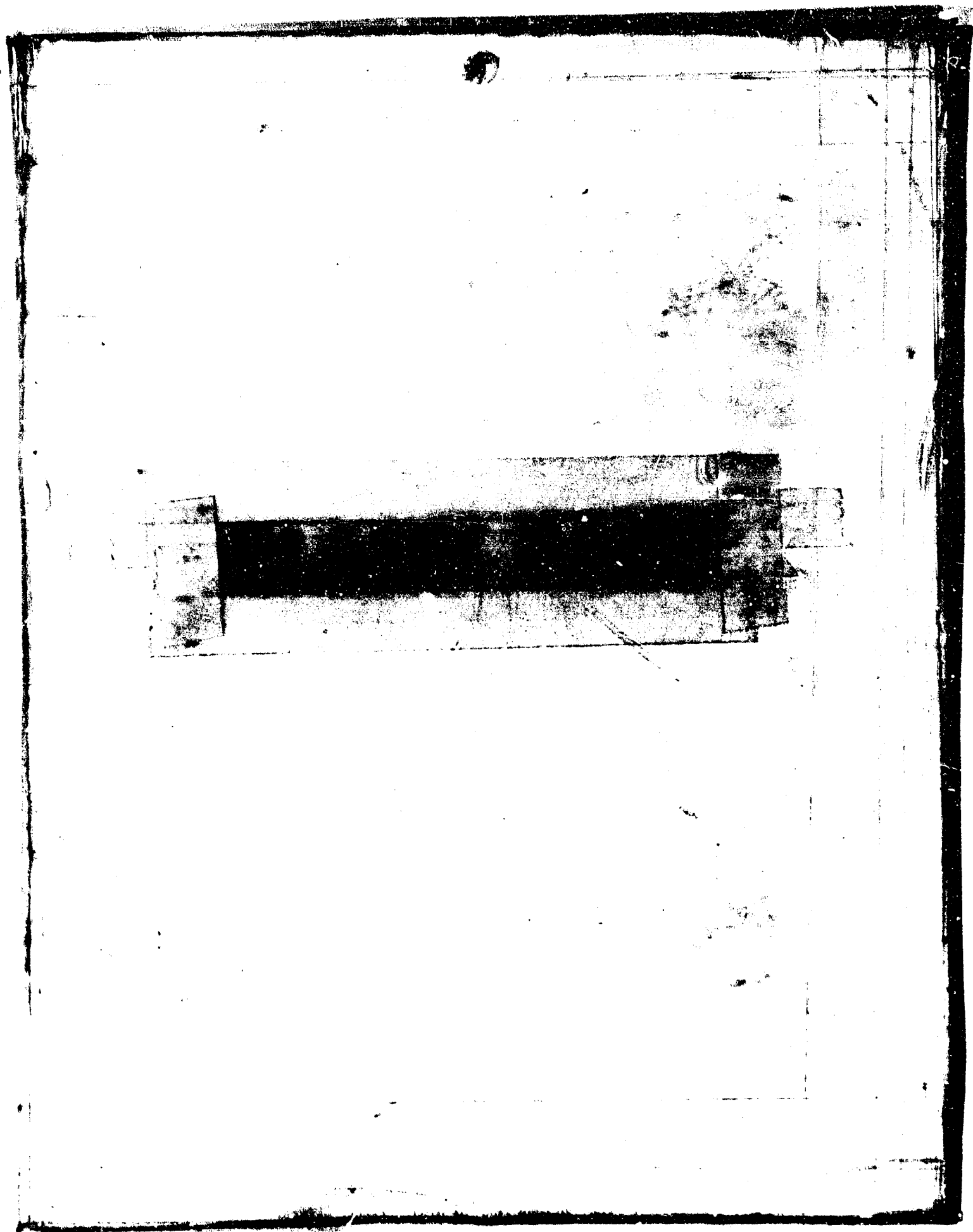


Figure 41 Magnetic Field Strength vs Winding Current at the Center of the APL Magnet.



C5871

Figure 42 Magnetic Field Distribution at 2.3 Tesla Center Field for the APL Magnet



## SECTION III

### APL FACILITY CHECKOUT

#### 1. SYSTEM CHECKS

Initial operation of the APL facility consisted of leak and flow checks of the cooling water and gas systems. No important problems were encountered in this phase, and it was established that all systems met their design requirements. During the facility checkout the interlocks and controls were adjusted to suit the operating conditions for the burner and magnet.

#### 2. BURNER TESTS

For purposes of burner testing, JP-4 fuel was used in place of cyanogen so as to minimize any risk in the event of some malfunction of the burner or facility. The circular 2.5 Mach number nozzle was used, and initially no channel or duct was used between the nozzle exit and the exhaust pipes. The first attempts at burner operation were always prematurely terminated by tripping of one or another of the interlocks. This problem was traced to acoustical vibration of the valve panel. The noise level was unusually high due to the absence of any channel or duct between the nozzle and the exhaust pipe and due to flow separation in the nozzle because of overexpansion. The noise level was reduced by installing a dummy channel which conducted the combustion products from the nozzle into the exhaust pipe. This dummy channel was simply a piece of heavy wall transite pipe which was ablatively cooled. With this dummy channel in place it was possible to operate the burner with all of the interlocks functioning. Burner operation appeared to be satisfactory in all respects.

#### 3. MAGNET TESTS

The magnet and its power supply were checked for satisfactory operation; at the same time, the magnet gap was surveyed for field strength and distribution. During initial magnet operation some of the cooling circuits became plugged with the residue which was inside of the newly installed pipe system. The thermal protection devices on the magnet coils shut off the power supply before overheating occurred. The residue was removed by reversing the water flow direction. The magnet was surveyed for field strength and distribution using a Rawson-Lish rotating coil gaussmeter. The maximum field was found to be only 4 percent lower than design and the longitudinal distribution was somewhat better than predicted so that the total flux through the generator channel is almost exactly as predicted. Uniformity surveys were taken at several stations. Within the channel gas passage volume the average nonuniformity was less than 2 percent.



The overload capacity of the power supply was investigated up to about 800 amps or 15 percent overcurrent. At this point the overcurrent protection device tripped, shutting off the power supply. Both the magnet and its power supply have large overload capabilities for short term operation. This feature makes possible generator experiments with higher interaction parameters for short time intervals.

#### 4. SEEDER

Testing and calibration of the seeder proved to be a somewhat time-consuming task. As originally built the seeder rotor had excessive end clearance which allowed a small amount of seed to flow when the rotor was not turning. After this was discovered, the seeder body was reworked to reduce this clearance. The first rotor had straight cut teeth which produced a pulsating or fluctuating seed flow. This rotor was replaced with one which had helical teeth. The helical rotor virtually eliminated the pulsation at high speeds but at speeds below 30 percent of the maximum speed, the pulsation was still evident. Finally a third rotor was made with more teeth of smaller size which would extend the lower end of the operating range.

Initially, the calibration technique used consisted of blowing the seed into a cloth bag which would be weighed before and after a timed run. This method was not successful due to the fact that the potassium carbonate seed material broke up into fine powder which flowed right through the cloth bag. The second calibration technique was more satisfactory. This consisted of blowing the seed into a plastic rubbish can which was about half full of water. The great solubility of the seed ensured that under proper conditions essentially all of the seed was collected. It was necessary to carefully adjust the gas flow through the seeder to ensure that the powder was transported but at the same time not blow water out of the can. Eventually a satisfactory calibration was obtained using granular potassium carbonate. The seeder is a volumetric feeder, and provided the physical form of different seeds is approximately the same, the mass flow should be proportional to the bulk density. In view of the high cost of cesium carbonate no attempt was made to calibrate with this material but the flow rate was inferred from its bulk density.

#### 5. CONCLUSIONS

At the end of the checkout it was concluded that satisfactory operation of all of the systems in the facility was achieved. All systems had met their design requirements within satisfactory margins.

## SECTION IV

### CONDUCTIVITY MEASUREMENTS AT APL

Some questions had been raised previously as to the relative effectiveness of cesium and potassium seeds. Other things being equal, the cesium seed should produce about twice the conductivity obtained with potassium. However, the enhanced conductivity expected with cesium could be greatly reduced if CsOH formation were greater than KOH formation. A search of readily available information indicated that at temperatures above 2600°K the hydroxide formation would be approximately equal and therefore, cesium should improve conductivity by a factor of two.

It was agreed that the facility should be used for conductivity measurements during the course of the facility checkout. The measurements were made using existing hardware with essentially no modification to the facility. The available ranges of pressures and temperatures were limited by the capability of the facility, specifically, the channel static operating pressures were much lower than those contemplated. With this as background, the methods used and the conditions under which the conductivity tests were made will now be described.

For the conductivity tests, JP-4 fuel and gaseous oxygen were burned stoichiometrically. The normal flow rate of the facility, 0.68 kg/sec, was used throughout the tests. The combustion products were seeded with dry powdered cesium or potassium carbonate which was injected into the burner with the oxygen flow. The seed rate was varied between approximately 0.1 and 2.0 mole percent.

The conductivity measurements were performed in a Hall channel composed of a number of water-cooled rings which are assembled with insulating spacers to form a cylindrical duct. The inside diameter of the duct increases slightly in the flow direction so as to compensate for boundary layer growth and the core flow is thus nominally at constant pressure. Two nozzles were used which produced flow Mach numbers of 1.5 and 2.5. The corresponding static pressures were 0.67 and 0.40 atmospheres, and the static temperatures are approximately 2850 and 2500° K, respectively.

Power from the magnet power supply was applied to the end rings of the channel. The magnet coil and a resistor were connected in series with the channel to help to stabilize the current. During a test, because of the applied axial voltage, an axial current flowed through the conducting gas in the channel. By measuring the voltage between intermediate rings of the channel, and by measuring the axial current flow through the gas, the conductivity can be calculated. Since only trivial currents flow into or out

of intermediate rings, the effect of electrode voltage drop is eliminated.

For these conductivity runs, temporary connections were made to voltmeters and ammeters on the instrumentation panel. Data was taken by photographing the panel with a Polaroid camera. The measured voltages were also recorded on an oscillograph in order to detect fluctuations in conductivity. At low seeder speeds some fluctuation was evident, but this disappeared at higher seeder speeds. For the same mass flows the stagnation pressure is approximately four times larger using the 2.5 Mach number nozzle while the burner flow velocity is approximately 4 times less than for the 1.5 Mach number nozzle. Since fluctuations appeared to be worse with the 1.5 Mach number nozzle, this supports the theory that larger burner residence times reduce fluctuations.

The results of these conductivity tests are shown on Figure 43. As may be seen, the conductivity is approximately twice as great with cesium seed as with potassium seed at a given mole percent. Thus, for the conditions of these tests there appears to be little difference in the amount of CsOH and KOH formation. Conductivity values from 6 to 68 mhos/meter were measured.

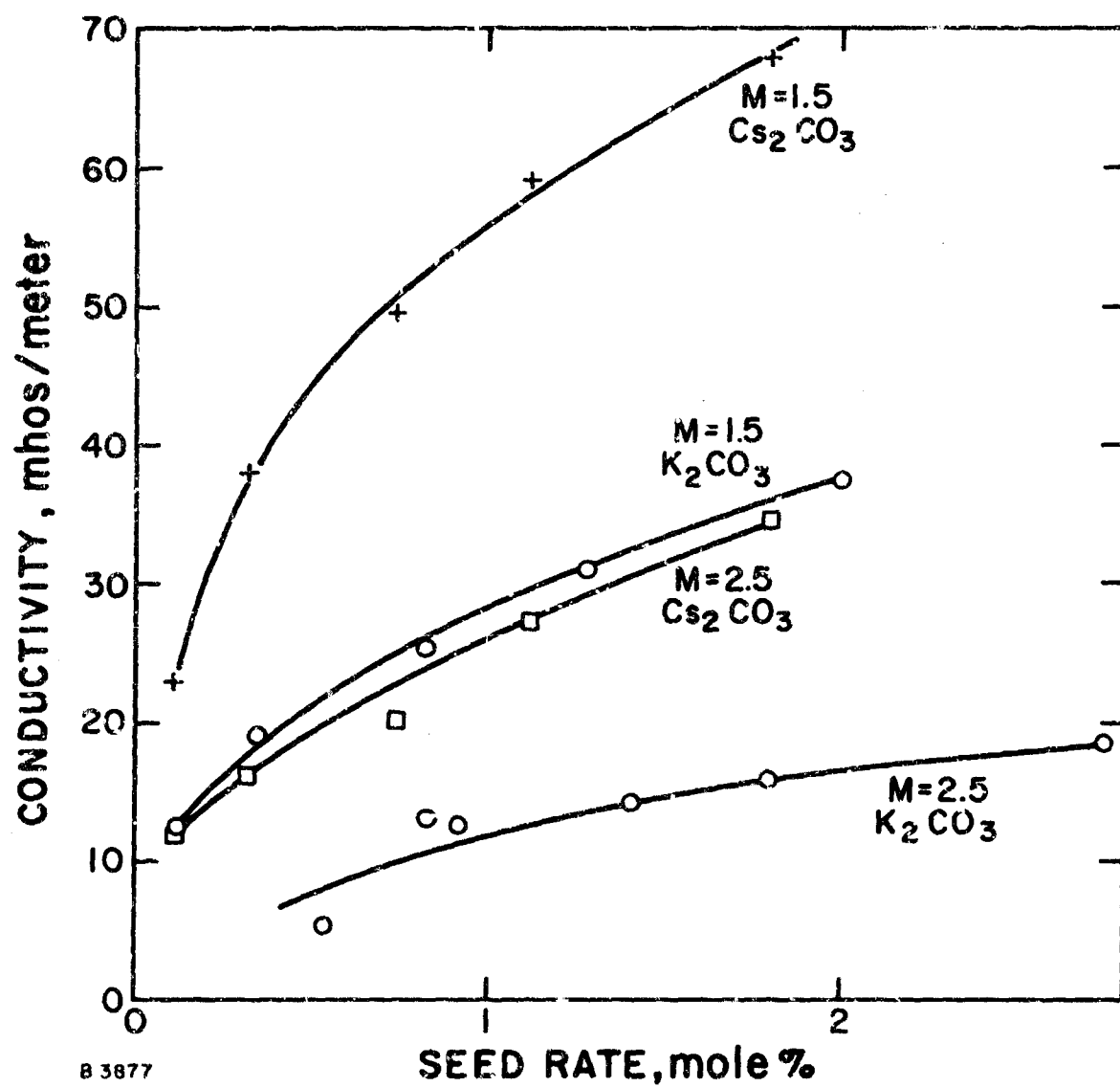


Figure 43 Results of Conductivity Tests with JP-4 and Oxygen.

**BLANK PAGE**

SECTION V  
INSTALLATION OF GENERATOR COMPONENTS  
IN THE AERL MARK II FACILITY

1. INTRODUCTION

Prior to investigating the performance of the generator using the combustion products of cyanogen and oxygen, AERL proposed moving the experiment to Everett because cyanogen had been burned at AERL and a team experienced with all aspects of handling cyanogen was readily available. The Air Force approved this plan and subsequently the generator components and certain essential equipment from the facility was shipped to AERL for installation in the Mark II generator facility. The Mark II facility has been described in several other reports\* and a detailed description will not be repeated here. The required modifications, however, will be discussed.

Due to the relatively great length of the Mark II magnet poles (1.52 m vs. 0.61 m for the APL magnet), the method of installing the generator components was given careful consideration. It was finally decided that it would be desirable to have the diffuser extend beyond the magnet poles into a region of low field so that pressure recovery would be relatively unaffected. This required that the burner be located in a high field region between the magnet poles. The operation of a burner in the presence of a magnetic field did not affect the performance.

2. MAGNET MODIFICATIONS

For the experimental work at AERL, a pair of auxiliary iron pole pieces were made for the Mark II magnet which reduced the air gap from 0.46 m to 0.2 m in the volume occupied by the channel. These pole pieces caused the field to increase by 3 to 4 kilogauss. Magnetic shunts were designed for installation adjacent to the burner so as to further increase the difference in field strength between the burner and the channel locations should poor burner performance be encountered. Subsequent testing showed these shunts to be unnecessary.

The system was designed so that a maximum field strength of 24 kilogauss (which is the same as the magnet in the APL facility) was to be obtained by passing 12000 amperes through the magnet. It developed that the auxiliary poles were overdesigned with the result that the available magnet

\*Louis, J. F., et al., "Studies of Fluid Mechanics Using a Large, Combustion Driven MHD Generator," AERL Research Report 145, March 1963.

Teno, J., et al., "Hall Configuration MHD Generator Studies," International Symposium on MHD Electric Power Generation, Salzburg, Austria (July 1966).

ballast resistor allowed a current slightly over 12000 amperes to circulate; for this current the maximum field was actually 26 kilogauss and the distribution was quite different from the APL magnet because of difference in size of the two magnets. The resulting field distribution is shown on Figure 44.

### 3. ASSEMBLY OF GENERATOR

The generator components were assembled into a frame constructed of aluminum channels with plastic crossmembers. The purpose of the frame was to hold the generator parts in alignment and also to adapt them to existing tracks in the magnet and an existing roll-out stand. A photograph of the frames and generator assembly is shown on Figure 45. The components shown are, starting at the bottom of the figure, the fuel-purge valve, burner plumbing, burner, nozzle, channel and diffuser, respectively. With the exception of the exit end of the diffuser, this entire assembly is located inside the magnet when in operating position. Also the seeder is visible at the top center of the figure.

### 4. MODIFICATION OF FACILITY

The Mark II facility required modifications to minimize the danger in handling of cyanogen fuel and to meet the operating requirements of the present experiment.

A complete new fuel system was constructed utilizing components from the APL facility. This fuel system is essentially the same as that constructed at APL. A fuel house was built to enclose the cyanogen cylinders and fuel piping. This fuel house has an exhaust fan that discharges into a 0.254-m diameter, 18.3 m tall stack erected on the roof of the building. Because of the location of the generator components inside the magnet it was found possible by a suitable arrangement of duct work to exhaust air from inside the magnet by means of the fuel house fan.

The exhaust system was modified by installing a fan in the exhaust stack and by extending the stack to a height of 6.1 m above the roof. These changes resulted in an exhaust system which is functionally very similar to that at APL.

The cyanogen detector was installed in the control room and six sampling lines were run to what were considered to be critical locations. The detector has been tested periodically with freshly prepared cyanogen-air samples. The sensitivity and response time have been completely satisfactory at all times. There has been some problem with occasional false alarms due to atmospheric pollution or sources of gases or vapors inside the building. The detector is, unfortunately, sensitive to many gases besides cyanogen.

Some revision to piping, valves, and controls were necessary to match the operating condition of this experiment. The generator output

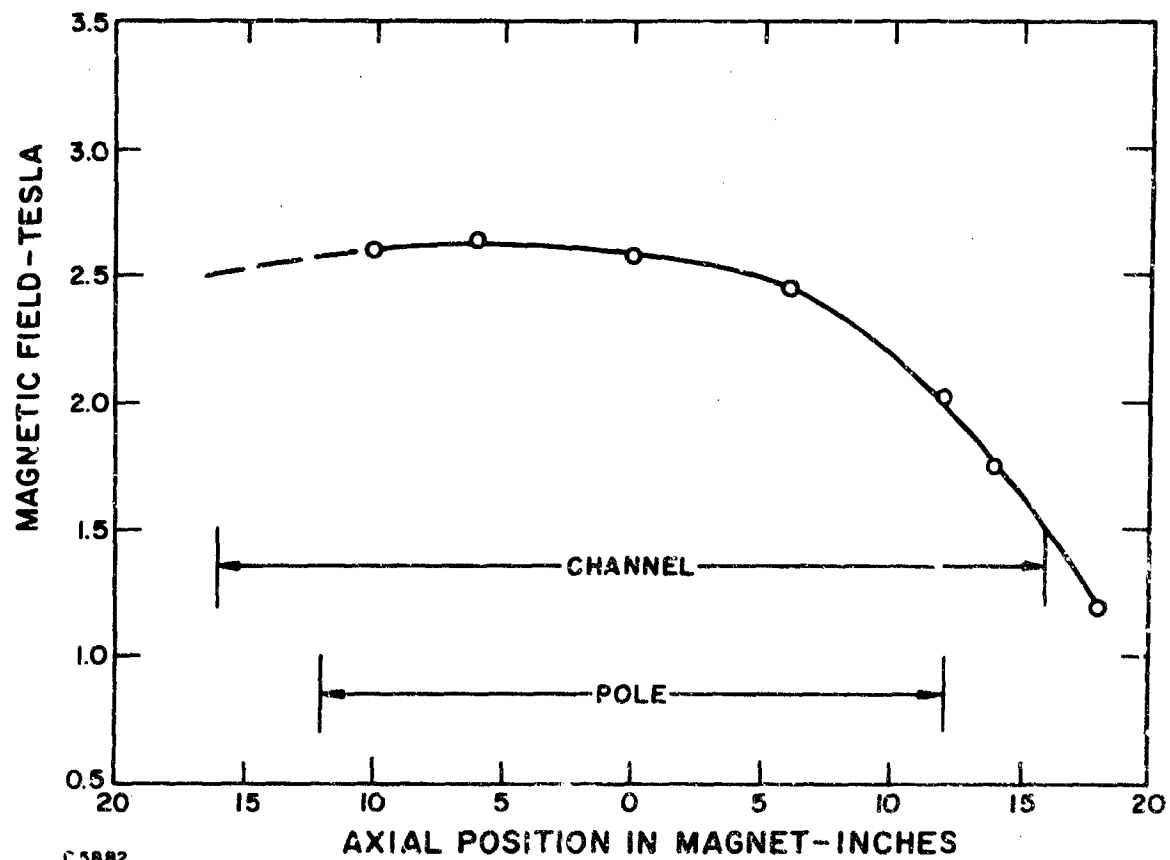


Figure 44 Axial Distribution of Flux Density of the Modified AERL Mark II Magnet.



NOT REPRODUCIBLE

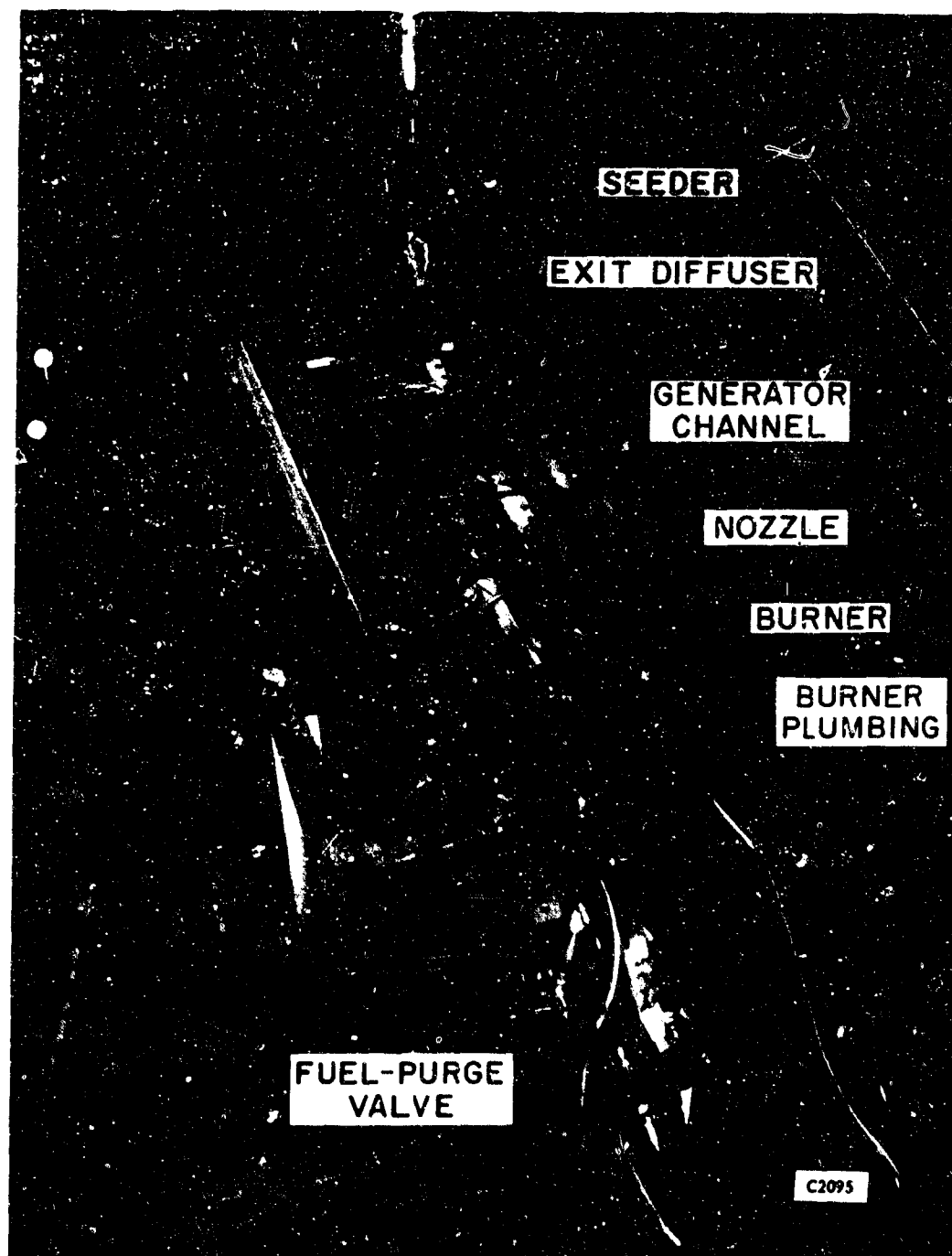


Figure 45 Photograph of the Generator Setup at AERL.

wiring and instrumentation also required changes. All of the revisions were individually relatively minor but collectively were very time-consuming.

## 5. BURNER MODIFICATION

The burner was originally designed for use with hydrocarbon fuels with an operating chamber pressure 6 atm and a mass flow rate of 0.68 kg/sec. In order to get satisfactory performance from the cyanogen-fueled channel it was necessary to increase the chamber pressure to 10 atm at the design flow rates. This change in chamber pressure and the change in oxidizer to fuel ratio required for stoichiometric combustion of cyanogen would have resulted in a condition where the oxidizer injectors would be operating subsonic. This situation could have produced low frequency instability. The remedy was to plug the inner row of oxidizer injectors, thereby changing the injector type from a triplet to a doublet. These plugs are removable so as to permit a return to the original configuration.

Burner operation was checked using toluene fuel and with a dummy channel made from transite pipe. Several runs were made to verify the action of the fuel system controls, check burner performance in a magnetic field, and to familiarize personnel with operating procedures. The modified burner has performed reliably with no evident change in combustion efficiency.

**BLANK PAGE**

## SECTION VI

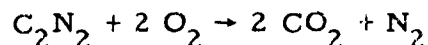
### EXPERIMENTS WITH CYANOGEN FUEL AT AERL

#### 1. INTRODUCTION

After the checkout of the burner operation and the facility were completed, and after the operating team was properly trained, cyanogen fuel testing was initiated. During a one-month test program, ten burner tests with cyanogen fuel were made. The electrical conductivity of the combustion products was measured in these tests, and in the last test the electron mobility was also measured. For safety reasons tests were only made under certain wind conditions. In particular, the wind velocity had to be 8 mph or more. The test program was slowed down considerably because of this requirement. The burner operated very well with the cyanogen fuel. No release of unburned cyanogen was detected at any of the sampling stations at any time.

#### 2. EXPERIMENTAL RESULTS

A stoichiometric mixture of cyanogen and oxygen was used burning to carbon-dioxide and nitrogen. The chemical equation for reaction is:



Since the heat of formation for liquid cyanogen is 68.5 kcal/mole, the preheat enthalpy for liquid cyanogen mixed with gaseous oxygen at room temperature is 650 cal/gm, see the Mollier chart for the mixture, Figure 46. The procedure for calculation of the preheat enthalpy is discussed in Section VII. The energy required to dissociate and heat the cesium carbonate seed is estimated to be about 10 cal/gm for each percent by weight of cesium. The estimate is based on data for potassium carbonate using the same mole fraction for the two seed materials. With the mass flow rate of about 0.68 kg/sec of cyanogen and oxygen, the heat transfer loss in the burner and nozzle is about 370 cal/gm. With these values the predicted burner stagnation conditions for the above combustion mixture with 2 percent seed are:

Enthalpy	260 cal/gm
Temperature	500° K
Pressure	10.5 atm
Entropy	2.14 cal/gm/°K

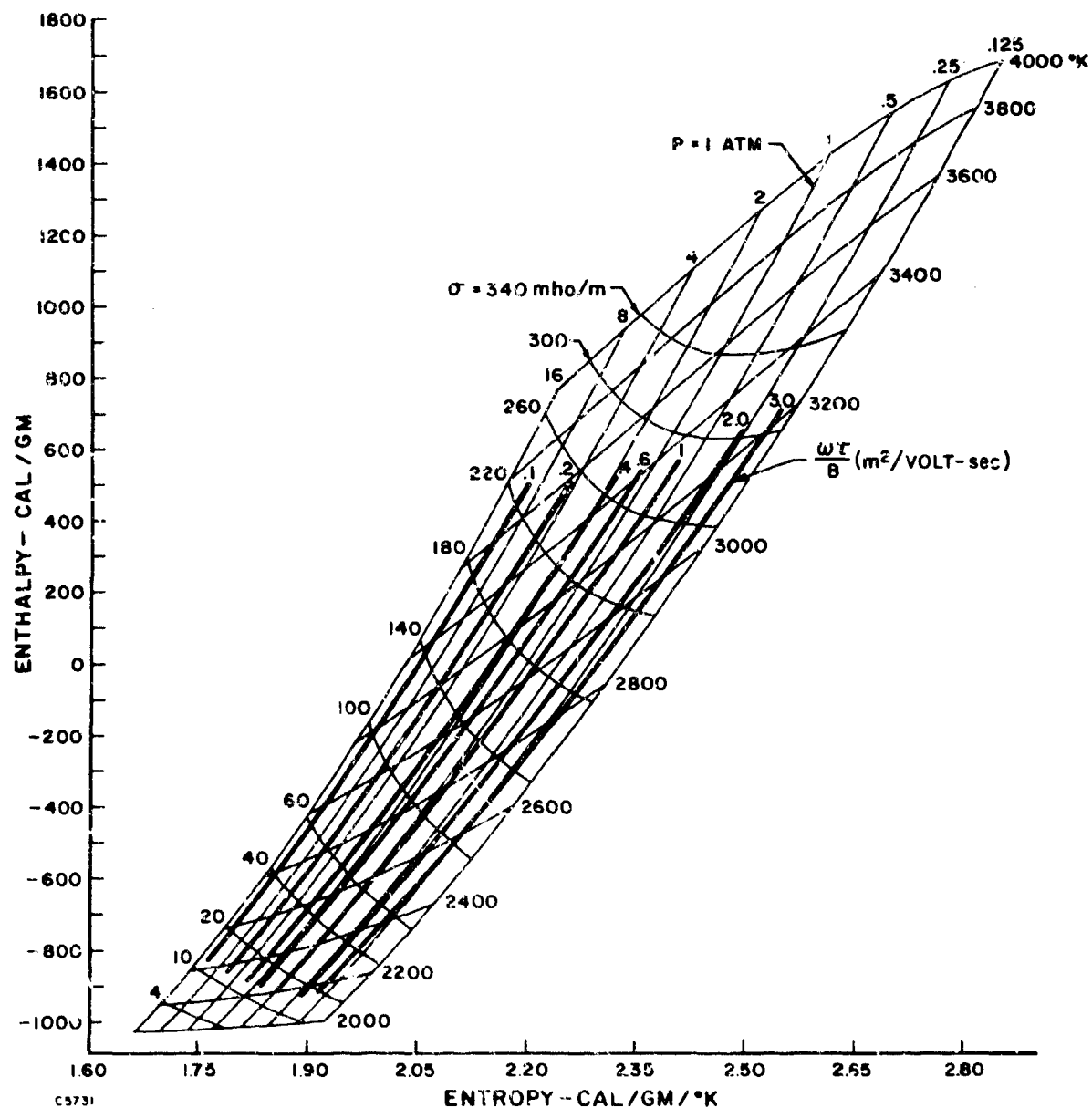


Figure 46 Mollier Curve for  $C_2N_2 + 2 O_2$  with 0.5% (Molar) Cs.

The pressure in the burner was measured and agreed within 2 percent with the predicted value. The duration of the tests varied from 5 to 7 seconds.

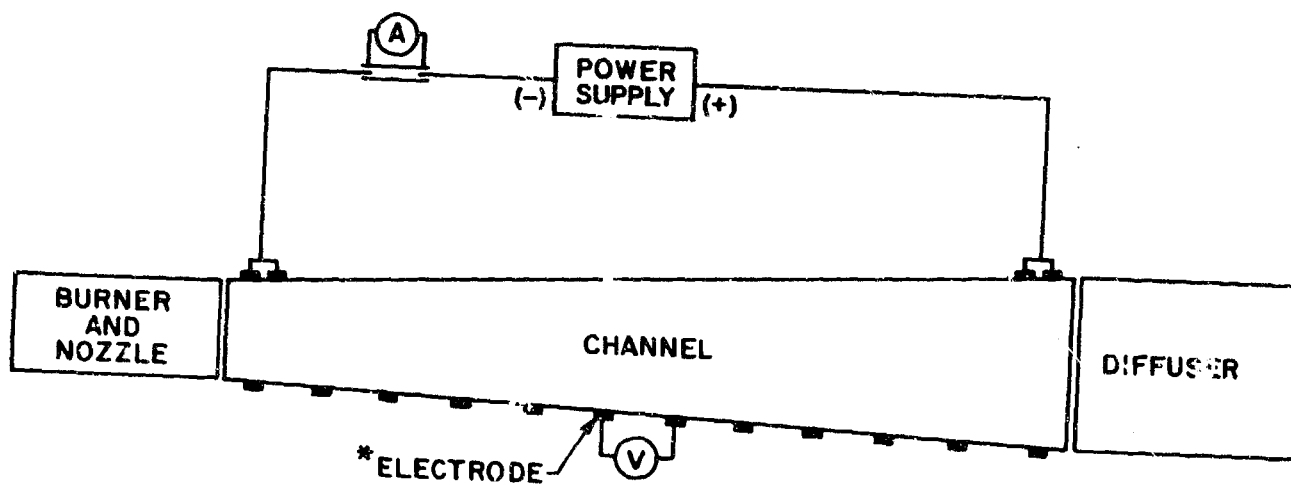
The electrical conductivity of the combustion products was measured both by applying a voltage along the channel from the exit to the inlet of the channel and by applying a voltage across the channel using seven electrode pairs. Two 55 kW Miller Welders (Miller Electric Manufacturing Company, Inc., Wisconsin) connected in series were used as power supply. The direct current open circuit voltage of this power supply was 325 volts. A ballast resistor was used to limit the current to 50 amps. The experimental set-ups are shown in Figures 47 and 48. A typical voltage distribution measured when the power supply is applied from the exit to the inlet of the channel (Figure 13) is shown in Figure 49, and an example of the voltage distribution measured when the power supply is applied across the channel electrode pair 28 (Figure 12) is plotted in Figure 50. The electrical conductivity of the gas,  $\sigma$ , was calculated by the following form of Ohm's Law,

$$\sigma = \frac{I \Delta l}{A \Delta V},$$

where  $I$  is the current flowing through area  $A$ , and  $\Delta V$  is the voltage difference over a segment of length  $\Delta l$ . It is seen that  $I/A$  is the local current density and  $\Delta V/\Delta l$  gives the absolute value of the local electric field. The accuracy of these measurements is 30 to 40 percent. The conductivity measured by applying a voltage across the channel was somewhat larger than the corresponding value measured when the power supply was applied along the channel. This is probably due to uncertainties in the values of the current densities.

The performance of the electrodes in terms of electrode voltage drop can be estimated from Figure 50. When the voltage distribution in the center of the channel is extended towards the walls as shown in Figure 50, the value of the electrode drops ( $V_{e1}$  and  $V_{e2}$ ) associated with the two electrode walls can be obtained. It is seen that for this test the cathode (electron emitter) drop is approximately 90 volts and anode drop is approximately 25 volts. The total electrode drop is then 115 volts. Boundary layer effects, electrode surface effects, and drops in the electrode material are all contributing to the measured electrode drops. As will be discussed later, the cyanogen fuel did contain appreciable amounts of impurities such as chlorine. With the chlorine impurity in the fuel removed, the electrode drop should be significantly smaller.

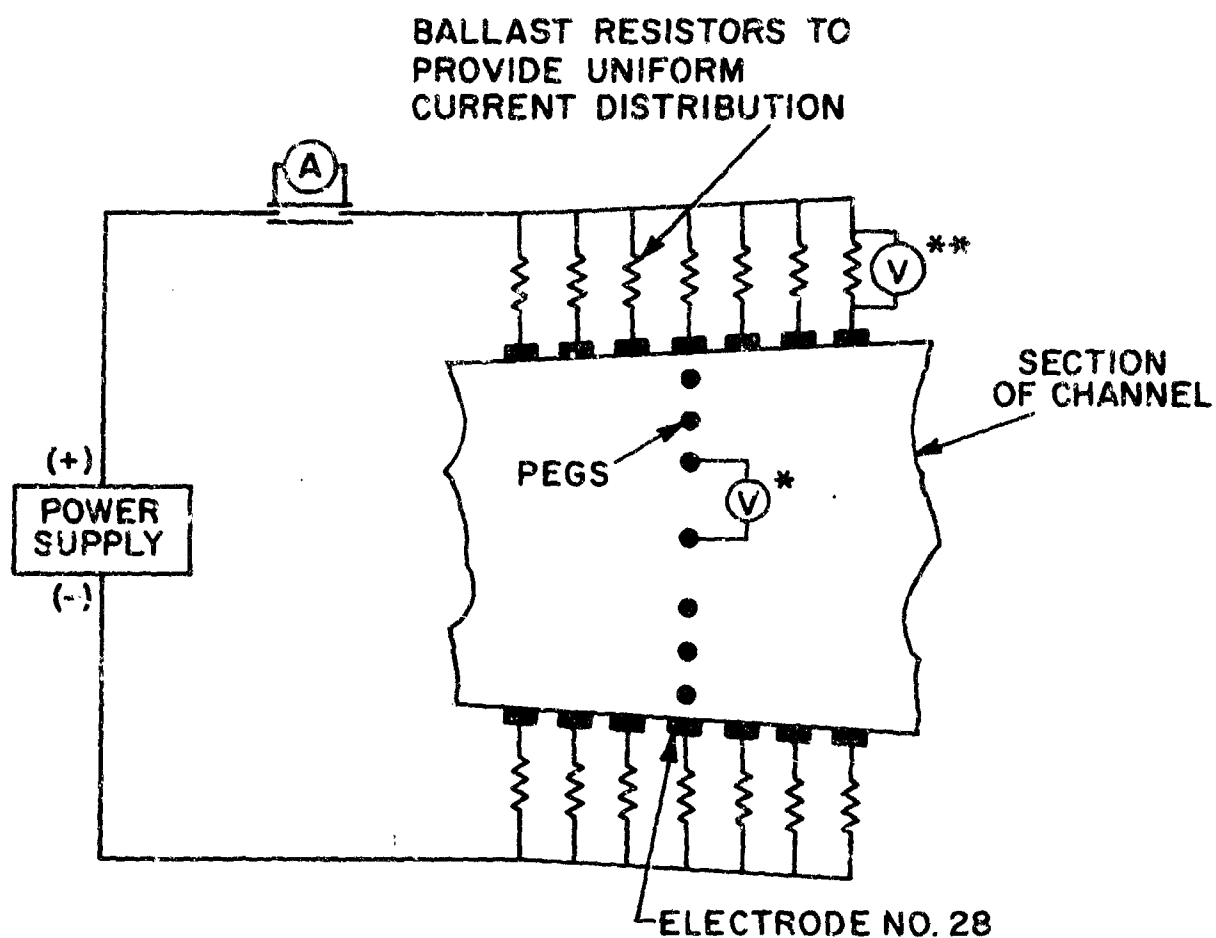
In these tests the flow rate of the cesium seed was varied from 0.7 to 4.5 percent by weight of the total flow of the combustion products, and at the 4.5 percent value a conductivity of 22 mhos/m was obtained. This is a factor of 7 to 7.5 lower than the anticipated value based on theoretical calculations. A systematic study was initiated to find the cause of this large discrepancy. The following possible causes were considered:



\* THE VOLTAGE BETWEEN ALL THE ELECTRODES SHOWN WERE MEASURED. ONE OF THE VOLTMETERS IS INDICATED.

C3032

Figure 47 Electrical Diagram for Conductivity Tests with Voltage Applied Along the Channel.



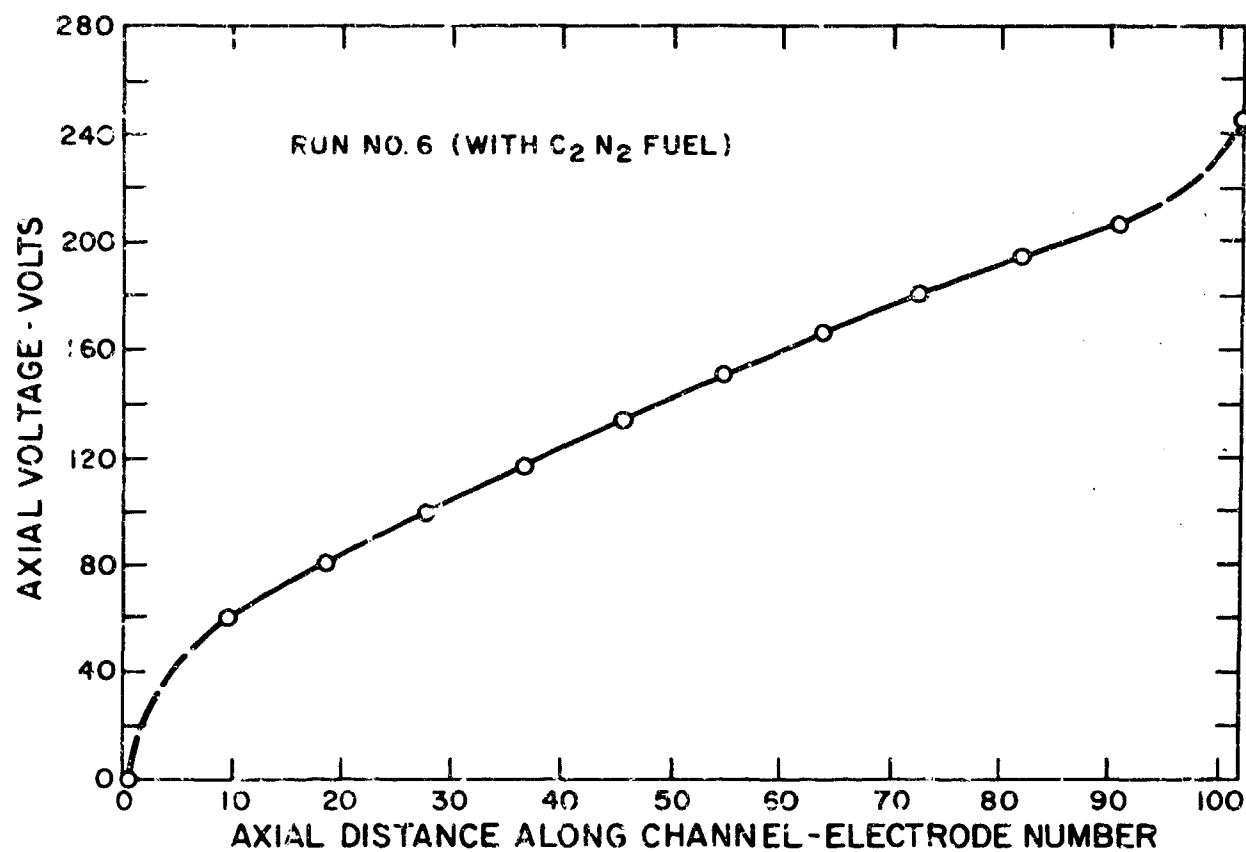
\*THE VOLTAGES BETWEEN ALL THE SEGMENTS SHOWN WERE MEASURED. ONE OF THE VOLTMETERS IS SHOWN.

\*\*VOLTMETERS FOR ALL THE RESISTORS WERE PROVIDED.

C 3C30

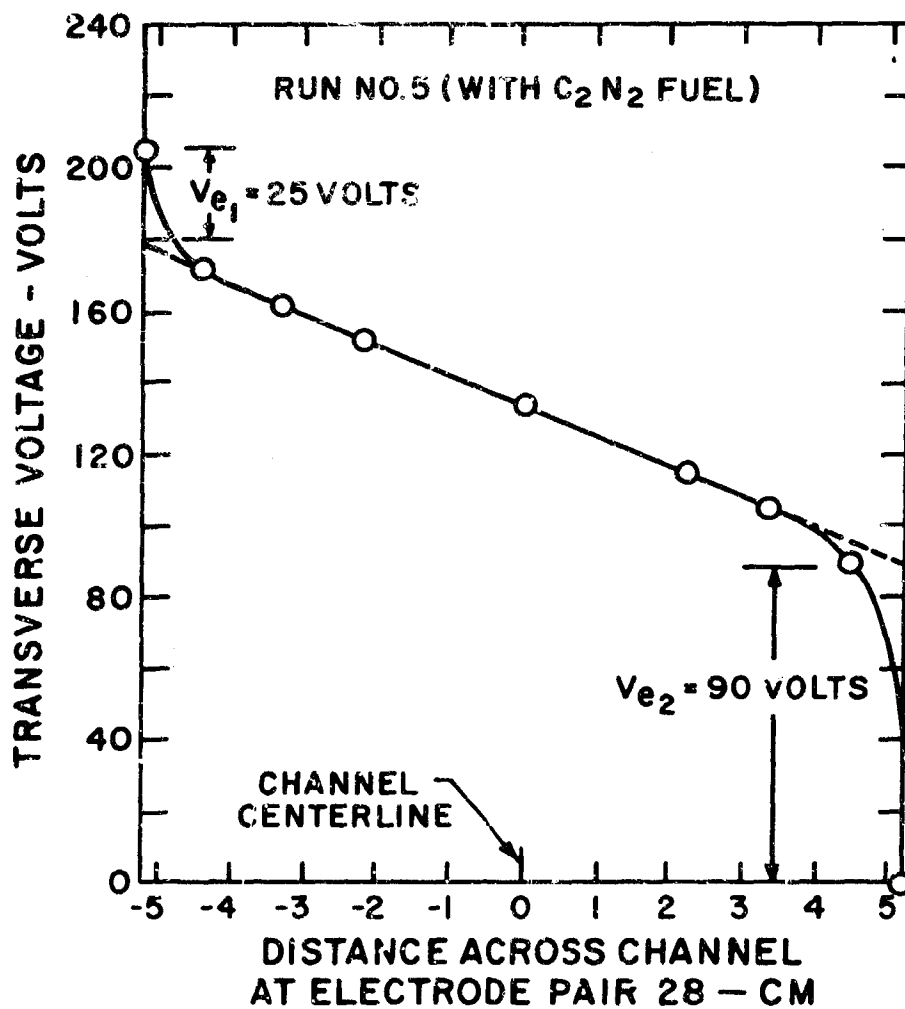
Figure 48 Electrical Diagram for Conductivity Tests with Voltage Applied Across the Channel at Electrode Pair 28.





C 3031

Figure 49 Observed Axial Voltage Distribution with Voltage Applied Along the Channel.



C3029

Figure 50 Observed Transverse Voltage Distribution with Voltage Applied Across the Channel at Electrode Pair 28.

- 1) Frozen flow and/or incomplete combustion.
- 2) Impurities in the fuel and/or in the oxidizer and/or in the seed.
- 3) Errors in fuel, oxidizer, and seed flow rates.
- 4) Faulty instrumentation.
- 5) Low burner efficiency (excessive energy losses).
- 6) Uncertainties in the theoretical calculations.

The first item on the list was checked both by theoretical and experimental means. The formation of carbon dioxide from carbon monoxide and oxygen was considered to be the critical reaction. If the formation of carbon dioxide were not completed in the burner or in the nozzle, the translational energy of the gas would be lower than the equilibrium value because the dissociation energy of the molecules involved has not been released. The translational temperature of the gas would therefore be lower than the equilibrium value. Since the electrical conductivity is a sensitive function of the gas temperature, a decrease in the temperature would reduce the conductivity significantly. Using a computer program for calculations of chemical nonequilibrium processes in supersonic nozzles available at AERL, it was concluded that the considered reactions were slow enough to cause some degree of freezing in the nozzle or incomplete combustion in the burner provided the amount of impurities was sufficiently small. Some contamination of the cyanogen and oxygen combustion products were provided by the pilot burner and by impurities in the fuel and oxygen. It was difficult to determine accurately the effect of these contaminants. In view of the fact that two or three mole percent of water in the flow would speed up the processes to insure chemical equilibrium, the facility was modified so that a small amount of methane could be injected into the burner. The methane burns forming water as one of the combustion products. Experiments with methane injection were then performed; however, no effects on the conductivity were observed. It was concluded that the gas was in chemical equilibrium and that the low conductivity value could not be explained by the effects discussed in this paragraph.

As far as impurities were concerned (Item 2) the oxygen and the seed was found to contain only insignificantly small amounts of impurities. However, tests on the cyanogen fuel revealed that the impurity content was more than an order of magnitude larger than the specifications called for. In particular, the chlorine content in the fuel was high. An accurate mass-spectrometer analysis of the cyanogen fuel was performed by the Gollob Analytical Service Corporation of Berkeley Heights, New Jersey. Measurable quantities of nitrogen, oxygen, carbon dioxide, hydrogen cyanide, cyanogen chloride, and chloroacetonitrile were discovered. The total amount of impurities was about 6 percent by weight, and the amount of chlorine was 2.1 percent by weight. These impurities lower the enthalpy of the gas since they are heated to the flame temperature in the burner. In addition, the cyanogen flow was smaller than planned because of the impurities, and the combustion mixture was therefore a few percent lean.

These effects in terms of conductivity should be relatively small and unimportant. The presence of the chlorine however would have a large effect on the conductivity because of two different effects. First, the attachment of electrons to the chlorine atoms decreases the electron density, and secondly, the formation of cesium chloride decreases the total number of cesium atoms available for ionization. Both effects tend to decrease the value of the conductivity. In Figure 51, a comparison between predicted and measured values of the conductivity near electrode pair 28 in the channel is shown as a function of the amount of cesium. With no impurities the theoretical conductivity varies from 86 mhos/m with 0.5 percent cesium to 158 mhos/m with 4.5 percent cesium. The chlorine impurity reduces the theoretical conductivity by a factor of 8.2 and 1.9 at 0.5 and 4.5 percent, respectively. The theory and experiments are seen to agree well at low seed rate, but at the high seed rate, the experimental values are lower than the theoretical values by about a factor of 3.5. It is concluded that the chlorine impurity in the fuel is the major factor in reducing the conductivity values; however, a significant discrepancy still exists at large seed rates. Clean cyanogen fuel was not available for testing. The predicted pressure (p), temperature (T), and conductivity ( $\sigma$ ) distributions for 3 percent seed (including the effects of the chlorine impurity) is shown in Figure 52. The channel area (A) distribution is also plotted.

As the next step in the procedure of establishing the cause of the discrepancy in the conductivity, Item 3 (Errors in the fuel, oxidizer, and seed flow rates) was investigated. The cyanogen fuel lines were cleaned so that the fuel turbine meter could be checked. The oxidizer and the seed flow meters were also recalibrated. It was concluded that these flow rates were, indeed, correct.

Item 4 (Faulty instrumentation) was investigated carefully; no faults were discovered. Redundant instrumentation was introduced into the experimental set-up and agreement on several different measurements was observed. The results of the two different conductivity measurements, discussed earlier, checked reasonably well. One further cross check on the data was made by measuring the Hall parameter. This measurement was made by applying a relatively small magnetic field across the channel normal to the peg insulator walls at the same time as an axial voltage was applied as in the conductivity tests. The test set-up is shown in Figure 53. For this situation where  $j_y = 0$ , Ohm's Law reduces to

$$j_x = \sigma E_x$$

$$j_y = 0 = \sigma E_y + \sigma u B - \omega \tau j_x$$

where  $j$ ,  $E$ ,  $\sigma$ ,  $u$ ,  $B$  and  $\omega \tau$  are the current density, the electric field, the conductivity, the velocity, the magnetic field and the Hall parameter, respectively. The subscripts indicate the vector components. The  $x$  and  $y$  directions are as shown in Figure 53. These equations combine to yield the following expression for the Hall parameter

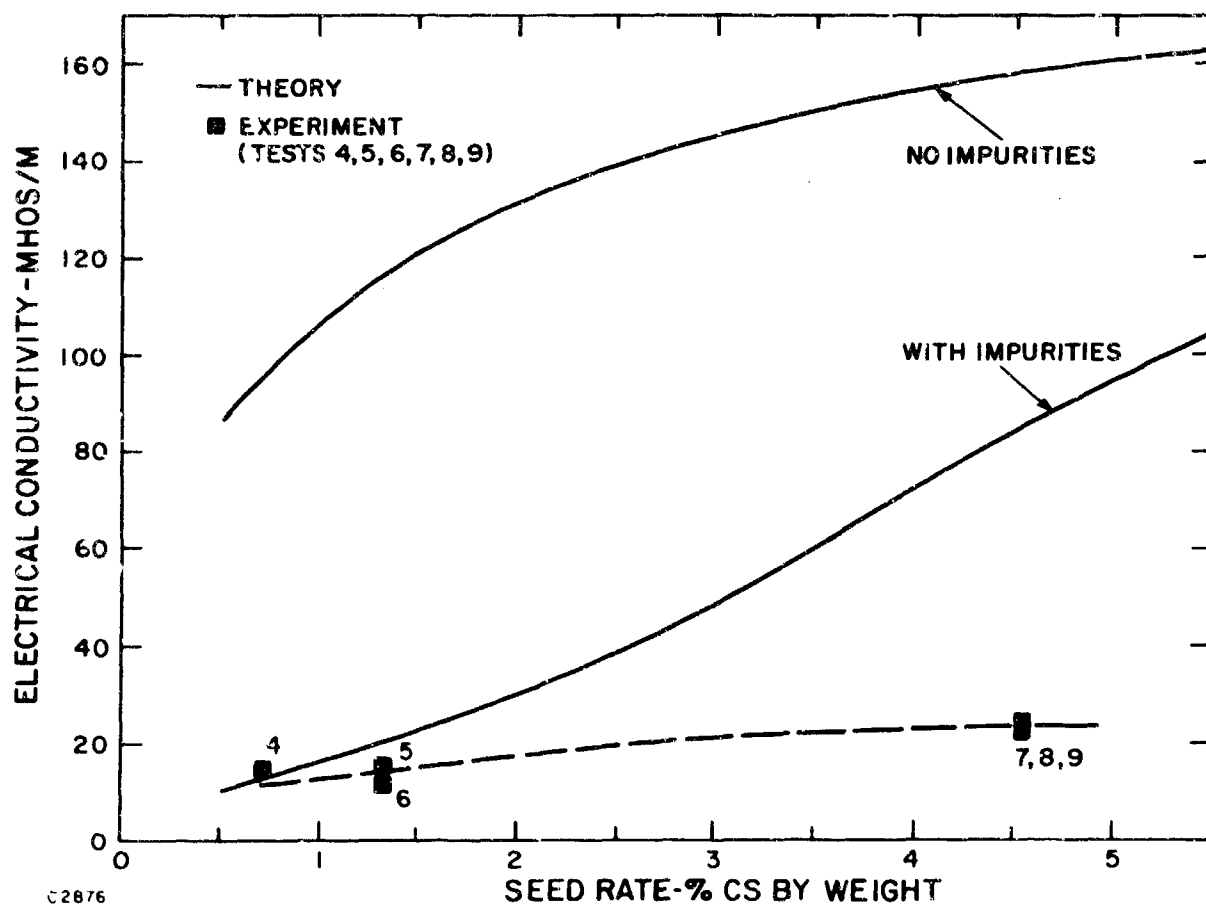


Figure 51 Observed and Predicted Values of Electrical Conductivity for Combustion Products of Cyanogen and Oxygen as a Function of Seed Rate;  $T = 2790^{\circ}\text{K}$  and  $P = 0.54 \text{ atm}$ .

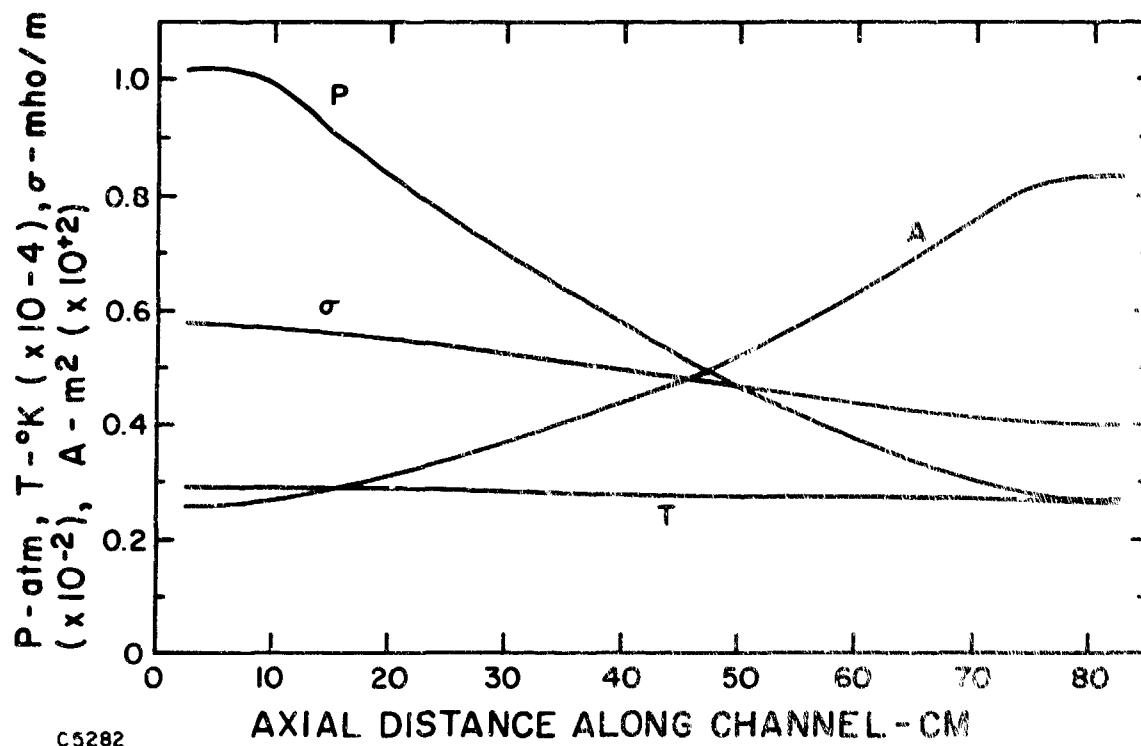
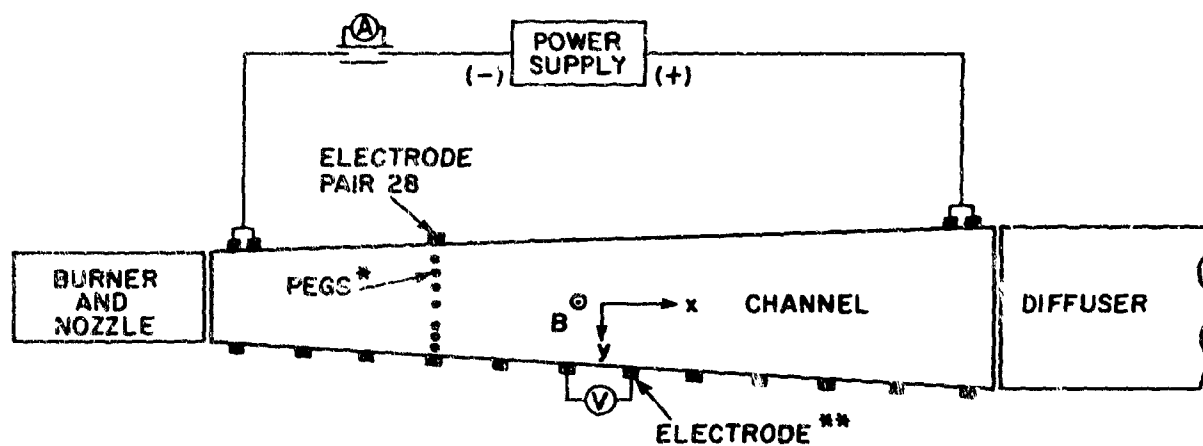


Figure 52 Predicted Distributions of Pressure, Temperature, Conductivity, and Area; Mass Flows of 0.68 kg/sec of Cyanogen and Oxygen.



\*THE VOLTAGES BETWEEN SEGMENTS WERE MEASURED

\*\*THE VOLTAGES BETWEEN ALL THE ELECTRODES SHOWN WERE MEASURED. ONE OF THE VOLTMETERS IS SHOWN.

C5283

Figure 53 Electrical Diagram for Hall Parameter Test.

$$\omega\tau = \frac{E_y + uB}{E_x}$$

Using this equation, the Hall parameter is evaluated from the observed voltage gradients  $E_y$  and  $E_x$ . The quantity  $uB$  is obtained from the transverse voltage profile at electrode pair 28 before the axial voltage is applied, and  $E_y$  and  $E_x$  is obtained from the transverse and axial voltage profiles, respectively, after the axial voltage has been applied. One test with cyanogen fuel was performed to measure the Hall parameter (or electron mobility). The experimental value of the Hall parameter was found to be lower than the theoretical value by a factor of about 1.4 to 1.7. The range in the value given here indicates the accuracy of these measurements. This result indicates that the discrepancy between the theory and the experiments in the conductivity values is due mainly to a difference in electron density rather than the electron mobility.

Item 5 (Low burner efficiency) was investigated next. To check the burner efficiency conductivity measurements were made with toluene fuel; good agreement between theory and experiments was observed indicating that the burner was operating as predicted. Of course, the flame temperature is higher with cyanogen than with toluene, and, therefore, the radiation loss in the burner will be larger with cyanogen. It is estimated that this will reduce the burner efficiency slightly; but considerably less than that required to explain the discrepancy in the conductivity. An overall burner efficiency of about 80 percent is estimated burning cyanogen.

The last item on the list of possible explanations for the difference that still exists, between the theoretical and experimental values of the conductivity is concerned with uncertainties in the theory. At this laboratory the conductivity calculations have been checked thoroughly using several different hydrocarbon fuels, and good agreement between theory and experiments have been observed. The most significant differences between the present experiments and the previous hydrocarbon fuel experiments appear to be the presence of chlorine and the absence of hydrogen in the gas in the present experiments.

The properties of chlorine used in the theory have been checked in other applications and are expected to be reasonably accurate; however, no measurement of the type discussed here has been made before. As discussed earlier, no change in the conductivity was observed. Of course, the amount of hydrogen introduced this way (in the methane) is small compared to the amount present when burning hydrocarbon fuels. Theoretical calculations indicate that in terms of the chemical reactions in the burner, a significant amount of hydrogen was injected. On the other hand, the value of the electron mobility, and, therefore, the conductivity depends on the concentration of hydrogen in the gas. However, the measured value of the mobility agrees fairly well with theory as discussed earlier. No obvious uncertainty in the theory that would explain the remaining discrepancy has been found.



If the burner losses are a stronger function of seed rate than estimated, this would tend to bring the theoretical and experimental values closer together. But previous experiments with the same seed material indicate that the losses have been correctly taken into account. The energy required to bring the seed material (cesium carbonate) into equilibrium with the gas has been estimated based on data for potassium carbonate using the same mole fraction for the two seed materials.

No power-generation tests were performed with cyanogen since the conductivity was so small. Therefore, to establish the power-generating capability of the channel a few power runs were made using toluene fuel. The channel was connected in the diagonal configuration at an angle of about 45 degrees. Grading resistors were used at the power take-off electrodes. The power generated was approximately 300 kW including the power in the grading resistors. The total axial voltage was 1370 volts. The mass flow was 0.59 kg/sec and the magnetic field at the middle of the channel was 2.6 Tesla. The electrode drop in the front of the channel was 40 volts and at the end it was about 115 volts. The generator worked well during these tests. The details of further power-generation tests with conventional hydrocarbon fuels such as toluene will be discussed in Section VIII. A maximum output of 400 kW was achieved in these tests.

### 3. CONCLUSIONS AND RECOMMENDATIONS

The measured values of the electrical conductivity of the combustion products of cyanogen and oxygen was a factor of 7 to 7.5 lower than the theoretically predicted values. The major cause of this discrepancy was found to be impurities in the cyanogen fuel. Tests revealed that the chlorine content of the cyanogen fuel was 2.1 percent by weight, more than an order of magnitude larger than the specifications called for. Theoretical calculations indicated that the chlorine would reduce the conductivity by a factor of 8 to 2, depending on the seed rate.

At high seed rates a significant further discrepancy still remains. The experimental values are lower than the theoretical values including the effects of chlorine by about a factor of 3.5 at a seed rate of about 4.5 percent by weight. No single cause of the remaining discrepancy has been discovered. Possibly a combination of the different phenomena considered is responsible for this behavior. To understand this behavior, more experiments must be performed.

No power generation tests were performed with cyanogen since the conductivity did not come close to its expected high values. However, the power-generating capability of the channel was established using conventional hydrocarbon fuels, in this case toluene.

It is recommended that additional experiments with cyanogen be performed. It is, of course, essential to use clean fuel so that the

effect of the chlorine can be eliminated. Furthermore, it would be very useful to add additional instrumentation. For example, a measurement of the temperature of the gas and the electron density would be valuable in determining the cause of possible discrepancies such as still exist in the present results.

**BLANK PAGE**

## SECTION VII

### ANALYSIS OF HALL MHD GENERATOR

As part of the work performed under this contract, a computer program, named Hall Generator Off Design Program, capable of calculating the performance of a Hall MHD generator system starting with the dimensions of the system, burner conditions and the composition of the working plasma was developed and checked out. In this section a general discussion is presented relative to the overall program. Appendix 2 has been included in this report for the purpose of explaining in detail the inputs, logic and subroutines used in this analytic program. The reader is referred to this appendix if the specifics of the program are desired.

The program is composed of a number of subprograms, these programs being used as follows:

- 1) Mollier chart subroutine - corresponding to a given gas composition, seed rate, temperature range and pressure range, this subroutine is used to establish a table and charts for enthalpy, temperature, conductivity, Hall coefficient, specific heat ratio, density, and entropy for the range of interest.
- 2) Hall Generator Off Design Program - "PP23" - subroutine beginning with burner stagnation pressure, mass flow, enthalpy and a nozzle contour, the channel inlet conditions are determined and then corresponding to a given channel axial area profile and channel loading, the performance of the channel is calculated. Simultaneously, the boundary layer thickness is computed and the core area determined at each point calculated along the length of the channel. Also, the mean Mach number and stagnation pressures are calculated for a number of points as an indication of the recovery capability of the working gas. As will be discussed, an unbounded growth of the shape factor associated with the boundary layer is taken to be an indication that the generator will stall for the conditions being analyzed. The program is arranged so that calculations stop if the shape factor becomes large.

The above subprograms will now be discussed in more detail.

#### 1. THERMODYNAMIC EQUILIBRIUM CALCULATIONS

The performance calculations of an MHD generator require a detailed knowledge of the thermodynamic properties of the combustion products for

a range which corresponds to the actual operating range to be analyzed or predicted. The Mollier chart subroutine calculates the equilibrium thermodynamic properties of the combustion products. This can be done for the combustion products of any mixture of C-H<sub>2</sub>-O<sub>2</sub>-N<sub>2</sub>. The combustion products are assumed to consist of CO<sub>2</sub>, CO, H<sub>2</sub>O, OH, O<sub>2</sub>, O, N<sub>2</sub>, N, H<sub>2</sub>, H, and NO. The calculations yield concentrations, enthalpy, entropy, and molecular weight as functions of temperature and pressure. In addition, the concentrations of CN, NH, and carbon vapor are estimated. Each component of the combustion products is assumed to be a "thermodynamically ideal" gas, and the calculations do not take account of any solid or liquid-phase components. The presence of a significant concentration of C<sub>gas</sub> in the products is indicative of insufficient O<sub>2</sub> to permit complete combustion of the C<sub>solid</sub> to CO and CO<sub>2</sub>, thus invalidating the calculation procedures.

Properties for a pressure range from 1/8 atm to 32 atm and a temperature range from 2000°K up to 5000°K can be calculated. The calculation is carried out using the techniques of statistical mechanics to determine the equilibrium concentrations of all the species in the working gas for the range of pressure and temperature of interest. The computer outputs the calculated equilibrium properties in tabular form with the various gas properties being listed as functions of the enthalpy and pressure for the range of interest (input data) which is used in conjunction with the performance calculations. Usually the data are displayed in the form of Mollier diagrams such as the chart shown in Figure 54 for the combustion products of cyanogen and oxygen with a carbon-to-oxygen ratio of one (1). The Mollier diagram shown in Figure 54 covers a pressure range from 1/4 atm to 16 atm and a temperature range from 2000-5000°K. The zero of the enthalpy scale is appropriate to solid carbon, gaseous N<sub>2</sub>, O<sub>2</sub>, and H<sub>2</sub> at 0°K. In order to determine the adiabatic flame temperatures of the fuel-oxidizer mixtures considered, the difference in enthalpy supplied with fuel and oxidizer from the defined zero value, the preheat enthalpy, must be established. It is pertinent to note that only the relative ratios of carbon, oxygen, hydrogen, and nitrogen need to be specified in order to determine a given Mollier diagram. The heat of formation for any given fuel and oxidizer does not affect the equilibrium calculations, but it must be taken into account in determining the preheat enthalpy and the burner stagnation enthalpy. The preheat enthalpies, H, in calories per gram of total mixture, are determined from the heats of formation ( $\Delta H_{fo}$ ) and heat contents ( $\int C_p dT$ ) of the reactants at the temperature at which they are mixed, expressed by the equation:

$$1. \quad H = \underbrace{\Delta H_{fo}}_{\substack{\text{Heat of form.} \\ \text{of fuel at } 0^\circ\text{K}}} + \underbrace{\Delta H_{fo}}_{\substack{\text{Heat of form.} \\ \text{of oxidizer at } 0^\circ\text{K}}} + \underbrace{\int_0^T C_p dT}_{\substack{\text{Heat content} \\ \text{of fuel}}} + \underbrace{\int_0^T C_p dT}_{\substack{\text{Heat content} \\ \text{of oxidizer}}}$$

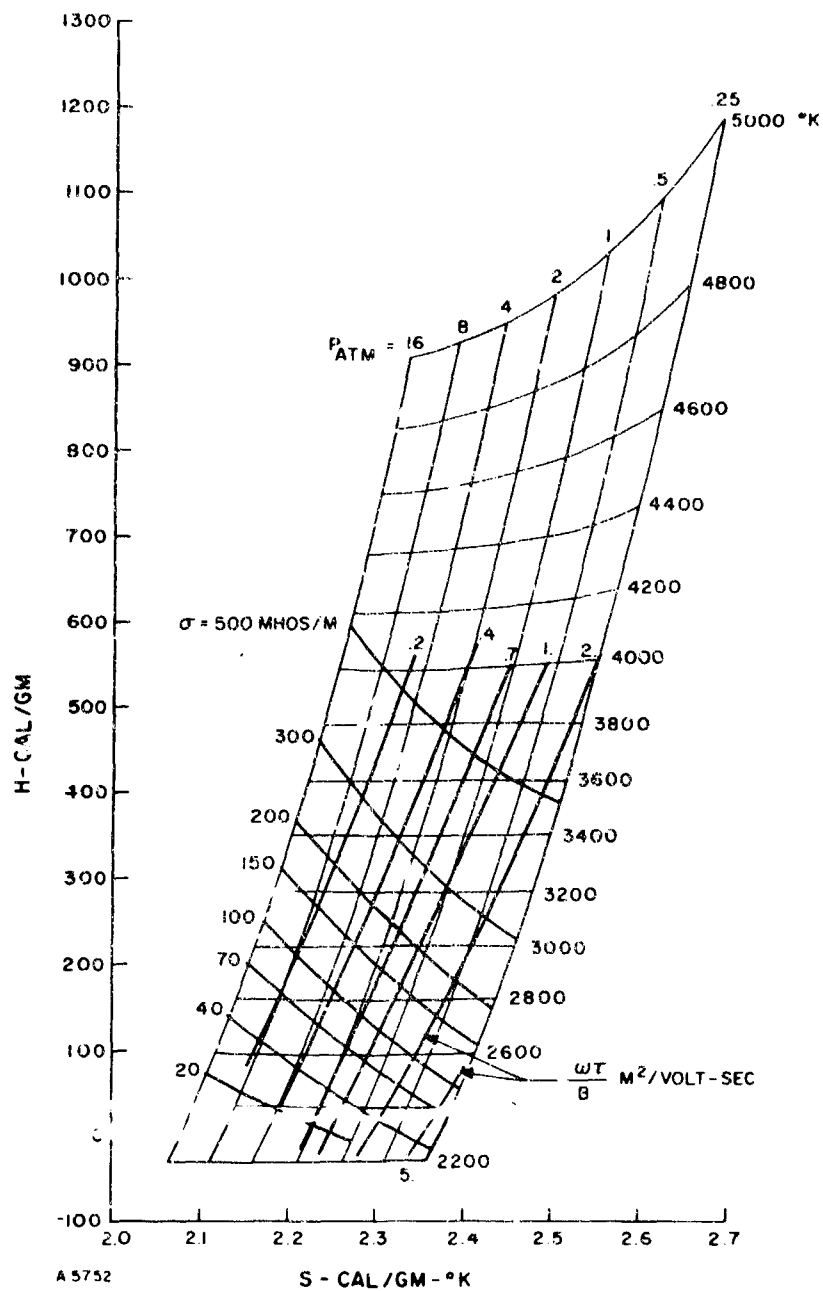


Figure 54 Mollier Chart,  $\text{C}_2\text{N}_2 + \text{O}_2$ , C/O = 1 Seeding Rate of 0.5 Mole %.

or

$$\begin{aligned}
 2. \quad H = & \Delta H_{fo} + \Delta H_{fo} + \int_0^T C_p dT + \int_0^T C_p dT \\
 & \text{Heat of form.} \quad \text{Heat of form.} \quad \text{Heat content} \quad \text{Heat content} \\
 & \text{of fuel at} \quad \text{of oxidizer at} \quad \text{of solid car-} \quad \text{of nitrogen} \\
 & \text{temp. } T \quad \text{temp. } T \quad \text{bon} \\
 & + \int_0^T C_p dT + \int_0^T C_p dT \\
 & \text{Heat content} \quad \text{Heat content} \\
 & \text{of oxygen} \quad \text{of hydrogen}
 \end{aligned}$$

T = temp. at which reactants are mixed.

An example of determining the preheat enthalpy and the adiabatic flame temperature for a mixture of  $C_2N_2$  and gaseous  $O_2$  is presented below:

#### Example of Preheat Calculations

Mixture $C_2N_2 + O_2$ (C/O = 1) mixed at $298^\circ K$		
Reactants	Mass	Heat of Formation at $298^\circ K$
$C_2N_2$ gas	52 gm	69 433 cal.
$O_2$ gas	32 gm	0
	84 gm	69 433 cal.

#### Heat Content at $298^\circ K$

2 C solid	2 x 250 =	500 cal.
1 $N_2$ gas	1 x 2072 =	2072 cal.
1 $O_2$ gas	1 x 2075 =	<u>2075 cal.</u>
		4647 cal.

Total Enthalpy (heat of formation + heat content) = Preheat Enthalpy =

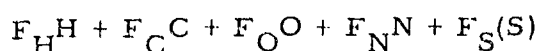
$$\frac{74080}{84} = 873$$

Entering the Mollier diagram Figure 54 an adiabatic flame temperature of  $4750^\circ K$  is predicted at 1 atm. The actual flame temperature, of course, depends on several factors including most notably the completeness of burning and the burner heat losses. Since these quantities are difficult to calculate depending on the burner geometry, material used in construction of the burner, residence time, etc., a burner efficiency is usually estimated based on prior experience. The burner efficiency is defined to be the ratio of the actual stagnation enthalpy of the combustion products to the predicted stagnation enthalpy. Prior experience indicates the losses to be 5 to 10 percent of the predicted stagnation enthalpy or that the burner efficiency is 90 to 95 percent for the type of burner used in this program.

As already mentioned, the zero of the enthalpy scale is appropriate to solid carbon, gaseous  $N_2$ ,  $O_2$ , and  $H_2$  at  $0^\circ K$ . The enthalpy difference between the zero of the enthalpy scale and absolute zero is referred to in the program as  $\Delta H_C$  and is computed from the following equation:

$$\Delta H_C = \frac{(9.3969 F_C + 2.8553 F_H + H_{foS} \times 10^{-4} F_S) \times 10^4}{12.011 F_C + 1.008 F_H + 16 F_O + 14.008 F_N} \text{ cal/gm}$$

where the  $F_i$  are the stoichiometric coefficients of the reactants:



and the symbols are defined as:

H	Hydrogen
C	Carbon
O	Oxygen
N	Nitrogen
S	Seed
$H_{foS}$	Heat of Formation of the Seed

The predicted stagnation enthalpy is the combination of  $\Delta H_C$  and the preheat enthalpy. Taking a value 90 to 95% of the predicted value and subtracting  $\Delta H_C$  yields the enthalpy corresponding to the predicted actual flame temperature. This number is an input constant for the present program ( $H_{B\phi}$  on the "INPUTS" sheet).

Following the computations of thermodynamic properties, the electrical properties of the combustion gases are computed as functions of temperature and pressure. The computed electrical properties are the electrical conductivity  $\sigma$  in mhos/m, and  $\omega\tau/B$  in  $m^2/\text{volt-sec}$ , the ratio of Hall coefficient for electrons to the magnetic field strength which is equal to the electron mobility,  $\mu$ , the electron drift velocity/unit electron field. These quantities have been computed using established cross-section data and the Saha equation. The equations used to calculate the conductivity and Hall coefficient are listed in Appendix 2. Different seed concentrations ranging from 0.1 to 1% by volume (seed concentration defined at  $3000^\circ K$  and 1 atm) of potassium and cesium have been considered, but only one concentration 0.5% has been indicated on the Mollier charts. Calculated values of gas conductivities,  $\sigma$ , in mhos/m, and electron mobilities,  $\omega\tau/B$  in  $m^2/\text{volt sec}$ , are plotted on the Mollier diagram of Figure 54 for a seed concentration of 0.5% cesium.



## 2. CALCULATION OF CHANNEL INLET CONDITIONS

On passing out of the burner, the combustion products pass through an expansion channel and then into the channel. (Typically, the flow exits the nozzle at supersonic speeds.) The program for calculating the inlet conditions for the channel requires as input data, dimensions of the nozzle, specifically the throat diameter and exit diameter, the burner stagnation enthalpy (corrected for losses, etc.,  $-H_{B\phi}$  above), the mass flow and the burner stagnation pressure. As a first step, the program directs the computer to look up all of the thermodynamic equilibrium data (a table is stored as output from the first subprogram) corresponding to the input values of stagnation pressure and temperature. Using the equilibrium data, the procedure to obtain the inlet conditions to the channel is:

- 1) Since  $H_{B\phi} = H_{TH} + 1/2 u^2$  for an isentropic process, at the throat of a supersonic nozzle this becomes  $H_{B\phi} = H_{TH} + 1/2 C^2$  (sonic velocity at the throat) or  $\Delta H = H_{B\phi} - H_{TH} = 1/2 C^2 = 1/2 (\gamma R)_{B\phi} T_{TH}$ ; however, for an isentropic process:

$$\frac{T_{B\phi}}{T_{TH}} = \frac{(1+\gamma)}{2} \text{ so that } C = \gamma R T_{TH} - \gamma R \frac{2}{(1+\gamma)} T_{B\phi} \quad \text{where:}$$

$H_{TH}$  is the static enthalpy at the throat

$u$  is the velocity

$C$  is the speed of sound

$\gamma$  is the specific heat ratio

$T_{TH}$  is the static temperature at the throat

$R$  is the universal gas constant

and

$T_{B\phi}$  is the burner stagnation temperature (obtained by lookup in the Mollier table corresponding to  $P_{B\phi}$  and  $H_{B\phi}$ )

- 2) From above,  $H_{TH}$  can be obtained from the equation,

$$H_{TH} = H_{B\phi} - 1/2 C^2.$$

Using  $H_{TH}$  and  $S_{TH} = S_{B\phi}$  (entropy), the thermodynamic properties of the combustion products at the throat can be determined by table lookup.

- 3) The value of  $C$  obtained in Step (1) above is not accurate because  $\gamma$  and  $\gamma R$  corresponding to burner conditions are used. A more accurate value of  $C$  can be obtained by using the  $\gamma$  and  $R$  determined in Step (2) or:

$$C = (\gamma R)_{TH} T_{TH}$$

- 4) Calculate the mass flow as

$$\dot{m} = \rho_{TH} C A_{TH}$$

- 5) The flow accelerates after passing the throat and expands to a lower pressure at higher velocities. The remainder of the calculation is to determine the inlet conditions starting at the throat by iteration knowing that

$$\Delta H = H_{TH} - H_{inlet} = 1/2 u^2 = 1/2 \left( \frac{\dot{m}}{\rho_{inlet} A_{inlet}} \right)^2$$

and that the process is isentropic. The iteration is begun by assuming a small  $\Delta H$  and then checking the above equation. This process is continued (with the increment being reduced as the point is reached) until the above equation is satisfied. With  $H_{inlet}$  and  $S_{inlet} = S_{TH} = S_{B\phi}$  the thermodynamic properties of the gas can be determined at the inlet of the channel again by table lookup.

### 3. MHD CHANNEL PERFORMANCE ANALYSIS (Hall Generator Off Design Program - "PP23" - Subroutine)

The performance analysis for the Hall connected MHD generator is an extension of one-dimensional methods previously developed for analysis of the Faraday configuration.\* One important difference is the treatment of the boundary layer. In previous analysis, the flow was considered to be fully developed. A friction term was included in the momentum equation, a heat transfer term in the energy equation, and the flow characteristics represented an average across the channel. However, due to the small length/diameter ratio which is typical for MHD channels, the flow is far from fully developed, but rather consists of an inviscid region occupying most of the channel area and a boundary layer confined to the immediate vicinity of the channel walls. Thus, the methods of boundary layer analysis have been employed for the present work, and the influence of the boundary layer in reducing the effective channel area has been considered. The appropriate one-dimensional momentum, energy and continuity equations are:

$$\rho u \left( \frac{du}{dx} \right) + \frac{dp}{dx} = J_y B = -\sigma U B^2 (1 - \alpha) \quad (\text{momentum}) \quad (1)$$

\*Louis, J. F. et al., "Studies of Fluid Mechanics Using a Large, Combustion Driven MHD Generator," Avco Everett Research Laboratory Research Report 145, March 1963.

$$\rho u \left( \frac{dh}{dx} + u \frac{du}{dx} \right) + J_x E_x + J_y E_y = -\sigma U^2 B^2 \left[ \alpha(1-\alpha) - \frac{\alpha^2}{(\omega_e \tau_e)^2} \right] \quad (2)$$

(energy)

$$\frac{1}{\rho} \left[ \left( \frac{\partial \rho}{\partial h} \right)_p \frac{dh}{dx} + \left( \frac{\partial \rho}{\partial p} \right)_h \frac{dp}{dx} \right] + \frac{1}{u} \frac{du}{dx} + \frac{1}{A} \frac{dA}{dx} = (\text{continuity}) \quad (3)$$

where sub y refers to the transverse direction; sub x refers to the axial direction; h is the static enthalpy;  $\rho$  is the density; u is the velocity; p is the static pressure; J is the current density; E is the field intensity, A is the area and

$$\alpha = \frac{\omega \tau J_x}{\sigma u B}$$

Note from the momentum Eq. (1) how the Hall generator loading coefficient plays the same role as  $E_y/UB$  for the Faraday generator. The last term in the energy Eq. (2) represents the effect of dissipation due to axial current.

In addition to the above equations several other equations are incorporated in the performance analysis. These are:

For determining  $J_x$  under a load condition

$$J_x = I/A \quad (4)$$

where I is the total current

For determining  $J_y$  ( $J_y'$  is introduced here to avoid positive current densities which would appear in the calculations if the electrode drop were greater than the generated voltage. As shown below, in this case  $J_y' = J_y = 0$ ).

$$J_y' = \frac{J V_e}{D_2} - (1 - \alpha) \sigma u B \quad (5)$$

$$\text{If } J_y' \geq 0 \quad J_y = 0, E_y = (1 - \alpha) u B, E_x = \frac{J_x}{\sigma} \quad (6)$$

$$J_y' \leq 0 \quad J_y = J_y', E_y = \frac{V_e}{D_2}, E_x = 1 - \alpha - \frac{\alpha}{\omega^2 \tau^2} - \frac{V_e}{D_2 u B} \omega \tau u B \quad (7)$$

For determining the electrode drop

$$V_e = K_1 GH + K_2 \quad (8)$$

where  $K_1$  and  $K_2$  are input constants;  $\Theta$  is the momentum thickness and  $H$  is the shape or  $\Theta H \equiv \delta^*$  which is the displacement thickness ( $\Theta$ ,  $H$  and  $\delta^*$  will be discussed below). The first term of the electrode drop is variable with the boundary displacement thickness.

For determining the core diameter

$$D_{\text{core}} = D_{\text{actual}} - 2 \Theta H \quad (9)$$

The momentum thickness of the boundary layer,  $\Theta$ , can be estimated using the momentum integral equation:

$$\frac{d\Theta}{dx} + \frac{\Theta}{U} \frac{dU}{dx} (2 + H) \frac{\Theta}{\rho} \frac{d\rho}{dx} = \frac{C_f}{2} \quad (10)$$

where  $C_f$  is the wall friction coefficient defined as the ratio of twice the wall shear,  $\tau$ , divided by  $\rho u^2$ ,  $U$  is the free stream velocity, and  $H$  is the so-called incompressible shape factor defined by  $H = \delta^*/\Theta$ , where  $\delta^*$  is the boundary layer displacement thickness. The value of  $H$  can be used to conjecture regarding the stability of the boundary layer for the case of low speed flow and small wall cooling using, for instance, the empirical correlation equation of Garner\*:

$$\left( \frac{U\Theta}{\nu} \right) \Theta^{\frac{1}{5}} \frac{dH}{dx} = e^{5(H-1.4)} \left[ - \left( \frac{U\Theta}{\nu} \right) \Theta^{\frac{1}{5}} \frac{\Theta}{U} \frac{dU}{dx} - 0.0135 (H - 1.4) \right] \quad (11)$$

where  $\nu$  is the kinematic viscosity. With a given velocity distribution, simultaneous solution of Eqs. (10) and (11) determines  $\Theta$ ,  $H$  and  $\delta^*$ . For an incompressible flow, the value of  $H$  for a turbulent flat plate with zero pressure gradient is 9/7, and a value of  $H = 1.8$  is believed to indicate incipient separation.

In an ordinary boundary layer analysis, velocity gradients arise due to the presence of curved surfaces or shock waves which lead to pressure discontinuities. In the case of a high speed compressible flow, the flow is generally at least streamwise isentropic except in the immediate neighborhood of shock waves or other discontinuities, so that there is a unique relationship between the pressure distribution and the velocity gradient in Eqs. (10) and (11) at the edge of the boundary layer. In an MHD flow with body forces, however, a careful distinction between electrode and insulating walls is necessary. On the electrode boundary layer, the current flows across the boundary layer normal to the flow so that the velocity gradient computed from Eq. (1) should be used for the solution of Eqs. (10) and (11). However, in the case of the insulating wall, the magnitude of the apparent velocity gradient depends on wall temperature.

\*Garner, H. C., "The Development of Turbulent Boundary Layers," ARC R & M 2133 (1944).

If the wall temperature is below that of the stream so that the gas near the wall in the region of high shear is a poor conductor of electricity, the body force on the insulating wall boundary layer will be small and the effective velocity gradient negligible or even favorable so that the insulating wall boundary layer is very stable, while, at the same time, the electrode boundary layer is experiencing an adverse gradient and may be near separation. Since separation at any location must be prevented, investigation of the electrode boundary layer only is required.

Unfortunately, there is scant data available to judge the stability of the boundary layer for a high speed flow with extensive wall cooling. However, Eqs. (10) and (11) have been used to estimate the boundary layer stability using the incompressible criteria for separation as described. It should be noted that the influence of the current on the boundary layer has been considered only in the momentum equation. The energy equation has not been considered, so that the dissipation in the boundary layer has been neglected.

It should be noted that the  $H$  predicted from Eq. (11) cannot be used directly to predict the actual geometric displacement thickness needed to correct the channel area in the case of a compressible flow and high wall cooling. However, under the assumption that the Prandtl number is unity, so that the temperature and velocity distributions are uniquely related, and that the velocity ratio  $u/U$  (where  $u$  is the velocity at some distance  $y$  measured from the wall) is equal to the ratio  $y/\delta$  raised to a power less than unity (where  $\delta$  is the boundary layer thickness)  $H$  as determined from Eq. (11) can be used to establish the boundary layer velocity distribution, which then determines the temperature and enthalpy distribution. Values of the power ( $\frac{1}{n}$  below) versus  $H$  are stored in the computer when the program is loaded. From this the density distribution, and hence, the geometric displacement thickness can be calculated.

Equations for the boundary layer written into the program, subroutine "H COMP", include:

$$\frac{u}{u_e} = \left(\frac{y}{\delta}\right)^{\frac{1}{n}} \quad (12)$$

$$\frac{h}{h_e} = \alpha + \frac{u}{u_e} \left[1 - \alpha + \beta\right] - \left[\frac{u}{u_e}\right]^2 \beta \quad (13)$$

$$\frac{\rho}{\rho_e} = \frac{1}{h/h_e} \quad (14)$$

$$\frac{\theta}{\delta} = \int_0^1 \frac{\rho}{\rho_e} \frac{u}{u_e} \left(1 - \frac{u}{u_e}\right) d\left(\frac{y}{\delta}\right) \quad (15)$$

$$\frac{\delta^*}{\delta} = \int_0^1 \left[ 1 - \frac{\rho}{\rho_e} \left( \frac{u}{u_e} \right) \right] d \left( \frac{y}{\delta} \right) \quad (16)$$

$$H_{inc} = \frac{\delta^*/\delta}{\theta/\delta} = \frac{\delta_{inc}^*}{\theta} ; D_{core} = D_{act} - 2 H_{inc} \theta \quad (17)$$

Where the subscript e refers to core or stream conditions, subscript w refers to the wall;  $a = \frac{hw}{he}$ ; and  $\beta = \frac{1}{2} \frac{u^2}{he}$ . A variable such as u, y or  $\sigma$  without a subscript refers to the local conditions in the boundary layer. The above equations can be found in any of the standard reference books on boundary layers as for example Schlichting's "Boundary Layer Theory."

The above set of equations are solved simultaneously at discrete points along the channel. (The distance between adjacent points along the axis of the generator is an input constant.)

Observed values of performance and predicted values of performance (predicted using this program) have shown excellent correlation, and even stall has been predicted with a high degree of accuracy.

#### 4. INPUTS AND OUTPUTS FOR THE HALL GENERATOR OFF-DESIGN PROGRAM

The required inputs for this program include:

- 1) For a round channel D versus X; For a rectangular channel  $D_1$  and  $D_2$  versus X
- 2) Flux density versus X
- 3) The time between printing in terms of the number of calculations --NBAR--the computer prints every NBARth calculation
- 4) The initial starting point XO
- 5) Increment of distance at which calculations are to be done DX
- 6) The dynamic viscosity MU
- 7) The initial value of length LO used in the calculation of Reynold numbers determined from the characteristics of the burner and nozzle
- 8) The initial momentum thickness THO
- 9) The axial load current I

- 10) A factor to indicate a round or rectangular channel. FD is 1 for rectangular channels and is  $\pi/4$  for a round channel.
- 11) A proportionality factor, FRIC I, for turbulent flow relating the friction factor  $C_f$  and the negative 1/5 th power of the Reynold's number.
- 12) A multiplier on the conductivity F1C. This number is one typically but can be any value as, for example, in estimating performance with a different seeding rate than the Mollier data with conductivity is calculated for.
- 13) A multiplier F2C like the above multiplier on the Hall parameter.
- 14) The proportionality factor, AK1, on the boundary layer portion of the electrode volt drop,  $V_e$  (See Eq. (8)).
- 15) The electrode drop, AK2, assumed to occur internal to the electrode (See Eq. (8)).
- 16) The maximum value of flux density, BMAX, used to obtain the local flux density as BMAX x B of Item 2 above. If Item 2 is not normalized then BMAX = 1.
- 17) The initial value of the compressible shape factor, HCOMPO
- 18) The burner stagnation enthalpy, HB $\phi$ .
- 19) The burner stagnation pressure, PB $\phi$ .
- 20) The area of the nozzle throat, ATH $\phi$ .

A typical output sheet is shown in Figure 55. The various symbols are defined as follows:

- 1) G Flow rate in kg/sec (output-m)
- 2) I Load current in amperes (input)
- 3) MU Dynamic viscosity (input)
- 4) FD Indicates round or rectangular channel (input)
- 5) DH  $\Delta H_C$  discussed earlier which is the elevation of the zero reference on the Mollier data above absolute zero in cal/gram (output)
- 6) F1 F1C previously discussed under inputs (input)  
correct
- 7) F2 F2C previously discussed under inputs (input)  
correct

# HALL GENERATOR-OFF DESIGN-NC56

FLOW RATE, G= 5.54697E 01 TOTAL CURRENT, I= 2000.0 MU= 6.5E-04 PD=0.785 FB1=0.0 FB2=0.0 D H= 1402. FRICTION F= 2.82000E-01 FI-CORRECTO.0400 FZ-CORRECTI.0000 KI= 1.00E 03 KZ= 1.25E 02 FICK= 0.0									
X B EFF GAMMA H BAR	P T U PT PO	Q H VE IV PCV	ALPHA D1 O2 CAPA IO	CAPM THETA A A-ACT NCOMP	MT RHO M RE DPOUT	SIGMA JK JV CF	V EX ZY P OUT	DELTA ALP BET DELM	
0.0	4.3948E-01	4.1932E 04	7.4110E-01	1.2500E 00	2.6593E 00	4.7532E 00	0.0	1.2344E-03	
1.900	2.3510E 03	-5.2884E 02	6.9509E-01	1.0000E-03	4.9861E-02	5.3010E 03	-1.1470E 03	5.0000E-01	
0.441	2.1045E 03	1.2624E 02	6.9509E-01	3.7729E-01	2.4855E 00	-4.0435E 03	1.8214E 02	6.0653E-01	
1.124	8.3882E 00	-2.8473E 01	3.7729E-01	3.7999E-01	4.5238E 03	2.0852E-02	0.0	8.0811E-02	
2.477	8.1614E 00	3.1679E 00	2.1509E 01	1.2368E 00	0.0				
0.250	4.4502E-01	4.0304E 04	7.0307E-01	1.2960E 00	2.6391E 00	4.8779E 00	3.0815E 02	4.4973E-03	
1.900	2.3509E 03	-5.2810E 02	7.0294E-01	3.6107E-03	7.0442E-02	5.1532E 03	-1.5649E 03	4.9674E-01	
0.444	2.0871E 03	1.2950E 02	7.0294E-01	3.8811E-01	2.4669E 00	-4.8450E 03	1.8422E 02	5.9257E-01	
1.124	8.0052E 00	-3.4603E 01	3.8811E-01	3.9610E-01	5.0892E 03	2.0367E-02	7.5260E 04	3.0540E 00	
2.430	7.5214E 00	3.0934E 00	2.2014E 01	1.2628E 00	6.1629E 05				
0.500	4.3438E-01	5.7529E 04	7.0122E-01	1.3114E 00	2.6999E 00	4.9199E 00	6.8802E 02	7.8775E-03	
1.900	2.3502E 03	-5.2270E 02	7.1027E-01	6.5257E-03	6.8770E-02	5.0477E 03	-1.6555E 03	4.9651E-01	
0.475	2.0791E 03	1.3280E 02	7.1027E-01	3.9622E-01	2.4518E 00	-4.8863E 03	1.8708E 02	5.8774E-01	
1.124	7.6733E 00	-3.5261E 01	3.9622E-01	4.1399E-01	5.4992E 03	2.0053E-02	3.2527E 05	6.6433E 00	
2.399	6.8994E 00	2.9482E 00	2.2451E 01	1.2459E 00	1.3760E 06				
0.750	4.2853E-01	5.5300E 04	6.9164E-01	1.3223E 00	2.7367E 00	4.9895E 00	1.0993E 03	1.1261E-02	
1.900	2.3600E 03	-5.2059E 02	7.1707E-01	9.0718E-03	6.7771E-02	4.9524E 03	-1.8013E 03	4.9532E-01	
0.484	2.0470E 03	1.3624E 02	7.1707E-01	4.0384E-01	2.4365E 00	-5.0939E 03	1.9003E 02	5.7955E-01	
1.124	7.3425E 00	-3.7111E 01	4.0384E-01	4.2961E-01	5.9266E 03	1.9754E-02	7.7232E 05	1.0538E 01	
2.362	6.3353E 00	2.8274E 00	2.4870E 01	1.2413E 00	2.1986E 04				
1.000	4.2405E-01	5.5293E 04	6.8020E-01	1.3317E 00	2.7668E 00	5.0703E 00	1.5493E 03	1.4675E-02	
1.900	2.3625E 03	-5.1789E 02	7.2372E-01	1.1883E-02	6.6903E-02	4.8418E 03	-1.9589E 03	4.9380E-01	
0.491	2.0528E 03	1.3960E 02	7.2372E-01	4.1137E-01	2.4183E 00	-5.3459E 03	1.9500E 02	5.6987E-01	
1.123	7.0081E 00	-3.9380E 01	4.1137E-01	4.4562E-01	6.3645E 03	1.9488E-02	1.4349E 06	1.4798E 01	
2.324	5.8162E 00	2.7149E 00	2.3287E 01	1.2350E 00	3.0986E 04				
1.250	4.2037E-01	5.1432E 04	6.6763E-01	1.3405E 00	2.7933E 00	5.1600E 00	2.0396E 03	1.8120E-02	
1.900	2.3637E 03	-5.1473E 02	7.3043E-01	1.4780E-02	6.6263E-02	4.7730E 03	-2.1207E 03	4.9205E-01	
0.496	2.0369E 03	1.4813E 02	7.3043E-01	4.1903E-01	2.3978E 00	-5.6242E 03	1.9595E 02	5.5906E-01	
1.123	6.6694E 00	-4.1753E 01	4.1903E-01	4.4166E-01	6.7485E 03	1.9249E-02	2.3316E 06	1.9440E 01	
2.284	5.3367E 00	2.6073E 00	2.3708E 01	1.2265E 00	4.0792E 04				
1.500	4.1723E-01	4.5674E 04	6.5430E-01	1.3494E 00	2.8175E 00	5.2580E 00	2.5709E 03	2.1642E-02	
1.900	2.3693E 03	-5.1120E 02	7.3729E-01	1.7784E-02	6.5633E-02	4.6845E 03	-2.2855E 03	4.9009E-01	
0.498	2.0192E 03	1.4664E 02	7.3729E-01	4.2694E-01	2.3749E 00	-5.9278E 03	1.9889E 02	5.4721E-01	
1.123	6.3275E 00	-4.4404E 01	4.2694E-01	4.7894E-01	7.1361E 03	1.9035E-02	3.4842E 06	2.4472E 01	
2.243	4.8922E 00	2.5028E 00	2.4137E 01	1.2168E 00	5.1418E 04				
1.750	4.1451E-01	4.7995E 04	6.4037E-01	1.3567E 00	2.8401E 00	5.3644E 00	3.1434E 03	2.5245E-02	
1.900	2.2734E 03	-5.0728E 02	7.4438E-01	2.0027E-02	5.5055E-02	4.5957E 03	-2.4500E 03	4.8795E-01	
0.499	1.9998E 03	1.5024E 02	7.4438E-01	4.3519E-01	2.3447E 00	-6.2473E 03	2.0184E 02	5.5438E-01	
1.122	5.9827E 00	-4.7248E 01	4.3519E-01	4.9623E-01	7.5054E 03	1.8944E-02	4.9127E 04	2.9900E 01	
2.200	4.6790E 00	2.4005E 00	2.4574E 01	1.2043E 00	6.2869E 04				
2.000	4.1716E-01	4.6975E 04	6.2589E-01	1.3687E 00	2.8413E 00	5.4790E 00	3.7571E 03	2.8955E-02	
1.900	2.2780E 03	-5.0290E 02	7.5178E-01	2.4234E-02	6.4520E-02	4.5057E 03	-2.6154E 03	4.8541E-01	
0.498	1.9785E 03	1.5394E 02	7.5178E-01	4.4388E-01	2.3222E 00	-6.5838E 03	2.0479E 02	5.7055E-01	
1.122	5.6364E 00	-5.0287E 01	4.4388E-01	5.1490E-01	7.0554E 03	1.8673E-02	5.6377E 06	3.5727E 01	
2.156	4.0946E 00	2.2999E 00	2.5038E 01	1.1948E 00	7.5142E 04				
2.250	4.1014E-01	4.4802E 04	6.1094E-01	1.3798E 00	2.8814E 00	5.4043E 00	4.4113E 03	3.2802E-02	
1.900	2.2831E 03	-4.9827E 02	7.5953E-01	2.7761E-02	6.4022E-02	4.4142E 03	-2.7783E 03	4.8964E-01	
0.495	1.9552E 03	1.5788E 02	7.5953E-01	4.5308E-01	2.2922E 00	-6.9355E 03	2.0776E 02	5.0573E-01	
1.121	5.5900E 00	-5.3520E 01	4.5308E-01	5.3473E-01	8.1845E 03	1.8520E-02	8.6799E 04	4.1952E 01	
2.110	3.7568E 00	2.2004E 00	2.5515E 01	1.1824E 00	8.8231E 04				

0A2171

/S

14581

CUU

RR

RR

PM

PR

PM

14591

180

1

0

0

0

0

CHALLON

JOB

15.783

G014-004-01-PP18

00.150

09110

CS999

0A2171

/6

1A581 CUU RM RR RN PW PR PH

18591 180 1 0 0 0 0 0

/HALLOO JOB 15.783 5019-006-81-PP18

00.150

09110

C5999

Figure 55 Typical Computer Output Data for Hall Generator Calculations.



- 8) K1 AK1 previously discussed under inputs (input)
- 9) K2 AK2 previously discussed under inputs (input)
- 10) X Distance in meters
- 11) B Flux density in tesla
- 12) EFF Generator efficiency defined as  $\left[ a - \frac{(\alpha/\omega T)^2}{1 - a} \right]$
- 13) GAMMA The ratio of a specific heat previously discussed
- 14) M BAR The average value of Mach number averaged across both the core and boundary layer
- 15) P The local static pressure in atms
- 16) T Local temperature
- 17) U Local velocity in m/sec
- 18) PT Local stagnation pressure in atms
- 19) PO The stagnation pressure corresponding to M BAR
- 20) Q Heat transfer in cal/m<sup>2</sup>
- 21) H Static value of enthalpy in cal/gm with reference to the Mollier chart 0
- 22) VE Electrode voltage drop
- 23) IY Transverse current in amperes in a width 1 cm wide
- 24) POY Stagnation pressure after a normal shock--corresponding to M BAR
- 25) ALPHA Loading factor previously defined
- 26) D1 Core width of channel in meters
- 27) D2 Core height of channel in meters
- 28) CAPA The area corresponding to D1 and D2
- 29) ID Internal diameter of the channel in inches (equivalent)
- 30) CAPH Incompressible shape factor of boundary layer
- 31) THETA Momentum thickness in meters
- 32) A Core area of flow in m<sup>2</sup>
- 33) A-ACT Total channel cross-sectional area in m<sup>2</sup>
- 34) HCOMP Compressible shape factor of boundary layer
- 35) WT Hall coefficient
- 36) RHO The local density in kg/m<sup>3</sup>
- 37) M Local Mach number

- 38) RE Reynolds number
- 39) DPOUT Increment of power output in Watts
- 40) SIGMA Conductivity of the gas in mhos/m
- 41) JX Axial current density in A/m<sup>2</sup>
- 42) JY Transverse current in A/m<sup>2</sup>
- 43) CF Friction coefficient previously discussed
- 44) V Terminal output voltage in volts
- 45) EX Axial field intensity in V/m
- 46) EY Transverse field intensity in V/m
- 47) POUT Power output in Watts
- 48) DELTA }  
ALP } The program is designed to do with the boundary layers  
BET } purposes of checking the program.  
DELH }

##### 5. DIAGONAL GENERATOR ANALYSIS PROGRAM

The Hall generator analysis program discussed here can be quickly converted to a Diagonal generator analysis program merely by changing the electrical boundary conditions from the Hall conditions to the diagonal conditions.

The diagonal boundary conditions include:

$$J_x = 0 \text{ (Hall current free generator)} \quad (18)$$

(The diagonal generator operating under ideal conditions is in reality a segmented Faraday generator (whose currents are strictly transverse) with those electrodes at the same potential on opposite sides of the channel connected in series to obtain a much greater output voltage. The diagonal connection is also used to reduce the number of output terminals. Therefore, an ideal diagonal generator is one where  $J_x = 0$ .)

$$I = I_y = A \phi J_y \quad (19)$$

$$\phi = \frac{E_y}{E_x} \text{ (Tangent of the diagonal angle)} \quad (20)$$

$$\Delta P_x = E_y I_y \Delta x \text{ (Incremental power output)} \quad (21)$$

$\Delta P_x$  and  $\Delta x$  as used here are the increments of power and axial distance

These changes were made to the program discussed, and the resulting program was used to analyze the generator performance as reported in this report.

BLANK PAGE

## VIII. GENERATOR TESTING WITH CONVENTIONAL HYDROCARBON FUELS AT AERL

### 1. INTRODUCTION AND SUMMARY

An important field for application of MHD power concerns generation of relatively large amounts of power for limited durations with lightweight systems carrying on-board oxidizer. Included are airborne systems as well as exo-atmospheric applications including ballistic systems and space systems. The experimental work described in Section VI under the present Contract is concerned with use of high energy fuels as typified by cyanogen plus oxygen, for these applications. The cyanogen-oxygen combination offers the maximum performance obtainable with systems using on-board oxidizer and commercially available high energy liquid fuels. High power output/unit mass flow of the order of one megawatt/kilogram-sec. at power levels of one megawatt and below is a prime requirement in these applications.

Since the inception of this contract, developments in ductile composite metastable superconducting materials by a number of suppliers now make it possible to design superconducting magnet systems with overall net current densities of  $1 - 2 \times 10^4$  amperes/cm<sup>2</sup> in the winding at field strengths up to and even above four Tesla. With these current densities, overall magnet system weight increases very little as the design field strength increases from two to four Tesla. Thus, magnet system weight vs. field strength no longer need be a prime consideration for MHD power supplies utilizing on-board oxidizer if the field strength can be held below four Tesla. With these relatively high magnetic fields, MHD generator systems using conventional hydrocarbon fuels and on-board oxidizer can be competitive at power levels of 300 kilowatts and up. The main objective of the work to be described in this Section was to demonstrate the feasibility of this type of generator system. It is extremely valuable to have experimental verification of these expectations, as this provides greatly increased flexibility in the design of on-board oxidizer MHD power supply systems and avoids logistic problems associated with cyanogen.

The work described in this Section consists of (1) an examination of alternative fuel-oxidizer combinations for MHD systems using on-board oxidizer and a selection of a combination which indicates close to optimum performance for the generator described in Section II (this generator was actually built for use with high energy fuel cyanogen), (2) an experimental testing program operating the previously discussed MHD generator equipment (Section II) on seeded combustion products of conventional hydrocarbon fuels and oxygen with the objective of optimizing the specific power output, and (3) a correlation between experimental results and theoretical performance calculations.

The results of this investigation demonstrate conclusively the high specific power capabilities of the MHD generators at power levels of 300 kilowatts and above. The experimental results are unique in terms of power output per unit mass flow rate for the considered power level. This fact is illustrated in Table VIII-1 where the specific power outputs are listed for combustion-driven generator test facilities which are or have been operated with liquid fuels (specifically, hydrocarbon fuels). (It is known that the University of Tennessee Space Institute facility has also been operated with solid fuel at about the same mass flow rate and has reached an electrical output of 200 kW in this case. This corresponds to a specific power of approximately 0.25 MJ/kg.) The table shows that the presently tested generator labeled "APL-Mark II Diagonal" generator significantly outperforms other generators of similar size and compares favorably with the performance of much larger generators. For this generator the mass flow rate 0.6-0.8 kg/sec, the power output is 300 and 400 kilowatts of the two mass flows, and the specific power output is 0.5 MJ/kg. The measured performance was found to agree closely with predictions.

It was found that the performance was adversely affected by three effects. First, because the Mark II magnet is large, the magnetic field extended too far into the end regions of the channel and caused excessive deceleration of the flow and inefficient power takeoff. Second, the electrode voltage drop in the downstream half of the channel was larger than used in the design calculations. Third, the observed diffuser-pressure recovery efficiency was quite low. With the proper improvement in these effects, it is estimated that the specific power output of this device will be about 0.7 MJ/kg.

## 2. EXAMINATION OF ALTERNATE FUEL-OXIDIZER COMBINATIONS

The selection of the specific fuel and oxidizer to use is part of the more complicated process of the design of an MHD generator power supply system. A naive selection of a fuel and oxidizer without regard to other considerations would undoubtedly not lead to an optimum overall system. In spite of the fact that in this investigation, the MHD channel and facility was in existence at the time testing began, still some freedom existed relative to the selection of the generator working gas. Before discussing this selection it is perhaps pertinent to present a discussion of the considerations which must be taken into account in the design of a MHD generator system. This discussion is presented in the next several paragraphs. It should be noted, in particular, that the amount of fuel and oxidizer expressed in terms of SFC (specific fuel consumption) is an extremely important factor in system design.

The MHD generator is the equivalent of a turbine and generator combined in a single device. Whereas, on the one hand, this leads directly to a number of outstanding advantages, e.g., elimination of moving parts (and as a corollary the elimination of the need for close tolerances), the capability of working at very high temperatures, very high volumetric

TABLE VIII-1  
LIQUID FUELED MHD GENERATOR TEST FACILITIES\*

	Mass Flow Rate (kg/sec)	Electrical Output(MW)	Max. Output Mass Flow Rate (MJ/kg)
<u>AERL</u>			
Mark II, Segmented Faraday <sup>1</sup>	2.7	1.5	0.55
Circular Hall <sup>2</sup>	4.3	1.0	0.23
LORHO Pilot, Circular Hall <sup>3</sup>	52	18	0.35
Mark V, Segmented Faraday† <sup>4, 5</sup>	52	32	0.62
Mark V, Two-terminal Faraday <sup>4, 5</sup>	50	25	0.52
A. P. L. - Mark II Diagonal(this report)	0.6-0.8	0.3-0.4	0.50
<u>Other U. S.</u>			
Stanford University <sup>6</sup>	0.27	.01	0.039
Univ. of Tenn. Space Inst. <sup>7, 8</sup>	0.8	.042	0.053
<u>Foreign</u>			
Electrotechnical Lab, Mark II Japan <sup>9</sup>	2.6	0.53	0.20
Krzhizhanovsky Power Inst. ENIN-2, Moscow, USSR <sup>10</sup>	50	2	0.04

\*References for this Table are given on the next page.

†Magnet excitation section was a two-terminal Faraday here.

# REFERENCES FOR TABLE VIII-1

1. Louis, J. F., Lothrop, J. and Brogan, T. R., "Studies of Fluid Mechanics Using a Large, Combustion Driven MHD Generator," March 1964. Physics of Fluids, 1, pp.
2. Teno, J., Brogan, T. R., DiNanno, L. R., "Hall Configuration MHD Generator Studies," Presented at the International Symposium on MHD Electrical Power Generation, Salzburg, Austria, July 1966.
3. Teno, J., Brogan, T. R., and Petty, S. W., "Studies with a Hall Configuration MHD Generator," Presented at the 10th Symposium on Engineering Aspects of MHD, MIT, March 1969.
4. Mattsson, A.C.J., Ducharme, E. L., Morrow, I. B., Brogan, T. R., "Design and Performance of a Single Circuit Output Self-Excited Faraday MHD Generator," Presented at Eighth Symposium on Engineering Aspects of MHD, Stanford, California, March 1967.
5. Mattsson, A., and Brogan, T. R., "Self-Excited MHD Generators," Presented at the International Symposium on MHD Electrical Power Generation, Salzburg, Austria, July 1966.
6. Rubin, E. S. and Eustis, R. H., "Electrode Size Effects in Combustion Driven MHD Generators," Proc. 11th EAM Symp., p. 35, Pasadena, Calif., March 1970.
7. Dicks, J. B. et al., "Theoretical and Experimental Studies of Two-Terminal MHD Generators," Electricity from MHD, 1968, p. 2718, IAEA, Vienna, 1968.
8. Dicks, J. B., et al., "The Performance of a Family of Diagonal Conducting Wall MHD Open-Cycle Generators," Proc. 11th EAM Symp. p. 16, Pasadena, Calif., March 1970.
9. Mori, F., Fushimi K. and Ikeda, S., "Experiments on MHD Generation with ETL Mark II," Electricity from MHD, 1968, p. 2761, IAEA, Vienna, 1968.
10. Zhimerin, D., Bashilov, V. and Motulevich, V., "The ENIN-2 Experimental Open Cycle MHD Generator Rig," Electricity from MHD, 1968, p. 2821, IAEA, Vienna, 1968.

electrical power densities; on the other hand, the merging of the turbine and generator combined with the fact that a conducting plasma is employed as the working medium leads to a number of interrelated considerations not previously encountered in any other technology.

In common with the specifications of other electrical power supplies, the specification of an MHD generator power supply includes, first, with respect to the electrical output

- 1) Power output
- 2) Terminal operating voltage
- 3) Regulation (external characteristics)
- 4) Stability
- 5) Starting requirements
- 6) Overload and fault requirements
- 7) Duty cycle

and second, with respect to the mechanical features

- 1) Weight restrictions, if any
- 2) Volume restrictions, if any
- 3) Working environment - altitude, ambient pressure, ambient temperature, etc.
- 4) Reliability

The designer of a combustion driven MHD generator power supply is faced with the task of manipulating the variables of the system to arrive at one or more optimum configurations in terms of the power supply specifications. The variables of an MHD generator system include:

- 1) The type of generator - two terminal Faraday, multi-circuit output segmented Faraday, diagonal, Hall, disc.
- 2) Mode of generator operation - impulse, reaction, or mixed.
- 3) Length/channel diameter (L/D) ratio of the MHD generator
- 4) Fuel and oxidizer
- 5) Combustion pressure and temperature
- 6) Seed material and concentration
- 7) Magnetic field intensity
- 8) Type of field coil
- 9) Cooling of burner, nozzle, channel, and exhaust system
- 10) Logistics of all materials handled
- 11) Utilization of auxiliary equipment - power conditioning, preheaters, pumps, etc.

The result(s) of the designer's effort is (are) one (or several systems) designated by

- 1) Total weight
- 2) Total volume
- 3) Fuel, oxidizer, and seed requirements



or, alternatively, by one or more of the following figures of merit:

- 1) SFC - pounds of fuel per kilowatt hour output
- 2) Specific power density - pounds of fixed weight per kilowatt capacity
- 3) Specific volume density - volume of system per kilowatt capacity
- 4) Specific energy output - kilowatt hours per pound of total weight (fixed weight plus fuel, oxidizer (if carried), and seed weights)

A good designer must have a comprehensive appreciation for certain basic facts related to the MHD generator. With specific reference now to airborne equipment where weight is a very important consideration, the first item of importance is the working gas which is obtained from the fuel, oxidizer, and seed. Ignoring other considerations for the time being, minimum weight implies obtaining the maximum output (kilowatts) for given mass flows of those items which must be carried onboard the aircraft. The reciprocal of this term is commonly referred to as the specific fuel consumption (SFC) which is defined as the weight of consumables carried per kilowatt hour output of the power supply. In basic terms, the SFC is related to the reciprocal of the product of the heat of combustion of the fuel,  $h_c$ , and overall energy extraction ratio,  $r$ , of the generating device, which is nothing more than the overall heat-to-electricity conversion efficiency,  $\eta$ . In equation form

$$\text{SFC} = \frac{1}{r h_c} \quad (22)$$

As is readily apparent, for a low SFC, high values of  $r$  and  $h_c$  are desirable.

If regeneration is excluded, so that the only power output of the system corresponds to the heating value of the fuel, the overall efficiency of the design is directly related to the expansion efficiency\* of the generator.

High expansion efficiency requires first a high electrical efficiency. This in turn requires proper matching of the load current and electrical properties of the gas throughout the length of the duct. It also requires a small electrode and boundary layer drop, fine enough segmenting to minimize Hall effect losses, uniform emission across the width of each electrode (i. e., in the direction of  $B$ ) - again to avoid local Hall losses, a moderately large  $L/D$  to minimize end Eddy current losses, and uniform gas properties to avoid gross Hall induced Eddy currents.

\* Defined as  $\eta_g = (\text{actual enthalpy change}) \div (\text{enthalpy change due to an isentropic expansion through the same pressure ratio})$ . For the range of pressure ratios and Mach numbers appropriate here,  $\eta_g$  will be approximately 5 points less than the electrical efficiency,  $\eta_e$ .

$$\eta_e \left( \equiv \frac{\int \tilde{j} \cdot \tilde{E}}{\int \tilde{j} \cdot (\tilde{u} \times \tilde{B})} \right)$$

High efficiency also requires smooth walls, a channel properly shaped to give the right pressure gradient, and the avoidance of boundary layer separation.

The SFC varies both with respect to efficiency and pressure ratio. For small pressure ratios, the SFC is very large primarily because the available enthalpy between the inlet and exit stagnation pressures is small thereby requiring a large mass flow to deliver the power. At higher pressure ratios the curves become flat because, as the pressure ratio is increased, the power requirement to compress the air is increasing at a faster rate than the available enthalpy between the two stagnation pressures. While a large pressure ratio is not necessarily bad in principle, it leads in practice to several complications. Among these are, higher heat transfer rates in the burner, nozzle, and upstream portions of the channel, a need for a high and rapidly tapering magnetic field strength in order to achieve a reasonable length and to keep the value of the Hall parameter within reasonable bounds, and greater difficulty in matching the electrical properties of up-and downstream portions of the duct in any hookup (Hall or diagonal) which is designed to achieve output to a single circuit or a not too unreasonably large number of circuits. In addition, of course, in a power cycle employing a compressor, the need to minimize compressor power provides another very strong incentive for high expansion efficiency.

The minimization of SFC happens to be only one of the facets to be considered in the design of high performance, lightweight MHD generator systems, and, in contrast to turbines, it cannot be selected independent of one other vital consideration. Whereas the turbine requires a clean working gas with a certain energy content at a given pressure and temperature, the electrical part of the MHD generator places other constraints on the working gas employed by the generator; the most important constraint is that the gas be a reasonable conductor of electricity. To examine the importance of the conductivity consider first, the interaction parameter,  $S$ , which is the ratio of the MHD force acting on the gas to the dynamic inertia force of the gas, or

$$S = \frac{J_y B L}{\rho u^2} = \frac{\sigma u B^2 L}{\rho u^2} = \frac{\sigma B^2 L}{\rho u} = \frac{\sigma B^2 L A}{\dot{m}} \quad (23)$$

( $S$  is Non Dimensional and Should be One or Larger)

where

$J_y$  is the transverse current density  
 $B$  is the magnetic field  
 $L$  is the length of the MHD channel  
 $\rho$  is the gas density  
 $u$  is the gas velocity  
 $A$  is the MHD channel cross sectional area  
 $\dot{m}$  is the total mass flow

As previously discussed, the mass flow is fixed by the power output requirements,  $P_{out}$ , the available enthalpy of the gas,  $\Delta H$ , and the efficiency,  $\eta$ , or

$$P_{out} = \eta \Delta H \dot{m} \quad (24)$$

alternately,

$$\dot{m} = \frac{P_{out}}{\eta \Delta H} \quad (25)$$

If the mass flow is fixed, the area is also fixed once the inlet conditions are established for the channel. The inlet conditions are selected on the basis of maximizing the volumetric power density as discussed below. If  $\dot{m}$  and  $A$  are fixed, then the interaction parameter is a function of  $\sigma$ ,  $L$ , and  $B$  only, or

$$S \approx \sigma L B^2 \quad (26)$$

which states that in the final analysis, to achieve a given value of interaction at a given flux density, the length of the generator varies inversely as the conductivity. This is not to say that there is unlimited freedom in the selection of  $L$ . A small  $L/D$  leads to large end effect losses; a large  $L/D$ , i. e., greater than 10, leads to large fixed weights and excessive heat and friction losses. Some optimization can be made in view of the trade offs which exist between length, weight, and neat losses versus the effect on SFC of carrying onboard various amounts of seed.

The importance of conductivity can be revealed still in another way. The volumetric electrical power density,  $P$ , of a working gas is given by

$$P = \alpha (1 - \alpha) \sigma u^2 B^2 \quad (P \text{ has the units: } \frac{\text{power}}{\text{unit volume}}) \quad (27)$$

where

$\alpha$  is the loading factor of the generator; for Faraday type generators

$\alpha = E_y/uB$ ;  $E_y$  is the transverse electric field. Also,  $\alpha$  happens to be equal to the electrical efficiency of Faraday generators

$\sigma$  is the gas conductivity

$u$  is the gas velocity

$B$  is the magnetic field flux density

In an efficient generator  $\alpha$  is typically between 0.5 and 0.8, and the product,  $\alpha (1 - \alpha)$ , is between 0.16 and 0.25. An alternate figure of merit of the working gases obtained from the previous equation is

$$\sigma u^2 = \frac{P}{\alpha (1 - \alpha) B^2} \quad (28)$$

As is evident from either equation, for a given power level at the same operating conditions, the volume, and hence, the fixed weight, is inversely proportional to the conductivity. Not as readily apparent from the equation is the fact that a given velocity implies a certain expansion, temperature level, and hence, conductivity. With small expansions  $u$  is small and the conductivity high, and vice versa as the expansion is increased the conductivity falls while  $u$  increases. Consequently, for a given set of stagnation conditions,  $\sigma u^2$  varies from a small value at small expansion to a maximum at moderate to high expansions and finally to reduced values at higher expansion (because of the conductivity drop off). Further, the maximum occurs at different pressure ratios for different inlet stagnation conditions. Barring other considerations, the conditions corresponding to the maximum  $\sigma u^2$  are selected as the channel inlet conditions. Table VIII-2 shows typical values for the various figures of merit which have been discussed to this point.

If it is tacitly assumed that minimum weight implies minimum volume (this is true at least to a first approximation), the discussion to this point can be summarized in terms of a single expression for the specific energy output,  $E$ , as

$$E = \frac{t}{W_D + \text{SFC} \cdot t} \quad (E \text{ has the units: } \frac{\text{energy}}{\text{weight (total)}}) \quad (29)$$

where  $t$  is the operating time, and  $W_D$  is the fixed weight per unit output power.

At the one megawatt level, the fixed weight and hence,  $W_D$  for MHD generators using either ordinary fuels and oxygen or high energy fuels and oxygen or preheated air, are less than turbo-alternator systems. The high SFC's (See Table VIII-2) of systems with oxygen however, lose any advantages for these systems compared with turbo-alternators for times greater than several minutes. However, certain future application seems to be in the 10 minute mission time regime in which case the use of high energy fuels and oxygen would be appropriate. If airbreathing MHD generator systems are used, the operating time for which the weight advantage exists extends to two hours for systems utilizing cyanogen as the fuel. Anticipating that a high energy fuel such as pentaborane ( $B_5H_9$ ) or a metallic slurry in hydrocarbon can be used and assuming that its properties will match those of hydrocarbon fuels at the same temperature, the MHD generator system could have weight advantages for all operating times. Since the weight of MHD generator systems grows only slowly with

TABLE VIII-2

Working Gas	Flame Temp. at 1 atm °K	Specific Heat of Combustion of Fuel BTU/#Fuel	$\sigma$ Mho/M	$u$ M/sec	$\sigma u^2$ Mho M/sec <sup>2</sup>	SFC
1. For Turbo-Alternators: Combustion Products of JP4 plus Air	-	19,000	-	-	-	0.61 (Typical of Advanced Turbo- Alternator Systems at low Altitudes)
For MHD Generators:						
2. Combustion Products of Commercial Fuels plus Preheated Air	2520	15,000	1	1,500	$2.2 \times 10^6$	Conductivity outside useful range for light weight system
3. Combustion Products of Kerosene Plus Oxygen	3120	19,000	20	2,000	$8 \times 10^7$	$\approx 6$
4. Combustion Products of Cyanogen Plus Oxygen	4800	9,000	200	2,000	$8 \times 10^8$	6.6
5. Combustion Products of Cyanogen Plus Preheated Air	3140	9,000	26	1,300	$4.4 \times 10^7$	1.42
6. Combustion Products of	2700	26,000	No actual information, $\sigma u^2$ assumed to be $5 \times 10^7$			0.57
7. Re-entry Air	-	-	400	4,000	$6 \times 10^9$	No fuel require <sup>d</sup> Note extremely high $\sigma u^2$

increases in power, the advantages are increased for higher power levels. There is little comparable weight advantage with increase of power level for turbo-alternator systems.

To recapitulate, strictly from a theoretical viewpoint, the goal of achieving high performance, light-weight MHD generator systems for airborne applications implies recognizing and staying within the constraints imposed through specification of weights, volumes, and performance. Briefly stated, these constraints or boundary conditions are:

- 1) The SFC should be a minimum
- 2) Low SFC's require fuels with high specific heats of combustion. Regeneration can aid in reducing the SFC
- 3) Low SFC's require high overall efficiencies
- 4) The efficiency of an MHD generator is determined by such things as heat losses, electrode losses, end effect losses, boundary layer thickness, losses due to nonuniformities in the working gas, losses due to circulating currents in the gas, and any exhaust system losses.
- 5) The fixed weight of the MHD generator system varies directly with the volumetric power density which is a function of the conductivity, gas velocity, and magnetic field strength
- 6) Conductivity is a function of temperature and seed concentration
- 7) As a consequence of (6), additional requirements on the fuel then are a high flame temperature, a minimum of water and alkali metal vapors in the combustion products, and the absence of any element in the combustion products which would deplete the supply of available electrons.

Apart from performance, weight and volume constraints which to a large degree steer the direction of the generator design, are another group of what might be referred to as constraints on the structures and physical system. These, too, result in narrowing down the range of selection of such things as fuels, coolants, power takeoff, etc. One of these constraints stands out, and it is pertinent to mention it here. With reference to fuel selection, it is particularly important at least for linear generators that the products of combustion be compatible with both the electrodes and insulators of the MHD channel both from the viewpoints of performance and duration. There exists a vast amount of experience with handling ash in the combustion products and, in fact, AERL employs a method of in situ flame spraying of zirconia to maintain channels for extensive periods of operation. It would, however, be necessary to establish by experiment the feasibility of handling gases where the ash is a major portion of the combustion products and to check that no deleterious effects on performance or duration result from the high concentration of ash encountered.

Before beginning the experiments discussed in this report a theoretical investigation was performed for a number of high energy fuels and various oxidizers with varying degrees of preheat. Table VIII-3 displays the results of the investigation with one typical high energy fuel,  $C_2N_2$ . Both on-board oxidizer and air were considered as the oxidizer. The on-board oxidizer systems as already mentioned are appropriate for mission operating times in the range of 10 minutes while the use of air permits the use of high power generation for many hours on a completely competitive weight and volume basis with other power supplies, even ignoring the considerations of power conditioning. The MHD generator output is DC and for the most part is inherently stable with most typical loads!

Consideration will not be given to applying the general theory as outlined in the above paragraphs to the specific generator system investigated under the present contract (see Section II). As the previous discussion revealed there are a number of tradeoffs that can be made even for the case of an existing system. With particular reference to the present system, the following points can be made.

- 1) In view of Eq. (28) maximum power density and hence power for a given volume of generator requires a high conductivity. In practice this implies the use of oxygen as the oxidizer (because of the resulting high flame temperature) and cesium as seed (because it results in high conductivity and gases due to the lower ionization potential compared to potassium).
- 2) Table VIII-2 reveals that the SFC's of kerosene-oxygen mixture versus cyanogen-oxygen mixture are approximately equal. Therefore, the advantage of the high energy fuel is mainly in terms of size (volume) and accordingly the fixed weight required to deliver a given power output. Even though higher magnetic field intensities will be required if hydrocarbon fuels are used, the weight change promises to be relatively minor due to the continual improvements in superconductor current carrying characteristics. Accordingly the hydrocarbon fuels should be considered as prime candidates for on board oxidizer MHD generator power supplies. This has the further advantage that the logistical problems associated with handling a second power supply fuel can be avoided.
- 3) With reference to diagonal generators of the present construction, the performance is relatively insensitive to the value of the Hall parameter and is directly sensitive to the magnitude of the conductivity. However, the variation of conductivity is relatively minor for any of the common hydrocarbons such as kerosene, JP4, JP5, toluene and benzene. At the relatively high magnetic field available in the Mark II facility, some variation in the conductivity can be tolerated without affecting the generator performance. Actually any of the above listed hydrocarbon fuel could be used.

TABLE VIII-3

## DIAGONAL MHD GENERATOR SYSTEMS COMPARISON\*

Fuel	Oxidizer	Preheat Fuel	Preheat Oxidizer	$\dot{m}_t$	B	P <sub>out</sub>	SFC $\frac{\# \text{Fuel}}{\text{KWHr}}$	Power Density $\frac{\# \text{Fixed}}{\text{KW}}$
1. C <sub>2</sub> N <sub>2</sub> **	N <sub>2</sub> O <sub>4</sub>	572°F	572°F	0.83 Kg/sec	2 W/M	1000 KW	6.6 #/KWHr	0.345 #/KW
2. C <sub>2</sub> N <sub>2</sub>	Bleed Air	572°F	572°F	2.0 Kg/sec	6 W/M <sup>2</sup>	615 KW	3.76 #/KWHr	1.8 #/KW
3. C <sub>2</sub> N <sub>2</sub>	Bleed Air	572°F	2200°F	1.0 Kg/sec	6 W/M <sup>2</sup>	825 KW	1.42 #/KWHr	1.45 #/KW
4. C <sub>2</sub> N <sub>2</sub>	Bleed Air	572°F	2200°F	2.0 Kg/sec	4 W/M	1200 KW	1.96 #/KWHr	0.5 #/KW
5. C <sub>2</sub> N <sub>2</sub>	Bleed Air	572°F	2200°F	2.0 Kg/sec	3 W/M	800 KW	2.92 #/KWHr	0.672 #/KW

\* T-A System 25 minutes - 1000 KW - 1971 system  
 SFC = 4.48 # Fuel/KWHr  
 Power Density = 1.149 # Fixed/KW  
 Uses onboard oxidizer

\*\* Uses onboard oxidizer -- Considerable improvement possible if oxidizer preheated to 2200°F



Based upon the above statements, for the present experiments oxygen was chosen as the oxidizer, and a hydrocarbon in this case toluene ( $C_7H_8$ ) was selected as the fuel. Avoidance of the handling problems associated with cyanogen plus the lack of a supplier of pure cyanogen were also important factors in the selection of the fuel.

### 3. EXPERIMENTAL PROGRAM

The test program associated with this contract spanned about a five-month period and included a total of fifty-four (54) tests out of which twenty six (26) were power generation tests. Some of the operating parameters and a few of the performance characteristics for this device are listed below:

Total mass flow	0.6 - 0.8 kg/sec
Fuel	toluene
Oxidizer	gaseous oxygen
Seed Material	$Cs_2CO_3$
Burner pressure	9 - 12 atm
Magnetic field	2.5 - 3.5 Tesla
Test time	5 - 8 sec
Active channel length	0.7 m
Channel dimensions:	
inlet	2.6 x 10.0 cm
outlet	7.2 x 11.6 cm
Generator configuration	diagonally connected
Hall parameter	1.0 - 4.0
Electric fields	1.0 - 5.0 kV/m
Electric current density	1.0 - 10.0 amp/cm <sup>2</sup>

The selection of the fuel and the oxidizer was made based on the results of the previous subsection. The Mollier chart for this mixture is shown in Figure 56. The magnetic field distribution for the case of 3.5 Tesla is shown in Figure 57. The dimensions of the active section of the channel are listed above (the channel construction and area distributions were discussed in previous sections). The Hall parameter, the electric field, and the electric current density ranges obtainable in this device are also listed.

Four different types of tests were performed during this program. A description of the different types of tests will be made below under the following headings: (1) Burner Tests, (2) Channel Heat Transfer and Static-Pressure Distribution Tests, (3) Conductivity Tests, and (4) Power Generation Tests.

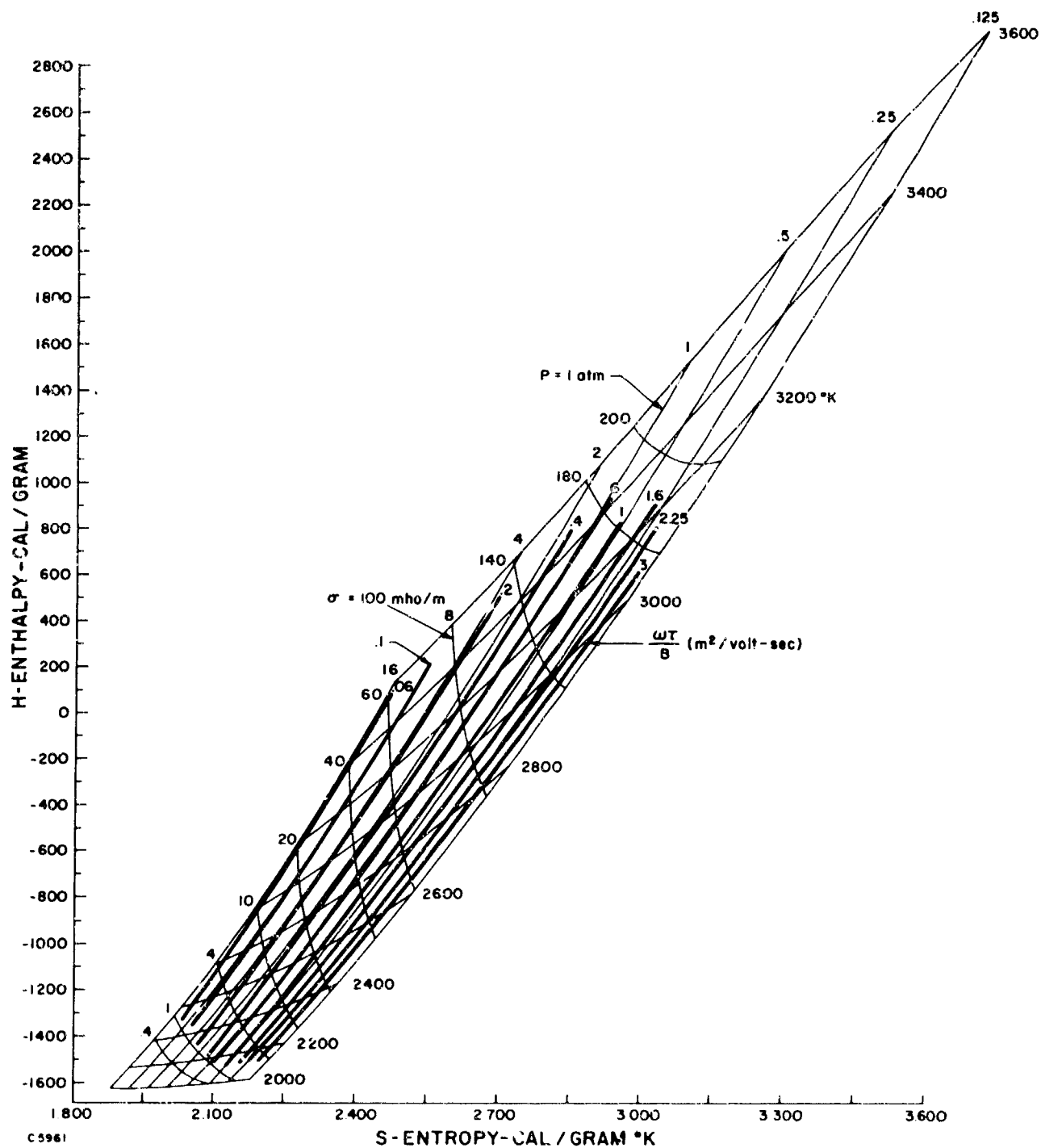


Figure 56 Mollier Chart for a Stoichiometric Mixture of Toluene and Oxygen with Two Weight Percent Cesium Added.

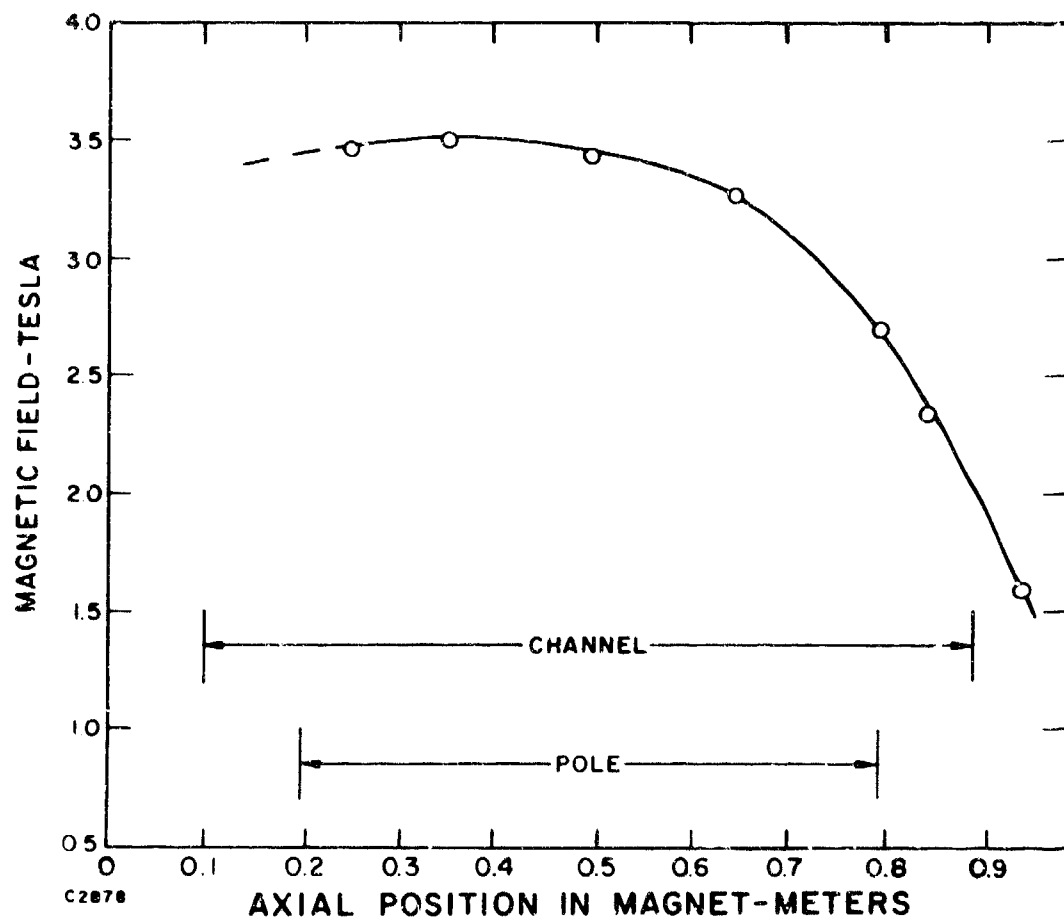


Figure 57 Magnetic Field Distribution of the Mark II Magnet with Short Pole Pieces at a Maximum Field of 3.5 Tesla.

Burner Tests. The purpose of these tests was to check and adjust the flow rates of the fuel, oxidizer, and seed and to check the overall performance of the system. A total of four such tests were performed.

Channel Heat Transfer and Static Pressure Distribution Tests. Eight tests were made for the purpose of measuring the heat transfer rates and the pressure distribution along the generator. The roughness of the channel walls and the recovery behavior of the diffuser were investigated.

Conductivity Tests. The electrical conductivity of the gas was measured along the channel by the technique described in Section VI. Three tests were performed with the powder seeder to check the agreement with the predicted values. Thirteen tests (during a two-week period) were made with a liquid seed system. The liquid seed system will be described later in this section.

Power Generation Tests. A total of twenty-six (26) tests were made for the purpose of generating electrical power output. The channel was connected in the diagonal mode of operation. Nineteen tests were made with the powder seed system and seven with the liquid seed system. With the powder seed, three initial tests were made with the channel in the closed position (see Section II), with a total mass flow of 0.6 kg/sec, with a magnetic field strength of 2.6 Tesla, and with a resistive load of 5 ohms. In the rest of the nineteen tests the channel was in the open position (see Section II), the mass flow was 0.8 kg/sec, the peak magnetic field was 3.5 Tesla, and the load resistance was 9 ohms except in the last test when it was 7.5 ohms. The tests with the liquid seed system will be discussed later in this section.

The testing program was significantly influenced by two effects that occurred during the testing as discussed below:

- 1) During the initial power tests (discussed above), it was observed that the power output capability of the channel was limited by the pressure recovery capability of the diffuser. To alleviate the recovery limitation and to increase the power out of this device, a number of relatively small modifications were made to the experimental set up so that the mass flow could be increased to 0.8 kg/sec and the peak magnetic field could be increased to 3.5 Tesla. It was found necessary to shield the burner solenoid valves and the seeder motor with iron.
- 2) The burner had been operated routinely and reliably under a wide variety of conditions prior to the above discussed modifications. However, after the modifications and at the higher flow rate of 0.8 kg/sec, the burner operated unreliably. In particular, at large seed flows, burnouts in the burner liner occurred. The cause of these failures was not determined,

but these operating conditions are considerably more severe than the design conditions for this burner. Three consecutive burner liners were damaged.

After the first burnout, an O-ring seal in the burner was observed to have failed and it was believed that this caused the failure. A new liner was installed; however, after two tests the burner again failed. In this case one oxygen injector in the outer set of injectors was plugged with seed material which could have resulted in directing a part of the flow towards the burner wall causing the burnout. The seed was filtered so that only seed particles smaller than about one third of the oxygen injector diameter was used. The injector subsequently remained clean, however, this did not prevent the liner from being damaged again. At this point it was realized that the flow pattern in the burner would have to be changed. Three improvements were made. First, the flow of cooling water in the burner was increased from 30-54 gpm. Second, the flow in the outer set of oxygen injectors was increased so that they carry 60 percent of the oxygen flow. This directs the flow towards the center of the burner and prevents the flow impinging on the burner walls. Third, a modification was made so that the fuel injectors could be aligned more accurately. In addition, since the failure occurred in conjunction with high seed flow, it was decided to try out a liquid seed system. This system did not perform satisfactorily and its use was discontinued. (A discussion of the liquid and system is given in Appendix I.) After the changes were made, the burner operated reliably using the powder seeder, and the testing was concluded without further difficulties.

The channel behaved well during this test program. Both the electrode walls and the peg insulator walls maintained their integrity very well when operated under normal conditions. During this program the channel was disassembled once, and the ceramic was repotted where required. Judging by the appearance of the electrode surfaces, the inlet end of the channel seemed to have slightly overheated during the previous testing. The last half of the channel and the diffuser were in excellent condition. The heat transfer in the front of the channel was larger than estimated in the design calculations. (Channel heat transfer measurements are discussed in the next subsection.) To avoid overheating any part of the channel the test time was reduced from eight to five seconds. During the burnout difficulties in the burner the channel was saturated with water and the ceramic in the walls absorbed seed material and the insulator characteristics of the walls deteriorated. The ceramic material in the walls was not replaced during this test program.

#### 4. EXPERIMENTAL RESULTS AND COMPARISON WITH THEORY

The description of the results will be made in the following manner: First, the burner and nozzle conditions will be discussed briefly. Secondly, the channel heat transfer data and their effects on the electrode voltage drop will be discussed. Thirdly, the pressure distribution along the

channel and the diffuser and the diffuser pressure recovery behavior will be described. Fourthly, the results of the power generation tests will be outlined and a detail comparison with theoretical calculation will be made.

The pressure in the burner was measured to be 9.2 and 12.25 atm at mass flow rates of 0.6 and 0.8 kg/sec, respectively. The temperature in the burner was estimated to be about 3300°K. The calculated Mach number at the exit of the nozzle is 2.18, and both the measured and calculated pressure at this position are 1.2 atm at the high mass flow rate and 0.9 atm at the low mass flow rate.

The channel heat transfer rates were inferred from the temporal behavior of the temperature measurements in five individual pegs along the channel. Experimental data from three tests are shown in Figure 58. The scatter in the data indicates the accuracy of these measurements. Theoretical curves for both turbulent and laminar boundary layer heat transfer rates are shown, and it is seen that the experimental data agree within about 20 percent with the predicted turbulent values. When the channel was designed, the transition from laminar to turbulent flow was estimated to occur in the first part of the channel, and the heat transfer rates for the first section (several inches) of the channel were expected to be between the laminar and turbulent values. Therefore, the measured heat transfer rates were higher than the design values near the channel inlet, and the electrodes overheated as mentioned above. To avoid this problem, the duration of the tests was reduced from 8 to 5 seconds. The heat transfer rate measured in the nozzle indicates that the heat transfer in that section was laminar. The transition from laminar to turbulent flow must therefore have occurred near the junction of the nozzle and the channel.

When the test time was reduced to five seconds as discussed above, the electrodes in the upstream section of the channel were heated properly however, the electrodes in the downstream section of the channel did not reach their design temperature with the result that the electrode voltage drop increased significantly. The increased electrode drop results, of course, in a loss in potential power output. The electrodes can easily be remachined to alleviate this problem.

Measurements of the static pressure distribution were made with no magnetic field applied with mass flow rates of 0.6 and 0.8 kg/sec. In Figure 59, the measured pressure distribution for a mass flow rate of 0.6 kg/sec is shown. It is seen that the diffuser recovery starts slightly into the channel which means that the diffuser performance is marginal at this pressure level. Modifications in the facility were made to increase the flow to 0.8 kg/sec to improve the recovery. The pressure distribution with this flow rate is plotted in Figure 60. It is seen that the pressure recovery now starts in the diffuser section rather than in the channel as was the case in the previous figure. This indicates a more favorable pressure recovery situation. Calculations show that the Mach number of the

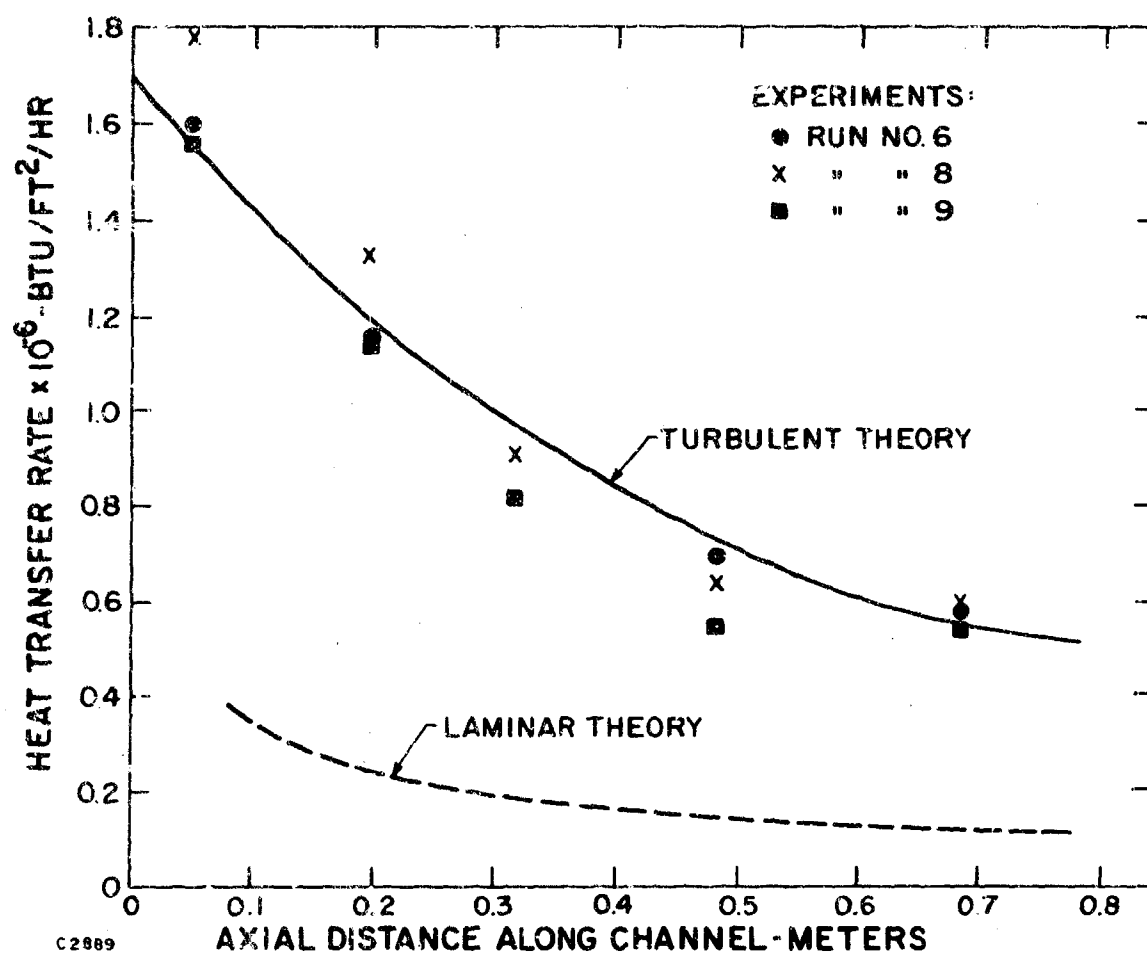


Figure 58 Insulator Heat Transfer as a Function of Axial Distance Along Channel When Burning Toluene and Oxygen; Mass Flow = 0.6 kg/sec; B = 0.

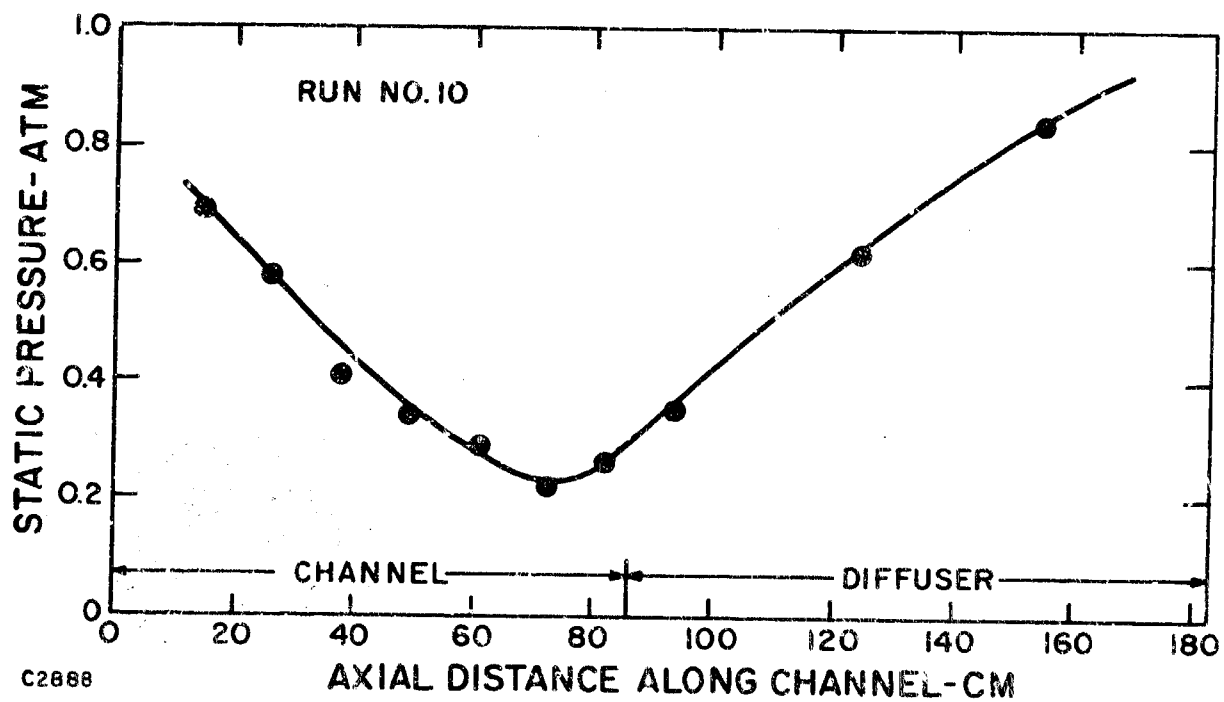


Figure 59 Measured Static Pressure Distribution in the Channel and the Diffuser when Burning Toluene and Oxygen; Mass Flow = 0.6 kg/sec;  $B = 0$ .



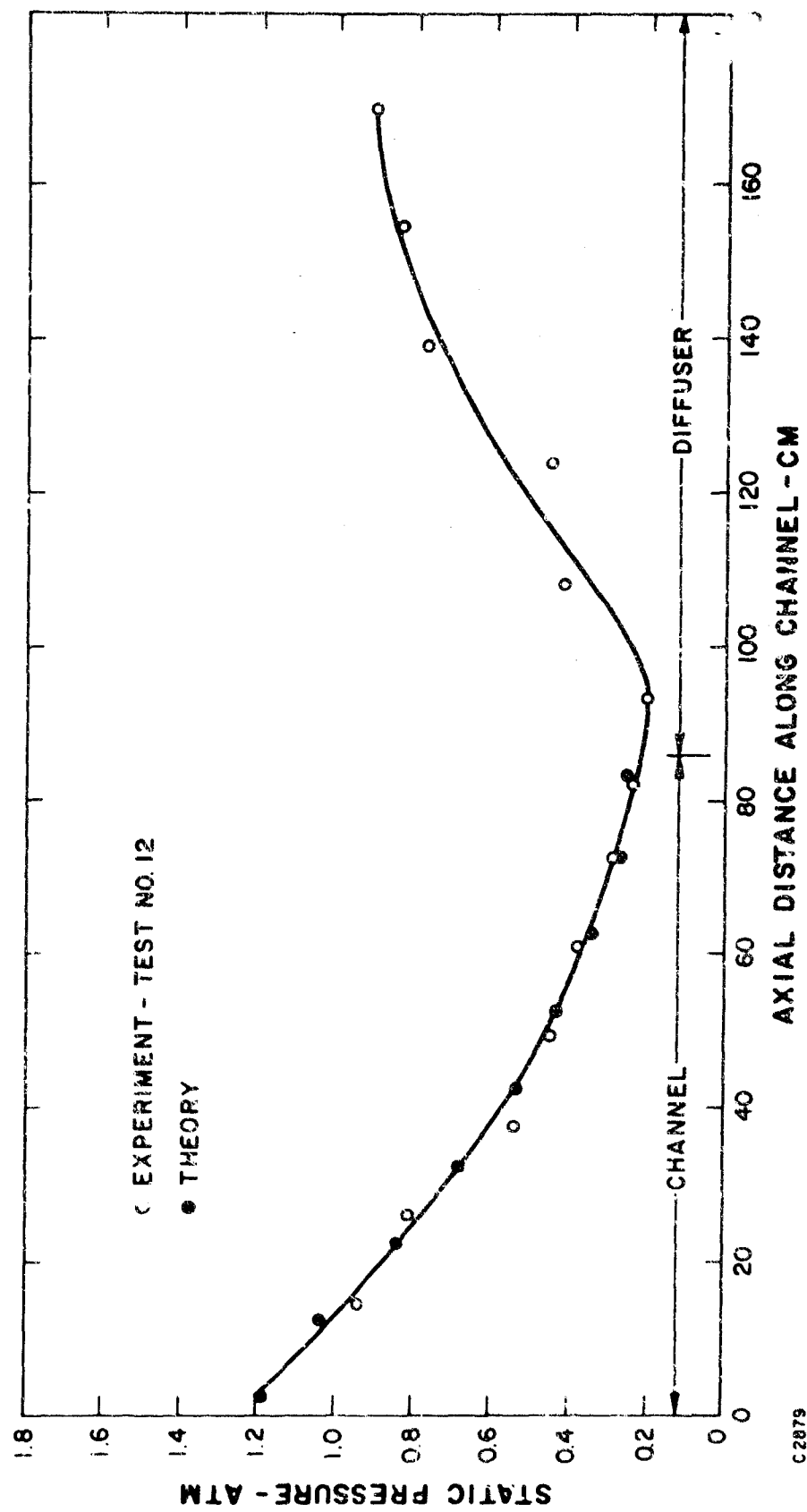


Figure 60 Static Pressure Distribution in the Channel and Diffuser when Burning Toluene and Oxygen; Mass Flow = 0.8 kg/sec;  $B = 0$ .

gas core at the exit of the channel is about 2.9 and that the normal shock recovery pressure averaged over the channel cross section is about 1.5 and 2.0 atm for the cases plotted in Figures 59 and 60, respectively. The required normal shock recovery pressure for this diffuser lies between these two values. The required value is probably about 1.75 atm. This value is considerably above the expected or anticipated value.

At AERL different circular diffusers have been tested previously under similar gas conditions\* and recovery pressure requirements ranging from 1.1 to 1.35 atm have been observed. A number of articles on supersonic diffusers tested under non-MHD gas conditions can be found in the literature.\*\* A wide range of performance characteristics are observed for different types of diffusers including data covering the requirement observed for the diffuser used here. The importance of the diffuser performance is illustrated by the fact that the power output under the present condition can be increased by about twenty-five percent if the recovery pressure requirement is reduced from 1.75 to 1.25 atm.

---

\* Teno, J., Brogan, T. R., Petty, S. W. et al., "Research Studies and the Development of MHD Generators and Accelerators," Final Report. Contract AF40(600)-1043 October 1969.

\*\* Neumann, E. P., and Lustwerk, F., "Supersonic Diffusers for Wind Tunnels," J. of Applied Mech., June, 1949, pp. 195-202.

Neumann, E. P., and Lustwerk, F., "High Efficiency Supersonic Diffusers," J. of the Aeronautical Sciences, June, 1951, pp. 369-374.

Lukasiewicz, J., "Diffusers for Supersonic Wind Tunnels," J. of the Aeronautical Sciences, September, 1953, pp. 617-626.

Crossen, J. W., and O'Brien, R. L., "Investigation of the Diffusion Characteristics of Supersonic Streams Composed Mainly of Boundary Layers," J. Aircraft, Vol. 2, No. 6, November-December, 1965, pp. 385-492.

In Figure 60, a theoretical pressure distribution is compared with the experimental results. Good agreement is observed. The theoretical predictions are based on smooth plate friction factors. This is encouraging since it implies that the smallest possible friction loss can be used in this type generator design.

The initial power generation tests were performed immediately after the conclusion of the cyanogen fuel program in order to establish the power-generating capability of the channel. The power output was raised to 280 kW in the third test. This corresponds to a specific power output of 0.47 MJ/kg. The "Closed position" area distribution was used during these tests, and the channel was connected in the diagonal configuration at an angle of about 45 degrees. Grading resistors were used at the power take off electrodes. The grading resistor and main load configurations will be discussed in a later paragraph. The maximum power generated was approximately 300 kW including the power in the grading resistors. The total axial voltage was 1370 volts. The mass flow was 0.6 kg/sec and the magnetic field at the middle of the channel was 2.6 Tesla. The electrode drop in the front of the channel was 40 volts and at the end it was about 115 volts. The generator worked well during these tests. A comparison between the theoretical and experimental axial voltage distribution is shown in Figure 61. Good agreement is observed. In Figure 62, the predicted voltage versus current characteristics are shown, and the predicted boundary layer stall limit is indicated. It is observed that it was possible to operate the generator close to the stall limit. A twenty-five percent deceleration of the flow velocity is estimated at these conditions. The pressure ports were inoperative during these tests, so no assessment of the pressure distribution and the pressure recovery situation could be made.

The fact that the generator output could be raised in a predictable manner to such a high performance level during the three initial power generation tests with this channel is extremely encouraging. It illustrates the present high level of understanding of generator channel performance.

To increase the power output, a second series of power generation tests (23 tests in all) were made. The channel was used in the "open position," and the mass flow and magnetic field were increased to 0.8 kg/sec and 3.5 Tesla, respectively. As in the previous series of tests, the channel was connected in a diagonal configuration with the equivalent insulating wall angle varying from about 50 to 43 degrees from the front to the back of the channel. As before, grading resistors were used at both power take-off electrodes. The active power generating section of the channel was about 70 cm.

For the initial power runs of this second set of tests, a small seed flow (less than one percent of  $\text{Cs}_2\text{CO}_3$  by weight) was purposely used to limit the output power level. The conductivity was about 20 mhos/m. The generated output power corresponding to this seed rate was approximately 245 kW at 150 amperes. The power in the grading resistors was relatively large in these tests because the present magnetic field tapers off very

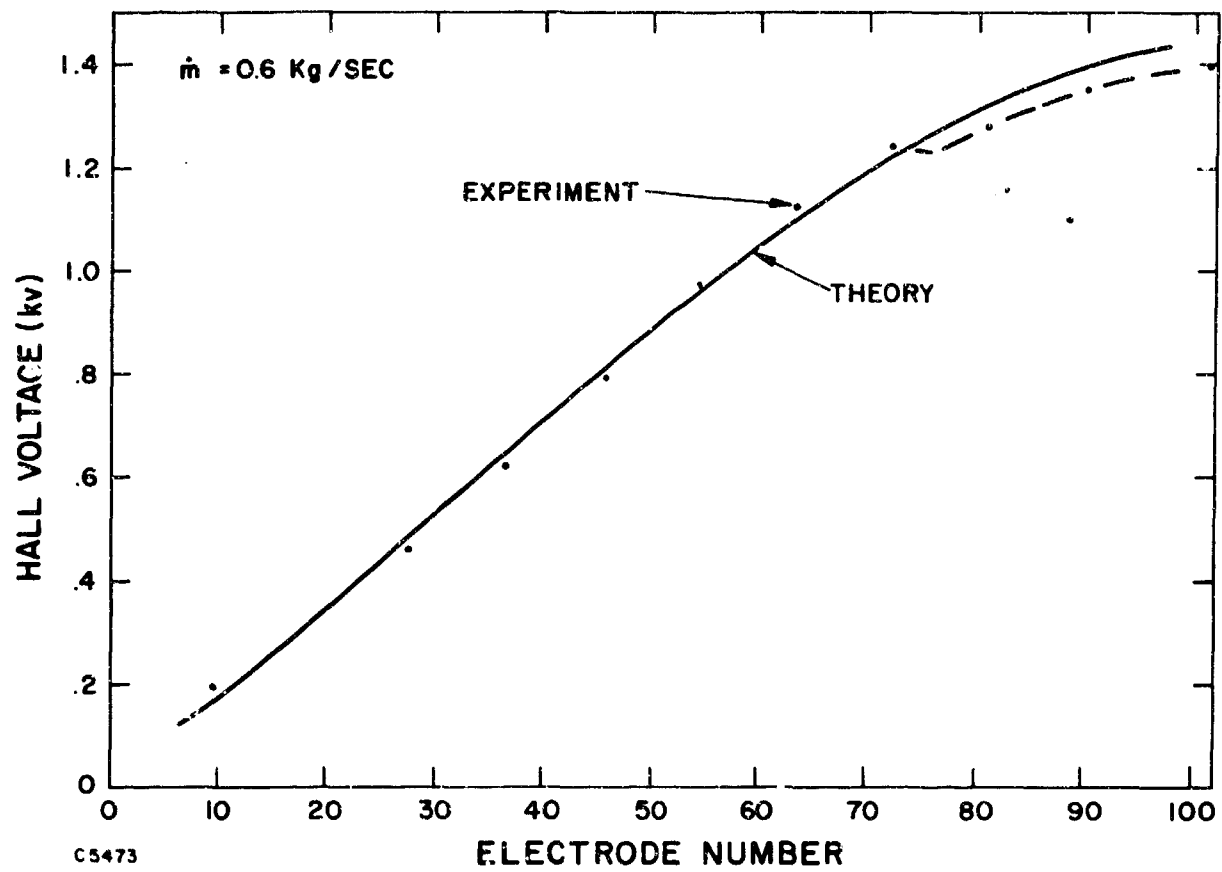


Figure 61 Observed and Predicted Axial Voltage Distributions for the APL Generator; Mass Flow = 0.6 kg/sec.

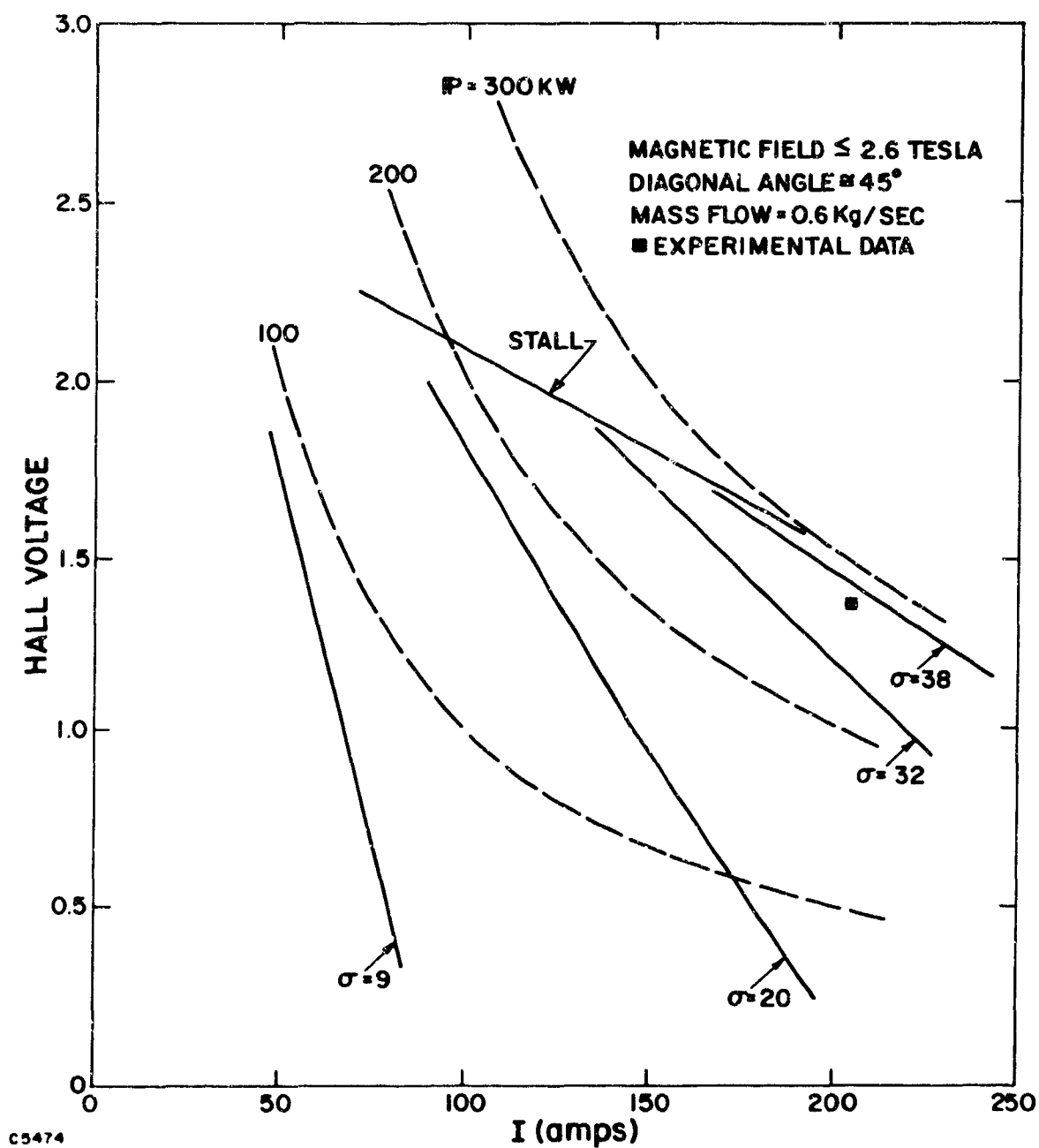


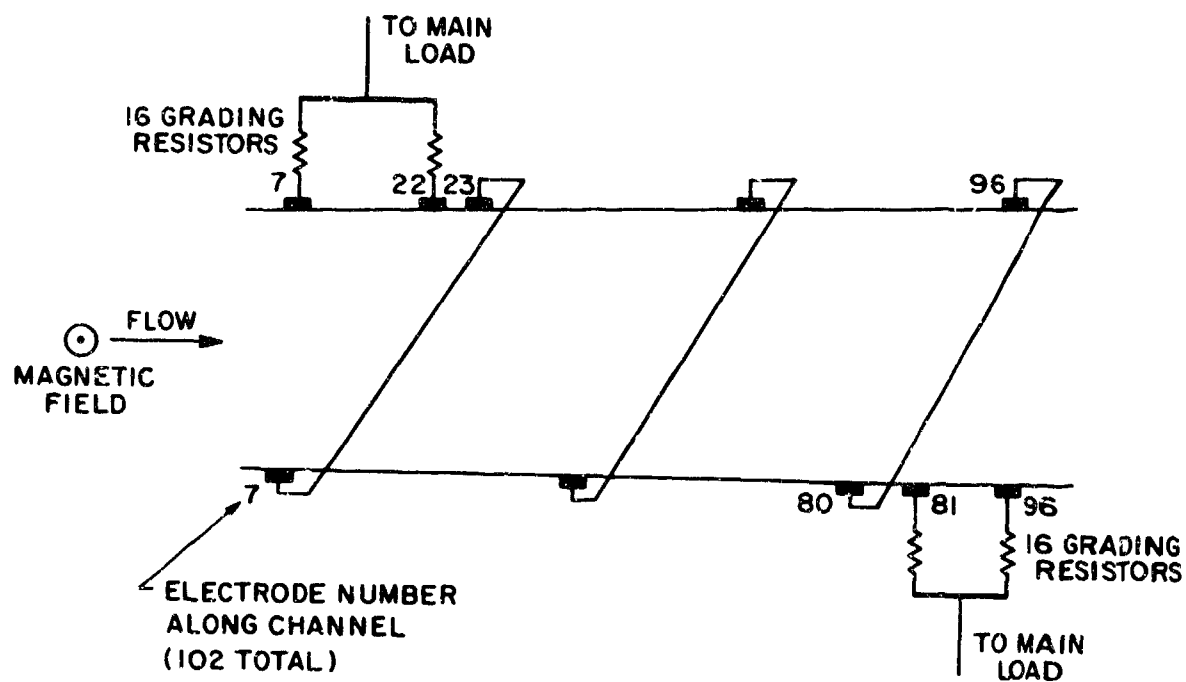
Figure 62 Predicted V-I Characteristics for the APL Generator with 0.8 kg/sec Mass Flow and a Peak Field of 2.6 Tesla.

slowly (see Figure 57) because of the large size of the magnet. With a magnet of appropriate size the grading resistors could be reduced considerably. During this test (Run No. 13), the detailed electrical circuitry for the channel connection was as follows: Ninety-six electrode pairs were used in the power section of the channel. The channel was connected in the diagonal mode. A schematic of the electrical wiring diagram is shown in Figure 63. Sixteen grading resistors were used at each end of the channel. The values of the resistors connected to electrodes 7 through 22 (Figure 63) were 19.8, 20.1, 20.4, 20.9, 21.4, 22.0, 22.7, 23.7, 21.3, 18.6, 15.9, 13.3, 10.7, 8.0, 5.4, and 2.7 ohms, respectively, and the resistors connected to electrodes 80 through 96 were 2.7, 5.7, 9.1, 12.2, 15.0, 18.1, 21.0, 24.1, 25.0, 22.4, 17.0, 14.6, 13.0, 11.6, 10.5, and 10.0 ohms, respectively. The values of these resistors were selected so that the generator performed satisfactorily in the end regions of the channel for these particular loading conditions.

More detailed results for this test are shown in the next four figures. The axial voltages along the two electrode walls are plotted in Figure 64. The transverse current is shown in Figure 65. The transverse voltage profiles measured on the pegs across the channel at electrodes 28 and 81 are shown in Figures 66 and 67 respectively. The test results agree with predicted performance as seen in Figures 64 and 65. Some relatively small discrepancies exist near the channel ends. From Figures 64 and 65, it is seen that the generated voltage increases evenly along the channel and that the transverse current is relatively uniform.

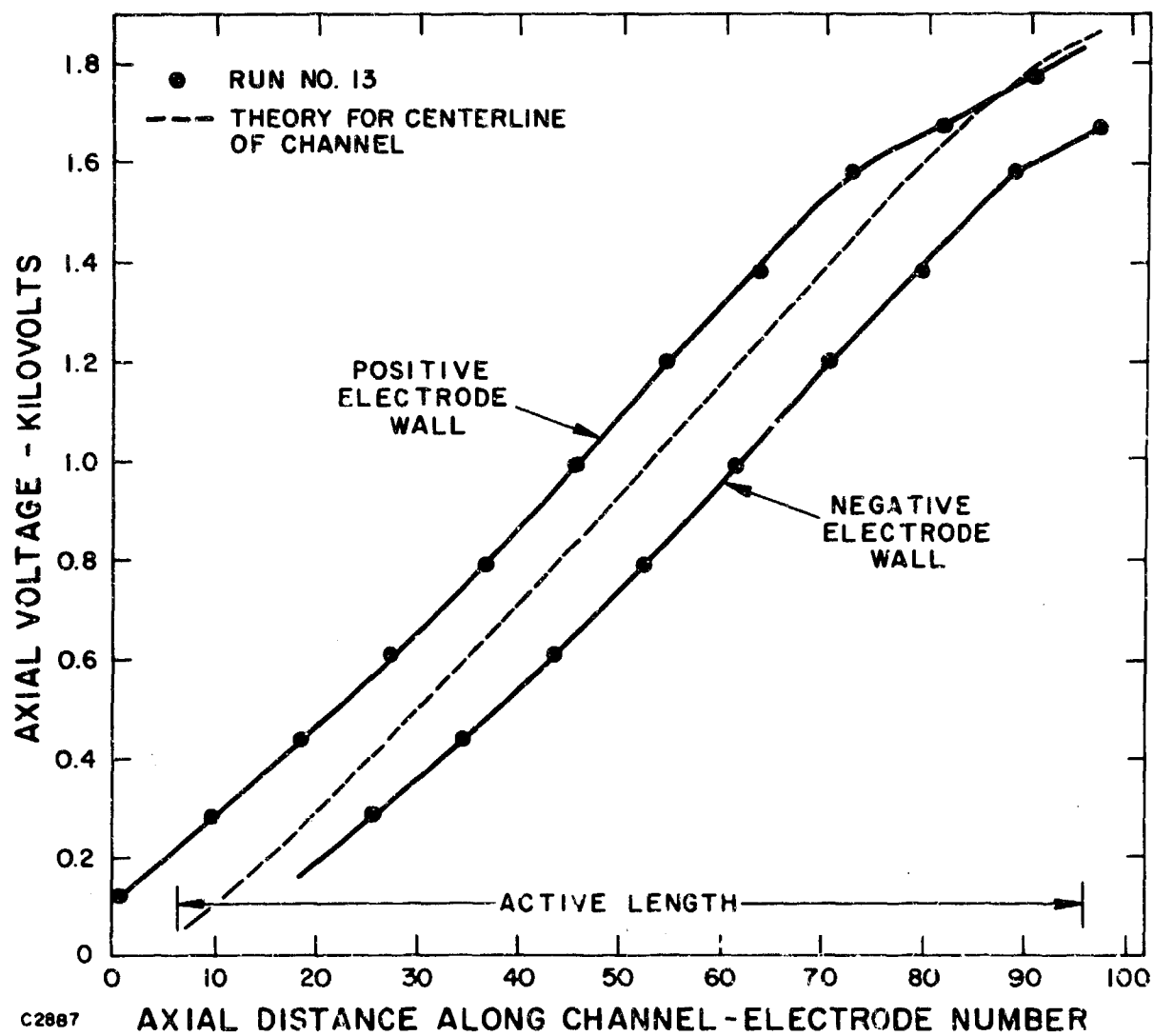
From Figures 66 and 67, the electrode voltage drops in this test are seen to be about 80 volts at electrode pair 28 and about 180 volts at electrode pair 81. The electric field at the center of the channel as determined from the test results agree within five percent of the predicted values. In fact, the agreement between experimental observations and analytical predictions was good in all respects for this test.

After the initial power runs of the second set of tests (as described above), testing at higher power levels was undertaken to establish the maximum power output capability of this machine. A power output of about 400 kW was generated. Some of the results for such a case are shown in Figures 68, 69, and 70. The experimental axial voltage and transverse current distributions are plotted in Figures 68 and 69, respectively. In Figure 70, the observed pressure distributions for both loaded and unloaded generator conditions are shown. The predicted pressure distribution under loaded generator conditions is seen to deviate from the observed values in the downstream section of the channel. The reason for this discrepancy is twofold. First, the magnetic field distribution (Figure 57) of the Mark II magnet because of its large size extends considerably into the diffuser and therefore, current flow is induced in the gas in this diffuser section which causes drag on the gas which in turn tends to increase the required pressure recovery level. To investigate this effect a few tests were made where the magnetic field was reduced by moving the channels further into the tapering and field section of the magnet. The pressure recovery improved some, but not enough to change the overall generator performance.



C 3020

Figure 53 A Schematic of the Electrical Wiring Diagram Used in Run No. 13.



C2887

Figure 64 Observed and Predicted Axial Voltage Distributions.



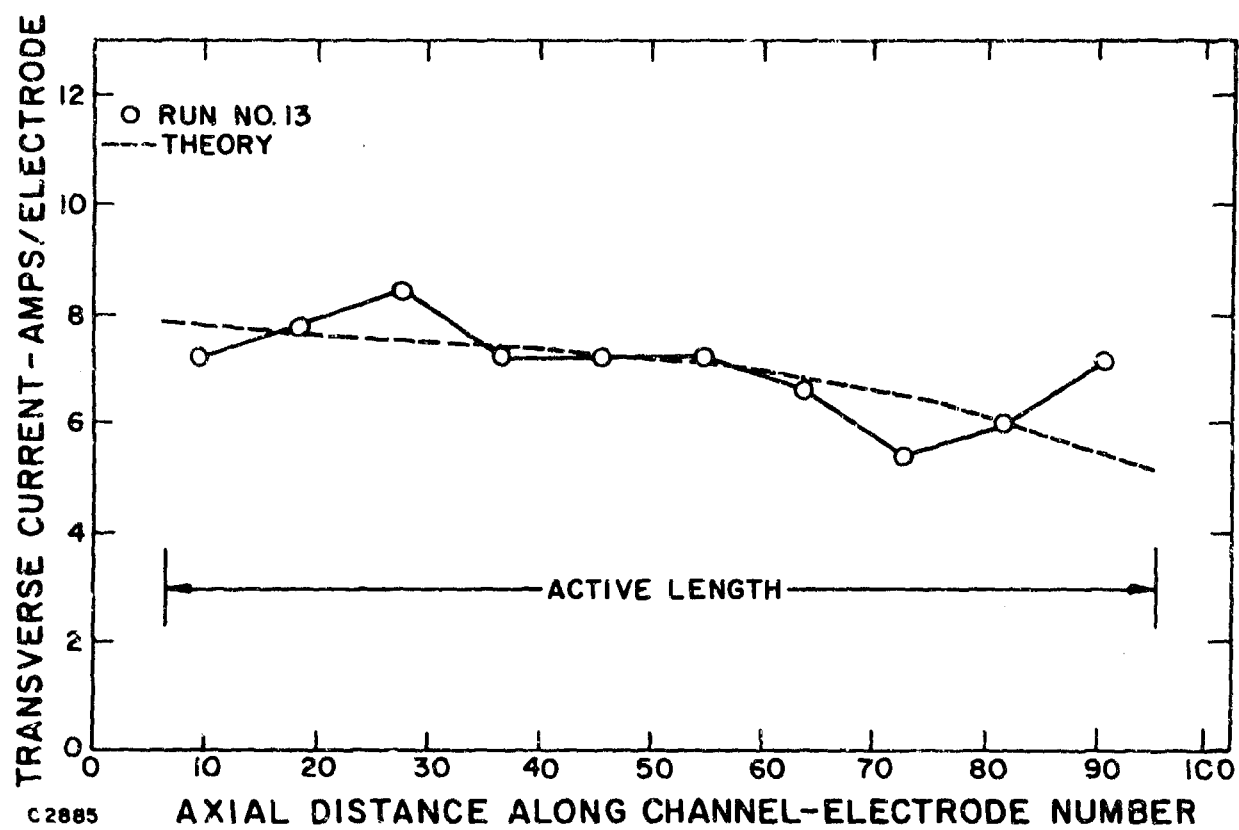


Figure 65 Transverse Current in Amperes per Electrode as a Function of Axial Distance Along the Channel.

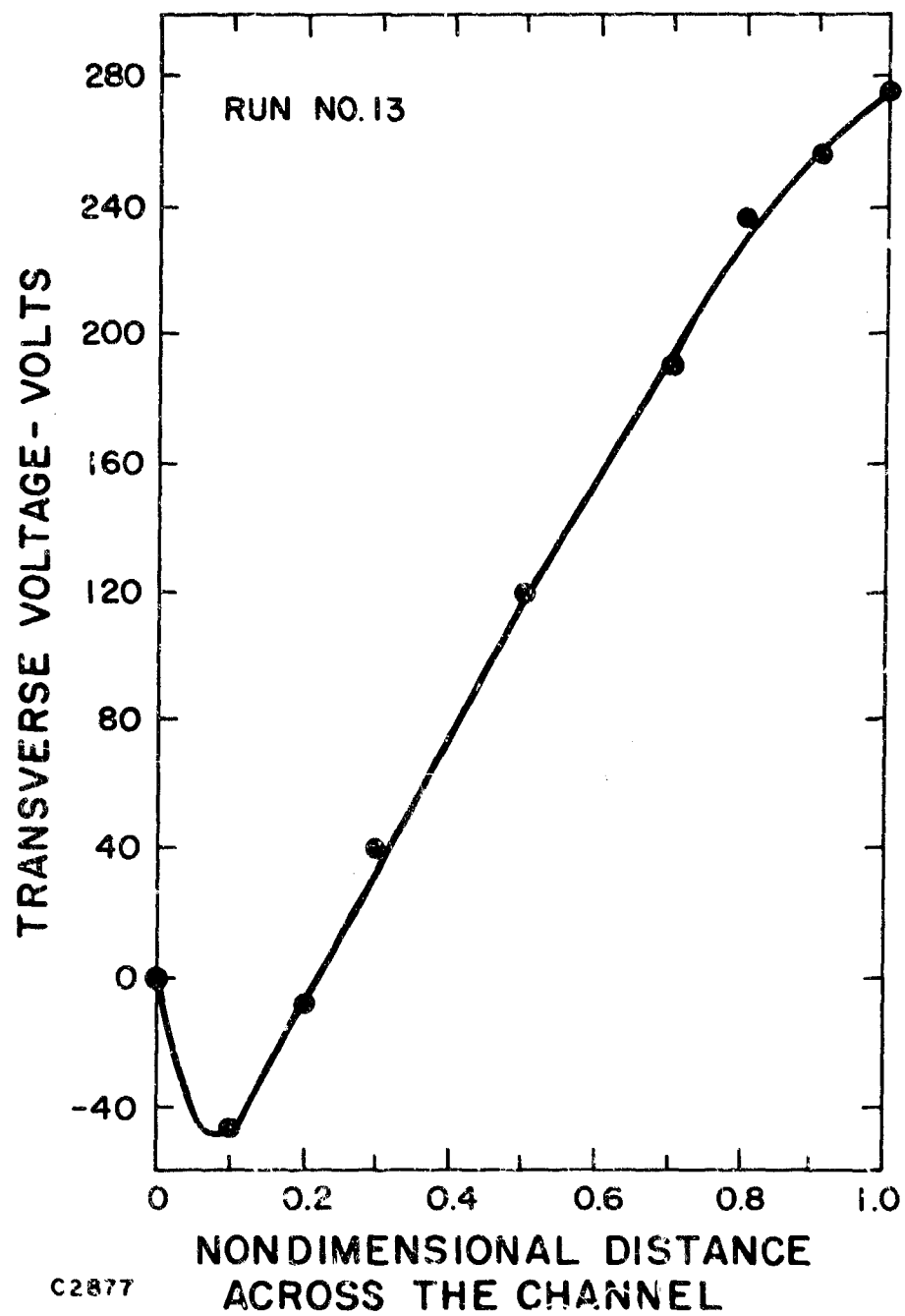


Figure 66 Transverse Voltage Distribution at Electrode Pair Number 28.

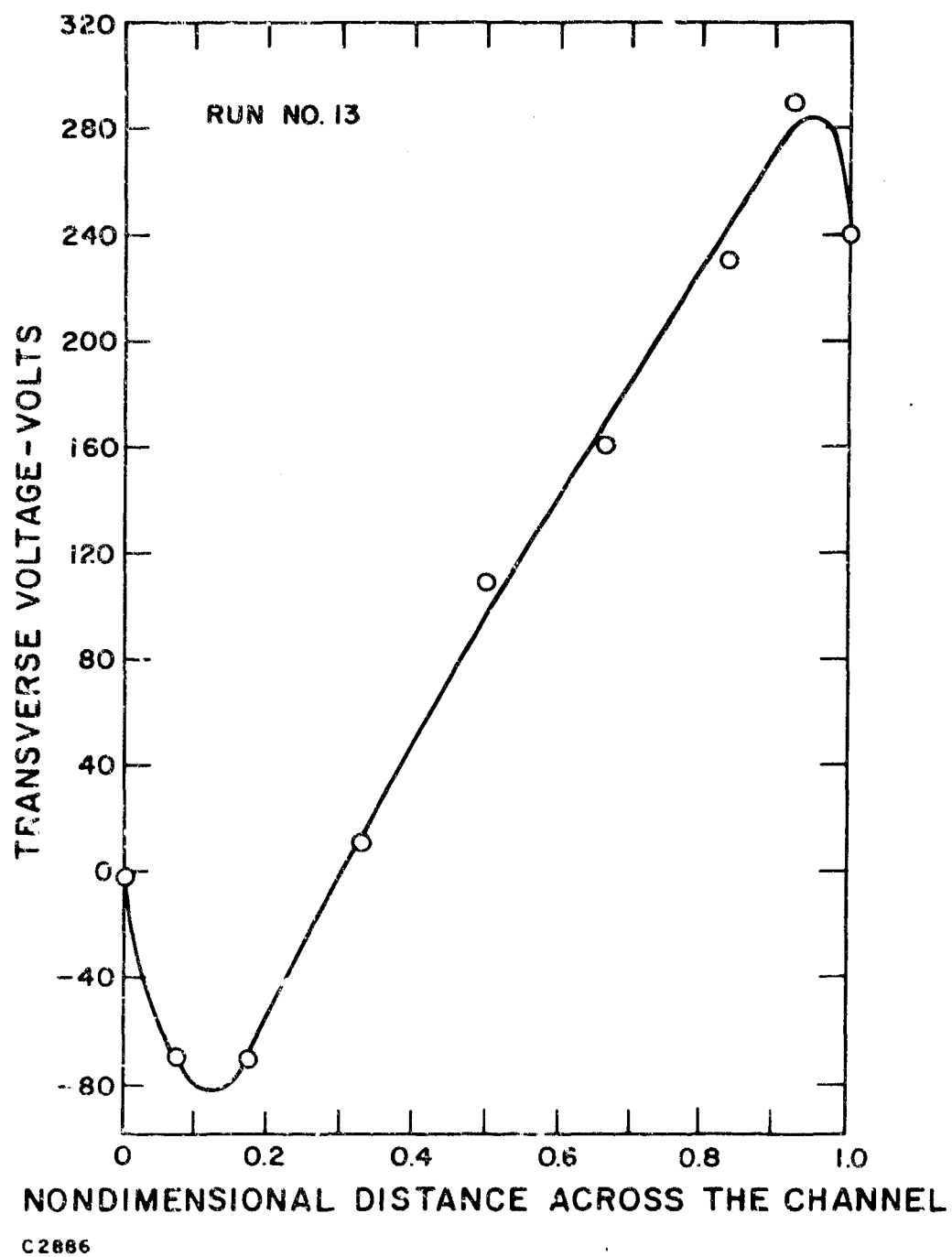
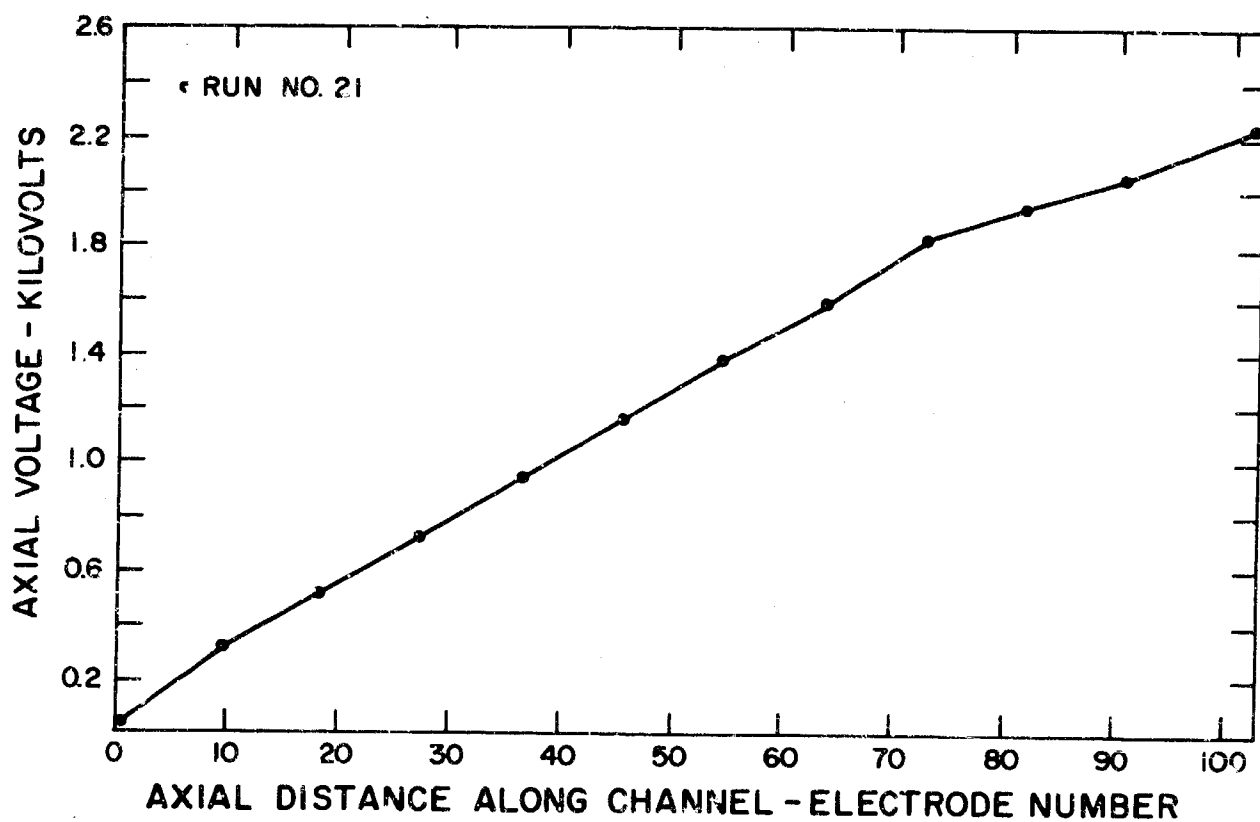
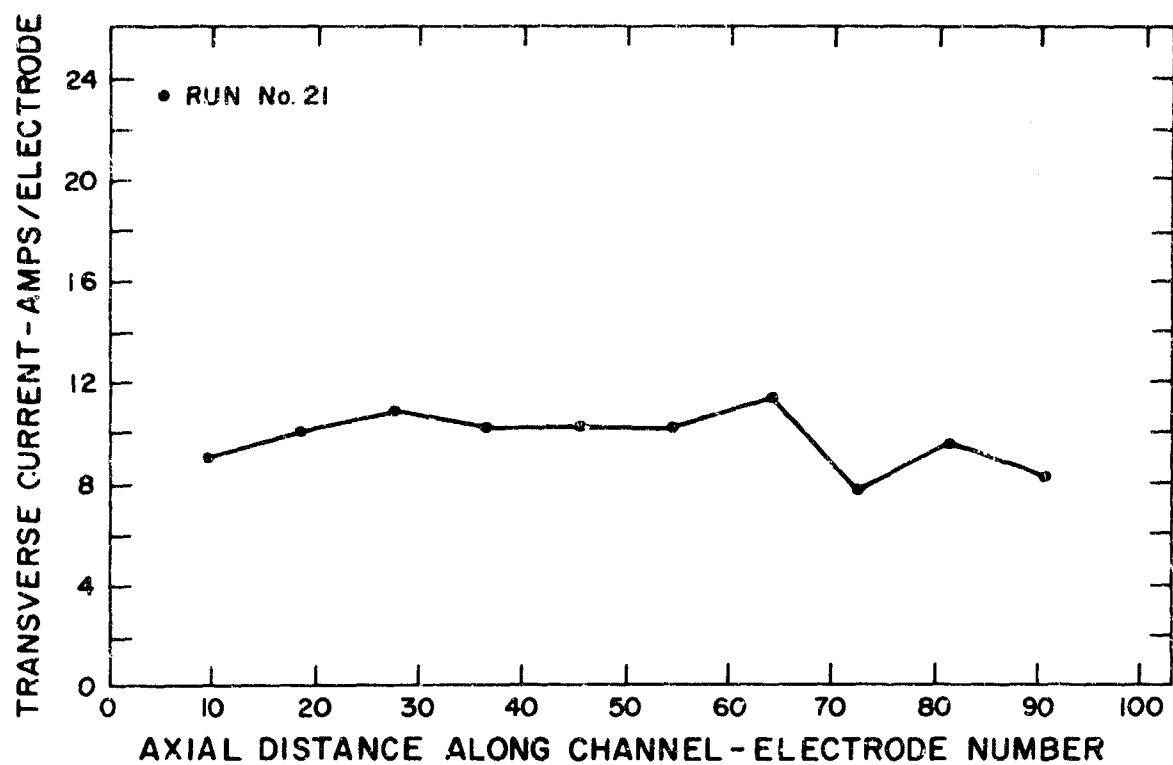


Figure 67 Transverse Voltage Distribution at Electrode Pair Number 81.



C5977

Figure 68 Axial Voltage Distribution for 400 kW Test.



C5976

Figure 69 Transverse Current Distribution in Amperes per Electrodes for 400 kW Test.

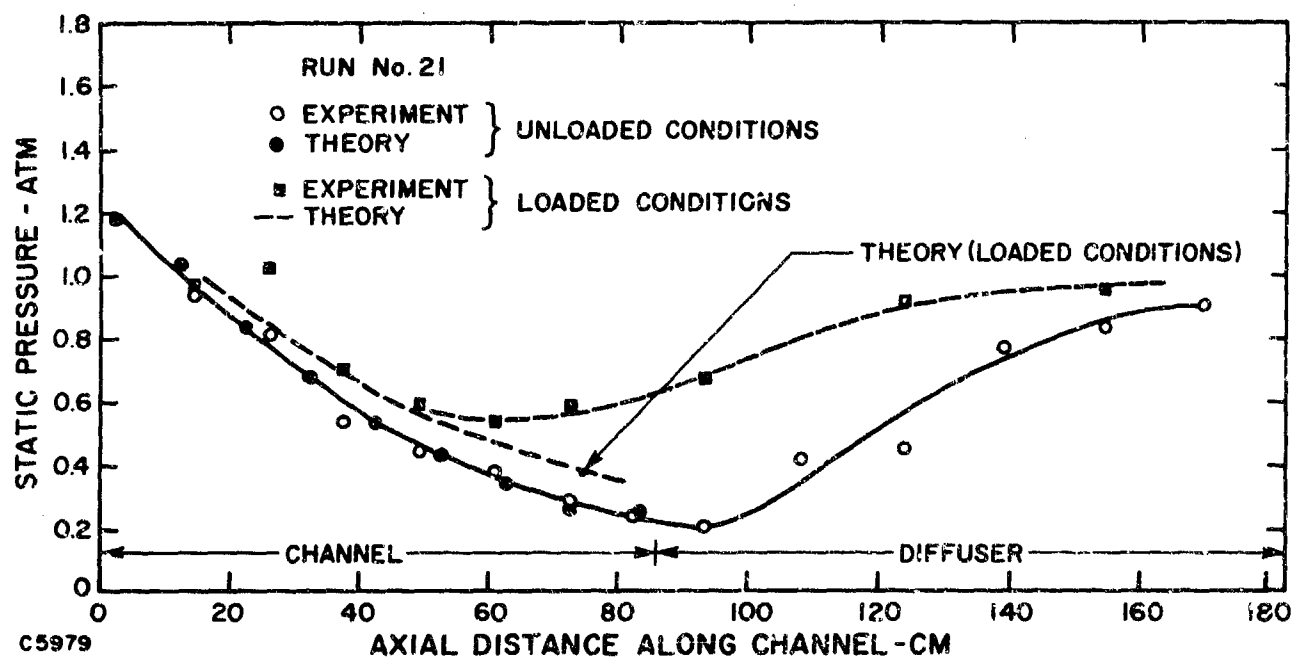


Figure 70 Axial Pressure Distributions for Unloaded and Loaded MHD Generator During 400 kW Test.

noticeably. To optimize the performance of the system investigated under this contract, a smaller magnet with a more rapidly decaying end field distribution would be required. For example, with the APL magnet (Section II) for which this generator was designed, this effect should be of no consequence. The second reason for this discrepancy has to do with the diffuser recovery efficiency. The theoretically calculated recovery pressure value at end of the channel under loaded conditions is about 1.7 atm. As discussed previously in this section, for unloaded generator operating conditions the diffuser required an estimated 1.75 atm to recover without changing the channel exit pressure. Under loaded conditions the required recovery pressure would naturally increase but not to the extent required to explain the observed data. It is predicted that a recovery pressure of approximately 2.25 atm is needed to explain the data. The degradation in performance can only be explained in terms of both the end losses and the pressure recovery requirement. The percent degradation caused by the individual effects was not examined. Further investigations would be required to resolve this matter.

A total of three tests at the 400 kW power level were made. Due to difficulties with the burner encountered at the higher seed rates (described earlier), it was not possible to achieve higher performance in this series of tests. Later in the study program the burner problem was eliminated as described in the previous subsection; however, since the channel walls were now contaminated with seed, current leakage limited the power output to about 360 kW even at considerably higher seed flows than previously used. (The seed contamination occurred because the channel was flooded with water during the three burner burnout tests.) Additional testing after a complete reconditioning of the channel would be required to establish the extent to which the 400 kW output might have been exceeded.

The predicted voltage versus current characteristics for the generator conditions of the second set of tests are shown in Figure 71. The characteristics at various conductivities are given. The mass flow was 0.8 kg/sec, the peak magnetic field was 3.5 Tesla. The channel is assumed to be connected in the diagonal mode by connecting the electrodes as shown in Figure 63. The values of the end bleed resistors vary depending on the current and voltage levels. The boundary layer stall curve is shown in this figure. It is seen that the generator stalls at about a power output of 500 kW. Therefore, it is concluded that if the diffuser performance could be improved and the current flow in the generator ends could be alleviated by using a magnet of the proper size for this channel (discussed above), a power output of 500 kW should be obtainable. Furthermore, by modifying the electrodes to increase the electrode temperature in the downstream section of the channel the electrode drop can be reduced significantly as discussed previously. It is estimated that the power output could then be raised to 550 kW, which corresponds to a specific power output of 0.7 MJ/kg. It is believed that it would be instructive and desirable to continue the testing of this channel with the objective of achieving this higher specific power output.

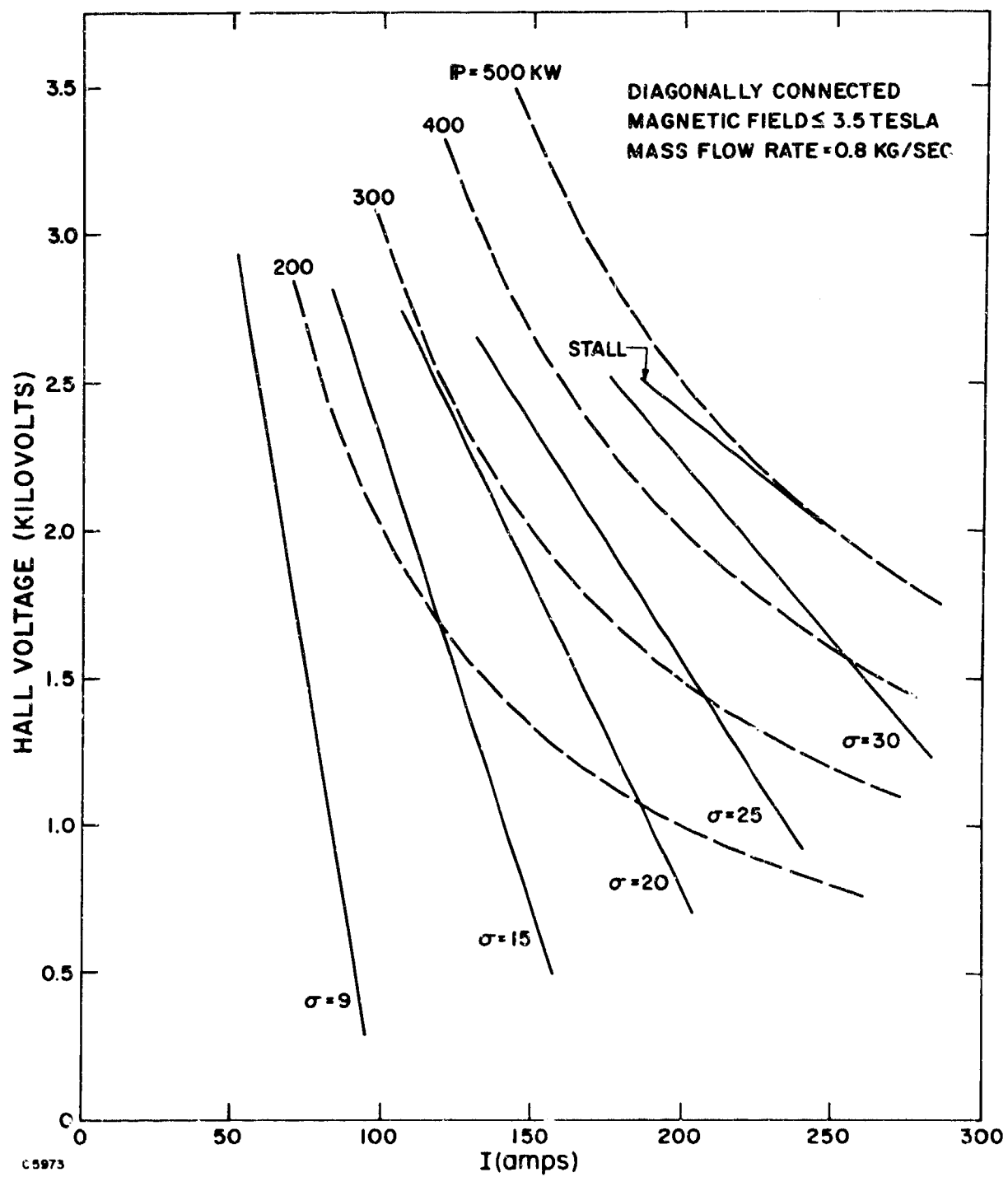


Figure 71 Predicted V-I Characteristics with 0.8 kg/sec Mass Flow and a Peak Field of 3.5 Tesla.



## 5. CONCLUSIONS AND RECOMMENDATIONS

In this test program the feasibility of compact, high power MHD power generation in the one megawatt range was demonstrated. Considerably higher performance than in previous generators of this size using conventional hydrocarbon fuels (see Table VIII-1) was achieved even though the channel was not designed for these conditions but rather for use with high energy fuels. The performance was predicted accurately by analytical techniques developed at AERL. In particular, performance characteristics such as axial voltage, current levels, pressure and heat transfer distributions, and electric fields could be predicted with good accuracy.

The diagonal generator configuration was used in this test program. A total power output of approximately 300 kW was generated with a mass flow of 0.6 kg/sec and a peak field of 2.6 Tesla, and a total power output of approximately 400 kW was generated with a mass flow of 0.8 kg/sec and a peak magnetic field of 3.5 Tesla. This corresponds to a specific power output of 0.5 MJ/kg. With some improvements in the equipment it is estimated that a specific power output of 0.7 MJ/kg (or 550 kW) can be achieved. The improvements referred to above involve 1) minor re-machining work on the electrodes to reduce the electrode drop and improve the generator performance, 2) redesigning the diffuser to obtain improved diffuser performance and 3) using a magnet of a size more suitable for the present channel.

If the above improvements were made, it would be desirable to further test this generator both to verify the estimated maximum output power of 550 kW and to make a more complete performance evaluation by testing the generator over a large range of output voltages and currents.

## APPENDIX 1

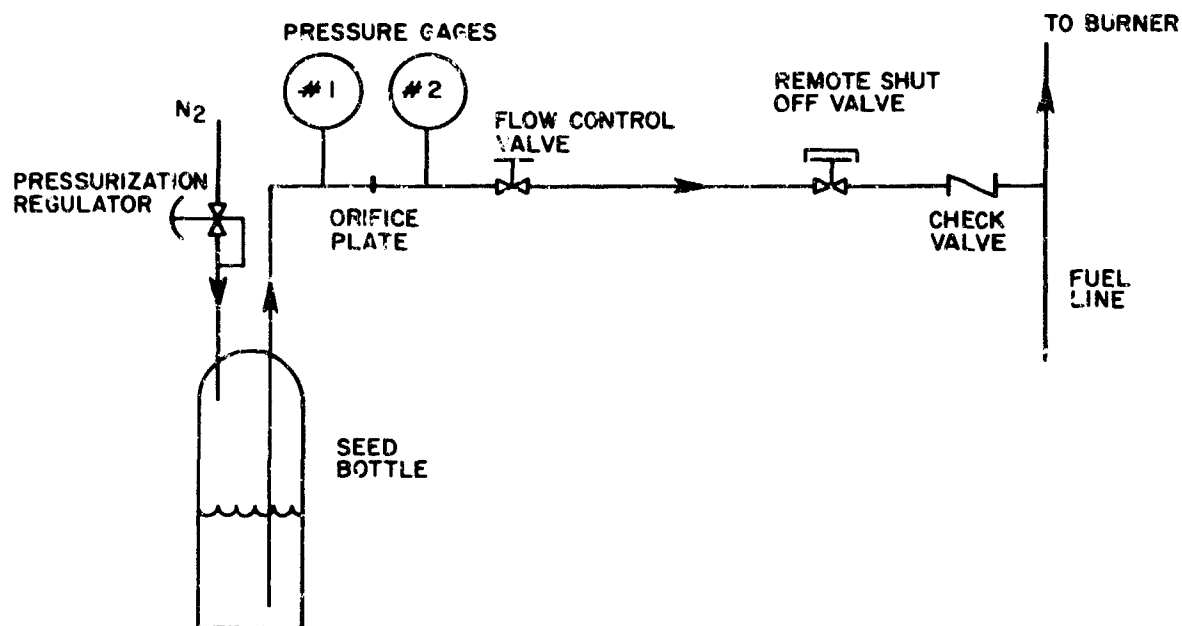
### LIQUID SEED SYSTEM

Tests to investigate the high power output performance of the MHD generator required that among other things the seeding rate be increased. Due to limits imposed on the dry powder seed system due to burner difficulties (see Section VIII), a liquid seed system was viewed as one method of seeding at the higher seed flow rates. As a consequence a liquid seed system was assembled, installed and checked out as part of the experimental program conducted at AERL. Cesium carbonate was dissolved in water, and the resulting solution was injected into the fuel line near the fuel manifold. A sketch of the seed system is shown in Figure 72. Because it was necessary to keep the amount of carrier water to a minimum, a saturated, heated mixture of cesium carbonate and water was used.

To heat the mixture and to avoid having the seed condense out of solution before the mixture was injected into the burner, the seed bottle and the copper tubes are wrapped with electrical heating tape and with one inch of thermal insulation so that the whole system was heated to approximately 210°F. At this temperature a solution of 2.5 to 1 by weight of cesium carbonate and water will stay in solution. The effect of a small amount of carrier water on the gas conductivity should have been small enough not to change the generator performance. The control valve shown in Figure 72 was used to change the seed flow during the run, and the pressure gages were used to determine the flow rate.

A good amount of time was spent during the test program trying to get the seeding system to operate in a predictable manner with the expected values of gas conductivity. The conductivities observed at lower seeding rates agreed with previous measured values but at higher seeding rates the observed results were erratic and nonrepeatable. Several difficulties in operating the system were observed, these included:

- 1) Seed blocking of the fuel injectors. (Although most of the seeding system was heated a small portion of tubing between the seed shutoff valve and the burner was cold and could have caused the seed to condense as the seed solution flowed through the tubing on the way to the burner.)
- 2) The seed had a tendency to settle out of solution unless continuously agitated thus leading to a non-uniform seed mixture.



C5084

Figure 72 Experimental Setup of Liquid Seed System at AERL.

- 3) There was apparently some tendency for the seed to chemically react with the system copper tubing. (It was not determined what effect this had on the solution).
- 4) The tubing heaters were fragile, and it was difficult to keep the system at a given temperature continuously.
- 5) When the system did operate as expected, the observed conductivity was not repeatable. Some of the tests did show good performance but the same performance could not be achieved twice in a row.

Because of the time consumed and the erratic performance, testing with this system was finally stopped and seeding with the powder seed system was resumed and because of the other changes made to the burner as discussed in Section VIII it was found that the burner was capable of being operated at any seed level using the powder seed system.

BLANK PAGE

## APPENDIX 2

### HALL MHD GENERATOR ANALYTIC COMPUTER PROGRAM

The purpose of this appendix is to explain in detail, the Hall MHD Generator Analytic Computer Program. To begin, the inputs to both the Mollier and Hall Generator Program are listed and explained; then, a typical set of input cards are displayed; and finally the program logic as well as various subroutines are explained.

#### Inputs To Mollier and Hall Generator Program

- |    |   |   |  |
|----|---|---|--|
| I  | [ | <ol style="list-style-type: none"> <li>1. ISEED, HEADIN (I1, 18A4)</li> <li>2. FC, FH, FN, FO, ZSEED (5E9. 0)</li> <li>3. NTEMP (I2)</li> <li>4. <math>T_1, T_2, T_3, \dots, T_{n_{temp}}</math> (8E9. 0)</li> <li>5. NPRES (I2)</li> <li>6. <math>P_1, P_2, P_3, \dots, P_{n_{pres}}</math> (8E9. 0)</li> <li>7. Blank Card</li> </ol>                                       |  |
| II | [ | <ol style="list-style-type: none"> <li>8. NATAB (I2)</li> <li>9. table of X, D1, D2 (one set per card) (3E9. 0)</li> <li>10. NBTAB (I2)</li> <li>11. table of X, B (one set per card) (2E9. 0)</li> <li>12. NAME LIST cards of form:<br/> NAME LIST/NAME/XO, DX, XMAX, MU, LO, NBAR, FHO,<br/> 1, FD, FRICT, F1C, F2C, AK1, AK2, BMAX, HCOMPO,<br/> HBO, PBO, ATHO</li> </ol> |  |

The program will cycle back to #12 after each case.

Set I read in phase one (1) or Mollier part of program.

Set II read in phase two (2) or Hall Generator part of program.

*Preceding page blank*

Explanation of inputs.

1. ISEED = 1                      cesium seeding  
              = 2                      potassium seeding  
       HEADIN = 72                character comment printed on first page of output
2. FC        = # of carbon atoms  
       FH       = # of hydrogen atoms  
       FN       = # of nitrogen atoms  
       FO       = # of oxygen atoms
3. NTEMP = # temperatures in the table which follows
4.  $T_1, T_2, T_3, \dots, T_{n\text{temp}}$  = list of temperatures in increasing order (8 per card)
5. NPRES = # pressures in the table which follows
6.  $P_1, P_2, P_3, \dots, P_{n\text{pres}}$  = list of pressures in increasing order (8 per card)
7. Due to its size, this program was split into two phases.

Phase one is the Mollier chart subroutine which for a given gas mixture and seed concentration is used to determine the complete thermodynamic properties of the mixture as well as conductivity and Hall coefficient for a given range of pressures and temperatures.

Phase two includes:

- a) Hall generator off design program = "PP23"
- b) Subroutine HCOMP - "HCOMP"
- c) Subroutine LIUTER - "LIUTER"

On the IEM 360-44 there exists the capability to overlay in core phase 2 over phase 1 after phase 1 is completed. This is known as a "COMPLETE PHASE OVERLAY" and is accomplished by the statement CALL LINK ('PHASE 2'). As a result of this, one card is skipped or lost in the input stream thus necessitating the need for a blank card at this point.

8. NATAB = # of  $X, D1, D2$  sets in the table which follows
9.  $X_1, D1_1, D2_1$   
        $X_2, D1_2, D2_2$   
        $\vdots, \vdots, \vdots$   
        $X_{n\text{atab}}, D1_{n\text{atab}}, D2_{n\text{atab}}$

10. NBTAB = # of X, B sets in the table which follows

11.  $X_1, B_1$

$X_2, B_2$

$\vdots$

$\vdots$

$X_{n\text{tab}}, B_{n\text{tab}}$

12. NAME LIST variables:

- a) XO (meters) initial x
- b) DX (meters) increment in x at which calculations are done
- c) XMAX (meters) final x
- d) MU dynamic viscosity
- e) LO (meters) initial value of length used in calculation of Reynold's numbers (i. e.  $REN = \rho * U * (LO + X) / MU$ )
- f) NBAR print control; the computer will print every NBAR-th step of the calculations
- g) THO initial momentum thickness
- h) I axial load current
- i) FD = 1. rectangular channel  
=  $\pi/4$  circular channel
- j) FRICT friction coefficient used in calculation of CF (i. e.  $CF = FRICT / REN^{**2}$ )
- k) F1C conductivity multiplier
- l) F2C hall parameter multiplier
- m)  $AK1 \left\{ \begin{array}{l} \text{constants for electrode drop } V_e \\ \text{ } \end{array} \right.$
- n)  $AK2 \left\{ \begin{array}{l} V_e = K_1 * \Theta H + K_2 \\ \text{ } \end{array} \right.$
- o)  $BMAX B_{\text{program}} = B_{\text{table}} * BMAX$
- p) HCOMPO initial value of compressible shape factor
- q) HBO (cal/gm) burner stagnation enthalpy
- r) PBO (atm) burner stagnation pressure
- s) ATHO (meters\*\*2) area of nozzle throat

NOTE: All NAME LIST variables are floating point except NBAR which is integer.



# FORTRAN CODING FORM

AUTHOR: STATEMENT NO. FORTRAN STATEMENT PROGRAM NUMBER PROGRAM DATE PAGE CF 1 2 IDENTIC

STATEMENT NO.	FORTRAN STATEMENT	PROGRAM NUMBER	PROGRAM	DATE	PAGE	CF	IDENTIC
1	C7H8 + 9N2 + 3O2 + .005 CESIUM SEEDING						
2	7.	18.	.005				
3	2000.	2100.	2200.	2300.	2400.	2500.	2600.
4	2800.	2900.	3000.	3100.	3200.	3300.	3400.
5	3600.	3700.	3800.	3900.	4000.		
6	1.	.2	.3	.4	.5	.6	.7
7	.9	1.	2.	4.	6.	8.	10.
8							12.
9	X VS. D1, D2						
10							
11	0.	.696	.712	.726	.740	.753	.767
12	.25	.712	.726	.740	.753	.767	.781
13	.50	.726	.740	.753	.767	.781	.795
14	.75	.740	.753	.767	.781	.795	.810
15	1.0	.753	.767	.781	.795	.810	.825
16	1.25	.767	.781	.795	.810	.825	
17	1.5	.781	.795	.810	.825		
18	1.75	.795	.810	.825			
19	2.00	.810	.825				
20	2.25	.825					
21	X VS. B						
22	0.	1.9					
23	3.25	1.9					
24	3.50	1.87					
25	3.75	1.84					
26	4.00	1.78					
27	4.25	1.65					

# FORTRAN CODING FORM

AUTHOR		PROGRAM NAME		PROGRAM NUMBER		DATE		PAGE OF	
STATEMENT NO.	1	2	3	4	5	6	7	8	9
1	2	3	4	5	6	7	8	9	10
10	11	12	13	14	15	16	17	18	19
19	20	21	22	23	24	25	26	27	28
28	29	30	31	32	33	34	35	36	37
37	38	39	40	41	42	43	44	45	46
46	47	48	49	50	51	52	53	54	55
55	56	57	58	59	60	61	62	63	64
64	65	66	67	68	69	70	71	72	73
73	74	75	76	77	78	79	80	81	82
82	83	84	85	86	87	88	89	90	91
91	92	93	94	95	96	97	98	99	100
IDENTIFICATION									

```

PNAME X0=0., DX=.25, XMAX=.2., MU=.6., SE-4, L0=2., NBAR=1., TH0=1.E-3, T=2000.,
FD=.785398, FRIC=.282, FIC=.84, ZC=1., AK1=1000., AK2=125., BMAX=1., H0MP0=1.25,
HB0=9., PB0=8.72, ATH0=9.2 SE-2, BEND
PNAME I=3000., BEND
    
```

Given these inputs and the Mollier tables (i. e. tables of h-enthalpy, t-temperature,  $\sigma$ -conductivity,  $\omega \tau / B$  - ratio of Hall coefficient for electrons to the magnetic field,  $\gamma R$  - product of specific heat ratio and universal gas constant,  $\rho$  - density,  $S$  - entropy, and  $\gamma$  - specific heat ratio for a range of pressures - p as well as DEH) from phase one (1), phase two (2) begins with the calculation of channel inlet conditions. From  $P = PBO$ ,  $h = HBO$  subroutine "LIUTER" does a series of double interpolations to obtain the Mollier table values -  $T_B$ ,  $\sigma_B$ ,  $(\frac{\omega \tau}{B})_B$ ,  $(\gamma R)_B$ ,  $\rho_B$ ,  $S_B$ ,  $\gamma_B$ .

$$h_{th} = h_B - (\gamma R)_B T_B / (1 + \gamma_B)$$

from  $h = h_{th}$ ,  $S = S_B = S_{th}$  another series of interpolations is done to obtain  $T_{th}$ ,  $(\gamma R)_{th}$ ,  $\rho_{th}$ .

$$GE = \rho_{th} (ATHO) \sqrt{(\gamma R)_{th}} T_{th} \quad \text{mass flow in}$$

$$A_o = (D1_1)(D2_1)(FD) = \text{AREA } (X = 0) \text{ area at inlet}$$

We now interpolate in the tables of  $\rho$ ,  $h$  for constant  $S = S_B$  to find  $h = h_o$  for which the following equation is satisfied:

$$h_B - h = 1/2 \left[ \frac{GE}{\rho A_o} \right]^2$$

From  $S = S_B$ ,  $h = h_o$  we get  $P = P_o$  from the Mollier tables.

The program now begins stepping off from  $X_o = XO$  in increments of  $\Delta X = DELX$  until  $X = XMAX$ . For each  $X$  a four (4) step RUNGE-KUTTA method is used to integrate the differential equations from  $X$  to  $X + \Delta X$ .

1. Set  $h = h_o$ ,  $P = P_o$ ,  $X = X_o = XO$ ,  $h_{inc} = HCOMPO$ ,  $\frac{da}{dx} = 0$ ,  
 $h_w = .5 (h_o + DEH)$ ,  $H = 1.25$ ,  $\Theta = THO$ ,  $V = 0$ .
2. "LIUTER" interpolates in the Mollier table to get  
 $T$ ,  $\sigma$ ,  $\omega \tau / B$ ,  $\gamma R$ ,  $\rho$ ,  $S$ ,  $\gamma$ ,  $\frac{\partial \rho}{\partial h}$ ,  $\frac{\partial \rho}{\partial p}$ ,  $\frac{\partial T}{\partial h}$ ,  $\frac{\partial T}{\partial p}$  at  $h$ ,  $P$ .
3.  $\alpha = \alpha * F1C$   
 $\omega \tau / B = \omega \tau / B * F2C$

4. Interpolate in X vs B input table to find B at current value of X.  
 $\omega \tau = \omega \tau / B * B$   
 $h_{\infty} = h + DEH$
5. Interpolate in X vs D1, D2, table to find  $D_{actual_1} = D_{A_1}$ ,  
 $D_{actual_2} = D_{A_2}$  at current value of X.
6. These calculations done only at  $X = X_0$   
 $\delta = 2 * \Theta * h_{inc}$   
 $u = \dot{m} / [\rho * (D1 - \delta) * (D2 - \delta) * FD]$   
 $\Delta h_0 = h_0 + 1/2 U^2$
7. Interpolate in H vs N table (defined in DATA statement) to find N at H. If H lies outside limits of table define  
 $D_{core_1} = D_{C_1} = D_{A_1} - 2\Theta H$   
 $D_{core_2} = D_{C_2} = D_{A_2} - 2\Theta H$   
 $\delta = \Theta H$   
 and skip to step 10.
8. Using  $\alpha' = h_w / h_{\infty}$  and  $\beta = 1/2 U^2 / h_{\infty}$ , "HCOMP" does the boundary layer calculations returning with  $h_{inc}$ .
9.  $\delta = (h_{inc}) * \Theta$   
 $D_{C_1} = D_{A_1} - 2\delta$   
 $D_{C_2} = D_{A_2} - 2\delta$
10.  $A_{core} = A_c = (D_{C_1}) (D_{C_2}) (FD)$   
 For  $X \neq X_0$ ,  $\frac{dA_c}{dx} = (A_c - A_c') / \Delta X$  where  $A_c' = A_c (X - \Delta X)$ .
11.  $J_x = I / A_c$   
 For  $X \neq X_0$   $U = \dot{m} / (\rho A_c)$   
 $V_e = (AK1) * (\Theta) * (h_{inc}) + AK2$   
 $\alpha = (\omega \tau / B) * J_x / \sigma * U$ ;  $\alpha \geq 1$  terminates program.
12.  $J_y' = \sigma * V_e / D_{C_2} - (1 - \alpha) \sigma * U * B$

If  $J_y' > 0$  set  $J_y = 0$ ,  $E_y = (1 - \alpha) * U * B$ ,  $E_x = J_x / \sigma$

If  $J_y' \leq 0$  set  $J_y = J_y'$ ,  $E_y = V_e / D_{C_2}$

$$E_x = - [1 - \alpha - \alpha / (\omega \tau)^2 - V_e / (D_{C_2} * U * B)] * \omega \tau * B * U$$

16.  $REN = \rho * U * (L_0 + X) / \mu$  : Reynold's number

$$C_f = FRIC / REN^2$$

$$17. \quad a) \quad \frac{du}{dx} = \left[ - \frac{dA_c}{dx} / A_c - \frac{\partial \rho}{\partial h} (J_x * E_y + J_y * E_x) / U - \frac{J_y * B}{U} \frac{\partial \rho}{\partial P} \right] / \left[ 1/U - \left( \frac{U}{\rho} \frac{\partial \rho}{\partial h} - \frac{\partial \rho}{\partial P} \right) \right]$$

$$b) \quad \frac{dp}{dx} = J_y * B - \rho * U * \frac{du}{dx}$$

$$c) \quad \frac{dh}{dx} = [J_x * E_x + J_y * E_y] / (\rho * U) - U * \frac{du}{dx}$$

$$\frac{d\rho}{dx} = \frac{\partial \rho}{\partial p} \frac{dp}{dx} + \frac{\partial \rho}{\partial h} \frac{dh}{dx}$$

$$d) \quad \frac{d\theta}{dx} = - \theta \frac{du}{dx} (2 + E_{inc}) / U - \theta \frac{d\rho}{dx} / \rho + C_f / 2$$

$$e) \quad \frac{dH}{dx} = ECP [5 (H - 1.4)] / [\theta (\rho * U * \theta / \mu)^{1/6}] * [ - (\rho * U * \theta / \mu)^{1/6} \theta \frac{du}{dx} / U - .0135 (H - 1.4) ]$$

$$f) \quad \frac{dP_{out}}{dx} = V * I$$

$$g) \quad \frac{dV}{dx} = EXM = - E_x$$

Equations a - g are then integrated using RUNGE-KUTTA.

Numbers 5 - 10 are done only at the first step of the 4-step Runge-Kutta; i. e. all values computed in 5 - 10 are assumed constant within the  $\Delta X$  range.

After each Runge-Kutta step the program cycles back to No. 2 with new values for  $U$ ,  $P$ ,  $h$ ,  $\theta$ ,  $H$ ,  $P_{out}$ ,  $V$ . After the fourth step  $X$  is updated by  $\Delta X$  and if  $NBAR = 1$ , the program will printout a block of data corresponding to the updated  $X$  position in the channel.

Subroutine "HCOMP" uses the following equations to compute  $h_{inc}$ :

N,  $\alpha'$ ,  $\beta$  (from numbers 7 and 8) are inputs to the subroutine.

$$\frac{U}{U_e} = \left(\frac{y}{\delta}\right)^{1/n}, \quad \frac{h}{h_e} = \alpha' + \frac{U}{U_e} (1 - \alpha' + \beta) - \left(\frac{U}{U_e}\right)^2 \beta$$

$$\frac{\rho}{\rho_e} = \frac{1}{h/h_e}$$

$$\frac{\Theta}{\rho} = \int_0^1 \frac{\rho}{\rho_e} \frac{U}{U_e} \left(1 - \frac{U}{U_e}\right) d\left(\frac{y}{\delta}\right)$$

$$\frac{\delta^*}{\delta} = \int_0^1 \left[1 - \frac{\rho}{\rho_e} \frac{U}{U_e}\right] d\left(\frac{y}{\delta}\right)$$

$$h_{inc} = \frac{\delta^*/\delta}{\Theta/\delta}$$

The subroutine uses a trap exoidal integration scheme with  $\Delta(\frac{y}{\delta})$  for  $0 \leq \frac{y}{\delta} \leq .25$  and  $\Delta(\frac{y}{\delta}) = .02$  for  $.25 \leq \frac{y}{\delta} \leq 1$ .

Subroutine "LIUTER" uses linear interpolation to compute gas properties and first differences to compute derivatives corresponding to given P - pressure and h-enthalpy.

## Conductivity and Hall Coefficient Equations

Listed below are the equations used to calculate the conductivity and Hall coefficient as part of the determination of gas properties in a typical calculation.

### Definitions:

EMM = molar weight (MW) from chart

EMG = initial molar weight (MW)

SUM1 =  $(7.3355 \times 10^{21}) P/T$

ENS =  $(Z_{\text{seed}})(\text{SUM1})(\text{EMM})/(\text{EMG})$

E =  $T/11605.4$

For K-Seed: CAYTM obtained from stored table

For Cs-Seed:  $\text{CAYTM} = \exp \left\{ 2.30259 [-3.87 (5040)K] - 1.5 \log_{10} \left( \frac{5040}{T} \right) + 26.9366 \times 10^{-6} \right\}$

X =  $4.0 (\text{ENS})/(\text{CAYTM})$

ENE =  $0.5 (\text{CAYTM}) [1 + \sqrt{1 + x}]$

OE =  $(2.23 \times 10^{-14}/E^2) \ln (1.09 \times 10^{10} \sqrt{E^3/(\text{ENE})})/0.88 \times 10^{-16}$

ENIQI =  $(1 - Z_{\text{seed}})(7.3355 \times 10^{21})P/T [O_2] C(O_2) + [O] C(O)$   
 $+ [H_2] C(H_2) + [CO] C(CO) + [CO_2] C(CO_2) + [H_2O] C(H_2O)$   
 $+ [OH] C(OH) + [N_2] C(N_2) + [NO] C(NO)$   
 $+ (\text{ENE})(\text{OE}) + (\text{ENS} - \text{ENE}) C(K)$

Where  $[~]$  is the concentration

and  $C(~)$  is the cross section

QT =  $\text{ENIQI}/\text{SUM1}$

$\alpha$  =  $\text{ENE}/\text{SUM1}$

### Conductivity Equation:

$\sigma = \left\{ 3.867 \times 10^{-8} \alpha / [\sqrt{T} (\text{QT})] \right\} / 0.88 \times 10^{-16}$

### Hall Coefficient:

$\omega \tau / B = \sigma / [1.602 \times 10^{-13} (\text{ENE})]$